Effects of Low-Intensity Pulsed Ultrasound on *Staphylococcus aureus* Biofilms, Antibiotic Tolerant Subpopulations, and Infected Tissue-Engineered Skin Models.

Hollie Shaw

A thesis submitted in partial fulfilment of the requirements for the degree of Doctor of Philosophy

The University of Sheffield
Faculty of Health
School of Clinical Dentistry

Submission Date: 22/12/2023

Acknowledgements

My first and foremost thanks go to my incredible supervisor Dr Joey Shepherd, she has demonstrated how to be a strong female lead in research, has put up with my nonsense and guided me gently through my PhD journey. I would also like to extend my gratitude to my co-supervisor Professor Graham Stafford, a great scientist and mentor.

The micro lab group Shivani, Samie, Sofia, Alice, Ash, Kittie, Hassan, Ahmed, and Cher, I am grateful to have had the opportunity to work with the incredible and supportive people. Thank you for all your help.

To my sisters-in-arms Karolina and Isabel, you have been the dream support network through this crazy ride that is our PhD's. We have each laughed, cried and helped each other through. Friends for life! Jon, Cathy and Luna, thank you for being part of the best, crazy group of friends, the tears of laughter I have shed with you all will forever be the greatest gift you've given me.

My mum and grandparents, I hope I have made you proud. I know you struggled to understand why I went on this crazy education journey, but you were still incredibly supportive. Mum, you gave me such a strong self of being and the confidence to go after what I wanted.

My children, Reuben and Imogen, you truly were my inspiration and my driving force to give you a better life. I hope I have shown you that you can accomplish anything you put your mind to. I want you to follow your dreams, in the same way I have followed mine.

Finally, and most importantly, my amazing husband, Chris, without you I would have never been able to complete this. The support and love you have shown me throughout has kept me going and allowed me to embark on a career I wouldn't have dreamed possible without you in my life. You have held down the fort, provided for the family, reassured me, made me laugh and wiped my tears. I will never be able to truly show you have grateful I am to you or repay you for all you have sacrificed and done for me, but I will show my gratitude for the rest of our lives!

Abstract

Chronic infections are often biofilm associated, these become persistent and require extended antibiotic use. Biofilm bacteria display increased antibiotic tolerance compared to their planktonic counterparts through several mechanisms, including decreased diffusion of antimicrobials through the extracellular matrix, enzymes within the matrix that degrade antimicrobials and the presence of persister cells. Antibiotic tolerant (AT) cells are dormant cells within a microbial population that lack common active targets for antimicrobials. Antimicrobials fail to kill these cells, which are then able to reactivate and repopulate an infection site prolonging the infection. This project aims to investigate whether ultrasonic treatment could be used to treat *Staphylococcus aureus* biofilm-associated infections, and how low-intensity pulsed ultrasound (LIPUS) affects biofilms, AT subpopulations and infected tissue.

Staphylococcus aureus biofilms at various stages of maturity were treated with clinically relevant LIPUS (30 mW/cm^2) to investigate changes in growth. Biofilms were treated with LIPUS in conjunction with gentamicin and vancomycin treatment to investigate the effects of ultrasound on antibiotic effectiveness. The permeability of biofilms and *S. aureus* membrane were investigated following LIPUS using fluorescence and microscopy, as well as structural changes in the biofilm using confocal microscopy. Changes in metabolism following LIPUS were investigated using ATP and oxygen levels, and gene expression patterns in biofilms treated with LIPUS were investigated via total RNA sequencing. AT populations were isolated from whole biofilm populations and treated with 30 mW/cm^2 LIPUS with and without gentamicin to assess growth and antibiotic sensitivity changes. Tissue-engineered skin models (TESM) were used to assess the efficiency of combined LIPUS and antibiotic treatment, as well as the effects of the LIPUS on cells used in the TESM. Permeability of cell monolayers were investigated using fluorescence, and proliferation and viability of cells used in the TESM were calculated using a metabolic assay (PrestoBlue) and quantifying number of cells. Effects of 2-hour 30 mW/cm^2 LIPUS on wound healing was investigated using monolayers of cells from TESM and migration assays were performed. Differences in ability to infect the TESM between a laboratory and a clinical strain of *S. aureus* were observed. *S.*

aureus infected TESM were treated with 2-hour LIPUS with and without gentamicin, and the number of viable *S. aureus* within the TESM was calculated to assess any changes in antibiotic sensitivity following LIPUS. ELISA assays were used to investigate the levels of the pro-inflammatory cytokine IL-6 in TESM treated with and without LIPUS treatment. To improve clinical relevance of the infected TESM, a synthetic *in vitro* wound milieu fluid (IVWM) was used as a carrier fluid for infection.

No changes in numbers of viable *S. aureus* cells were identified after up to 3-hours LIPUS treatment, and dispersal of the biofilm did not occur in up to 2-hours LIPUS treatment. Antibiotic sensitivity increased in LIPUS treated biofilms for gentamicin only, with no changes to vancomycin sensitivity. Structural changes to the biofilm showed no visual changes in the biofilms at 1- and 7-days when treated with LIPUS. Increased biofilm permeability to small molecular weight dextran was observed in 1-day and 7-day *S. aureus* SH1000 biofilms with 2-hours LIPUS treatment. However, methods used to investigate changes in cell membrane permeability did not show any changes. ATP levels of older biofilms (5- and 7-day) were significantly altered by LIPUS treatment with a reduction in ATP release from the biofilms, which was not observed in younger biofilms. Oxygen levels were higher in the media of the LIPUS treated biofilms, but the mechanisms behind this observation remain unclear. Antibiotic tolerant populations were isolated and treated with LIPUS, the growth and viability of these populations remained unchanged when treated with 2 hours LIPUS, while antibiotic sensitivity increased.

RNA sequencing and gene ontology representation analysis indicated the cell and plasma membrane were cellular components with the most changes to gene expression, while gene expression for proteins associated with transmembrane transport and the cytocidal processes against other organisms were over-represented biological functions with the most changes to gene expression when *S. aureus* SH1000 biofilms were treated with LIPUS.

Proliferation and metabolism of mammalian cells used in the tissue-engineered skin model remained unchanged, as did the permeability of a monolayer of keratinocytes (HaCaT) and fibroblast (HDF) cells following LIPUS. Wound healing in HaCaT monolayers was not impacted by LIPUS treatment, but in HDF the rate of healing was reduced. Nonetheless total closure of all wounds was observed at 48-hours post treatment. IL-6 production was increased in LIPUS treated skin models. Changes to antibiotic sensitivity in infected skin models were not observed with LIPUS treatment, however it is noted the experimental conditions did not represent proposed treatment set up in a clinical setting.

A laboratory strain of *S. aureus (S. aureus* SH1000*)* was unable to infect the TESM, unlike the clinical strain used *(S. aureus* S235). There was a reduction in numbers of viable cells in the laboratory strain when incubated in media from the keratinocytes and the fibroblasts as well as when incubated in the presence of the human cells, indicating release of a substance antimicrobial to SH1000 but not S235 cells. Lastly, the use of a synthetic wound fluid caused clustering of *S. aureus* within the TESM, closely representing a physiologically relevant infection.

This study found that LIPUS increased antibiotic sensitivity to gentamicin in *S. aureus* SH1000 biofilms, although mechanisms remain unclear, data collected in this study suggest changes to biofilm structure and permeability is unlikely to be the cause. Data collected in this study also suggests membrane permeability is unlikely to be the cause of the increased sensitivity and more work would be required to elucidate the mechanisms of increased sensitivity. The treatment regime investigated in this study did not increase the efficacy of antibiotics in infected wound models but repeated LIPUS and antibiotic treatment should be investigated in the future, as repeated LIPUS treatment is used in other clinical settings, such as bone healing.

Table of Contents

Table of Figures

Abbreviations

Agr – Accessory gene regulator

AMP – Antimicrobial peptides

AMR – Antimicrobial resistance

AT – Antibiotic tolerant

BHI – Brain Heart Infusion

CFU – Colony forming units

CHIPS – Chemotaxis inhibitory protein of *Staphylococcus aureus*

ClfA – Clumping factor A

ClfB – Clumping factor B

CP5 – Capsule polysaccharide type 5

CWA – Cell-wall anchored proteins

FnBPA – Fibronectin binding protein A

FnBPB – Fibronectin binding protein B

GO – Gene ontology

Hla – α-haemolysin

Hlg – γ-haemolysin

Il-6 – Interleukin 6

IV – Intravenous

IVWM – *in vitro* wound milieu

LIPUS – Low-intensity pulsed ultrasound

MIC – Minimum inhibitory concentration

MRSA – Methicillin-resistant *S. aureus*

MSCRAMM – Microbe surface recognising adhesive matrix molecules

NHS – National Health Service

NO – Nitric oxide

PAMPs – Pathogen-associated molecular pattern

PBP – Penicillin binding proteins

PCA – Principal component analysis

PSM – Phenol-soluble modulins

PIA – Polysaccharide intracellular adhesins

ppGpp – Guanosine pentaphosphate

PRR – Pattern recognition receptor

PVL – Panton-Valentine leucocidin

RSH – ReIA/SpoT homolog proteins

SAgs - Superantigens

SAK – Staphylokinase

SE – Staphylococcal enterotoxin A

SpA – Protein A

SSTI – Skin and soft tissue infections

TA – Toxin-antitoxin

TCS – Two-component System

TLR – Toll-like receptor

TSST-1 – Toxic shock syndrome toxin

US – Ultrasound

WHO – World Health Organisation

1 Introduction

The skin is part of the innate immune system, acting as a physical barrier against pathogens. When the skin is compromised, pathogens can invade the body and infections can occur (Ki & Rotstein, 2008). These can be acute, and resolve within weeks with or without treatment, or in some cases these infections fail to improve even with appropriate treatment, becoming chronic (Pulido-Cejudo *et al*., 2017). Chronic infections can require repeated antibiotic treatments or long-term antibiotic usage. This is poor antibiotic stewardship as extended use of antibiotics results in selective pressure on the bacteria and causes development of antimicrobial resistance (AMR) (Llor & Bjerrum, 2014).

The World Health Organisation (WHO) identifies AMR in microorganisms as a global crisis which requires urgent action. In 2015, the WHO formulated an action plan to address AMR, and has surveillance systems in place to monitor its spread (World Health Organisation, 2018). AMR is currently one of the biggest threats to human health, partly due to the reliance of modern medicine on the ability of antibiotics to prevent and treat bacterial infections (World Health Organisation, 2020). In addition to acquired antibiotic resistance, bacteria are often found in biofilm which are commonly associated with chronic infection (James *et al*., 2008). Biofilms have a protective extracellular polysaccharide barrier, protecting the bacteria from host immune responses and antimicrobial agents (Hall & Mah, 2017).

Bacteria in biofilms can display increased antibiotic tolerance for several reasons, including the presence of a subpopulation of antibiotic tolerant (AT) cells (Fisher *et al*., 2017). These cells are dormant and lack many common targets of antibiotics activity, therefore are able to withstand doses of antibiotic lethal to actively dividing cells. These cells can then reactivate when growth conditions are optimal potentially contributing to recurring infection (Lewis, 2007). The ability to reactivate these AT cells during antibiotic treatment would reduce their antibiotic tolerance and increase

the likelihood of effective treatment of infection (Lewis, 2007). This could improve the treatment outcomes for patients with chronic skin and soft tissue infections (SSTI).

Ultrasound (US) is widely used clinical settings for a range of applications, from imaging to bone healing. High intensity US can destroy biofilms, while low intensity US has been found to induce increased growth of biofilms (Jiao Li *et al*., 2018; Pitt *et al*., 1994; Pitt & Ross, 2003). The mechanism which results in the increased growth is not understood although increased movement of nutrients and oxygen has been suggested as a cause (Pitt & Ross, 2003).

The aim of this project is to assess the effects of low intensity pulsed US (LIPUS) on antibiotic sensitivity of bacterial cells in biofilms, isolated AT populations and infected tissue-engineered skin models (TESM), and the mechanisms by which LIPUS affects biofilms, AT subpopulations and infected TESM.

2 Literature Review

2.1 Skin and Health

The skin is the largest organ in the human body and is crucial for maintaining health and homeostasis. It provides a barrier against the outside world, protects the body from the adverse effects of heat, prevents dehydration , and is one of the first lines of defence against potentially harmful pathogens. Several components make up the barriers of the immune system, from tears and stomach acid to mucous membranes, specialised cells, enzymes and commensal bacteria (**Figure 1**). The largest component by far is the skin.

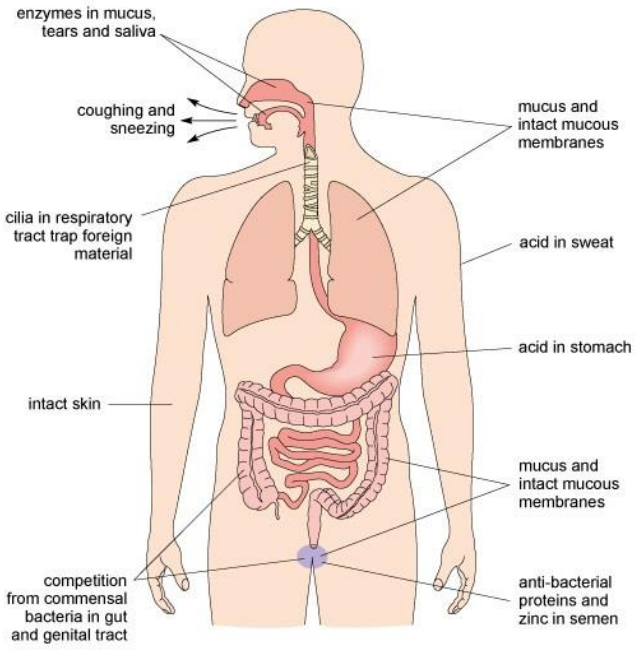

Figure 1: The barriers of the immune system include intact skin and mucous layers, high acidity of sweat and the stomach, commensal bacteria, enzymes and ciliated cells and automated response to stimuli such as coughing and sneezing. Taken from Open University (2023)

The skin is composed of three layers, all of which play a key role in maintaining health and protecting the body (**Figure 2**). The uppermost layer of the skin is the epidermis, containing mainly keratinocytes, but also melanocytes, Merkel cells and

specialised immune cells. This thin layer of tissue protects the body from pathogens, UV radiation, and dehydration. The topmost layer of the epidermis, the stratum corneum, is comprised of dead keratinocytes. The stratum corneum acts as armour, preventing microbial invasion and regularing water loss. Live keratinocytes within the lower layers of the epidermis are immune competent cells, able to recognise and respsond to pathogens, modulate immune response and produce antimicrobial peptides (Quaresma, 2019). Melanocytes found in the skin produce melanin, pigments found in skin, hair and eyes which provide protection against photodamage caused by UV radiation (Cichorek *et al*., 2013). Merkel cells are associated with peripheral nerves, allowing for the perception of soft touch (Abraham & Mathew, 2019). Langerhans cells are skin specialised antigen presenting cells, activated during infection (Quaresma, 2019).

The midlayer of the skin is the dermis, providing structure to the skin and housing important components such as blood vessels, sweat and sebaecous glands, hair follicles, receptors to sense, heat, and touch, nerves, lympatic vessels and immune cells (Pfisterer *et al*., 2021). These components all assist sensing the enviroment, maintaining health of the skin and protecting the body from harm. The dermal extracellular matrix is comprised mainly of elastin and collagen proteins produced by fibroblast cells which populate the dermal layer (Pfisterer *et al*., 2021). The deepest layer of the skin is the hypodermis, which is made up of adipocytes and connective tissue. The hypodermis provides the body with insulation, energy storage and connects the skin to deeper tissues (T.M. & K., 2022). The different layers of the skin can be visualised by haemotoxylin and eosin staining of thin slide mounted sections of skin (**Figure 3**).

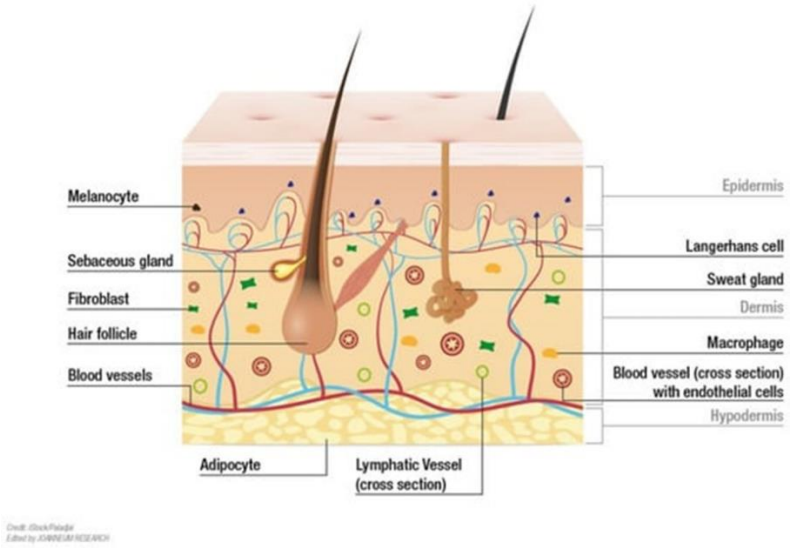

Figure 2: Cross section diagram of human skin. (https://www.mdpi.com/2227-9059/11/3/794#)

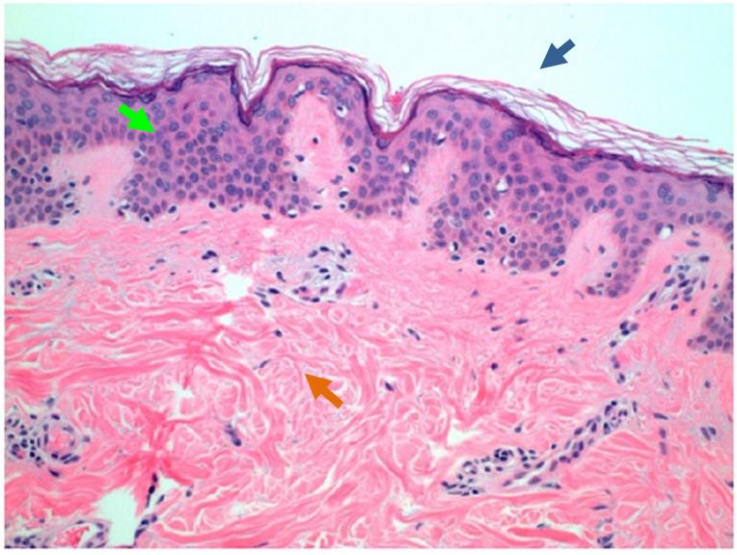

Figure 3: Haematoxylin and Esosin histology stain of human skin arrows highlighting the stratum corneum (blue), epidermis (green) and dermis (orange). (Ji & Li, 2016)

Due to its proximity to the outside world, the skin is at high risk to disease and infection which impacts its ability to protect human health. There are a plethora of diseases which impact the skin including autoimmune diseases, dermatitis, eczema, acne and psoriasis. All these diseases negatively impact the integrity of the skin and cause disruptions which make the skin vulnerable to microbe invasion. Infections of

the skin are often minor and quickly resolved with treatment, however, a large burden of health is the development of chronic infections.

2.2 Injury and Skin and Soft Tissue Infection

Patients with skin wounds are susceptible to developing infections. Wounds are categorised as acute or chronic depending on length of healing; wounds healing within 4 weeks are considered acute, while failure to heal beyond 4 weeks is categorised as chronic (DiNubile & Lipsky, 2004). Injuries which commonly become infected include minor abrasions, surgical incisions, burns, bites, vascular ulcers, diabetic ulcers, and pressure sores (Bowler *et al*., 2001). Patients with underlying skin conditions, which compromise the skin barrier, such as eczema and atopic dermatitis, are also at increased risk of infection (Boguniewicz & Leung, 2011). Skin and soft tissue infections (SSTI) can lead to complications including deeper penetrating infections and systemic infections (Ki & Rotstein, 2008). Cellulitis and abscess are common types of SSTI. Cellulitis is the infection of the dermis and subcutaneous tissues (Yarbrough *et al.*, 2015). Patients often present with localised infection, pain, swelling and redness (Gunderson, 2011), while abscesses are a collection of pus surrounded by a membrane (Cheng *et al*., 2011). These manifestations of SSTI are not mutually exclusive and a patient may present with an abscess with surrounding cellulitis. Cellulitis and abscesses are commonly minor infections, responding well to treatment, however, they can develop into a serious condition. In 2022-23, around 140,000 emergency hospital admissions were recorded due to SSTI and 168,000 total admissions were attributed to SSTI (NHS, 2023; Service, 2023).

Burns are a common trauma which damage the skin, and severity of burns varies from a first degree to a fourth-degree burn (Jeschke *et al*., 2020). These are characterised by the depth of the injury. First and second degree burns are superficial, affecting the epidermis. Second degree burns may result in scarring and increased discomfort for the patient and may penetrate into the dermis. Third degree burns penetrate into the dermal layer, while fourth degree burns involve deeper

tissues, such as muscle. Both third and fourth degree burns often require surgery (Jeschke *et al*., 2020). Due to the damage in the skin's barrier against pathogens, infections are a complication associated with burn injury with increased scarring risk, and invasive and systemic infection (Greenhalgh, 2017; Singer & McClain, 2002). Chronic wounds are skin injuries with extended healing times, total healing failure or recurring infections (Frykberg & Banks, 2015). Chronic wounds are susceptible to infection and pressure sores and diabetic foot ulcers (DFU) are examples of injury which may develop into chronic wounds. Pressure sores (also known as pressure ulcers) are skin injuries caused by prolonged pressure on areas of the skin, resulting in reduced blood flow to the area, and are found on patients with reduced mobility and are commonly associated with elderly patients (Boyko *et al.*, 2018). Insulin resistant diabetes increases the risk of developing a diabetic foot ulcer (DFU), due to peripheral diabetic neuropathy and compromised blood flow (Reiber *et al.*, 1999). Both pressure sores and DFU may become infected, with chronic sores often being found to be colonised by biofilm bacteria (Bhattacharya & Mishra, 2015).

2.3 Chronic SSTI

Chronic SSTIs are recurrent or persistent infections which fail to resolve after several weeks of appropriate treatment. Some skin conditions are often associated with recurring infections, such as hidradenitis suppurativa, an inflammatory skin disorder commonly resulting in recurring abscesses (Bukvić Mokos *et al*., 2023). Chronic infections can also occur when typically acute infections such as cellulitis, abscesses and impetigo recur or persist after treatment. Alternatively, chronic wounds such as pressure sores and DFU can become infected, leading to long term infection and further inhibiting healing of the chronic wound. A study published in 2018 found that 45% of patients with DFU were prescribed antimicrobial dressings or medication when they initially presented, suggesting these ulcers were already infected or were suspected to be at high risk of developing infection. By the end of the 12-month study 75% of the sample had developed an infection (Guest *et al*., 2018). Kee *et al*. (2019) assessed the healing time of DFU in Malay patients and found infection significantly increased the healing time of CFU from a median of 1 months in

uninfected DFU to 5 months in infected DFU. There are several contributing factors to the development of chronic infections including obesity, patient lifestyle, poor circulation, poorly controlled diabetes, advanced patient age, and patients with compromised immune systems (Cieri *et al*., 2019; Dryden *et al.*, 2015; Hemmige *et al*., 2015).

2.4 Burden of DFU Infection

Chronic SSTIs carry high costs to patients' quality of life and healthcare organisations, as well as the wider community. When looking at chronic wounds DFU alone cost the NHS an estimated £900 million annually (Kerr *et al*., 2019), and DFU failing to heal cost an average 400% more than DFU which heal within 12 months (Guest *et al.*, 2018). The National Health Service (NHS) have estimated that 10% of diabetic patients will develop a skin ulcer during their lifetime, with 40% of patient with an ulcer not surviving five years (Mackenzie, 2017).

The difficulties in treating these infections with drug therapy results in more drastic treatment options and are commonly a contributing factor to the need for amputation (Tabur et al., 2015; Ugwu et al., 2019; D. D. Wang et al., 2016). DFU are the most common cause of diabetic hospitalisation and the leading cause of limb amputation (Casqueiro *et al*., 2012; Mavrogenis *et al*., 2018). The percentage of patients requiring amputation due to infected DFU varies in a number of studies with estimates between 6% and 17% (Guest *et al.*, 2018; Lu & McLaren, 2017; Ndosi *et al*., 2018). Seth *et al* (2017) reported 39% of study participants required a minor amputation and 8% major amputation, however it is unclear how major and minor amputation were classified. This study included less participants than others which may be the reason for the higher percentages reported. Management of amputation costs on average £16900 per patient, more than double the average cost of treatment of an infected DFU and eight times the cost of treating an uninfected DFU (Guest *et al.*, 2018).

Amputation of a limb due to a DFU is also an indicator of premature death, with patients with leg amputations as a result of DFU being at the highest risk of premature death than diabetic patients not requiring amputation. Huang *et al.* (2018) reported a 5-year survival rate of 40% in patients with major or minor lower extremity amputation, with the mean survival time of 3.1 years. Patients classified as having a major amputation, having an amputation above the ankle, experienced worse outcomes than patients with minor amputation. Izumi *et al.* (2009) similarly found that major amputations had a significant impact on the 5-year mortality, the average age of death was 61 compared to the average life expectancy at the time of data collection in the USA which was between 75.5-77.4 years (Centre for Disease Control and Prevention, 2007).

2.5 Treatment of Chronic SSTI

In SSTI, the first line of antibiotic treatment is dependent on the type of SSTI and the condition of the patient. For instance, patients presenting with superficial non-bullous impetigo will be offered topical antibiotics in the first instance, while blistered impetigo is treated with oral antibiotics (NICE, 2020a). Uncomplicated deeper infections such as abscesses, cellulitis and infected leg ulcers are also treated with oral antibiotics (NICE, 2019a, 2020b). Seriously unwell patients, or patients presenting with infections at risk of serious complications are offered intravenous (IV) antibiotics with review to move to oral antibiotics if improvement is observed within 48 hours. Infections demonstrating a failure to resolve or patients exhibiting worsening condition may require specialist intervention and hospitalization (NICE, 2019a, 2020a).

Physical removal of damaged tissue and infection may be required in wounds failing to resolve. Debridement is a standard procedure in caring for chronic wounds, the process involves the removal of dead tissue and infection from within a wound. Debridement can be achieved using different methods: biological, enzymatic, and mechanical (Thomas *et al.*, 2021). Biological debridement, also known as larval

therapy, refers to the use of sterile *Lucilia sericata* larvae to remove dead tissue and bacteria from a wound. The larvae ingest necrotic tissue and bacteria and the digestive enzyme secretions (metalloproteases, proteases, glycosidases, and lipases) from the larvae have antimicrobial and anti-inflammatory effects on the wound (Cazander *et al*., 2013; Tombulturk & Kanigur-Sultuybek, 2021). Larval therapy results in quicker debridement than traditional debridement methods and an increased healing rate of the wound (Dumville *et al.*, 2009; Mudge *et al*., 2014). Yet, the idea of larval therapy can be disagreeable for patients, resulting in reluctance to undertake this treatment (Spilsbury *et al*., 2008). Enzymatic debridement involves the use of exogenous enzymes to degrade dead tissue to allow removal. Patients receiving enzymatic debridement reported lower pain, with wound healing to a greater extent than patients receiving mechanic wet-to-dry debridement (Onesti *et al*., 2016). Mechanical debridement is the removal of dead tissue through surgery, high pressure wound irrigation, wet-to-dry debridement, or ultrasonic treatment. Surgical debridement involves the total removal of wound tissue, leaving only healthy tissue, this type of debridement is invasive and may result in larger wounds initially (Vowden & Vowden, 1999). Another mechanical debridement technique is wet-to-dry debridement. Wet-to-dry debridement involves the application of a wet dressing to the wound, this is allowed to dry before removal to manually remove dead and infected tissue. This is reported by patients as painful and may cause damage to otherwise healthy tissue (Young, 2012).

Failure of treatments for SSTI resulting in long term SSTI are a risk factor in developing osteomyelitis, this is often seen in osteomyelitis caused by *Staphylococcus aureus* (Cunningham *et al.,* 1996; Prieto-Pérez *et al.,* 2014). Osteomyelitis treatment involves IV antibiotic treatment followed by long-term oral antibiotic treatment (NICE, 2019b). Severe osteomyelitis requires surgical interventions that can include amputation (Zhong *et al*., 2023). Effective treatment of SSTI with first line antibiotic treatment would reduce the occurrence of such complications and decrease the need for further treatment and reduce harm to patients.

2.6 Microbiology of Chronic SSTI

Opportunistic pathogens found colonising the skin surface can invade the body when the protective barrier of the skin is compromised, which can then multiply to quantities which overwhelm the immune system causing clinically significant infections (Jneid *et al*., 2017). Several of the pathogens which are found in SSTI are part of a collective group of clinically significant pathogens known as ESKAPE pathogens. The ESKAPE pathogens are *Enterococcus faecium, S. aureus, Klebsiella pneumoniae, Acinetobacter baumannii, Pseudomonas aeruginosa,* and *Enterobacter spp.* (Mulani *et al*., 2019). These pathogens are becoming increasingly virulent and drug resistant, and are commonly associated with nosocomial infection. Infections of burn wounds are often initially infected by *S. aureus* and as the infection ages *P. aeruginosa* becomes the predominant pathogen (Church *et al*., 2006). *S. aureus* is also commonly the causative organism in abscesses, and infection with *S. aureus,* along with β haemolytic streptococci, often causes cellulitis (Sullivan & de Barra, 2018).

DFU infections are complex and predominantly polymicrobial infections, the identification of single species infections are attributed to inadequate use of antibiotics, causing partially clearing infections allowing single species colonisation of wounds (Rastogi *et al*., 2017). All patients in the study conducted by Rastogi *et al.* who did not receive antibiotics prior to presentation had polymicrobial infections, this is due to ineffective use of antibiotics which may eradicate sensitive bacteria but leave resistant or tolerant bacteria present. Therefore, when a patient presents after antibiotic treatment samples taken from that patient will only contain the bacteria not eradicated by treatment (Rastogi *et al*., 2017). Gram-negative bacteria are commonly found in DFU infections, with one study finding 71% of isolates identified were Gram-negative (Seth *et al*., 2019). *Escherichia coli* is one such Gram-negative bacteria, isolated in 30% of patient samples (Malik *et al*., 2013; Seth *et al*., 2019; Shahi & Kumar, 2015). *Enterobacter spp.* and *P. aeruginosa* have also been identified in high proportions of DFU infection, 73 % and 14 % of infected DFU respectively (Xie *et al*., 2017). Gram-positive cocci, such as *Staphylococcus spp.*

and *Enterococcus spp.* are also commonly isolated from DFU infections (Mavrogenis *et al.*, 2018). Several studies found *S. aureus* accounted for 30%-40% of bacteria isolated from DFU patients (Gardner *et al*., 2013; Kateel *et al*., 2018; Seth *et al*., 2019; Shahi & Kumar, 2015), and one study found *Enterococcus spp.* made up 47% of the isolates from samples (Malik *et al., 2013)*. However, the culturing techniques used in studies to identify bacteria in DFU leads to bias in the species found with easily cultured bacteria, such as *S. aureus* and *E. coli* being detected more readily, leading to the assumption that these are the most prevalent bacteria in these infections (Dowd *et al*., 2008). These bacteria are aerobic or facultative anaerobic and are believed to cause the majority of DFU infections, however severe infections can also have anaerobic bacteria present (Shahi & Kumar, 2015), such as *Bacteroides fragilis* and *Peptostreptococcus spp*. (Percival *et al*., 2018).

2.6.1 Staphylococcus aureus in SSTI

In this study, *S. aureus* was the focus as *S. aureus* is a significant pathogen in SSTI infections (Dryden, 2010; Seth *et al*., 2019; Shahi & Kumar, 2015), often resulting in difficult to treat infections. These Gram-positive bacteria live commensally on the skin and colonise the nostrils of approximately 30-50% of the human population (Ryu *et al*., 2014). Despite being commensal these bacteria are recognised as a major human pathogen causing some of the most common infections, including bacteraemia, endocarditis, pleuropulmonary infections and SSTI (Tong *et al*., 2015). *S. aureus* has the ability to invade host cells, allowing the evasion of both the immune system and antibiotic treatment (Bien *et al*., 2011).

2.6.2 S. aureus Virulence Factors in SSTI

S. aureus has multiple virulence factors making it an efficient and effective pathogen (listed in **Table 1**). *S. aureus* is surrounded by a polysaccharide capsule, preventing phagocytosis (Kuipers *et al*., 2016). Several cell-wall anchored proteins (CWA) have been identified in *S. aureus* that allow the bacteria to adhere to the host cells to

colonise and infect. Microbe surface components recognising adhesive matrix molecules (MSCRAMM) are a prominent group of CWA associated with infection (Foster, 2019). Clumping factors are a type of MSCRAMM and bind with fibrinogen (Foster, 2019), fibrinogen is a host glycoprotein present in wounds, playing a role in healing (Laurens *et al*., 2006). Clumping factor B (ClfB) also binds to loricrin (Mulcahy *et al*., 2012) and cytokeratin 10 (Walsh *et al*., 2004), proteins found in keratinocytes on the outer layer of the epidermidis, these proteins facilitate colonisation of nasal passages (Hohl *et al*., 1991; Mulcahy *et al.*, 2012). Expression of cytokeratin is enhanced when the epidermal barrier is damaged (Ekanayake-Mudiyanselage *et al*., 1998). ClfB has been associated with skin infections and abscess formation (Lacey *et al*., 2019). Fibronectin binding proteins A and B (FnBPA and FnBPB) are also MSCRAMMs, binding to fibronectin, fibrinogen and elastin (Foster, 2019). As with clumping factor fibronectin binding proteins are important during early infection, aiding in the adhesion to host cells. Fibronectin binding proteins are also associated with the internalisation of *S. aureus* within host cells *(Agerer et al*., 2005; Schröder *et al*., 2006). There is evidence *S. aureus* FnBPA facilitates internalisation of non-invasive species (Pontes *et al*., 2012).

S. aureus also produces enzymatic virulence factors, breaking down host extracellular components to aid infection. Hyaluronidase breaks down hyaluronan (Ibberson *et al*., 2014), a glycosaminoglycan which is a component of the extracellular matrix; it plays a role in granulation and cell migration as well as other stages of wound repair (Oksala *et al*., 1995; Stern *et al*., 2006). Hyaluronidases allow the bacteria to use the hyaluronan as a carbon source, and in addition to providing a nutrient source, allows the bacteria to penetrate tissues allowing infection to spread (Hynes & Walton, 2000). *S. aureus* also produces lipase which break down fatty acids. The function of this enzyme is thought to be to allow the bacteria to penetrate tissues through the breakdown of extracellular components, this is evidenced by the increased lipase activity in invasive infections in comparison to superficial infections (Rollof *et al*., 1987). Lipase appears to play a role in biofilm formation, *S. aureus* mutants lacking lipase demonstrated reduced biofilm forming capability (Hu *et al*., 2012). *S. aureus* also produces two types of enzymes which interact with proteins found in the plasma of the blood. The first, coagulase, converts fibrinogen to fibrin,

allowing for the formation of clots, through the activation of thrombin (McAdow, Missiakas, *et al*., 2012). This aggregation of fibrin around the bacteria protects the bacteria from host immune response and facilitates the formation of abscesses (Cheng *et al*., 2010). Immunization against coagulase reduces abscesses in murine models (McAdow, DeDent, *et al.*, 2012). The second, staphylokinase (SAK), can digest these fibrin clots through activation of plasminogen, facilitating the invasion activity of *S. aureus* (Peetermans *et al*., 2014).

To successfully establish an infection and survive *S. aureus* must evade the host immune system. *S. aureus* produces both secreted proteins and membrane bound proteins which inhibit the immune response of the host. An exoprotein secreted by *S. aureus*, chemotaxis inhibitory protein of *S. aureus* (CHIPS), inhibits neutrophil migration through binding with receptors, blocking neutrophil activation via ligand binding (Postma *et al*., 2004). Protein A (SpA) is a protein on the surface of *S. aureus* which binds antibodies at the tail domain, preventing the activity of antibodies during infection, aiding the survival of *S. aureus (Falugi et al*., 2013).

Toxins produced by *S. aureus* damage cell membranes, causing cell lysis. These toxins target immune cells. Panton-Valentine leucocidin (PVL) is a toxin which induces cell lysis by forming β-barrel pores within the host cells membranes (Yoong, 2013). PVL targets leukocytes, reducing the immune response to *S. aureus.* The presence of the PVL gene in MRSA increases the patients likelihood of poor outcome *(Ahmad et al*., 2020). α-haemolysin (Hla) and γ-haemolysin (Hlg) also induces cell lysis by the formation of β-barrel pores (Vandenesch *et al*., 2012). Phenol-soluble modulins (PSM) are able to induce cell lysis in many types of cells including monocytes (Cheung *et al*., 2014). Superantigens (SAgs) are exotoxins produced by *S. aureus* which induce a strong immune response, inducing excessive inflammatory cytokine production by T-cells (Oliveira *et al*., 2018). These superantigens are commonly associated with toxic shock syndrome and food poisoning caused by *S. aureus* (Xu & McCormick, 2012).

Table 1:The role of S. aureus virulence factors involved in SSTI

Table 2: Virulence factor	Role in SSTI	Reference
MSCRAMMs – Clf & FnBP	Adhesion and invasion of host cells.	(Lacey *et al*., 2019), (Agerer *et al.,* 2005), (Schröder *et al*., 2006)
Enzymes – Hyaluronidase, Lipase Coagulase & Staphylokinase	Breakdown of extracellular matrix components to allow the spread of infection. Abscess formation	(Cheng *et al*., 2010; Hynes & Walton, 2000; Peetermans *et al*., 2014; Rollof *et al*., 1987)
Immune evasion proteins – CHIPS & SpA	Prevention of neutrophil migration. Binding of antibodies and blocking humoral immune response.	(Falugi *et al*., 2013), (Postma et al., 2004)
Toxins – PVL, Hla, Hlg, & PSM	Immune cell killing, evading immune response. Degradation of host cell-cell adhesion	(Cheung *et al*., 2014; Vandenesch *et al.*, 2012; Yoong, 2013)

Along with virulence factors expressed by these bacteria, many strains of *S. aureus* are also antibiotic resistant. MRSA (methicillin resistant *S.aureus*) strains are becoming more prominent in healthcare-associated infections and chronic wounds (see 2.7). This increases the difficulty in treating infections caused by *S. aureus*.

2.7 *S. aureus* Antibiotic Resistance and Tolerance

Antimicrobial resistance is the ability of microbes to avoid growth inhibition and killing by antimicrobial agents. Bacteria may avoid antimicrobials through intrinsic resistance, where the bacteria naturally lack the target for the antibiotic, or through acquisition of resistance genes, through a mutation, transformation, transduction or conjugation (Abushaheen *et al*., 2020). Mechanisms of resistance (**Figure 4**) include the inactivation of the antimicrobial through the production of enzymes which can modify the antibiotic, such as beta-lactamase which inactivates beta-lactam antibiotics (Kong *et al*., 2010), through the hydrolysis of the beta-lactam ring (Shaikh *et al.*, 2015). Bacteria may also alter the target site of antibiotics to prevent the activity, such as the emergence of vancomycin resistance seen in Gram-positive bacteria through the acquisition of *van* genes which causes structural changes to peptidoglycan precursors, which are the target of vancomycin activity. The changes to this precursor, D-alanyl-D-alanine, reduce vancomycin binding allowing cell wall synthesis to continue even in the presence of vancomycin (Reygaert, 2018). Another change to a target site is responsible for resistance to macrolide antibiotics, which bind to the 50S ribosomal subunit, through the modification of 23S rRNA (Foster, 2017). Reduction of antibiotic uptake into the cell as well as increased efflux also protects the bacteria against antibiotics (Kumar & Schweizer, 2005), this mechanism of resistance is seen in *S. aureus* against tetracycline in which efflux pumps have been described which transport tetracycline out of the cell (Foster, 2017).

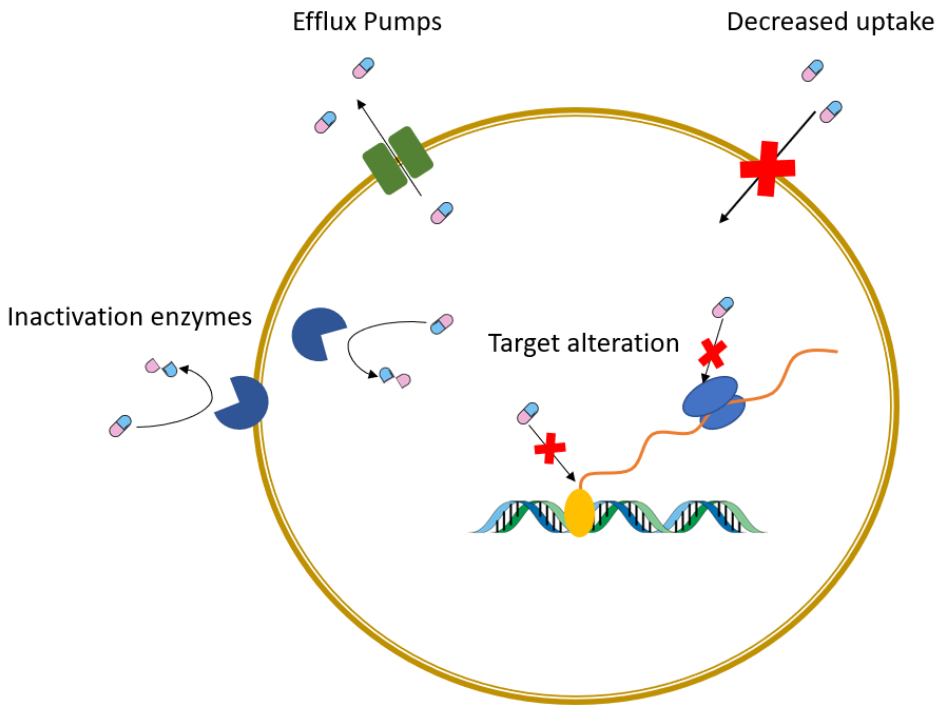

Figure 4: Mechanisms of antibiotic resistance in S. aureus. These mechanisms include enzymes which inactivate antibiotics, efflux pumps that pump the antibiotic out of the cell, changes to the cell wall to prevent antibiotic uptake and changes to the antibiotic target to prevent antibiotic activity. Adapted from Guo et al, 2020 (Guo et al., 2020)

S. aureus is often associated with antibiotic resistance. Penicillins are the first line antibiotic in the treatment of infections caused by *S. aureus.* Penicillin is a beta lactam antibiotic, and their mechanism of action is to prevent crosslinking of peptidoglycans during cell wall synthesis through the binding of bacterial penicillin binding proteins (PBP) (Soares *et al*., 2012), responsible for the building of the peptidoglycan cell wall (Navratna *et al*., 2010). The lack of cell wall exposes the bacteria to the osmotic pressures of the environment, resulting in cell lysis. Penicillin has been heavily used in clinical settings since its discovery, which has produced an environment of selective pressure that resulted in the development of resistance in some *S. aureus* strains. The production of beta-lactamase enzyme by *S. aureus,* inactivates beta-lactam antibiotics, preventing the antibiotic from binding PBP (Kong *et al*., 2010). As well as producing enzymes to combat antibiotics *S. aureus* exhibits all resistance mechanisms as shown in **Figure 4**. The resistance to tetracycline is achieved through pumping the antibiotic out of the cell to prevent tetracycline binding

to the 30S subunit of ribosomes (Foster, 2017). As well as the change in drug target to prevent vancomycin activity, there is evidence to suggest *S. aureus* are able to prevent vancomycin from entering the cell through thickening of the cell wall (Lambert, 2002).

MRSA exhibit resistance to methicillin antibiotic, a semisynthetic beta-lactam antibiotic. These strains gain resistance to beta-lactams through the expression of PBP with poor beta-lactam binding. The expression of the *mecA* gene, a resistance gene, produces PBP2a, which has a low affinity for the beta-lactam ring in the antibiotics (Lowy, 2003). This allows PBP2a to continue crosslinking the molecules in peptidoglycan, allowing cell wall synthesis to continue even in the presence of beta-lactam antibiotics (Katayama *et al*., 2000). MRSA are not only resistant to beta-lactam antibiotics but have been shown to have significantly higher resistance to quinolone antibiotics, which inhibit DNA replication (Jacoby, 2005), than methicillin sensitive *S. aureus* (Gade & Qazi, 2013) and macrolide antibiotics (Liu *et al*., 2017), which target ribosomes, preventing protein synthesis by binding to the 50S unit (Leclercq, 2002). Erythromycin, clarithromycin and azithromycin are all examples of macrolide antibiotics.

In addition to these acquired mechanisms of antibiotic resistance*, S. aureus* are biofilm-forming. Biofilms provide multiple mechanisms for resident microbes to be inherently insensitive to antibiotic treatment (see 2.8).

2.8 *S. aureus* Biofilm

Biofilms are communities of bacteria, that are often multispecies, surrounded in an extracellular matrix (ECM) made up of polysaccharides, enzymes, extracellular DNA and other molecules (Otto, 2008). Existing in a biofilm provides benefits to the bacteria, such as a nutrient source, protection from host immune response and protection against antimicrobial agents due to the ECM. The ECM provides a barrier

against immune cells, preventing phagocytosis by macrophages (Roilides *et al*., 2015). Cells communicate through secretion of molecules into the ECM, resulting in regulation of genes coding for virulence factors (Gupta *et al.*, 2016). Gene transfer also occurs in the ECM; DNA released by lysed cells can be taken up by living cells in the biofilm. These genes can be antimicrobial resistance genes which increases virulence of the bacteria (Lewis, 2001). Bacteria in biofilm are able to withstand mechanical stress and shear force (Gloag *et al*., 2020).

This means biofilms are clinically significant as biofilm associated infections are difficult to treat. James *et al.* (James et al., 2008) observed 60 % of chronic infections had biofilms present while only 6 % of acute infections had biofilms. Biofilms are less susceptible to antibiotic activities, resulting in less effective treatment of infections. Marcia *et al.* (Macià et al., 2014) showed biofilm bacteria could tolerate up to 1000x higher concentrations of antibiotic than planktonic bacteria. Tolerance displayed by biofilms is caused by a number of factors. The extracellular matrix reduces antibiotic diffusion as molecules are unable to penetrate the biofilm efficiently (Hall & Mah, 2017). Extracellular enzymes, such as β-lactamase released by lysed cells in the biofilm, can also be present in the biofilm, preventing antibiotic activity (Hoiby *et al*., 2010).

2.8.1 Formation and Regulation

Stages of biofilm formation are categorised as attachment, multiplication, maturation and dispersal (**Figure 5**). MSCRAMMS are important molecules in the initial phase of biofilm attachment, these allow the initial formation of biofilms on biotic surfaces by binding to proteins on the hosts cells, such as fibrinogen or fibronectin (Foster, 2019). Once attached, with adequate nutrients the adhered cells will begin to divide, these cells have little protection from the environment so a crucial step in biofilm is the intracellular adhesion between bacterial cells. MSCRAMMs which facilitate bacterial adhesion to host cells, also allow for the intracellular attachment of bacterial cells and therefore the multiplication of *S. aureus* in the initial stages of biofilm formation (Speziale et al., 2014). *S. aureus* also begin to upregulate the production

of extracellular polysaccharides, including capsular polysaccharides, to allow aggregation of cells (Riordan & Lee, 2004). Polysaccharide intercellular adhesins (PIA) are produced as part of the extracellular matrix; PIA is positively charged attracting the negatively charged cell wall of the bacteria, fixing cells together through electrostatic interactions (Otto, 2008).

S. aureus cells within the biofilm will undergo programmed cell death and lysis to allow for the release of DNA from the cytoplasm into the biofilm (Sadykov & Bayles, 2012). This lysis is regulated by a protein coded by *cidA* acting as a holin, a pore forming membrane protein, and an antiholin protein coded by *lrgA*. Both proteins are required for normal biofilm development (Mann et al., 2009). Extracellular DNA is present in the biofilm to provide structural integrity (Sugimoto *et al*., 2018), through electrostatic interactions between the eDNA molecules and cells (Dengler *et al*., 2015). As well as offering structural support, the release of DNA enables gene transfer to surrounding bacteria within the biofilm. eDNA also exhibits antimicrobial resistance activity on vancomycin through direct interaction with the antibiotic preventing the antimicrobial activity (Doroshenko *et al*., 2014).

The established biofilm matures into a 3D structure, often characterised by mushroom-like structures, known as microcolonies. The formation of these structures occurs during maturation. The formation of these microcolonies results in differential concentrations of nutrients and oxygen within the biofilm, inducing changes to metabolism throughout the biofilm allowing for increased resistance to changes in the environment or stressors (Gupta et al., 2016). Channels within the biofilm form to allow the flow of nutrients in the mature biofilm (Mann *et al*., 2009), PSM are thought to be key to the formation of these fluid channels (Periasamy *et al*., 2012).

Intracellular chemical signalling occurs within the biofilm, known as quorum sensing. In *S. aureus,* the *Agr* locus contains several genes for quorum sensing. This is known as the accessory gene regulator (Agr) system, which allows *S. aureus* to

sense and respond to bacterial cell density through changes to gene expression for virulence factors (Le & Otto, 2015). The final phase of biofilm development is dispersal, this is the release of bacteria back into the environment to colonise other surfaces. The Agr system is implicated in the dispersal of the biofilm. The accumulation of signalling molecules within the biofilm is detected by *S. aureus* within the biofilm though membrane receptors which induces the expression of virulence factors which breakdown the extracellular matrix of the biofilm through protease activity and PSM (Moormeier & Bayles, 2017; Periasamy et al., 2012).

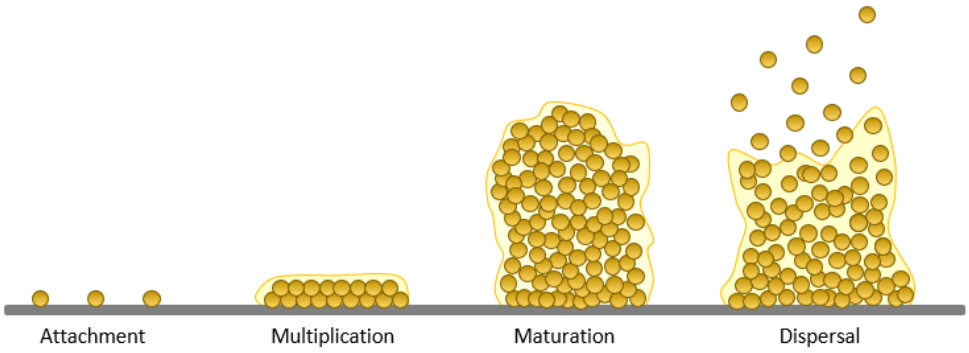

Figure 5: The development of Staphylococcus aureus biofilm over time. Attachment: bacteria reversibly attach to a surface and if conditions are suitable bacteria will multiply. Multiplication: bacteria reproduce and produce an extracellular matrix. Maturation: biofilm builds up to 3D microcolonies, fluid channels form within the extracellular matrix. Dispersal: bacteria are released back into the environment. Adapted from Muhammad et al (2020) Created in BioRender.

Within bacterial populations, including biofilms, not all cells are phenotypically identical, even if their genotype is clonal (Veening *et al*., 2008). This phenomenon is sometimes called population hedge betting, the production of non-identical daughter cells from replication leaving one daughter cell lacking the ability to grow making this cell tolerant of environmental stresses, or bistability, where cells in the same conditions may have high or low activity (Veening *et a*l., 2008). This results in a small population of inactive cells, or persister cells. Persister cells present a problem in

infection treatment, while not resistant to the effects of antibiotics, these cells do display tolerance to antibiotic treatment (Keren *et al*., 2004). These tolerant cells can go on to repopulate the infection site after treatment has ceased.

2.9 Microbial Persistence

2.9.1 Antibiotic tolerant populations

AT cells, or persister cells, were identified within 20 years of the discovery of penicillin, showing tolerance but not resistance to penicillin treatment (Lewis, 2007). AT cells are thought to be a protective state bacteria enter during times of stress and are hypothesised to occur in all bacteria (Fisher *et al.*, 2017). AT cells are genetically identical to the rest of the population, with phenotypical differences – a reduction or loss of metabolic activity without death. Due to the dormancy in these subpopulations, there is no protein synthesis, DNA synthesis, and cell wall synthesis; all processes which are targets for antibiotics, this lack in cell growth leads to tolerance of antibacterial agents (Lewis, 2007). Although this subpopulation make up a small percentage of the total population, (around 1 %), the ability to survive stressors (e.g. antibiotics), as well as the ability to resurrect in favourable conditions, AT cells are considered partially responsible for recurring infection (Kussell *et al.*, 2005). The mechanism for this recurrence of infection driven by AT populations is when the infection is treated with appropriate levels of antibiotics, killing active cells within the biofilm along with host immune response clearing pathogens, the dormant cells can withstand these lethal doses of antibiotics as well as evade the immune system of the host (Fisher *et al.*, 2017; Lewis, 2007). When treatment is halted, and conditions return to growth favourable conditions the dormant persister cells reactivate and repopulate the infection site (Fisher *et al*., 2017; Lewis, 2007). This results in the infection returning (**Figure 6**).

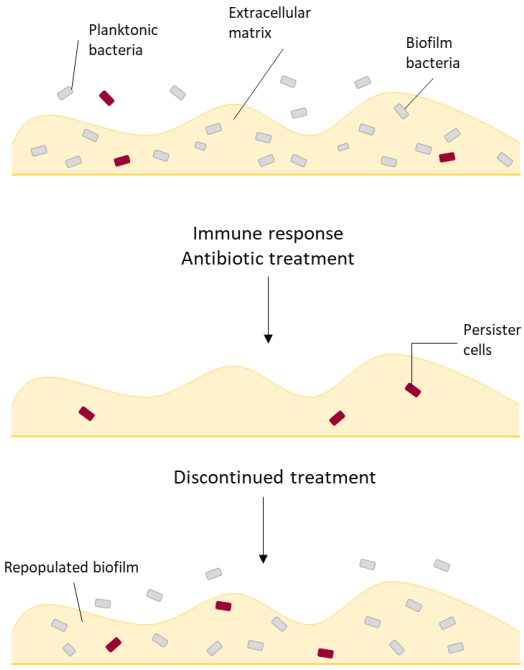

Figure 6: Repopulation of a biofilm via reactivation of antibiotic tolerant persister cells: Dormant cells in biofilm tolerate the activity of host immune cells and antimicrobials during treatment, reactivating once conditions return and repopulating the biofilm. Adapted from Lewis 2007 (Lewis, 2007)

2.9.2 Formation and resurrection

Screening has failed to identify a single gene which causes persistence, rather changes in persistence levels changes with some mutations (Lewis, 2007). For example, in *E. coli* the presence of a *hipA7* allele of *hipA*- which codes for the HipA toxin in the HipAB toxin/antitoxin (TA) system (Korch *et al*., 2003); results in a 1000-fold increase in persister cell levels in the population, HipA toxin inhibits bacterial cell growth causing dormancy, HipB is the antitoxin which inhibits the activity of HipA. The HipA7 mutation reduces the binding activity of HipB while still inhibiting cell growth (Feng *et al.*, 2014), this causes the increase in persister formation observed in this mutant. This finding resulted in the association of TA systems with persister formation. TA systems are gene pairs of a toxin and a corresponding antitoxin, the antitoxin is often plasmid a gene (Gelens *et al*., 2013). The toxins are proteins which target cellular processes vital for cell survival while the antitoxins may be proteins or RNA which prevent the activity of the toxin, either by preventing translation of the toxin protein or through binding to the toxin, neutralising its activity (Wang & Wood,

2011). When activated, the toxin from the TA system can interrupt crucial processes for cell survival, and it was understood that this causes dormancy in cells (Lewis, 2007). Deletion of single TA systems rarely decrease persister levels, indicating other pathways to dormancy are also relevant (Wang & Wood, 2011).

Other studies have linked the stress alarmone or 'magic spot' Guanosine tetraphosphate and pentaphosphate (p)ppGpp activation of TA systems to the formation of persister cells. These are second messenger molecules which regulate the stringent bacterial stress response which results in the downregulation of protein synthesis and upregulation of stress related genes to increase bacterial survival in response to environmental stressors (Boutte & Crosson, 2013). However, this paper was later retracted due to the identification of bacteriophage contamination in the *E. coli* strain used in the study potentially contributing to the observations made (Harms *et al*., 2017). The group have since been unable to replicate the findings of this study, instead finding that while ppGpp and Lon have an important role in persister formation (Harms *et al.*, 2017), Lon is an ATP-dependant stress protease, which degrade antitoxins, allowing toxins to induce dormancy (Ramisetty *et al.*, 2016).

In *S. aureus* during stress, ReIA/SpoT homolog proteins (RSH), which synthesize and hydrolyse ppGpp, are activated (Irving & Corrigan, 2018). When the stringent response is activated translation stalls allowing the bacteria to preserve energy and prioritise processes which aid survival. A model proposed by Wood and Song suggests the dimerization of inactive 70S ribosomes into persister 100S ribosomes in response to stress is a process crucial to persister formation (**Figure 7**) (Wood & Song, 2020). In this model the activation of ppGpp and cAMP inhibits ribosome activity through the activation of Ribosome-associated inhibitor A and dimerizes the 70S ribosome through ribosome modulation factor, which binds the ribosomes at the 30S subunit forming the 90S inactive ribosome. Finally ppGpp activates ribosome hibernation promoting factor to form the 100S ribosome which is associated with persistence (Wood & Song, 2020). In addition to translation stalling ppGpp is known to inhibit DNA primase, preventing DNA synthesis in *E. coli* (Maciag *et al*., 2010).

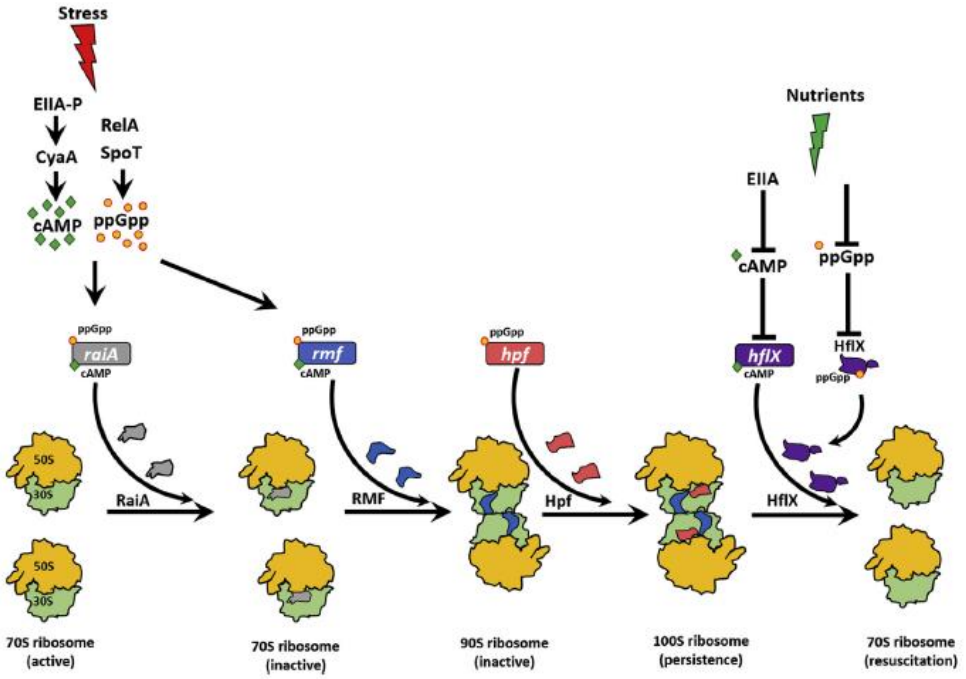

Figure 7: Dimerization of 70S ribosomes to persister 100S ribosomes in response to stress. Stress activates RSH proteins, activating ppGpp and cAMP. This activates raiA and rmf which inactivates 70S ribosomes and dimerizing 70S ribosomes at the 30S subunit. Hpf converts the inactive 90S dimerized ribosomes to 100S persistence ribosomes. Nutrients prevent the activity of ppGpp and cAMP causing resuscitation of persister ribosomes to active 70S ribosome. Taken from Wood & Song, 2020 (Wood & Song, 2020)

Conlon *et al.* (Conlon et al., 2016) found that *S. aureus* with mutations in ppGpp pathway proteins still produced persister cells which displayed tolerance to antibiotics, suggesting that the stringent response was not the sole mediator of persistence in *S. aureus* (Conlon et al., 2016). Instead, they suggested low levels of ATP were the cause of persistence in *S. aureus* due to the reduction of antibiotic targets in response to a drop in ATP. Zalis *et al.* (Zalis et al., 2019) also indicated ATP levels were correlated with persister levels, this study found disruption of TCA cycle through the deletion of genes coding for citrate synthase, α-Ketoglutarate dehydrogenase, succinyl-coenzyme A synthetase, and fumarate hydratase, all enzymes involved in TCA cycle, resulted in increased persistence (Zalis *et al*., 2019). The formation of persister cells is still a topic without a clear mechanism, with the potential for overlapping systems. Similarly, the mechanisms of resurrection of

persister cells are also unclear and treatment options are limited. However, reawakening these dormant cells could lead to more effective treatment and prevention of chronic and recurring infections by increasing antibiotic targets within the AT cells.

2.10 Detection and Response to *S. aureus* Infection

During S. *aureus*-instigated and other infections, the immune system activates in an attempt to clear the infection. Several processes are activated in the initial stages of infection. Keratinocytes are immune competent cells found in the upper layers of the skin. Keratinocytes express pattern recognition receptors (PRR), specialised receptors for the detection of microbes via pathogen associated molecular pattern molecules (PAMP). Keratinocytes express several PRRs, including Toll-like receptors (TLR) (Pivarcsi *et al*., 2003). In *S. aureus* infection, TLR-2 is heavily implicated in the detection of infection by *S. aureus*. Lack of TLR-2 receptors severely impacts the survival of mice infected with *S. aureus* (Takeuchi *et al*., 2000). TLR-2 detects peptidoglycan and PSM produced by *S. aureus* (Hanzelmann *et al.*, 2016; Takeuchi *et al*., 1999). Activation of TLR2 induces the production of cytokines. Several cytokines are released by cells during infection, modulating inflammation and immune response, including interleukins (IL), and Tumour Necrotic Factor-α (TNF-α) (Lebre *et al.*, 2007). Ngo *et al*. (2022) reported an increase in IL-6 and IL-8 expression when *S. aureus* was internalised by keratinocytes. IL-8 is a proinflammatory cytokine, which recruits neutrophils to the site of infection as part of the innate immune response (Pace *et al.*, 1999). IL-6 is also a proinflammatory cytokine which is released promptly after injury and infection (Gebhard *et al.*, 2000; Yao *et al.*, 1997). IL-6 also works to support innate immune response, and influences monocyte differentiation to macrophages (Chomarat *et al.*, 2000).

Antimicrobial peptides (AMPs) are produced by many cells throughout the body in an effort to combat infection. Cytokines such as IL-6 enhance the production of AMPs (Ching *et al.*, 2018; Erdag & Morgan, 2002). Keratinocytes produce human

cathelicidin (LL-37) and defensins, both AMPs are found to have bactericidal effects against *S. aureus,* as well as acting to influence migration of immune cells (Kang *et al*., 2019; Midorikawa *et al.*, 2003). Defensins and CAP37 (the protein origin of LL-37), have been shown to be chemoattractant for T-cells (Chertov *et al.*, 1996). CAP37 is also a chemoattractant for neutrophils (Chertov *et al.*, 1997), while defensins are implicated in the migration of macrophages (Soruri *et al.*, 2007).

2.11 Wound Infection Model

Interactions between pathogens and host cells must be studied to understand the mechanisms of infection and the efficacy of treatments. Several models are used in infection research including 2D monolayer models, 3D models and the use of whole systems in *in vivo* studies. These models each present benefits and limitations. The use of monolayers to investigate infection has been standard in *in vitro* modelling of infections due to the simplicity and high reproducibility of these models, however these models lack physiological features, such as the structure of the skin, extracellular matrix interaction and gradients of factors for growth (Kapałczyńska *et al*., 2018). Animal models are also often used in infection models to understand infection in complex systems, however animal models are subject to ethical considerations and are constrained by the differences in skin structure and immune response between humans and animals, meaning findings in animal models may not translate to humans (Salgado *et al*., 2017; Uhm *et al.*, 2023). The use of 3D wound models to investigate infection allows the use of human cells in a more physiologically relevant environment to understand the potential treatment of infections. *In vitro* 3D skin models allow for control of the cells within the skin as well as sterility and adaptation to fit research questions, for example the use of primary cells, cell lines, or cells with different gene expressions (Rademacher *et al.*, 2018). The skin model used in this study was a tissue-engineered skin model (TESM) developed by Shepherd *et al*. (Shepherd *et al.*, 2009), using decellularised dermis seeded with keratinocytes and fibroblasts and grown at air-liquid-interface.

While 3D wound models provide several benefits in research there are limitations to the use of these models. Human skin is a complex organ with several cell types such as keratinocytes, fibroblasts, nerve cells and immune cells, as well as the presence of secretions such as sebum and sweat (Pfisterer et al., 2021; Quaresma, 2019). Current cultured 3D skin models do not contain all the elements that would be seen in the normal skin environment. The TESM used in this study lacks immune cells, sebum and sweat all of which contribute to the prevention and eradication of infection (Makrantonaki et al., 2011; E. Wang et al., 2016). While the use of a 3D model allows for control and adaptability in investigations, it must also be considered that these lack the complexity seen in whole systems and findings may not translate into clinical settings.

2.12 Ultrasound

2.12.1 Frequency and Intensity

Ultrasound (US) is sound with a frequency greater than 20 kHz. It has a number of industrial and clinical applications based on the frequency. The frequency of US is defined by the number of waves which pass a given point during per second (Abu-Zidan *et al*., 2011). Low frequency US (20 kHz – 200 kHz) is often used in industrial settings with some clinical treatments, whereas higher frequencies (1 MHz – 15 MHz) are used in therapy and clinical imaging (Mason, 2011). Frequency and wavelength, the distance a wave travels, are inversely correlated, where high frequency US has shorter wavelength than low frequency (Powles *et al*., 2018). In US imaging, the area imaged determines what wavelength and therefore frequency used, short wavelengths, generated at 5-10 MHz, are unable to penetrate tissues deeply while longer wavelengths, generated at 2-5 MHz, have greater penetration but lower resolution images (Powles *et al*., 2018). US intensity is measured by power applied to an area. High-intensity US is often used to clean surfaces (Gallo *et al*., 2018). Intensities >10 W/cm^2 US can detrimentally affect prokaryotic and eukaryotic cell walls, resulting in cell lysis. High-intensity focused ultrasound can be used to eliminate tumours through extreme heating of tissue (Izadifar *et al*., 2020). The ability

of high-intensity US to clean surfaces and damage cells and tissues is due to inertial cavitation. Cavitation is the expansion and contraction of bubbles within a liquid. Inertial cavitation is the unstable oscillation of these bubbles, resulting in unstable growth in diameter before the sudden collapse of the bubble (Fabiilli *et al*., 2009). The bubble collapses with high energy, producing heat, shockwaves, shear force and free radicals (Fabiilli *et al*., 2009; Shanei & Sazgarnia, 2019). Low-intensity US (<2 W/cm^2), on the other hand, results in stable cavitation where bubbles in liquid will expand and contract at a stable rate allowing the bubble to stay intact (Izadifar *et al*., 2017) (**Figure 8**). The waves of US may be generated continuously or pulsed, continuous US is known to cause thermal effects, while pulsed ultrasound is non-thermal (Fisher *et al.*, 2003). It is important to consider both the intensity and the generation of the waves when proposing the use of therapeutic US, as these can impact the effects on tissues.

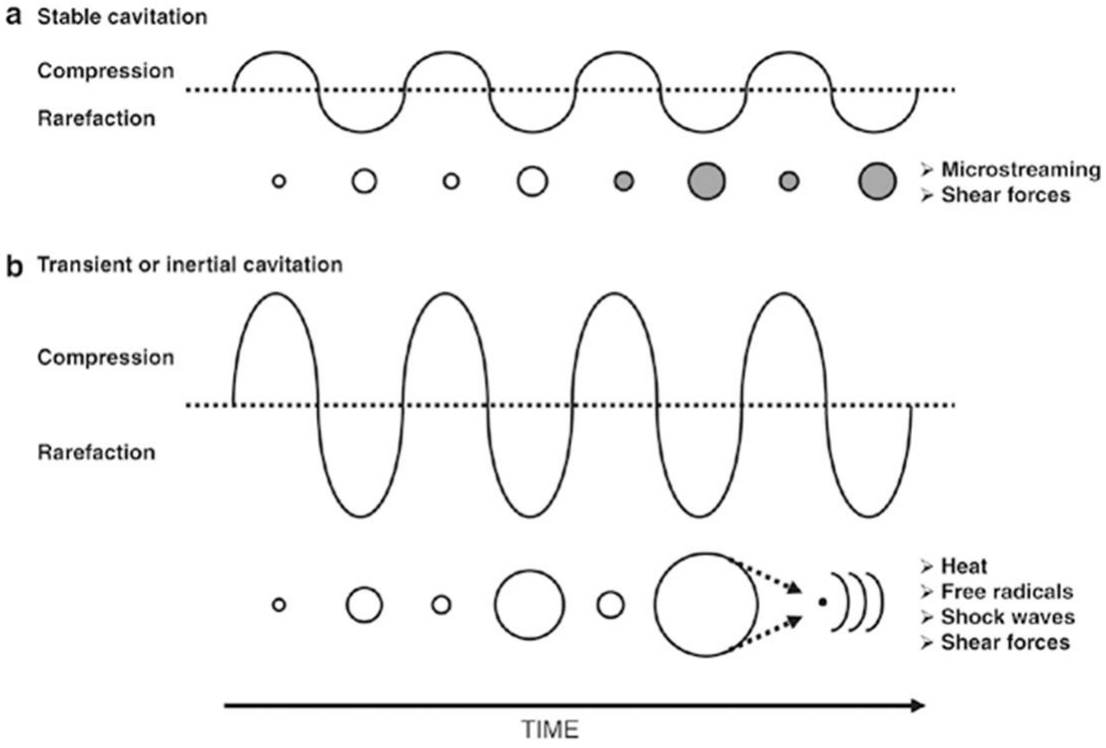

Figure 8: Ultrasound intensities: a) low intensity ultrasound results in stable cavitation, unidirectional movement of fluids and force. B) high intensity ultrasound results in high pressures causing collapse of bubbles which generates heat, shockwaves, free radicals. Taken from Newman & Bettinger 2007(Newman & Bettinger, 2007)

2.12.2 Therapeutic Applications

Low-intensity pulsed ultrasound (LIPUS) is currently used in fracture clinics to assist fracture healing (Rutten *et al*., 2008). Several mechanisms have been suggested for the enhanced fracture healing, including stimulation of prostaglandins, mediation of cell differentiation (Della Rocca, 2009), and enhanced angiogenesis (Erdogan & Esen, 2009). Production of nitric oxide (NO) in response to US treatment is also thought to be crucial in the mechanisms of bone healing (Diwan *et al*., 2000; Sugita *et al*., 2008). Evidence also indicates that soft tissue wound healing can be accelerated with the use of LIPUS. Roper *et al.* (Roper *et al.,* 2015) found the application of US to wounds in murine models increased wound healing times. The application of LIPUS increased cell proliferation in human foreskin cells *in vitro* via the activation of the ERK pathway (Zhou *et al*., 2004). In addition to stimulating wound healing through cellular proliferation, US can be used to debride chronic wounds, promoting healing. MIST therapy is a system to provide combination treatment of saline solution and low intensity US, traditionally used in wound irrigation, (Ramundo & Gray, 2008). When used as MIST therapy, US has been evidenced to heal 69% of wounds significantly quicker than patients who historically did not receive MIST treatment (Ennis *et al*., 2006).

2.12.3 Ultrasound and Microbes

Interactions between microbes and US have previously been studied to varying degrees. Sonication is often used to disrupt biofilms and kill bacteria at high intensities, and biofilm prevention by US has been reported (Bharatula *et al.*, 2020; Iqbal *et al.*, 2013; Wang *et al*., 2017). Evidence presented by Koibuchi *et al*. (2021) suggested that low-intensity US treatment of *S. epidermidis* prior to incubation inhibits short-term biofilm formation. The use of US on medical indwelling devices has also shown positive results in the prevention of biofilm formation (Hazan *et al*., 2006; Wang *et al.*, 2017). However, Pitt & Ross (Pitt & Ross, 2003) studied the

effects of US on both planktonic and biofilm associated bacteria and found low-intensity US increased growth in *Pseudomonas aeruginosa, E. coli* and *S. epidermidis*. In biofilms the bacteria remained attached to a surface, with no indication that US treatment caused the removal of bacteria from the rods used as support for growth. No mechanism for this increased growth was elucidated however the authors speculated that it may be due to increased nutrient flow (Pitt & Ross, 2003). Bochu *et al*. (2003) found the increased permeability of yeast cells to Ca^{2+} during US treatment (intensity of 2 W/cm^2) was responsible for the increased proliferation of *Saccharomyces*, however, *S. cerevisiae* is eukaryotic and therefore the composition of the cell wall is different to prokaryotic cells, and these findings may not translate into bacteria. Still, there is evidence that US results in cell permeability in bacteria; Li *et al. (J. Li et al., 2018)* suggested cell permeability caused by US treatment led to the death of *E. coli* through leakage of cellular content, the intensities of US used in this study were much greater than the US used in the study by Pitt & Ross (Pitt & Ross, 2003) and Bochu *et al. (Bochu et al., 2003)*. Therefore, high intensity US may cause an increase in cell wall permeability which the bacteria cannot survive, while low intensity US may cause a level of permeability which is beneficial to survival and proliferation.

When used in combination US and antibiotics have been shown to have synergistic activity in planktonic bacteria. Pitt *et al. (Pitt et al., 1994)* established that the use of a combination of US and gentamicin increased the killing of *P. aeruginosa* and *E. coli* in comparison to gentamicin only treatment. The effects on *S. epidermidis* and *S. aureus* were also studied but there was no significant difference between samples treated with US and samples receiving gentamicin only. The mechanisms were not elucidated but physiological differences between Gram-positive and Gram-negative bacteria cell wall may be the underlying reason for the differences observed (DeLongchamp *et al*., 2011). Selan *et al. (Selan et al., 2019)* treated *S. aureus* with US in the presence of ampicillin and found samples treated with US had a greater killing effect than the sample with only ampicillin (Selan et al., 2019), showing US can enhance the activity of antibiotics against Gram-positive bacteria. There is also growing evidence to support the use of US in combination with microbubbles to enhance the activity of antibiotics, this is thought to be due to the increase in

cavitation at lower US intensities. Zhu *et al. (Zhu et al., 2014)* demonstrated this using *E. coli* treated with gentamicin and US as well as gentamicin and microbubble mediated US. Cell death was higher in the bacteria exposed to gentamicin and microbubble mediated US. The use of microbubbles in Gram-positive bacteria has also been demonstrated in *S. epidermidis*, when treated with vancomycin and microbubble US there was increased antimicrobial activity when compared against US and vancomycin without the presence of microbubbles (Dong *et al*., 2018).

The use of clinically relevant LIPUS may be a viable adjunctive to antibiotic therapy to improve antibiotic stewardship of chronic SSTI, which commonly require repeated and extended antibiotic therapy, by enhanced antibiotic sensitivity, reducing antibiotic concentrations required to successfully treat infections and reducing risk of more invasive treatments and complications. This study aims to investigate LIPUS as an adjunctive therapy.

2.13 Hypothesis, Aims and objectives for the project.

Hypothesis: LIPUS will increase *S. aureus* biofilm susceptibility to antibiotic treatment.

Aims:

- To investigate the effect of clinically relevant LIPUS (30 mW/cm^2, 150kHz) on growth and metabolic activity of *S. aureus* bacteria, within a biofilm and antibiotic tolerant populations, and response to antibiotics.
- To investigate the effects of LIPUS (30 mW/cm^2, 150kHz) on TESM as a potential adjunct treatment to antibiotics for infected wounds

Objectives

- Measure growth and metabolic activity in planktonic and biofilm *S. aureus* with and without varying LIPUS treatments
- Measure sensitivity of S aureus (biofilms and antibiotic tolerant populations) to antibiotics with and without use of varying LIPUS treatments
- Measure permeability and structural changes within the *S. aureus* biofilms
- Measure skin model cells metabolic activity, proliferation and migration, and permeability with and without LIPUS treatment
- Measure antibiotic sensitivity in *S. aureus* within a wound infection model.

The LIPUS device used in this study is commercially available and currently used in clinical settings therefore the intensity and frequency of the LIPUS used throughout this study remained equal to the intensity and frequency used in the clinical setting to understand if this commercially available device could be repurposed in skin infection treatment.

3 Materials and Methods

3.1 Materials

3.1.1 Bacteria, Mammalian cells and Virus

Table 3: Bacterial species

	Supplier
Staphylococcus aureus SH1000 (Horsburgh *et al.*, 2002)	Dr J. Shepherd (University of Sheffield, Sheffield, UK)
Staphylococcus aureus S235 (Doroshenko *et al.*, 2018)	Dr J. Shepherd (University of Sheffield, Sheffield, UK)
Staphylococcus aureus RN4220 LacZ (O'Neill et al., 2004)	Professor Alex O'Neill (University of Leeds, Leeds, UK)

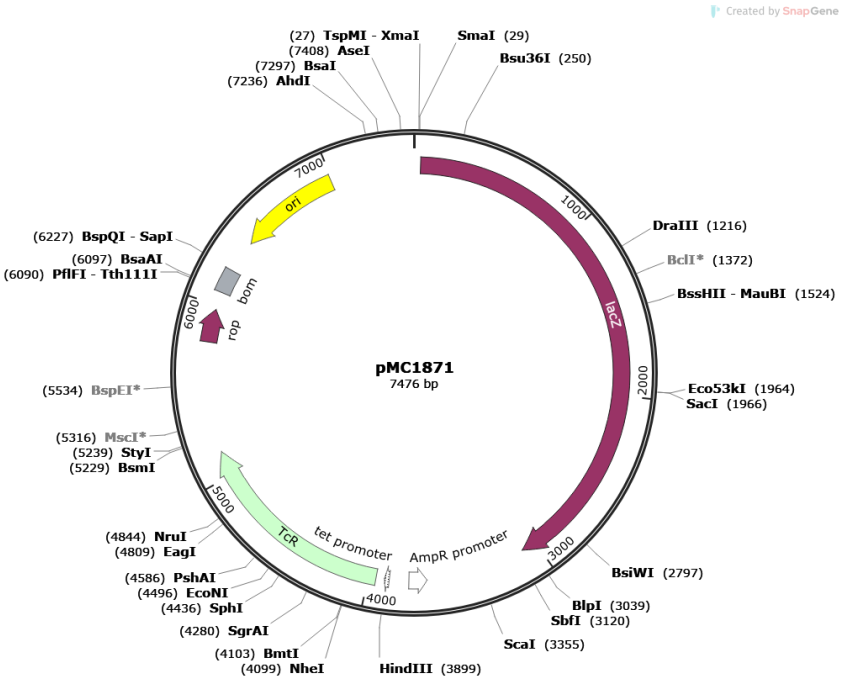

***Figure 9: Plasmid map of pMC1871* containing *lacZ gene* used in *S. aureus* RN4220 (O'Neill *et al*., 2004).**

Table 4: Mammalian cells

	Supplier
HaCaT (human dermal keratinocytes)	Thermo Fisher Scientific, Altrincham, UK
Adult Human Dermal Fibroblast	Thermo Fisher Scientific, Altrincham, UK

Table 5: Bacteriophage

	Supplier
Φ11	Professor Simon Foster (University of Sheffield, Sheffield, UK)

3.1.2 Growth Media

Table 6: Bacterial growth media

	Recipe	**Supplier**
Brain Heart Infusion agar	Supplied complete	Oxoid, Basingstoke, UK
Brain Heart Infusion broth	Supplied complete	Oxoid
LK Broth	10 % w/v Tryptone 5 % w/v Yeast Extract 7 % w/v Potassium Chloride	
Tryptic soy agar	Supplied complete	Oxoid
Tryptic Soy Broth	Supplied complete	Oxoid

Table 7: Mammalian Growth Media

	Recipe	Supplier
3D Model Media	KGM (recipe below) 2 ng/ml TGf-α	 BioLegend
Fibroblast Medium	Dulbecco's Modified Eagle Medium (DMEM) 10 % Foetal Bovine Serum 2 mM L-Glutamine 5ml Penicillin/Streptamycin (10,000 U/ml) 5ml Amphotericin (250 µg/ml)	Sigma-Aldrich, Gillingham, UK Thermo Fisher Scientific, Altrincham, UK Sigma-Aldrich, Gillingham, UK Sigma-Aldrich, Gillingham, UK Sigma-Aldrich, Gillingham, UK
Keratinocyte Growth Medium (KGM)	DMEM Ham's F-12 Nutrient Mixture 10 % Foetal Bovine Serum 5 ml Penicillin/Streptamycin (10,000 U/ml) 2 mM L-Glutamine 0.18 mM Adenine 0.5 µg/ml Hydrocortisone 0.5 ng/ml Insulin 10 ng/ml EGF 5 ml Amphotericin (250 µg/ml) 1 ng/ml TGF-α	Sigma-Aldrich, Gillingham, UK Sigma-Aldrich, Gillingham, UK Thermo Fisher Scientific, Altrincham, UK Sigma-Aldrich, Gillingham, UK Sigma-Aldrich, Gillingham, UK Sigma-Aldrich, Gillingham, UK Sigma-Aldrich, Gillingham, UK Sigma-Aldrich, Gillingham, UK Sigma-Aldrich, Gillingham, UK BioLegend

3.1.3 Other Materials

Table 8: Chemicals

	Supplier
4% Paraformaldehyde	Thermo Fisher Scientific, Altrincham, UK
4-Methylumbelliferyl β-D-galactopyranoside	Sigma-Aldrich, Gillingham, UK
Ampicillin	Sigma-Aldrich, Gillingham, UK
BacLight LIVE/DEAD stain	Thermo Fisher Scientific, Altrincham, UK
BacTiter-Glo microbial cell viability assay	Promega, Southampton, UK
Calcium chloride	Sigma-Aldrich, Gillingham, UK
Chloramphenicol	Sigma-Aldrich, Gillingham, UK
Ciprofloxacin	Sigma-Aldrich, Gillingham, UK
Donor skin	ETS-Biolife, The Netherlands
DPX mountant	Sigma-Aldrich, Gillingham, UK
Ethanol	Sigma-Aldrich, Gillingham, UK
Extracellular oxygen consumption assay	Abcam, Cambridge, UK
Fibrinogen	Sigma-Aldrich, Gillingham, UK
Fibronectin	Sigma-Aldrich, Gillingham, UK
FilmTracer™ SYPRO™ Ruby biofilm matrix stain	Thermo Fisher Scientific, Altrincham, UK
FITC-Dextran 250kDa	Sigma-Aldrich, Gillingham, UK
FITC-Dextran 4kDa	Sigma-Aldrich, Gillingham, UK
FITC-Dextran 70kDa	Sigma-Aldrich, Gillingham, UK

Foetal bovine serum	Thermo Fisher Scientific, Altrincham, UK
Gentamicin	Sigma-Aldrich, Gillingham, UK,
Glycerol	Sigma-Aldrich, Gillingham, UK,
IL-6 ELISA kit	Sigma-Aldrich, Gillingham, UK
Mitomycin C	Sigma-Aldrich, Gillingham, UK
Lactic acid	Thermo Fisher Scientific, Altrincham, UK
Lactoferrin	Sigma-Aldrich, Gillingham, UK
Lysostaphin	Sigma-Aldrich, Gillingham, UK
Lysozyme	Sigma-Aldrich, Gillingham, UK
Peptone	Sigma-Aldrich, Gillingham, UK
Rat tail collagen	Sigma-Aldrich, Gillingham, UK
RNA Protect bacteria reagent	Qiagen, Manchester, UK
RNase Free DNase kit	Qiagen, Manchester, UK
RNeasy kit	Qiagen, Manchester, UK
Sodium citrate	Sigma-Aldrich, Gillingham, UK
Ultrasound gel	Henleys Medical Supplies, Welwyn Garden City, UK
Vancomycin	Sigma-Aldrich, Gillingham, UK
VECTASHIELD HardSet Antifade mounting medium with DAPI	2BScientific, Kidlington, UK
Wheat Germ Agglutinin, Alexa Fluor™ 488 conjugate	Thermo Fisher Scientific, Altrincham, UK
X-gal (5-Bromo-4-Chloro-3-Indolyl β-D-	Sigma-Aldrich, Gillingham, UK

Galactopyranoside)	

Table 9: Equipment

	Supplier
µ-Dish 35 mm, high Glass bottom	Thistle Scientific, Rugby, UK
6-well plates	Thermo Fisher Scientific, Altrincham, UK
6-well deep well plates	Thermo Fisher Scientific, Altrincham, UK
12-well plates	Thermo Fisher Scientific, Altrincham, UK
96-well plates	Thermo Fisher Scientific, Altrincham, UK
Cell culture 0.4µm pore insert (12- & 6-well)	Thermo Fisher Scientific, Altrincham, UK
Swann-Morton disposable scalpel	SLS, Nottingham, UK
Exogen LIPUS device	Smith and Nephew, Watford, UK
Gosselin square petri dish 120mm	Thermo Fisher Scientific, Altrincham, UK
Tecan Infinite 200 plate reader	Tecan, Reading, UK
Tecan Sunrise plate reader	Tecan, Reading, UK
Epredia Citadel 2000 tissue processor	Thermo Fisher Scientific, Altrincham, UK
Olympus microscope	Olympus Life Sciences, Southend-on-Sea, UK
Leica ST 4040 linear stainer	Leica, Milton Keynes, UK

Leica Histocore Arcadia H tissue embedder	Leica, Milton Keynes, UK
Lecia RM2235 microtome	Leica, Milton Keynes, UK
Leica Thunder fluorescent microscope	Leica, Milton Keynes, UK
Spinning disk confocal microscope	Nikon, Surrey, UK
Epredia Superfrost microscope slides	Thermo Fisher Scientific, Altrincham, UK

3.1.4 Buffers

Table 10: Buffers

	Recipe	**Supplier**
Phage buffer	1 mM $MgSO_4$	Sigma-Aldrich, Gillingham, UK
	4 mM Calcium chloride	Sigma-Aldrich, Gillingham, UK
	50 mM Tris-HCl (pH 7.8)	Sigma-Aldrich, Gillingham, UK
	0.6 % Sodium chloride	Sigma-Aldrich, Gillingham, UK
	0.1 % Gelatin	Sigma-Aldrich, Gillingham, UK
Phosphate buffered saline	Supplied complete	Sigma-Aldrich, Gillingham, UK

3.2 Methods

3.2.1 Biofilm

3.2.1.1 Bacterial culture

3.2.1.1.1 Maintenance of S. aureus

S. aureus SH1000 were grown from -80 ^{o}C glycerol stocks overnight in a static incubator at 37 ^{o}C on Brain Heart Infusion (BHI) agar and stored at 4 ^{o}C for 4 weeks before subculture onto fresh agar to maintain stocks. Overnight cultures of *S. aureus* S235 were grown in BHI broth in a shaking incubator at 37 ^{o}C, 150 rpm. *S. aureus* containing *lacZ* gene (RN4220 *LacZ)* were grown on Brain Heart Infusion agar containing 10 µg/ml chloramphenicol and broth for this strain was supplemented with 20 µg/ml chloramphenicol.

3.2.1.1.2 Biofilm Growth

Overnight cultures of *S. aureus* SH1000 were diluted 1:100 in 3 ml BHI broth in 6-well plates or 6-well plate inserts, then incubated in a humid environment for 1-, 2-, 5-, and 7-days at 37 ^{o}C in a static incubator. Media were replenished every 2 days throughout the incubation period and humidity was visually monitored throughout the growth period. Spent media was discarded and fresh media added to the wells at the beginning of each experiment.

3.2.1.2 Determination of minimum inhibitory concentration (MIC)

Stock solutions (2X) of gentamicin 128 µg/ml, ciprofloxacin 128 µg/ml, and vancomycin 128 µg/ml in sterile water were prepared. 100 µl BHI broth was added to each well of a 96-well plate, 100 µl of each 2X stock solution of antibiotic was added to the first well with a concentration of 128 µl/ml before serially diluting to a final concentration of 0.031 µg/ml. *S. aureus* SH1000 bacterial suspension (OD_{600} 0.05) was added to each well and plates incubated at 37 ^{o}C overnight. After the incubation period plates were removed from the incubator and light absorbance at OD600nm was measured on a Tecan plate reader to measure growth (the more bacterial growth, the higher the turbidity and absorbance read). Sterile broth was used as a negative control and bacterial suspension without the presence of antibiotics was used as a growth control. Gentamicin and vancomycin were used in antibiotic sensitivity experiments with LIPUS treatment. Ciprofloxacin was used to induce

antibiotic stress persistence to isolate antibiotic tolerant (AT) populations in further experiments.

3.2.1.3 Ultrasonic treatment

An EXOGEN LIPUS machine (Smith & Nephew) was used to deliver pulsed ultrasound at 1.5 MHz, with an intensity of 30mW/cm2. An adaptor allows 6-well plates to sit on transducers coated with US gel (**Figure 10**). Initial bacterial growth, antibiotic sensitivity and permeability assays were treated with LIPUS for 1-, 2- and 3-hours. Further LIPUS treatment experiments were treated for 2- hours.

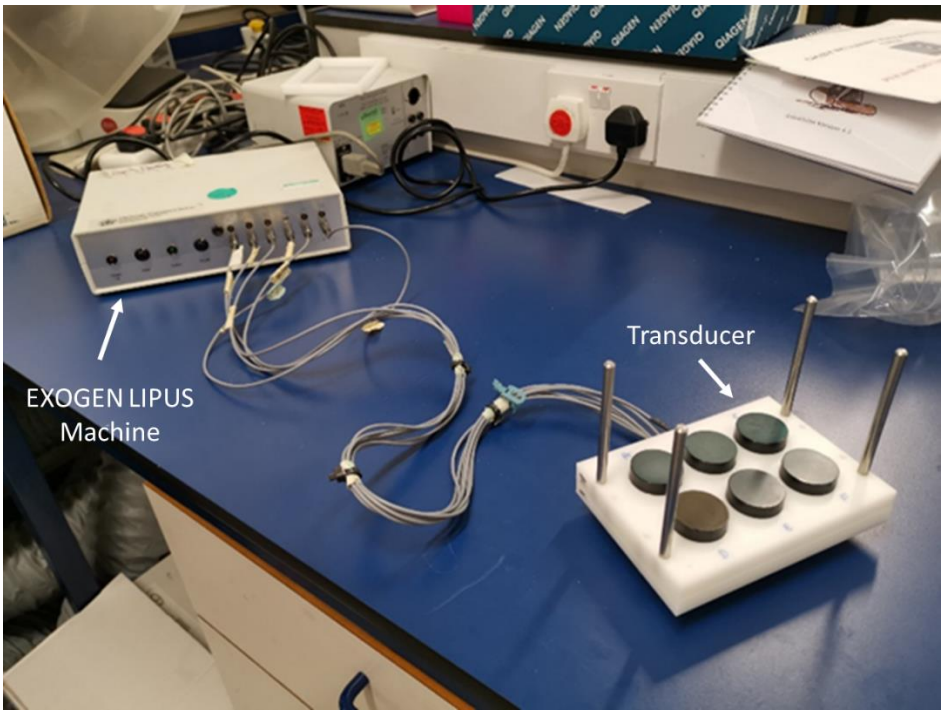

Figure 10: EXOGEN low intensity pulsed US machine used to deliver US to bacteria and mammalian cells in 6-well plates. Each well sits on a transducer covered with US gel.

3.2.1.4 Bacterial Growth with LIPUS

3.2.1.4.1 Colony-Forming Units

Established biofilms were grown for 1-, 3-, 5-, and 7-days as described above (3.2.1.1.2) in 6-well plates. Spent media was discarded and fresh media was added

immediately prior to LIPUS treatment. Biofilms were treated with LIPUS for 1-, 2-, and 3-hours and incubated for a further 24-hours. Media were removed and plated on BHI agar using Miles-Misra to assess biofilm disruption, while the biofilm was manually disrupted using a pipette and plated using Miles-Misra to assess growth changes. Colonies were counted and CFU/ml were calculated.

3.2.1.4.2 Crystal Violet Staining

Established biofilms were grown for 1-, 3-, 5-, and 7-days as described (3.2.1.1.2) above in 6-well inserts. Biofilms were treated with LIPUS for 2-hours and incubated for 24-hours before media was removed, and 0.1 % crystal violet was added to each insert for 30 minutes. Crystal violet was removed, and inserts were allowed to dry before images were taken for analysis. Images were analysed using ImageJ.

3.2.1.5 Antibiotic sensitivity

Biofilms were grown as described above, for 1-, 3-, 5-, and 7-days (3.2.1.1.2) Spent media were removed and BHI supplemented with 1 mg/ml gentamicin or 2 mg/ml vancomycin was added to the biofilms either pre or post LIPUS treatment. Biofilms were treated with LIPUS for 1-, 2-, and 3-hours, described in **Error! Reference source not found.**, then incubated for 24-hours in the presence of the antibiotic of interest. Biofilms were washed with PBS twice before being manually disrupted in 3 ml PBS with a pipette and 200 µl was plated using Miles-Misra technique on BHI agar plates. Colonies were counted and colony-forming units per ml (CFU/ml) were calculated.

3.2.1.6 BacTiter-Glo ATP assay

S. aureus SH1000 biofilms grown for 1-, 3-, 5-, and 7-days (3.2.1.1.2) were treated with LIPUS (3.2.1.3). Media were removed from the biofilm and the biofilms

mechanically disrupted with a pipette. BacTiter-Glo kit was prepared as manufacturer's instructions. 100 µl of bacterial cell suspension from the biofilm and the media removed from the biofilm were added to a black 96-well plate from both LIPUS treated and untreated samples. Sterile PBS was used as a control for background luminescence. Samples were allowed to sit at room temperature for 15 minutes to equilibrate temperature. 100 µl prepared BacTiter-Glo was added to each well and allowed to mix. The plate was incubated for 5 minutes at room temperature before luminescence was recorded in a Tecan plate reader.

3.2.1.7 Biofilm Permeability Assay

S. aureus SH1000 biofilms were grown as described above 3.2.1.1.2) in 6-well plate inserts for 1-, 2-, 5-, and 7-days at 37 ^{o}C in a static incubator. Spent media were removed, then BHI supplemented with 1 mg/ml 4 kDa, 70 kDa or 250 kDa FITC-Dextran was added into the well-insert and BHI without FITC-Dextran was added to the well to surround the well-insert. The biofilms were treated with LIPUS for up to 3-hours. 200 µl BHI was removed from the well insert at 1-hour intervals and the wells were replenished with 200 µl BHI. The fluorescence of the removed BHI was measured in a Tecan Plate Reader with an excitation of 495nm and emission of 517nm. The changes in fluorescence were compared against the fluorescence of BHI removed from wells of biofilms without LIPUS treatment.

3.2.1.8 Bacterial cell membrane permeability

3.2.1.8.1 Transduction of LacZ using Φ11 Phage

Staphylococcus aureus RN4220 construct containing *lacZ* were used as the donor strain. 150 µl of overnight culture of *S. aureus* RN4220 containing the *lacZ* plasmid were added to 1:1 mixture of TSB growth media and phage buffer, 100 µl phage lysate was added and incubated at 25 ^{o}C overnight until clear. Lysate was then filtered using syringe filters with 0.22 µm pores to sterilise.

Staphylococcus aureus SH1000 was the recipient strain. 50 ml LK broth was inoculated with *S aureus* SH1000 and incubated overnight at 37 ^{o}C 250 rpm. Overnight cultures were centrifuged at 5000 rpm for 10 minutes and resuspended in 3 ml LK broth. Transduction broths were prepared using LK broth supplemented with 10 mM calcium chloride. The broth was inoculated with 500 µl recipient strain and 500 µl phage lysate. A control of transduction broth inoculated with recipient strain without the phage lysate was prepared. These were incubated for 25 minutes in a static incubator at 37 ^{o}C before being incubated at 250 rpm 37 ^{o}C for a further 10 minutes. Ice cold sodium nitrate was added to the mixture to give a final concentration of 10 mM and incubated on ice for 5 minutes. The mixture was then centrifuged at 5000 rpm for 10 minutes at 4 ^{o}C. The supernatant was removed, and pellet was resuspended in ice cold 20 mM sodium nitrate and incubated on ice for 45 minutes before 100 µl was spread on 0.05 % sodium citrate LK agar plates containing 10 µg/ml chloramphenicol.

Single colonies grown on the ciprofloxacin plate overnight at 37 ^{o}C were selected and streaked onto TSB broth containing 100 µg/ml X-gal to confirm the presence of β-galactosidase activity, blue colonies from the X-gal plate were used in further experiments due to the presence of β-galactosidase activity.

3.2.1.8.2 B-Galactosidase Assay

An overnight culture of *S. aureus,* containing a *LacZ* plasmid, was diluted to OD_{600} 1 and treated with LIPUS as described above for 2 hours. 200 µl BHI was removed from each well and spun in a centrifuge at 5000 rpm for 5 minutes and the supernatant was removed and added to a black 96-well plate. 25 µl of 1mg/ml 4-Methylumbelliferyl β-D-galactopyranoside (4-MUG) was added to each well and incubated in the dark at room temperature for 90-minutes. After incubation fluorescence was read in the Tecan Plate Reader with excitation 365nm and emission 445nm. LIPUS samples were compared against untreated samples.

3.2.1.8.3 Propidium Iodide Assay

An overnight culture of *S. aureus* SH1000 was diluted to OD_{600}=1. 2 ml were added to 6-well plates and stained using a BacLight LIVE/DEAD kit according to manufacturer instructions. Equal parts Syto60 and propidium iodide (PI) were combined and 6 µl was added to each well. The bacterial suspension was then treated with LIPUS for 2 hours and 20 µl was immediately removed from each well and placed on a microscope slide and imaged using a Leica Fluorescence microscope. 100 bacterial cells from each slide were imaged and percentage of PI-stained cells was calculated, and comparisons were made between the samples which received LIPUS treatment and samples without LIPUS treatment.

3.2.1.9 Biofilm structure

Biofilms were grown in glass-bottom µ-dish for 1- and 7-days before being treated with LIPUS for 2-hours. Biofilms were then fixed with cold ethanol for 30 minutes then washed with PBS 2x. A stain solution of PBS and 5 µg/ml WGA-AlexaFluor-488 was prepared and the biofilm was covered with 300 µl stain solution then incubated for 10 minutes at room temperature in the dark. The stain solution containing WGA-AlexaFluor-488 was removed and biofilm was washed 3x with PBS to remove excess staining. 300 µl FilmTracer Sypro Ruby Biofilm Matrix Stain was added to the biofilm and incubated for a further 30 minutes in the dark at room temperature. The Biofilm Matrix stain was then removed, and the biofilm was washed 3x with PBS. 300 µl Vectashield Hardset Antifade Mounting Media with DAPI was used to mount the biofilms and incubated at room temperature for 15 minutes before being left at 4 ^{o}C overnight to set. The stained biofilms were imaged on the Nikon Spinning Disk confocal microscope at 100x magnification with oil. The excitation/emissions for each stain were: FilmTracer Spyro Ruby Biofilm Matrix Stain: excitation 450nm emission 610nm, WGA-AlexaFluor-488: excitation 498 emission 526nm, DAPI: excitation 350 emission 470. Z-stacks were taken throughout the biofilm and images were analysed using ImageJ.

3.2.1.10 Oxygen concentration

Biofilms were grown as described above (3.2.1.1.2) for 1-day. The spent media was removed, and 1.5 ml fresh BHI was added to each well. The Extracellular Oxygen Consumption Reagent was prepared to manufacturer instructions and 100 µl was added to each well. The well was covered with mineral oil as per manufacturer instructions and biofilms were treated with LIPUS for 2-hours in the dark. 200 µl BHI was removed from each well and the fluorescence was read in the Tecan Plate Reader excitation 380 and emission 650.

3.2.1.11 RNA extraction

A Qiagen RNeasy mini kit was used to extract RNA from *S. aureus* SH1000 biofilms. All reagents were prepared to manufacturer's instructions prior to the RNA extraction. *S. aureus* SH1000 biofilms grown as above (3.2.1.1.2) and treated with LIPUS (3.2.1.3) for 2-hours. The biofilms were mechanically disrupted with a pipette in 1 ml PBS and 500 µl of the cell suspension was removed and added to 1 ml RNAprotect Bacterial reagent and incubated for 5 minutes at room temperature before centrifuging at 5000 x g for 10 minutes. The pellet was stored overnight at -20 ^{o}C to be used for RNA extraction. The pellet was resuspended in 200 µl TE buffer containing 65 µg/ml Lysostaphin and lysozyme and incubated for 45-minutes at 37 ^{o}C with regular vortexing to mix every 5 minutes. 700 µl RTL buffer was added and mixed and 500 µl 100 % ethanol was added and pipetted to mix. 700 µl lysate was placed in an RNeasy Mini spin column and centrifuged for 15-seconds at 10000 rpm, flow-through was discarded and this was repeated until all lysate had been centrifuged. 700 µl buffer RW1 was added to the column and centrifuged at 10000 rpm for 15-seconds. 500 µl Buffer RPE was added to the column and centrifuged at 10000 rpm for 15-seconds, this was repeated with the second centrifuge step for 2-minutes. The spin column was placed in a collection tube and 50 µl of nucleotide-free water was added to the column and centrifuged at 10000 rpm for 1-minute. RNA elution was measured using a nanodrop to quantify the RNA and check quality of RNA extracted. RNA was used in sequencing.

3.2.1.12 RNA Sequencing analysis

RNA samples extracted as above (3.2.1.11) from *S. aureus* SH1000 biofilms treated with 2-hour LIPUS, and untreated control samples were sent for RNA sequencing analysis to GENEWIZ by Azenta Life Sciences (Leipzig, Germany). Bioinformatic data was analysed by GENEWIZ by Azenta Life Sciences and supplied analysed. The reference genome was *S. aureus* NTCC 8325 (the parent strain of SH1000), quantities of RNA were compared between untreated and LIPUS treated samples to identify changes to gene expression between the samples. Biological process changes were identified using Gene Ontology Analysis. Overexpressed genes were identified using DEseq analysis in Galaxy. The biological process, molecular function or cellular component associated with those genes were identified using Gene Ontology Resource. Overrepresented genes were analysed and visualised using goseq analysis in Galaxy.

3.2.2 Antibiotic Tolerant Populations

3.2.2.1 Antibiotic tolerant cell isolation

Bacterial biofilms were grown as above, then mechanically disturbed with a pipette before treatment with 1x, 10x, 100x, 1000x, 2000x and 5000x MIC ciprofloxacin identified in the MICs performed on *S. aureus* SH1000 (3.2.1.2) in PBS for 24h at 37 ^{o}C in a shaking incubator. Bacterial suspensions were then washed 4x in PBS before being plated using Miles-Misra method to count colony forming units to determine the concentration of antibiotic which causes reduction of bacterial number indicating an antibiotic tolerant (AT) population. This step was then repeated removing cell suspension at 2-, 6-, 20-, 24- and 30-hours, to determine antibiotic treatment times for successful isolation of antibiotic tolerant (AT) populations.

Following results from earlier determination of concentration and time experiments, isolation of antibiotic tolerant populations was performed using 2.5 mg/ml (5000x MIC) ciprofloxacin for 20h in a shaking incubator at 37 ^{o}C. Whole biofilms were mechanically disrupted using a pipette and incubated in PBS to be used as a control population. All populations were washed 4x in PBS prior to validation and LIPUS treatment experiments to remove all ciprofloxacin.

3.2.2.2 Growth curves of AT populations

AT populations were isolated as above (3.2.2.1) and diluted in 200 µl BHI to OD_{600} 0.05 and incubated in the Tecan Sunrise Plate Reader at 37 ^{o}C for 18-hours with regular shaking throughout the incubation. Absorbance was read at 30-minute intervals at 600 nm. Whole biofilm populations were used as untreated controls to confirm AT population isolation as slow growth is an indicator of AT.

3.2.2.3 MIC of regrown AT Population

Antibiotic tolerant (AT) populations were isolated as above (3.2.2.1) and used to inoculate fresh BHI and grown overnight at 37 ^{o}C in a shaking incubator. Stock solutions (2X) of gentamicin and ciprofloxacin were prepared and diluted as above in 96-well plates and the regrown cultures were diluted to OD_{600} 0.05 then used to inoculate the broth containing antibiotics along with whole biofilm populations as controls. The 96-well plates were incubated at 37 ^{o}C overnight and absorbance at 600 nm was measured in the Tecan plate reader. MICs were conducted on regrown AT populations to assess for resistance to antibiotics used in experiments.

3.2.2.4 Growth of LIPUS treated AT populations.

AT populations were isolated as above from 1-day biofilm (3.2.2.1) and diluted to OD_{600} 1 before LIPUS treatment for 2-hours in PBS before incubation for a further 24-hours. 200 µl was then plated using Miles-Misra to calculate CFU/ml. Whole biofilm populations and non-LIPUS treated samples were used as untreated controls.

3.2.2.5 Growth curves of LIPUS treated AT populations.

AT populations were isolated from *S. aureus* SH1000 as above (3.2.2.1) and were diluted to OD_{600} 0.1 before treatment with LIPUS for 2-hours. Whole biofilm population was also diluted to an OD_{600} 0.1 and treated alongside the antibiotic tolerant sample. After LIPUS treatment the LIPUS treated antibiotic tolerant bacteria and whole biofilm bacteria were used to inoculate BHI broth in a 96-well plate to OD_{600} 0.05 incubated in the Tecan Sunrise Plate Reader at 37 ^{o}C for 18-hours with regular shaking throughout the incubation. Populations without LIPUS treatment were used as untreated controls to identify if LIPUS impacts the growth of AT populations.

3.2.2.6 Antibiotic Sensitivity with LIPUS Treatment

AT populations were isolated from *S. aureus* SH1000 as above (3.2.2.1) and diluted to OD_{600} 1. The AT cells were treated with 10 µg/ml gentamicin in PBS and treated with LIPUS described in 3.2.1.3, for 2-hours then incubated for 24-hours at 37 ^{o}C. Bacterial cell suspensions were then washed 2x in PBS before being resuspended in 2ml PBS, 200 µl was plated using Miles-Misra on BHI agar plated. Colonies were counted and CFU/ml were calculated to identify if LIPUS treatment impacts the antibiotic sensitivity of AT populations.

3.2.3 Human cells and Tissue-engineered Skin

3.2.3.1 Mammalian cell culture

Human keratinocytes (HaCaT) and Human dermal fibroblasts (HDF) were grown from liquid nitrogen storage in keratinocyte growth media and fibroblast medium

respectively, in 5 % CO_2 incubators 37 ^{O}C until 80 % confluent. When cells reached 80 % confluency, cells were passaged. Media were removed from the flasks and cells washed 3x with sterile PBS. Cells were detached from the flask by incubating at 37 ^{o}C for 5 minutes for the HDF and 15 minutes for the HaCaT, with 3 ml 1 % trypsin-EDTA. 7 ml warmed DMEM containing 700 µl FBS was added to neutralise the trypsin, cells were spun down for 5-minutes at 1000 RPM, counted, plated out into fresh media in T-75 flasks, maximum seeding density of 2.1 x 10^6 cells per flask. Cultured cells were routinely visually monitored for infection and cell growth rate, and slow growing cells were discarded.

3.2.3.2 Mammalian Cell Permeability

Human dermal fibroblasts and HaCaT cells were seeded in DMEM in 0.4 µm pore cell culture inserts and grown to confluency. Growth media from within the well and insert was removed and 2 ml DMEM containing 1 mg/ml Dextran 70 kDa was added into the well, 2 ml DMEM was added to the well surrounding the well inserts. The monolayers were treated with LIPUS for 2 hours, at 20-minute intervals permeability of the monolayer was measured by removing 200 µl DMEM from the bottom well and dextran fluorescence was measured at a 494-nm excitation and 521-nm emission. The bottom well was replenished with 200 µl DMEM after each measurement.

3.2.3.3 Proliferation of cells with LIPUS treatment

HaCaT and HDF cells were seeded in a 6-well plate at 0.1x10^6 per well and incubated overnight at 37 ^{o}C in 5 % CO_2. Cells were then treated with LIPUS for 2 hours and incubated again at 37 ^{o}C in 5 % CO_2. Cells were detached from the 6-well plate using trypsin (3.2.3.1) at day 0, 1, 2 and 3, and counted using a haemocytometer and a 1:2 dilution trypan blue to reveal non-viable cells. Changes in cell number over time were compared to cells without LIPUS treatment.

3.2.3.4 PrestoBlue

HaCaT and HDF cells were seeded at a density of $0.1x10^6$ in 6-well plates and grown overnight at 37 ^oC in 5 % CO_2. The spent media was removed and 1800 µl fresh media was added to the wells. Cells were then treated with LIPUS as above (3.2.1.3) for 2 hours. 200 µl PrestoBlue solution was added to each well and incubated for 30-minutes at 37 ^oC. Absorbance was measured in the Tecan Plate Reader at 570 nm. This was repeated over a 3-day period, measured at 0-, 24-, 48- and 72-hours.

3.2.3.5 Wound healing

HaCaT and HDF cells were seeded in a 6-well plate and grown to confluency. Cells were treated with media supplemented with 10 µg/ml mitomycin C for 2 hours at 37 ^oC before removal of the media and washed 3x with PBS. The cell monolayer was then scratched using a 200 µl pipette tip, cells were washed 2x with PBS and 2 ml media was added to the well. The cells were then treated with LIPUS for 2 hours and imaged at 0-, 5-, 24 and 48-hrs post LIPUS for the HDF cells and 0-, 5- and 24-hrs post LIPUS for the HaCaT cells. The closure of the wound in the monolayer was compared against a wound in a monolayer without LIPUS Treatment.

3.2.3.6 Decellularisation of donor skin

Donor skin was washed in sterile PBS at 37 ^oC for 7-days, with the PBS changed daily to remove the glycerol the skin was preserved in. On day 7 the PBS was removed and 1M NaCl was added to completely submerge the skin. The skin in NaCl was incubated overnight at 37 ^oC before epidermis was removed using a scalpel. The acellular dermis was then added to 50 ml Falcon tubes and covered with DMEM; this was incubated for a further 24-hours to ensure sterility of the dermis. All decellularised dermis was stored at 4 ^oC.

3.2.3.7 Tissue-engineered skin model construction

Sterile decellularized dermis (DED) from the donor skin was cut to size to fit 6-well cell culture inserts and placed reticular layer up. Human keratinocytes (HaCaT) and human dermal fibroblasts (HDF) were seeded onto the DED within the inserts, $3x10^6$ and $6x10^5$ respectively, in Green's Media supplemented with penicillin/streptomycin and amphotericin B, plus 2 ng/ml TGF-α both within and surrounding the well insert. For 12-well cell culture inserts $1x10^6$ HaCaT and $3x10^5$ HDF were seeded onto DED (**Figure 11**).

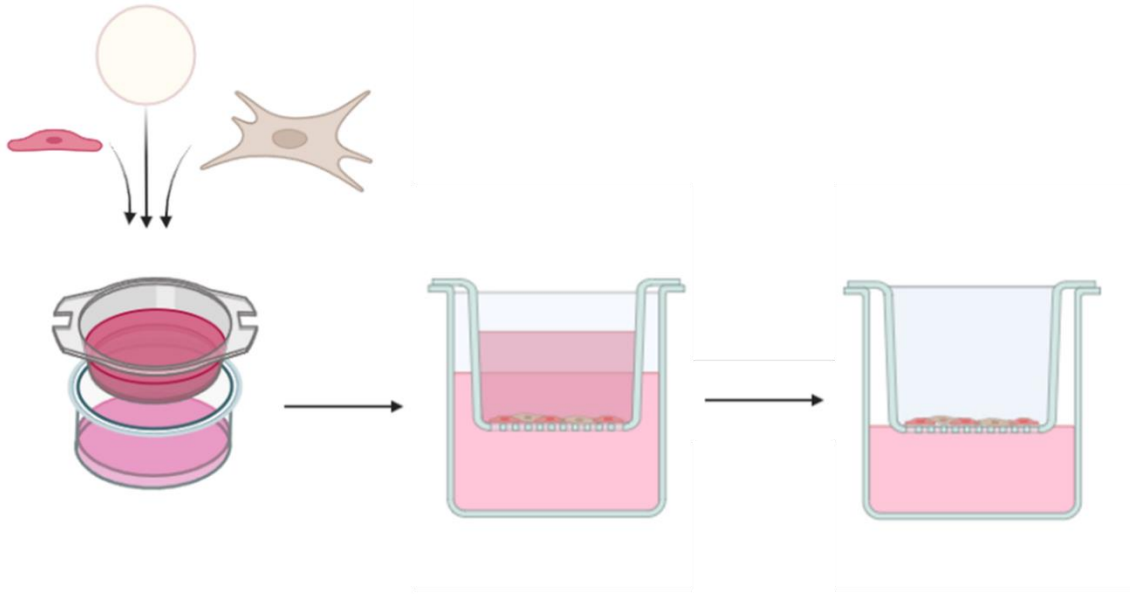

Figure 11: HaCaT and HDF cells seeded onto DED in well inserts containing DMEM, media is then removed from within the well insert and skin constructs are grown at air-liquid-interface. Created in BioRender.

Skin constructs were incubated in 5 % CO_2 incubator at 37 ^oC. At day 3 post seeding the media was removed from within the insert to allow cell differentiation at air-liquid-interface (**Figure 11**) and the media surrounding the insert was replenished at regular intervals over 14 days. For skin constructs being used for bacterial infection, at day 12 media containing antibiotics were removed and wells were washed with

sterile PBS before KGM without penicillin/streptomycin was added to the well for the last 2 days of incubation. The completed skin model can be seen in **Figure 12** and **Figure 13**.

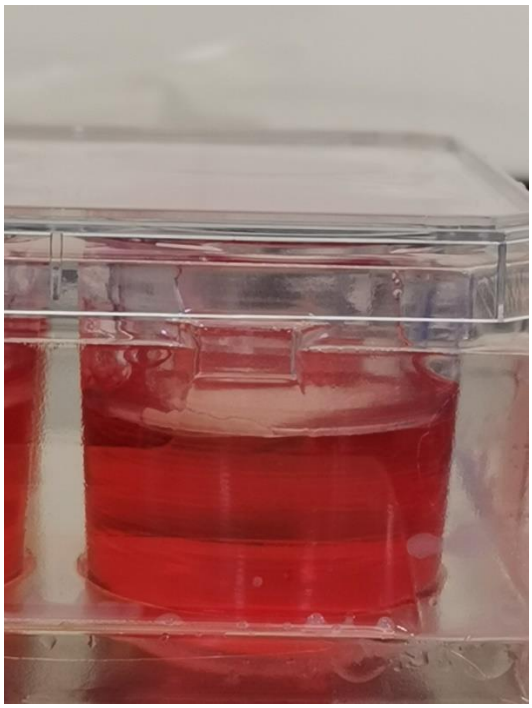

Figure 12: Skin construct at air-liquid-interface

Figure 13: Top view of skin construct in well-insert

3.2.3.8 Tissue-engineered skin model infection

To provide a break in the epidermal skin barrier, skin constructs were thermally injured using a heated loop held against the epidermal surface for 5 seconds. *S. aureus* SH1000 and S235 were grown overnight in BHI broth, the number of bacteria in the cultures was counted using a haemocytometer and diluted to $1x10^6$ bacteria/ml. For constructs grown in 12-well inserts 10 µl of bacterial suspension was added containing 1×10^4 *S. aureus* S235 and for constructs grown in 6-well inserts 30 µl bacterial suspension containing 3×10^4 *S. aureus* S235 was added to the injured model. Infected models were then incubated for 24-hours to allow an infection to establish.

3.2.3.9 LIPUS & Antibiotic treatment of Tissue Engineered Skin Models (TESM)

3 ml PBS containing 20 µg/ml gentamicin were dropped onto the surface of TE skin infected with *S. aureus* S235 then treated with 30 mW/cm^2 LIPUS. The infected TESM were then incubated with the antibiotics for a further 24-hours, alongside infected models treated with 20 µg/ml gentamicin which did not receive LIPUS treatment. The models were cut in two, half the models were weighed and homogenised by vortexing in 1 ml PBS to release bacterial cells from the model. The suspensions were serially diluted and then plated on BHI agar plates using Miles-Misra technique before being incubated in a static incubator overnight at 37 ^oC. Colonies were counted and CFU/g tissue were calculated. The rest of the model was fixed in 4% Paraformaldehyde for a minimum of 24 hours before being processed for histology and imaging analysis. Infected models and uninfected models treated with and without LIPUS were also used as controls.

3.2.3.10 Histology

Fixed models were secured in an appropriately sized histology cassette to be processed in the tissue processor overnight. The tissue processing programme is described below.

Tissue Processing:

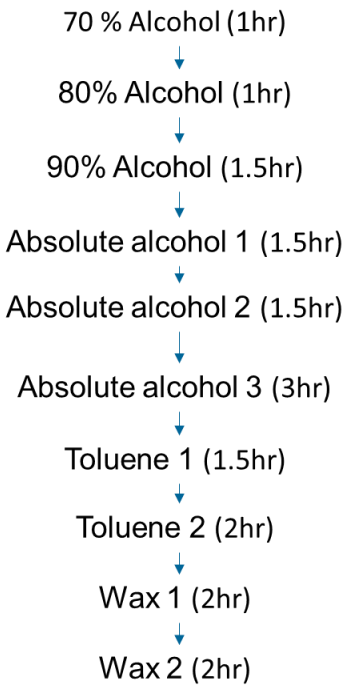

Skin models were removed from the tissue processor and embedded in wax to prepare for sectioning and staining. Embedded tissue was sectioned using a microtome and mounted on frosted microscope slides and placed in a histology oven at 70 ^{o}C for an hour. The slides were then placed in the linear stainer for H&E staining. Sections for each sample were stained using H&E or Gram staining. H&E staining and Gram staining procedures are described below.

H & E Staining (45 seconds in each stage):

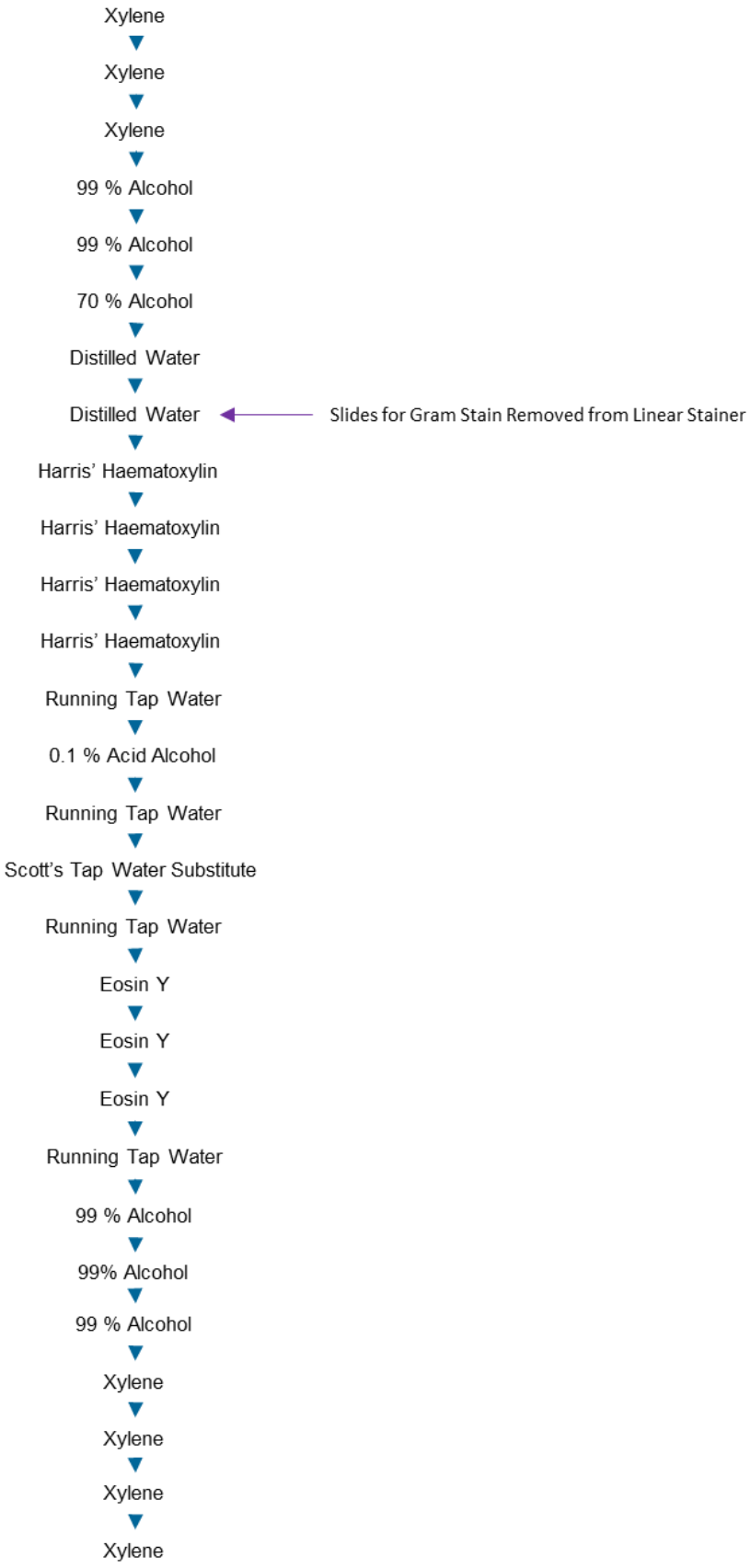

Gram Staining:

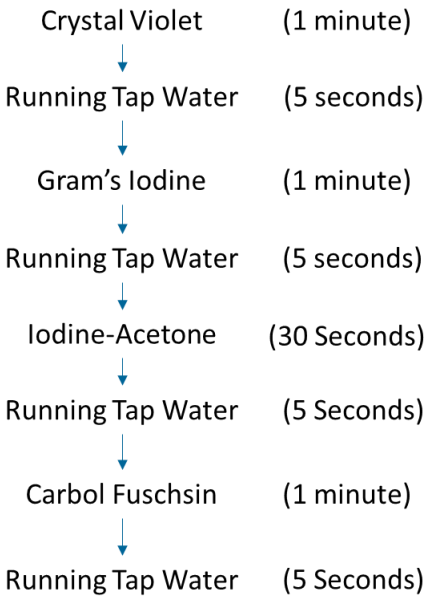

Post staining the samples were covered with a coverslip, mounted with DPX mountant for histology and imaged using the Olympus Microscope.

3.2.3.11 Staphylococcus aureus strains co-culture with mammalian cells

Human dermal fibroblasts and HaCaT cells were seeded at a density of 0.1 x 10^6 in the appropriate media, as described above (**Table 7**, without antibiotics), in 12 well-plates and incubated at 37 ^oC in 5 % CO_2 overnight. Media were removed and centrifuged at 1000 RPM for 5 minutes and the supernatant was carefully removed and added to a 12 well-plate. Fresh antibiotic-free media was added to the cells. Overnight cultures of *S. aureus* SH1000 and S235 were diluted to OD_{600} 0.1 and added into the wells containing both cells and cell culture media removed from the cells. The plate was incubated overnight at 37 ^oC in a static incubator. 200 µl was removed after incubation from each well and plated using Miles-Misra to calculate CFU/ml. Bacteria were also grown in fresh cell-culture media, FBS and BHI as controls.

3.2.3.12 IL-6 ELISA

Tissue-Engineered skin models were grown and treated with LIPUS for 2-hours. 100 µl of media was removed from inside the well at 0-hour, 2-hour and 24-hour post LIPUS treatment and used to perform an ELISA to measure IL-6 levels. An IL-6 ELISA kit was used according to manufacturer's instructions and all reagents were prepared as instructed as follows. 100 µl of cell supernatant was added to the precoated ELISA plate from the kit and incubated for 2.5-hours at room temperature before removing the supernatant and washing 4x with 300 µl 1x wash buffer. 1x IL-6 detection antibody was added to each well and incubated for 1-hour at room temperature before removal and repeated washing as before. 100 µl Streptavidin solution was added to each well and incubated at room temperature for 45-minutes with gentle shaking, washing was repeated as above. 100 µl TMB One-Step Substrate Reagent was added to each well and incubated at room temperature for 30-minutes in the dark, 50 µl Stop Solution was added to each well and absorbance was read at 450nm in Tecan Plate Reader. TESM which did not receive LIPUS treatment were used as untreated controls.

3.2.3.13 IVWM in infection of skin model

The *in-vitro* wound milieu (IVWM) was prepared as described in (Dhekane *et al.*, 2022) and shown in the table below.

Component	Concentration
FBS	70 %
Rat-tail collagen	12 µg/ml
Fibrinogen	300 µg/ml

Fibronectin	30 µg/ml
Lactoferrin	20 µg/ml
Peptone Water	0.0005 %
Lactic Acid	11 mM

Skin constructs were grown in 12-well plates as above (3.2.3.7) and infected with *S. aureus* S235 for 24-hours in the presence of the IVWM or BHI at 37 ^{o}C in 5 % CO_2. After 24-hours, models were cut in two, half the model was weighed, homogenised and vortexed in 1ml PBS for 30-seconds to release bacterial cells from the model. Bacterial cell suspensions were serially diluted and plated onto BHI agar plates using Miles-Misra technique before being incubated in a static incubator overnight at 37 ^{o}C. Colonies were counted and CFU/g were calculated. The rest of the model was fixed in 4% Paraformaldehyde for a minimum of 24 hours before being processed for histology as described in 3.2.3.10.

3.2.3.14 Growth of bacterial cells in IVWM

Overnight cultures of *S. aureus* S235 and SH1000 were diluted to OD_{600} 0.1 and used to inoculate IVWM, prepared as above (3.2.3.13) and BHI in 96-well plates. The plates were incubated in a Tecan Sunrise Plate reader for 18-hours at 37 ^{o}C, absorbance was read at 30-minute intervals at 600nm. At the end of incubation 20 µl was removed from each well and fixed onto a microscopy slide for Gram Staining. Slides were imaged on Olympus microscope at 100x magnification.

3.2.4 Data Analysis and Statistics

All statistical analyses were performed in Prism Graphpad using t-test or one-way ANOVA with Tukey's or Dunnett's multiple comparison. A p-value <0.05 was determined to be statistically significant. MICs were calculated using Gompertz fit for MIC in Prism Graphpad. Images were analysed using ImageJ.

4 Results

4.1 Biofilm

Biofilms are associated with chronic infection therefore treatment of biofilm infections is an important area of investigation. LIPUS is an option to be explored in treating biofilm-related infections. In this study *S. aureus* SH1000 biofilms were used to assess the effects of LIPUS on biofilm growth, disruption, permeability, and antibiotic sensitivity. Whole biofilms were treated with LIPUS to assess how the LIPUS treatment affects the biofilm and *S. aureus* SH1000 planktonic cells were also used to investigate the effects of LIPUS treatment on the permeability of the bacterial cells.

4.1.1 Growth

Changes in the number of viable cells in *S. aureus* SH1000 biofilms treated with LIPUS were assessed by counting colony-forming units taken from a LIPUS-treated sample and compared to an untreated sample of biofilm. The dispersal of the biofilms was also measured by counting viable bacteria within the media taken from the biofilm. Changes in the presence of organic matter in the whole biofilm were conducted by staining biofilms with crystal violet.

4.1.1.1 CFU

S. aureus SH1000 biofilms were grown for 1-, 3-, 5-, and 7-days, and then treated with 30 mW/cm^2 LIPUS for 1-, 2-, and 3-hours. The biofilms were incubated for 24-hours at 37 ^{o}C before the media was removed and the biofilms mechanically disrupted in PBS. The media and biofilms were both serially diluted, plated and allowed to grow overnight to determine the number of colony-forming units (CFU) present. An increase in CFU/ml from the biofilm would indicate an increase in

bacterial growth, where an increase in CFU/ml from media samples would indicate an increase in dispersal of the biofilm.

4.1.1.1.1 1-day old S. aureus biofilm

S. aureus SH1000 biofilms, grown for 1-day, which did not receive LIPUS treatment were used as untreated controls against 1-, 2-, and 3-hour LIPUS treated biofilms. The biofilms were disrupted and serially diluted to calculate the CFU/ml of *S. aureus* SH1000 in the biofilm. When calculating the number of viable bacteria from 1-day old biofilms the number of CFU/ml can be seen in **Table 11**. When analysed using a one-way ANOVA there were no significant changes to the number of bacteria when comparing the untreated biofilms with the LIPUS treated biofilms for 1-, 2-, and 3-hours (**Figure 14a**). These data indicate no change to growth of the 1-day old biofilm when treated with LIPUS.

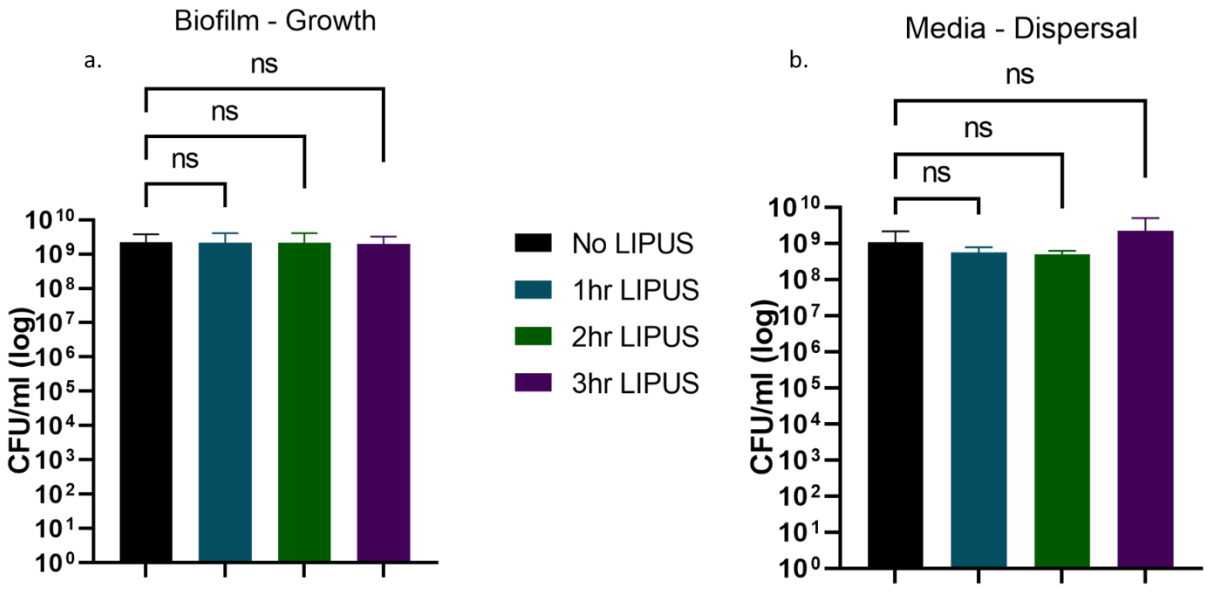

Figure 14: 1-day old S. aureus SH1000 biofilm was treated with 30 mW/cm² LIPUS for 1-, 2- and 3-hours, incubated for 24-hours then plated to quantify bacterial numbers in the biofilm (a) and the media (b) through CFU/ml. Error bars = +/-SEM. Analysed using one-way ANOVA with Dunnett's multiple comparison. ns = not significant. N=3

Media was removed from the 1-day old *S. aureus* SH1000 biofilm and serially diluted to calculate the number of viable cells within the media (**Figure 14b**). An untreated *S. aureus* SH1000 biofilm was used as a control. The CFU/ml for each test condition can be seen in **Table 11**. When analysed using one-way ANOVA there were no statistically significant changes in CFU/ml in the media from the untreated biofilm when compared to the 1-, 2-, and 3-hour LIPUS treated biofilms. These data indicate no change to dispersal of the 1-day old biofilms following LIPUS.

Table 11: Summary of CFU/ml of biofilms and media from 1-day old S. aureus biofilms treated with/without LIPUS.

	Biofilm – Growth		**Media – Dispersal**	
LIPUS time (Hours)	CFU/ml	p-value (against untreated)	CFU/ml	p-value (against untreated)
0	2.22×10^9		1.10×10^9	
1	2.14×10^9	0.99	5.71×10^8	0.8
2	2.12×10^9	0.99	5×10^8	0.74
3	1.98×10^9	0.98	2.36×10^9	0.25

4.1.1.1.2 **3-day old S.** *aureus biofilm*

3-day old *S. aureus* SH1000 biofilms which did not receive LIPUS treatment were used as untreated controls, the untreated and 1-, 2-, and 3-hour LIPUS treated biofilms were mechanically disrupted and serially diluted to calculate the number of viable cells within the biofilm (**Figure 15a**). The CFU/ml for each test condition can be seen in **Table 12**. Again, there were no discernible differences across the data and when analysed statistically using a one-way ANOVA in comparison to the untreated samples. This indicates that the overall growth in 3-day biofilm was not affected by the LIPUS treatment used in this study.

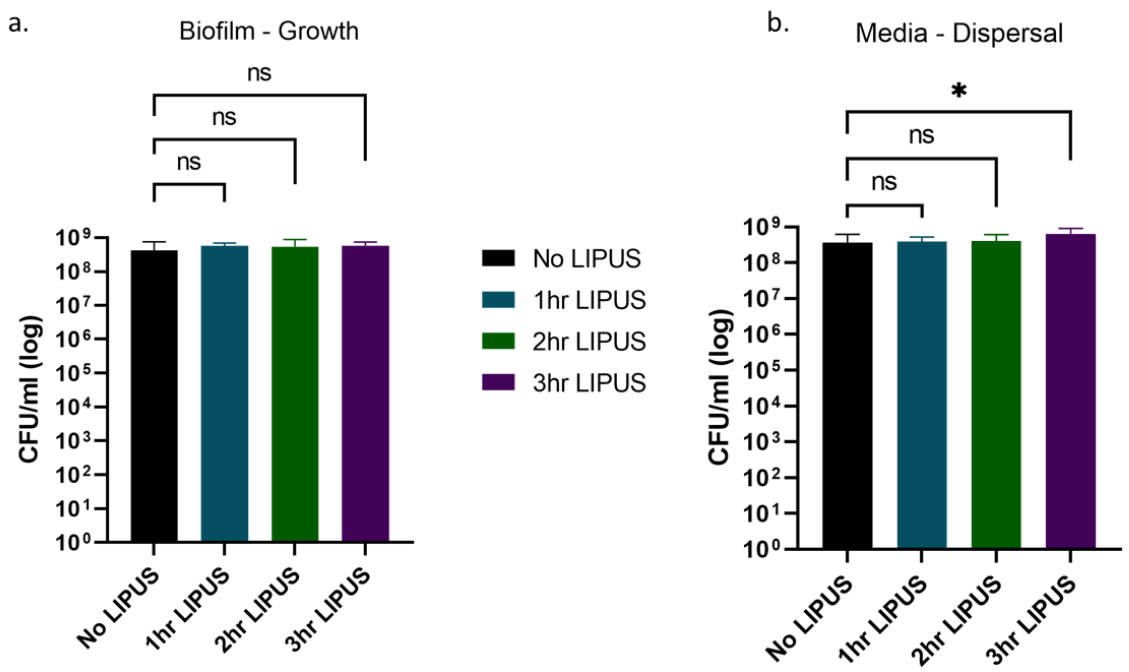

Figure 15: 3-day S. aureus SH1000 biofilm was treated with 30mW/cm² LIPUS for 1-, 2- and 3-hours, incubated for 24-hours then plated to quantify bacterial numbers in the biofilm (a) and the media (b) through CFU/ml. Error bars = +/-SEM. Analysed using one-way ANOVA with Dunnett's multiple comparison. ns= not significant. * = p-value >0.05. N=3

Media was taken from 1-, 2-, and 3-hour LIPUS treated biofilms along with media from an untreated biofilm and serially diluted to calculate the number of viable cells within the media (**Figure 15b**). The CFU/ml from the media of each test condition can also be seen in **Table 12**. When analysing statistically using a one-way ANOVA, the biofilms treated with LIPUS for 1-, and 2-hours were not statistically different when compared to the media from the untreated biofilm. However, the 3-hour treatment did yield a significant increase in CFU/ml indicating potential disruption of the biofilm. Both 1- and 2-hour 30mW/cm^2 LIPUS treatment did not affect the rate of disruption of the 3-day old biofilm, however, 3-hour LIPUS treatment used in this study may have increased the disruption of the biofilm.

Table 12: Summary of CFU/ml of biofilms and media from 3-day old S. aureus biofilms treated with/without LIPUS.

	Biofilm – Growth		**Media – Dispersal**	
LIPUS time (Hours)	CFU/ml	p-value (against untreated)	CFU/ml	p-value (against untreated)
0	4.18×10^8		3.64×10^8	
1	5.67×10^8	0.48	3.87×10^8	0.99
2	5.38×10^8	0.64	3.96×10^8	0.98
03	5.76×10^8	0.44	6.40×10^8	0.03

4.1.1.1.3 5-day old S. aureus biofilm

5-day old *S. aureus* SH1000 biofilms were treated with 1-, 2-, and 3-hour 30 mW/cm^2 LIPUS along with an untreated biofilm as an untreated control. The biofilms were mechanically disrupted and serially diluted to calculate the number of viable cells within the biofilm (**Figure 16a**). The average CFU/ml recovered from each test condition can be seen in **Table 13**. When analysed statistically using a one-way ANOVA all 2 timepoints of LIPUS treatment did not cause statistically significant changes in the number of bacteria within the 5-day biofilm when compared to the untreated 5-day biofilm, indicating the 30mW/cm^2 LIPUS treatment used in this study did not affect the growth of the 5-day old biofilms.

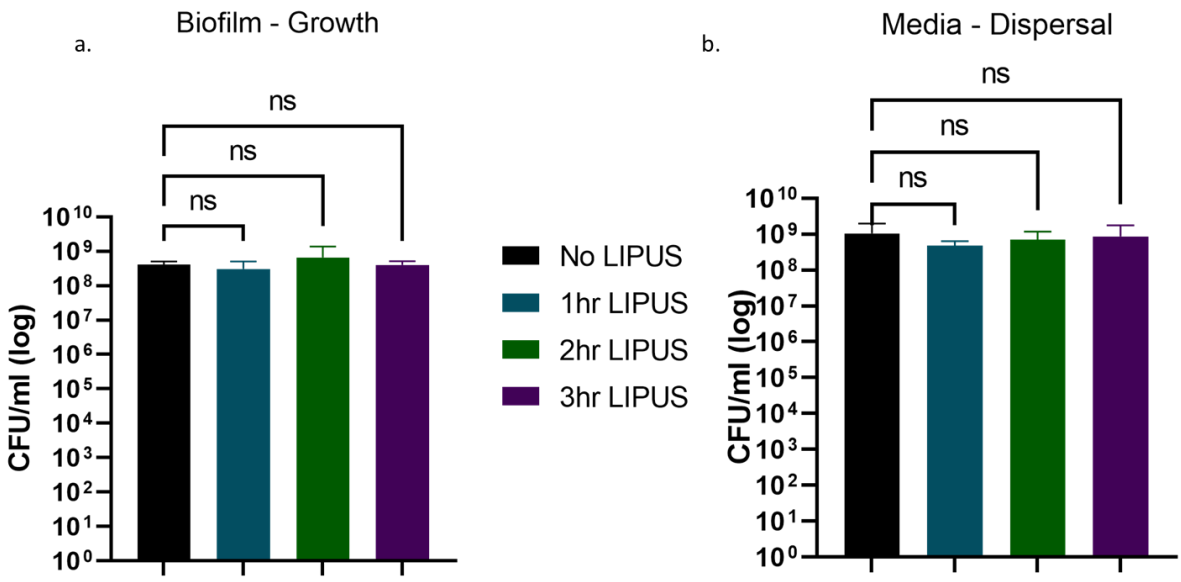

Figure 16: 5-day S. aureus SH1000 biofilm was treated with 30 mW/cm^2 LIPUS for 1-, 2-, and 3-hours, incubated for 24-hours then plated to quantify bacterial numbers in the biofilm (a) and the media (b) through CFU/ml. Error bars = +/-SEM. Analysed using one-way ANOVA with Dunnett's multiple comparison. ns = Not significant. N=3

Disruption of the 5-day *S. aureus* SH1000 biofilms was assessed by comparing number of bacteria in the media of 5-day biofilms without LIPUS treatment against LIPUS treated biofilms. (**Figure 16b**). The average CFU/ml from the media of each test condition can also be seen in **Table 13**. When analysed statistically using a one-way ANOVA the changes in CFU/ml from the media of each of the timepoints of LIPUS treatment were not statistically significant when compared to the media of the untreated biofilm.

Table 13: Summary of CFU/ml of biofilms and media from 5-day old S. aureus biofilms treated with/without LIPUS.

	Biofilm – Growth		**Media – Dispersal**	
LIPUS time (Hours)	CFU/ml	p-value (against untreated)	CFU/ml	p-value (against untreated)
0	3.36 x 10^8		1.04 x 10^9	

1	3.08 x 10^8	0.89	4.80 x 10^8	0.23
2	6.64 x 10^8	0.34	7.02 x 10^8	0.61
3	4.04 x 10^8	<0.999	8.69 x 10^8	0.92

4.1.1.1.4 7-day old S. aureus biofilm

The oldest biofilms used in this study were 7-day old biofilms. The *S. aureus* SH1000 biofilms grown were then treated with 30 mW/cm^2 LIPUS for 1-, 2-, and 3-hours, before being mechanically disrupted and serially diluted (**Figure 17a**). The average CFU/ml for each timepoint of LIPUS treatment can be seen in **Table 14**. When analysed using one-way ANOVA there was no statistical difference in the number of viable cells in the biofilms when comparing the untreated biofilm to all LIPUS treatment timepoints. This demonstrates that the 30 mW/cm^2 used in this study did not affect the growth of the 7-day biofilms.

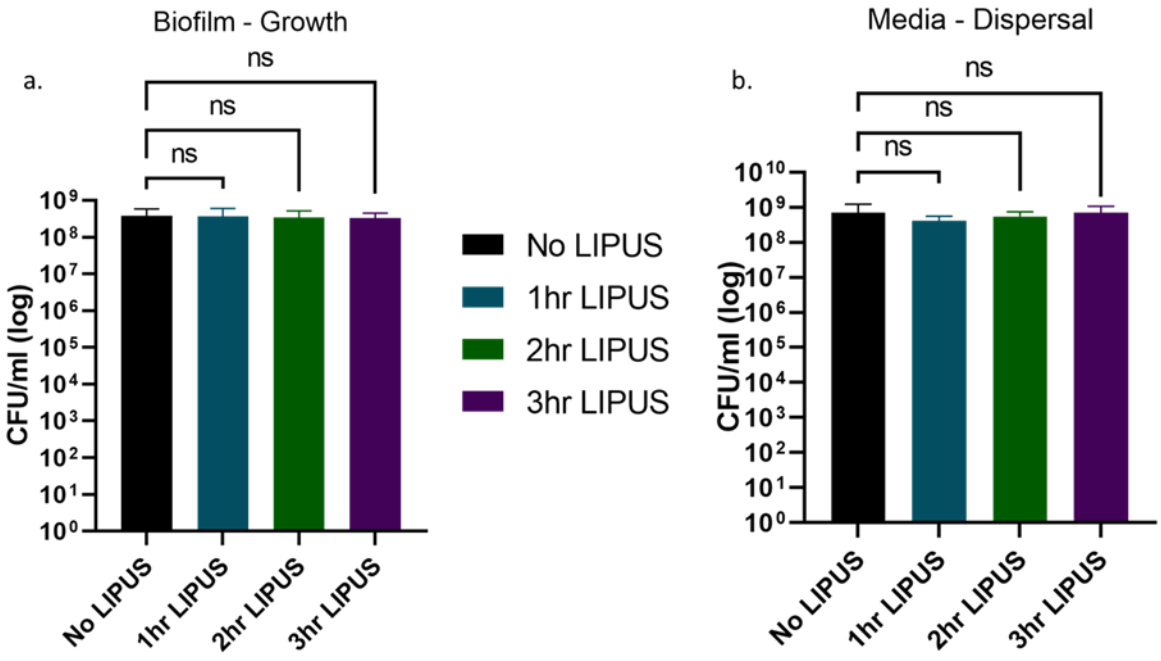

Figure 17: 7-day S. aureus SH1000 biofilm was treated with 30 mW/cm^2 LIPUS for 1-, 2-, and 3-hours, incubated for 24-hours then plated to quantify bacterial numbers in the biofilm (a) and the media (b)

through CFU/ml. Error bars = +/-SEM. Analysed using one-way ANOVA with Dunnett's multiple comparison. ns = Not significant. N=3.

Media removed from 7-day old *S. aureus* SH1000 biofilms treated with 1-, 2-, and 3-hour LIPUS were serially diluted to calculate the number of viable cells within the media and compared to the number of viable cells in the media removed from biofilms without LIPUS treatment which were used as an untreated control (**Figure 17b**). The average CFU/ml from each test condition can be seen in **Table 14**. This indicated that 30 mW/cm^2 LIPUS treatment used in this study for up to 3-hours does not increase the dispersal of 7-day old biofilm.

Table 14: Summary of CFU/ml of biofilms and media from 7-day old S. aureus biofilms treated with/without LIPUS. Analysed using one-way ANOVA with Dunnett's multiple comparison.

	Biofilm – Growth		**Media – Dispersal**	
LIPUS time (Hours)	CFU/ml	p-value (against untreated)	CFU/ml	p-value (against untreated)
0	3.78 x 10^8		6.96 x 10^8	
1	3.66 x 10^8	0.99	4.07 x 10^8	0.19
2	3.40 x 10^8	0.94	5.44 x 10^8	0.67
3	3.27 x 10^8	0.88	9.96 x 10^8	>0.999

4.1.1.2 Crystal violet staining

S. aureus SH1000 biofilms were grown for 1-, 3-, 5-, and 7-days in 6-well plate inserts, before treatment with 30 mW/cm^2 LIPUS for 2-hours, the biofilms were incubated for 24-hours before removal of the media, the biofilms were stained with CV and images were captured. The images were analysed in ImageJ to calculate the

percentage of coverage of the well-insert by the biofilm. The whole culturable area of the inserts is 420 mm^2.

4.1.1.2.1 1-day old S. aureus biofilm

When *S. aureus* SH1000 biofilms were grown for 1-day the area of the well-inserts covered with biofilm was visually similar between the untreated (**Figure 18a**) and biofilm treated with 30 mW/cm^2 LIPUS (**Figure 18b**). When analysing the images using ImageJ the biofilm in the untreated sample covered 90 % of the well-insert, while the biofilm in the sample treated with LIPUS covered 96 % of the well-plate insert (**Figure 18c**). When comparing the percentage of well-plate coverage between the treated and untreated sample statistically using a t-test the p-value was 0.168 which is not statistically significant.

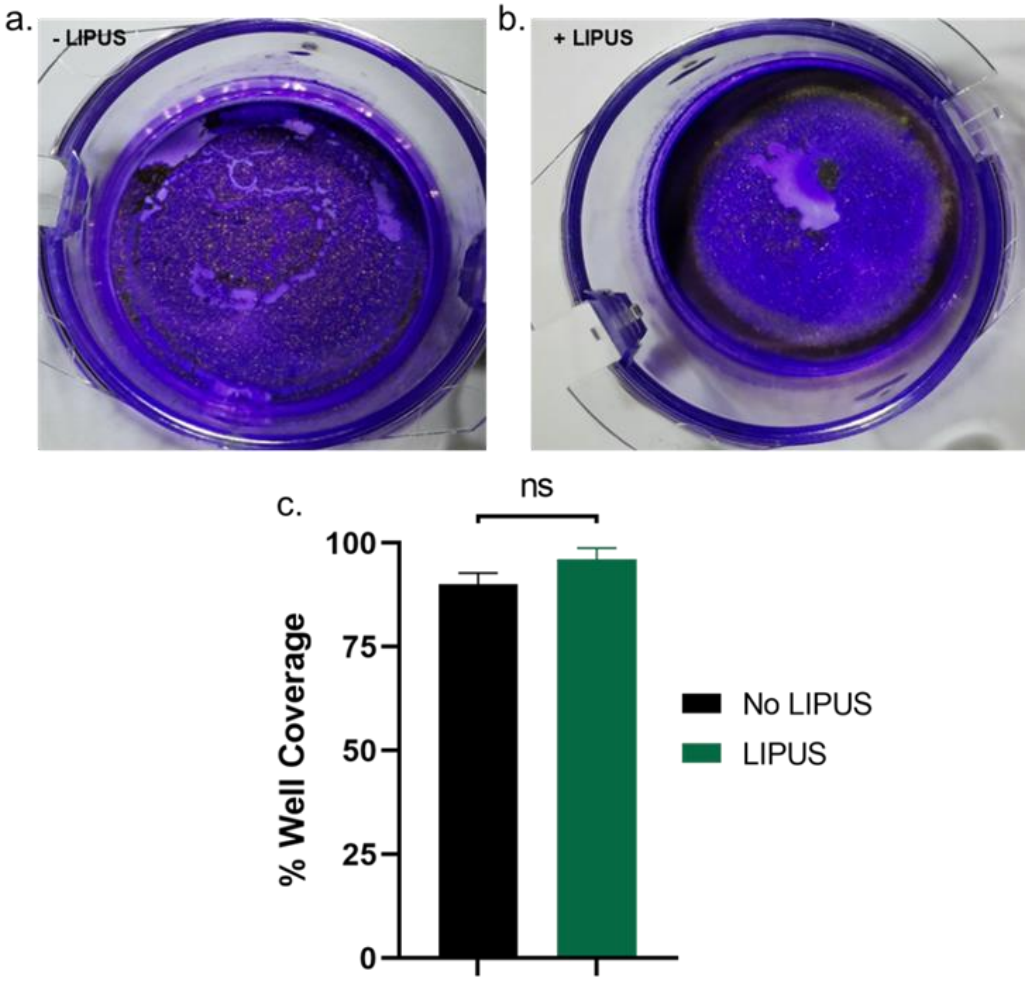

Figure 18: 1-day S. aureus SH1000 biofilm without LIPUS treatment (a) and with 30 mW/cm^2 LIPUS treatment (b) with similar area of coverage. The percentage of the area of coverage was calculated (c). Error bars = +/-SEM. Analysed using t-test. ns=not significant N=3.

4.1.1.2.2 3-day old S. *aureus biofilm*

The area in which the 3-day *S. aureus* SH1000 biofilm covers was lower than the 1-day biofilm, however the area covered by the untreated biofilm (**Figure 19a**) was visually similar to the biofilm treated with 30 mW/cm^2 LIPUS (**Figure 19b**). When the percentage of area covered was calculated with ImageJ the untreated biofilm covered 88 % of the well-plate while the area of coverage by the LIPUS treated biofilm was 90 % (**Figure 19c**). When comparing the percentage of coverage of the well-plate inserts statistically using a t-test the p-value calculated was 0.79 which is not statistically significant.

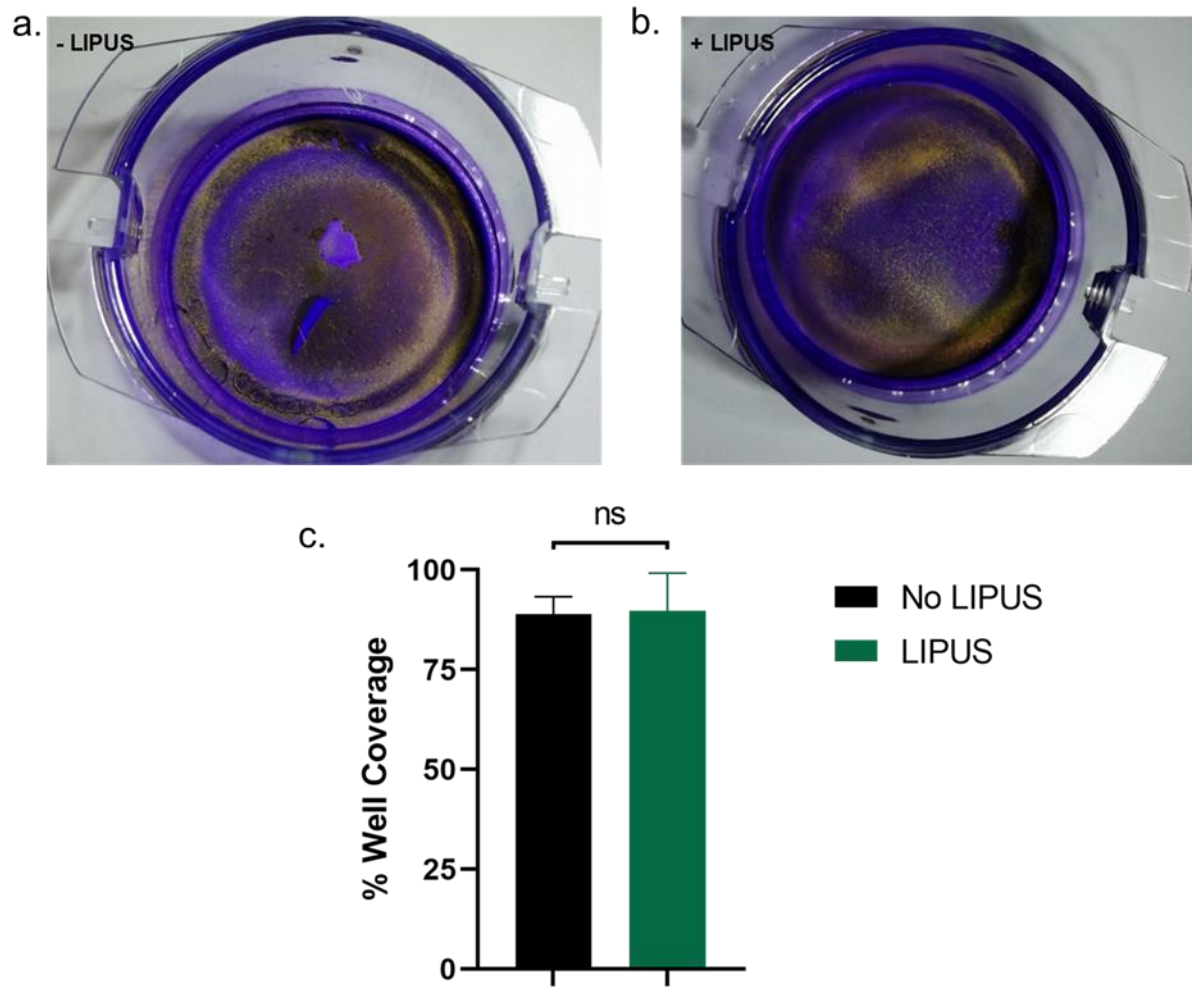

Figure 19: 3-day S. aureus SH1000 biofilm without LIPUS treatment (a) and with 30 mW/cm^2 LIPUS treatment (b) with similar area of coverage. The percentage of the area of coverage was calculated (c). Error bars = +/-SEM. Analysed using t-test. ns=not significant N=3.

4.1.1.2.3 5-day old S. aureus biofilm

When the *S. aureus* SH1000 biofilms were grown for 5-days in the 6-well inserts, the area covered by the biofilms was again lower than the 1-day and 3-day old biofilms with some loss of biofilms around the outer edge of the well-plates as seen in **Figure 20a** and **Figure 20b**. There was not a large visual difference between the untreated control biofilm (**Figure 20a**) and the 2-hour LIPUS treated biofilm (**Figure 20b**). When analysing the percentage of area covered by biofilm using ImageJ the untreated biofilms covered 83 % of the well insert, compared to 86 % coverage of the well insert covered by the biofilm treated with LIPUS (**Figure 20c**). When

comparing the treated and untreated biofilms coverage of the well inserts statistically using a t-test the p-value calculated was 0.47 which shows an insignificant difference between the treatment conditions.

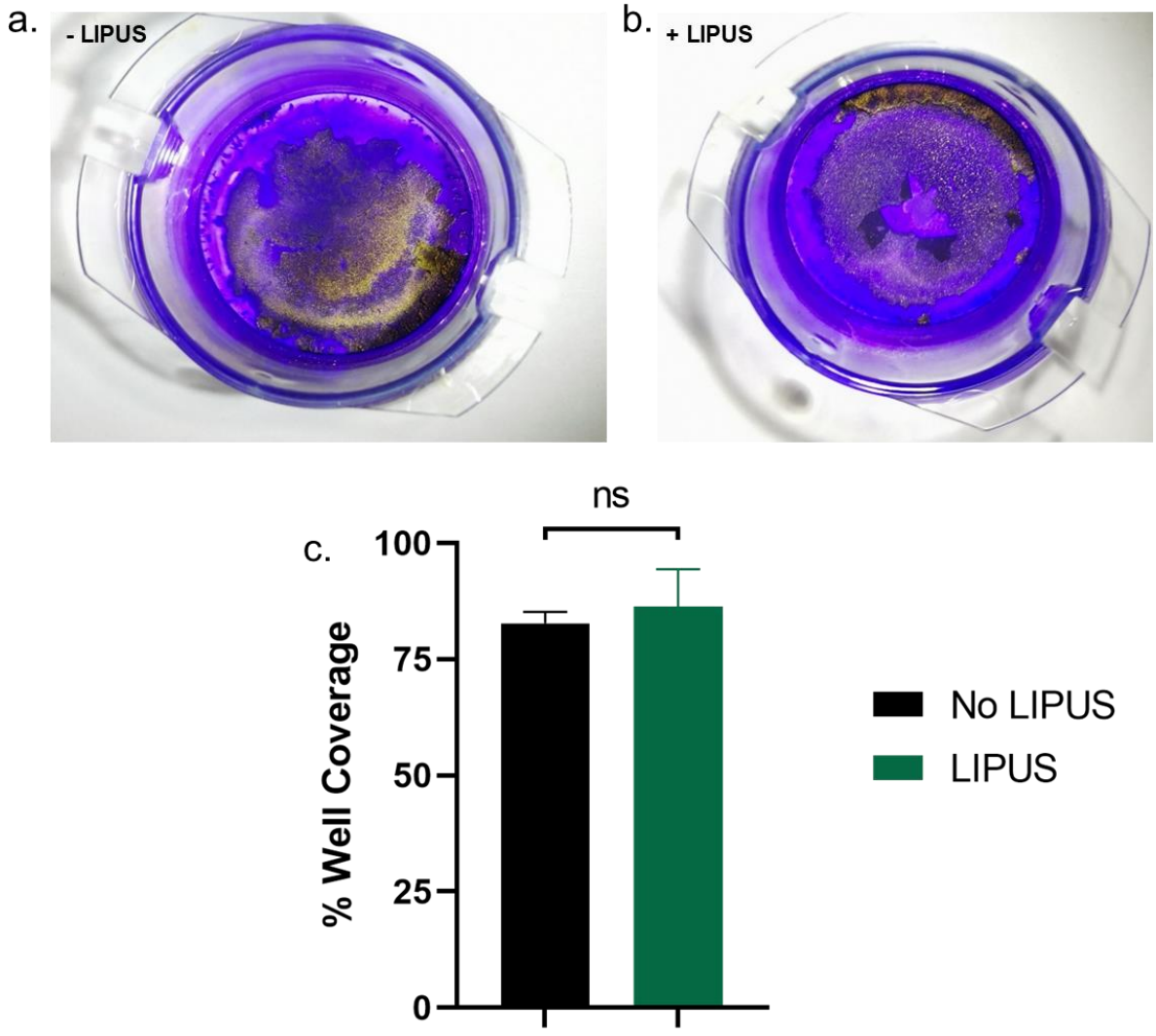

Figure 20: 5-day S. aureus SH1000 biofilm without LIPUS treatment (a) and with 30 mW/cm² LIPUS treatment (b) with similar area of coverage. The percentage of the area of coverage was calculated (c). Error bars = +/-SEM. Analysed using t-test. ns=not significant N=3.

4.1.1.2.4 7-day old S. aureus biofilm

Again, when the older *S. aureus* SH1000 biofilms grown for 7-days (**Figure 21a**) had a lower coverage of the 6-well inserts than the younger 1-day (**Figure 18**), 3-day (**Figure 19**), and 5-day biofilms (**Figure 20**). The untreated biofilm (**Figure 21a**) was visually similar to the LIPUS treated biofilm (**Figure 21b**), with loss of biofilm spread throughout the well insert, with higher areas of staining indicating denser areas of biofilm surrounded by areas of lower staining with sparser areas of biofilm. When the images were analysed with ImageJ the untreated biofilm covered 73 % of the area of the insert, while the LIPUS treated biofilm covered 76 % of the area of the insert (**Figure 21c**). When analysing these percentages using a t-test the p-value calculated was 0.57 which is not statistically significant.

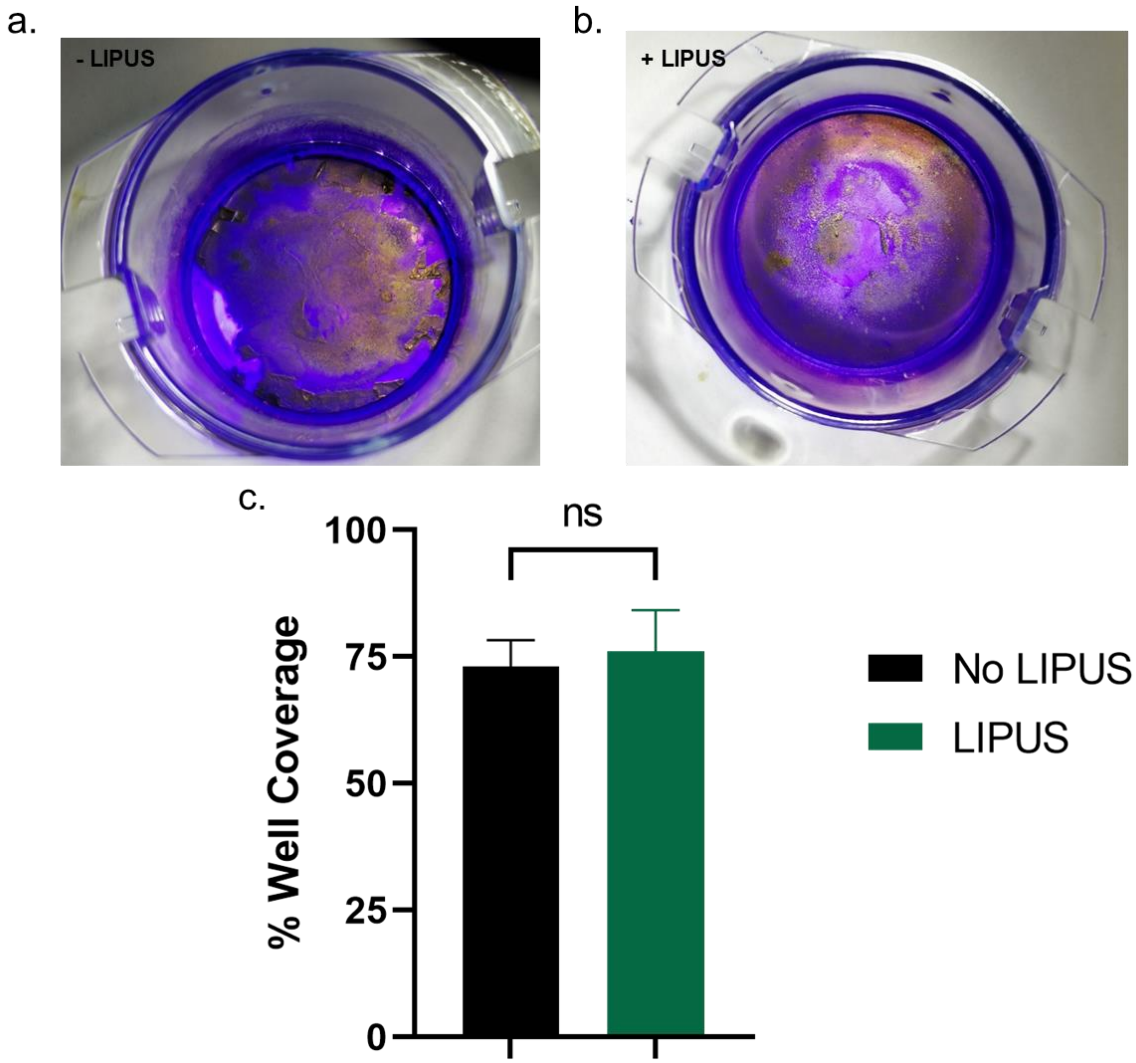

Figure 21: 7-day S. aureus SH1000 biofilm without LIPUS treatment (a) and with 30 mW/cm² LIPUS treatment (b) with similar area of coverage. The percentage of the area of coverage was calculated (c). Error bars = +/-SEM. Analysed using t-test. ns=not significant N=3.

4.1.2 Antibiotic Sensitivity

The aim of this experiment was to measure changes in sensitivity to gentamicin in biofilm associated *S. aureus* when treated with LIPUS. Biofilms were cultured for up to 7 days and exposed to 1000x MIC gentamicin and vancomycin and treated with LIPUS for up to 3-hours.

Results from this section are summarised below all individual results in **Table 15** (p.69)

4.1.2.1 MIC

Minimum inhibitory concentrations (MICs) were calculated for the *S. aureus* SH1000 strain to discern the orientative concentrations for clinically relevant antibiotics. *S. aureus* were grown in the presence of gentamicin, vancomycin, and ciprofloxacin for 24-hours before optical density was measured at 600nm to establish the MIC for each antibiotic. MIC for gentamicin was calculated at 1.34 µg/ml using Gompertz fit for MIC (**Figure 22a**). The MIC for vancomycin was calculated to be 1.8 µg/ml (**Figure 22b**) and for ciprofloxacin the MIC was calculated to be 0.5 µg/ml (**Figure 22c**). When comparing MIC identified against the EUCAST breakpoints all three antibiotics showed some level of susceptibility, with the EUCAST breakpoint for gentamicin and vancomycin susceptibility being <2 mg/L, for ciprofloxacin intermediate susceptibility was identified as susceptibility is characterised by inhibition with <0.001 mg/L and resistance is identified if MIC is >1 mg/L.

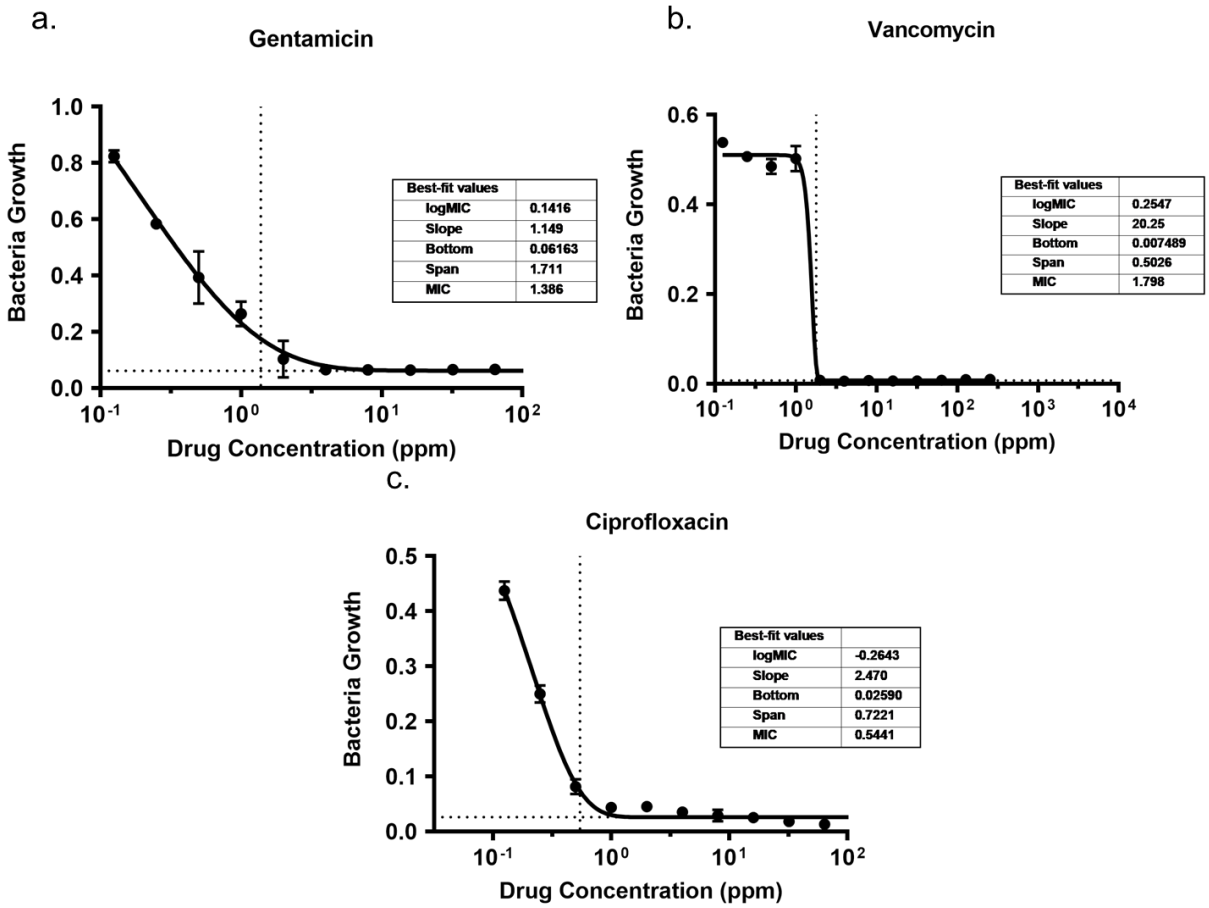

Figure 22: Minimum inhibitory concentrations of gentamicin (a), vancomycin (b), and ciprofloxacin against S. aureus SH1000. Error bars = +/-SEM. MIC calculated using Gompertz fit for MIC.

The MIC for gentamicin against *S. aureus* S235 was also calculated for orientative concentrations. *S. aureus* S235 was grown in BHI supplemented with gentamicin 0.125 µg/ml – 256 µg/ml for 24-hours at 37 ^{o}C, the optical density was read at 600nm and the MIC for gentamicin was calculated at 1.94 µg/ml using Gompertz fit for MIC (**Figure 23**). As this is below 2 µg/ml and below the EUCAST breakpoint *S. aureus* S235 is susceptible to gentamicin.

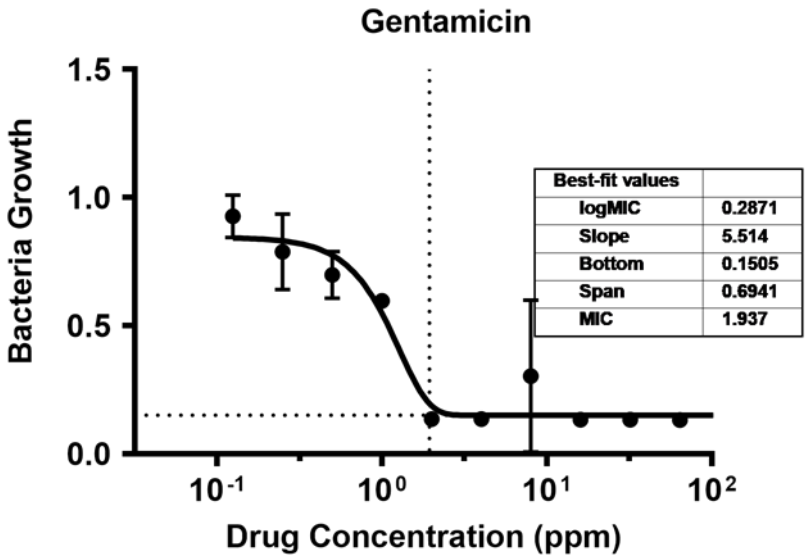

Figure 23: S. aureus S235 grown for 24-hours in the presence of 0.125 µg/ml - 256 µg/ml gentamicin at 37 ºC, absorbance was read at 600nm, MIC calculated using Gompertz fit for MIC. Error bars = +/-SEM.

4.1.2.2 Gentamicin and LIPUS

Results from this section are summarised in **Table 15**.

4.1.2.2.1 1-day old S. aureus biofilm

S. aureus SH1000 1-day old biofilms were treated with LIPUS (30mW/cm^2) for 1-hour (**Figure 24a**) and challenged with gentamicin 1 mg/ml pre and post LIPUS treatment. LIPUS significantly increased antibiotic sensitivity in these biofilms when gentamicin was added both pre and post LIPUS treatment. When the biofilms were exposed to gentamicin without LIPUS treatment the average CFU/ml was 1.45x10^7, this decreased to 1x10^6 when the biofilm was exposed to 1 mg/ml gentamicin prior to LIPUS treatment (one-way ANOVA p=0.0006, highly significant). Gentamicin treatment post LIPUS treatment also resulted in a significant decrease in CFU/ml compared to gentamicin alone.

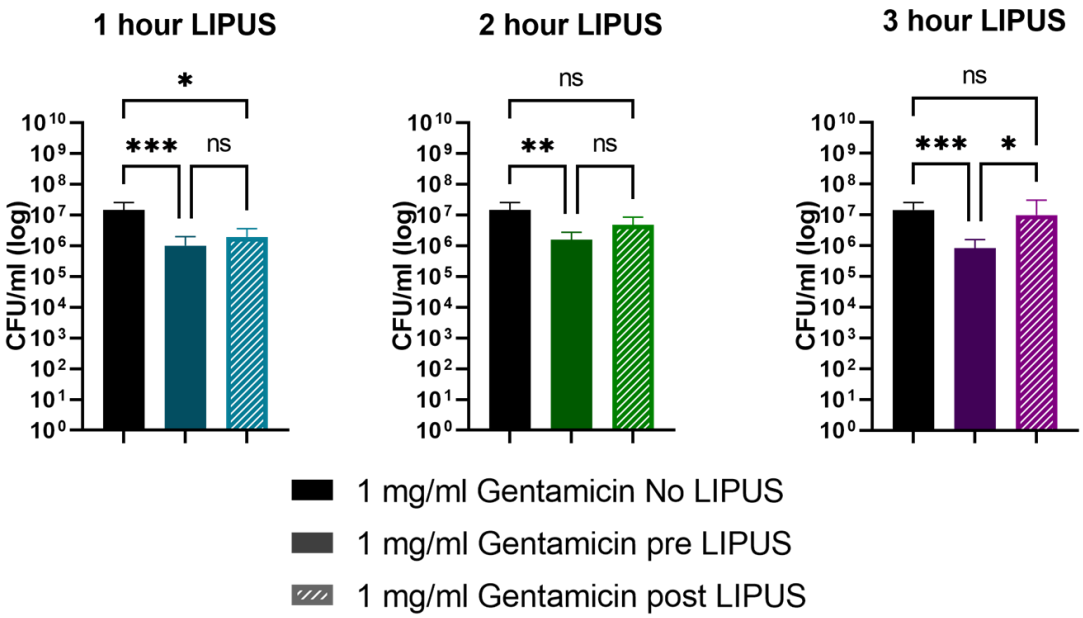

Figure 24: 1-day S. aureus SH1000 biofilms treated with 30 mW/cm² LIPUS for 1-, 2-, and 3-hours and 1 mg/ml gentamicin pre and post LIPUS treatment. Error bars = +/-SEM. Analysed using one-way ANOVA with Tukey's multiple comparison. ns = not significant, * = p-value <0.05, ** = p-value <0.01, *** = p-value <0.005. N=3.

Similarly, when treated with gentamicin 1mg/ml prior to 2-hour LIPUS treatment (**Figure 24b**), *S. aureus* SH1000 1-day biofilms had significantly increased sensitivity to gentamicin, when treated with gentamicin only the CFU/ml recovered from the biofilm was 1.45 x 10^7, compared to 1.58 x 10^6 CFU/ml when biofilms were exposed to gentamicin after LIPUS pretreatment (p=0.04, one-way ANOVA). When exposed to 1 mg/ml gentamicin post-LIPUS treatment the CFU/ml was 4.79 x10^6, this was lower than the untreated sample but not significantly lower (p=0.16). There was no significant difference in CFU/ml recovered from 1-day old biofilm treated with gentamicin pre or post LIPUS (p=0.62)

When treating the 1-day biofilm with 3-hour LIPUS treatment (**Figure 24c**) the CFU/ml of the gentamicin only sample was 1.45 x 10^7. When the biofilm was exposed to 1 mg/ml gentamicin pre LIPUS treatment the CFU decreased to 8.4 x 10^5 (p=0.0002, one-way ANOVA). When the biofilm was exposed to gentamicin post LIPUS treatment the CFU/ml was 9.93 x 10^6 (p=0.63, one-way ANOVA). When

comparing the gentamicin pre LIPUS treatment to the post LIPUS treatment the p-value was 0.019, indicating the difference in gentamicin sensitivity is significantly higher in samples exposed to gentamicin prior to LIPUS treatment.

4.1.2.2.2 3-day old S. aureus biofilm

S. aureus SH1000 biofilms were grown for 3-days and treated with LIPUS for 1-hour (**Figure 25a**) and treated with 1 mg/ml gentamicin. When the 3-day old biofilm was treated with 1 mg/ml gentamicin only the CFU/ml was 2.95 x 10^7, compared to gentamicin pre LIPUS 2.53 x 10^6 CFU/ml (p=0.048, one-way ANOVA). When the biofilm was exposed to gentamicin post LIPUS treatment the CFU/ml recovered from the biofilm was 6.67 x 10^5, significantly lower than the gentamicin only treated biofilm (p= 0.0002, one-way ANOVA). The increased gentamicin sensitivity in 3-day biofilms treated with 1-hour LIPUS is not dependent on the time of gentamicin exposure relative to LIPUS treatment.

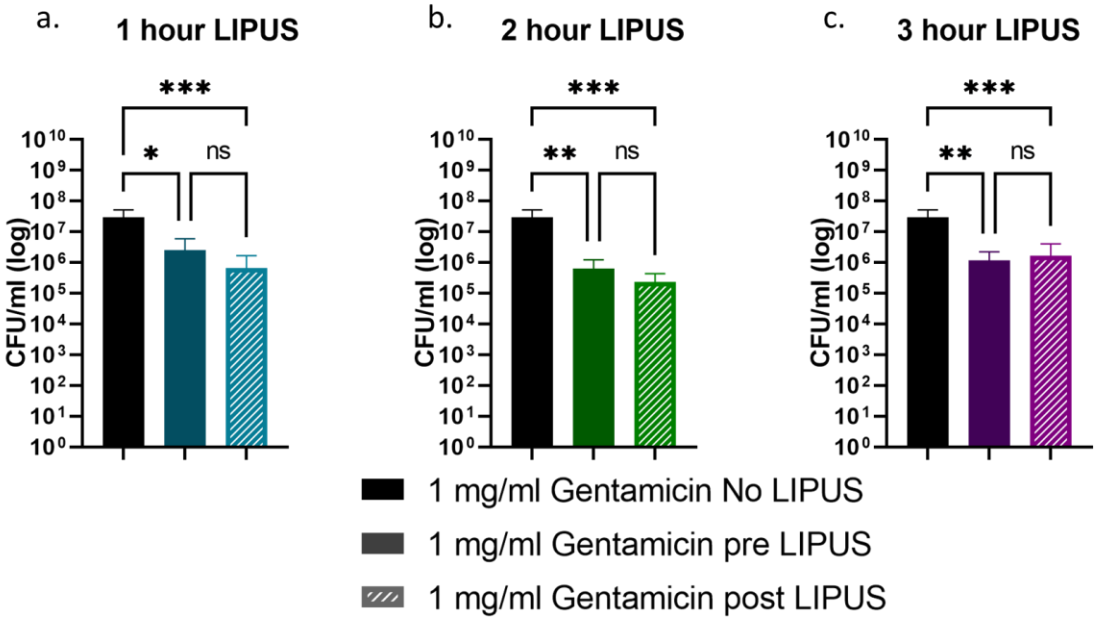

Figure 25: 3-day S. aureus SH1000 biofilms were treated with 30 mW/cm² LIPUS for 1-, 2-, and 3-hours and 1 mg/ml gentamicin pre and post LIPUS treatment. Error bars = +/-SEM. Analysed using one-way

ANOVA with Tukey's multiple comparison. ns = not significant, * = p-value <0.05, ** = p-value <0.01, *** = p-value <0.001. N=3.

When the 3-day *S. aureus* SH1000 biofilm was treated with 1 mg/ml gentamicin only the CFU was 2.95 x 10^7, however when treated with gentamicin prior to 2-hour LIPUS treatment (**Figure 25b**) the CFU/ml was 6.2 x 10^5 (p=0.006, one-way ANOVA). When the biofilm was exposed to gentamicin post LIPUS treatment the CFU/ml was 2.3 x 10^5, significantly reduced in comparison to the gentamicin only treated biofilm, (p=0.0001, one-way ANOVA). The number of bacteria in samples exposed to gentamicin pre LIPUS treatment was not significantly different to the number of bacteria in the biofilms exposed to gentamicin post LIPUS (p=0.89, one-way ANOVA). This suggests, as with 1-hour LIPUS treatment, that 2-hour LIPUS treatment increases gentamicin sensitivity, and the sensitivity was not dependent on whether the gentamicin exposure was pre or post LIPUS treatment.

A similar trend is identified in 3-day *S. aureus* SH1000 biofilms treated with LIPUS for 3-hours (**Figure 25c**). The 1 mg/ml gentamicin only treated biofilm had 2.95 x 10^7 CFU/ml, this was significantly reduced in biofilms treated with gentamicin pre LIPUS treatment with 1.15 x 10^6 CFU/ml (p=0.008, one-way ANOVA), showing increased gentamicin sensitivity with LIPUS treatment. When the biofilm was exposed to gentamicin post LIPUS treatment the CFU/ml was significantly reduced to 1.6 x 10^6 (p=0.0007, one-way ANOVA). The gentamicin exposure pre LIPUS treatment biofilm no significant changes in number of viable bacteria when compared to gentamicin exposure post LIPUS treatment (p >0.9999). This again suggests that LIPUS treatment does increase gentamicin sensitivity and not dependant when the biofilm is exposed to gentamicin in relation to LIPUS treatment.

4.1.2.2.3 5-day old S. aureus biofilm

5-day *S. aureus* SH1000 biofilms were treated with 1 mg/ml gentamicin and 1-hour 30 mW/cm^2 LIPUS (**Figure 26a**). When the 5-day biofilms were treated with

gentamicin only the CFU/ml was 3.3 x 10^7, however, this was significantly reduced when the biofilm was exposed to gentamicin pre LIPUS treatment with 4.9 x 10^3 CFU/ml (p=0.0008, one-way ANOVA). When the biofilm was exposed to gentamicin post LIPUS treatment the number of bacteria was not significantly reduced when compared to the gentamicin only treated biofilm with 1.1 x 10^4 CFU/ml (p=0.08, one-way ANOVA). This shows the 5-day old biofilm does have increased gentamicin sensitivity but only if the biofilm is challenged with gentamicin prior to LIPUS treatment.

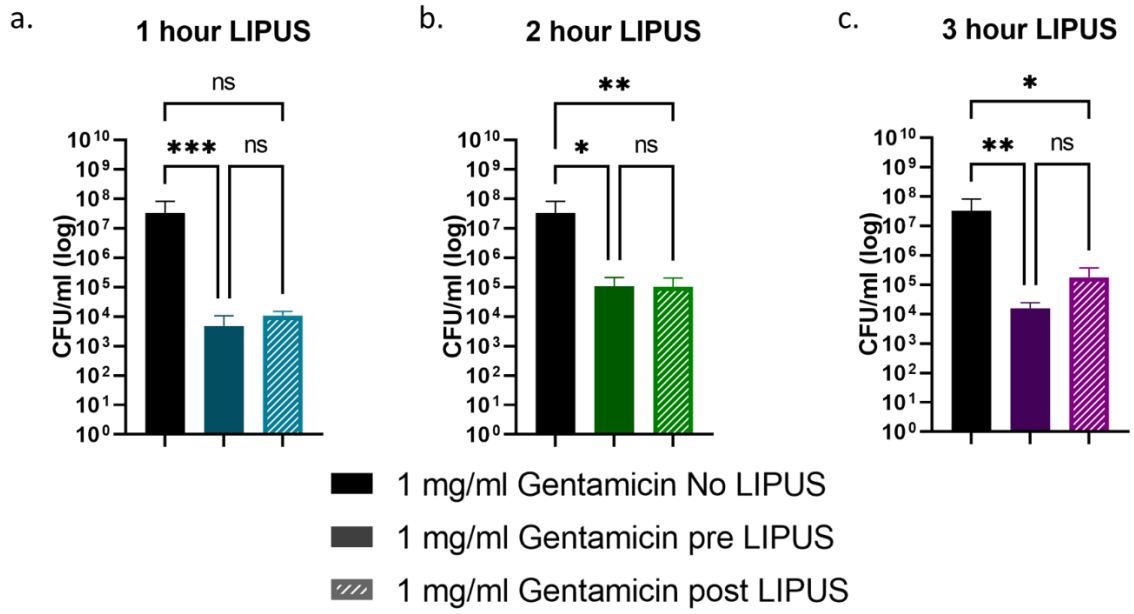

Figure 26: 5-day S. aureus SH1000 biofilms were treated with 30 mW/cm^2 LIPUS for 1-, 2-, and 3-hours and 1 mg/ml gentamicin pre and post LIPUS treatment. Error bars = +/-SEM. Analysed using one-way ANOVA with Tukey's multiple comparison. ns = not significant, * = p-value <0.05, ** = p-value <0.01, *** = p-value <0.001. N=3.

However, when the 5-day *S. aureus* SH1000 biofilm is treated with 2-hour LIPUS (**Figure 26b**), the increased sensitivity to gentamicin is not dependent on time of exposure in relation to the LIPUS treatment. The biofilm exposed to gentamicin only had CFU/ml of 3.26 x 10^7, while the gentamicin pre LIPUS biofilms had significantly reduced number of viable bacteria with 1.06 x 10^5 (p=0.013, one-way ANOVA). When the biofilm was exposed to gentamicin post LIPUS treatment the number of

bacteria was again significantly reduced when compared to the gentamicin only treated biofilms with a CFU/ml of 1.02 x 10^5 (p=0.007, one-way ANOVA). When the CFU/ml for the gentamicin pre and post LIPUS treatment the changes in CFU/ml were not significantly different (p>0.999, one-way ANOVA).

When the 5-day *S. aureus* SH1000 biofilm was treated with LIPUS for 3-hours, the gentamicin only treated biofilms had CFU/ml of 3.26 x 10^7 and the biofilms treated with 1 mg/ml gentamicin pre LIPUS treatment had a significantly lower CFU/ml of 1.57 x 10^4 (p=0.004, one-way ANOVA). The biofilms treated with LIPUS post gentamicin exposure also had a significantly reduced CFU/ml of 1.81 x 10^5, (p=0.02, one-way ANOVA). When comparing the pre and post LIPUS treated biofilms the changes in CFU were not significant (p>0.99, one-way ANOVA). This would indicate, again, that 3-hour 30 mW/cm^2 LIPUS treatment does increase the sensitivity of *S. aureus* SH1000 biofilms and is not dependent on time of gentamicin exposure in relation to LIPUS treatment.

4.1.2.2.4 7-day old S. aureus biofilm

7-day old *S. aureus* SH1000 biofilms were exposed to 1 mg/ml gentamicin and 1-hour 30 mW/cm^2 LIPUS treatment before disruption and serial dilution to calculate number of viable bacteria in the biofilm (**Figure 27a**). The number of viable bacteria recovered from the 7-day gentamicin only treated biofilm was 4.49 x 10^7, when the biofilm was exposed to gentamicin prior to LIPUS treatment the number of viable bacteria significantly decreased to 2.19 x 10^6 (p=0.02, one-way ANOVA). When the biofilm was treated with gentamicin post LIPUS treatment the number of viable bacteria was also significantly reduced to 1.5 x 10^5, (p=0.0001, one-way ANOVA). The number of viable bacteria from the gentamicin pre LIPUS biofilm was not significantly different to the gentamicin post LIPUS (p=0.29, one-way ANOVA). This shows increased gentamicin sensitivity in LIPUS treated biofilms, not dependent on the time of gentamicin challenge in relation to the LIPUS treatment.

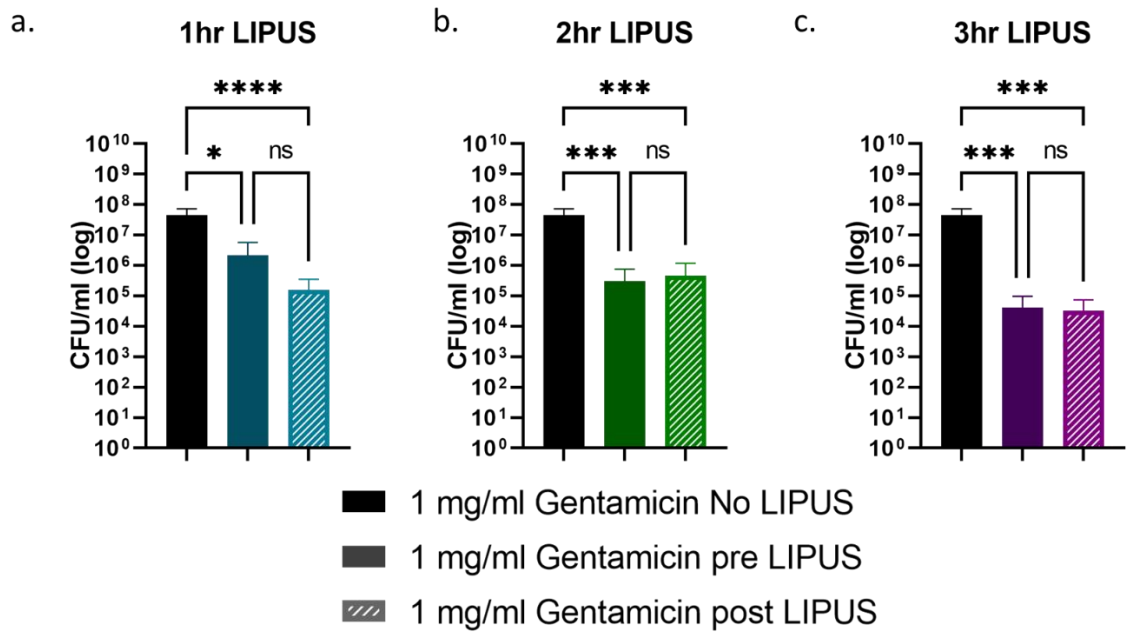

Figure 27: 7-day S. aureus SH1000 biofilms were treated with 30 mW/cm^2 LIPUS for 1-, 2-, and 3-hours and 1 mg/ml gentamicin pre and post LIPUS treatment. Error bars = +/-SEM. Analysed using one-way ANOVA with Tukey's multiple comparison. ns = not significant, * = p-value <0.05, ** = p-value <0.01, *** = p-value <0.001, **** = p-value <0.0001. N=3.

When the 7-day *S. aureus* SH1000 biofilm was treated with LIPUS for 2-hours, The gentamicin only treated biofilm had CFU/ml of 4.49 x 10^7, the number of viable bacteria significantly decreased with gentamicin exposure pre LIPUS treatment with a CFU/ml of 3.06 x 10^5, this was a significant reduction and the p-value calculated was (p=0.0047, one-way ANOVA). When the biofilms were exposed to gentamicin post LIPUS treatment the number of viable bacteria was again significantly reduced when compared to the gentamicin only treated biofilm with a CFU/ml of 4.73 x 10^5, (p=0.02, one-way ANOVA). When comparing the difference in CFU/ml of the gentamicin pre and post LIPUS treatment the difference was not significant (p>0.999, one-way ANOVA). This indicates an increase in gentamicin sensitivity with LIPUS treatment when gentamicin treatment was applied both pre and post LIPUS treatment.

In 7-day *S. aureus* SH1000 biofilms treated with 3-hour 30 mW/cm^2 LIPUS (**Figure 27c**) the CFU/ml for the gentamicin only treated biofilm was 4.49 x 10^7, which

significantly reduced when the gentamicin was applied pre LIPUS treatment to 4.16 x 10^4 (p=0.001, one-way ANOVA). When the biofilm was exposed to gentamicin post LIPUS treatment the number of viable bacteria again was significantly reduced in comparison to the gentamicin only treated biofilm with a CFU/ml of 3.29 x 10^4 (p=0.0009, one-way ANOVA). The difference in CFU/ml for the biofilms exposed to gentamicin pre and post LIPUS treatment was not significant (p>0.999, one-way ANOVA). Again, this would indicate an increase in gentamicin sensitivity when biofilms are treated with LIPUS which in independent of the time of gentamicin exposure in relation to the LIPUS treatment.

4.1.2.3 Vancomycin and LIPUS

Results from this section are summarised in **Table 15**.

4.1.2.3.1 1-day old S. aureus biofilm

S. aureus SH1000 biofilms were treated with 1-hour LIPUS and 2 mg/ml vancomycin (**Figure 28a**). When the biofilms were treated with vancomycin only the number of viable bacteria recovered was not significantly different to the number of viable bacteria recovered from the vancomycin pre LIPUS treatment biofilms (4.58 x 10^8 CFU/ml vs 8.12 x 10^8, p>0.99, one-way ANOVA). When the vancomycin was added post LIPUS treatment the CFU/ml was 7.86 x 10^8, again this was not significantly different to the vancomycin only treated biofilms or the biofilms treated with vancomycin pre LIPUS treatment with p-values of 0.54 and 0.33 respectively.

The same is seen in the *S. aureus* SH1000 biofilms treated with 2-hour LIPUS (**Figure 28b**). The biofilms treated with 2mg/ml vancomycin did not yield significantly different number of viable cells when compared with vancomycin only treated biofilms (5.02 x 10^8 vs 4.58 x 10^8, p>0.99, one-way ANOVA). Exposure to vancomycin post LIPUS treatment the changes in CFU/ml (6.91 x 10^8) was not significantly different to the vancomycin only treated biofilm (p=0.37, one-way ANOVA) or the vancomycin pre LIPUS treatment (p=0.96, a one-way ANOVA).

When the *S. aureus* SH1000 biofilms were treated with LIPUS for 3-hours (**Figure 28c**) the CFU/ml recovered from the biofilms exposed to vancomycin only (4.59 x 10^8) was which was not significantly different to the vancomycin pre LIPUS CFU/ml (2.08 x 10^8) ($p>0.999$, one-way ANOVA). The CFU/ml recovered from the biofilms treated with vancomycin post LIPUS treatment was 5.12 x 10^8 which was not significantly higher than either the vancomycin only treated biofilms ($p=0.37$, one way ANOVA) or the vancomycin pre LIPUS treated biofilms ($p=0.96$, one-way). This would indicate that 30 mW/cm^2 LIPUS treatment of 1-, 2-, and 3-hours does not change the vancomycin sensitivity of *S. aureus* SH1000 1-day biofilms.

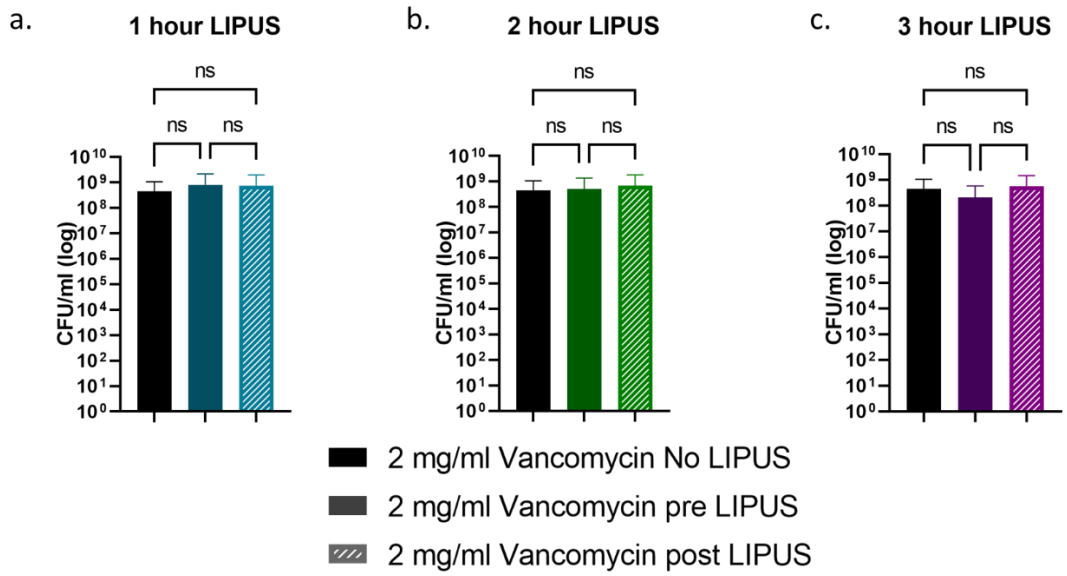

Figure 28: 1-day S. aureus SH1000 biofilm treated with 30 mW/cm^2 LIPUS for 1-, 2-, and 3-hours and treated with 2 mg/ml vancomycin pre and post LIPUS treatment. Error bars = +/-SEM. Analysed using one-way ANOVA with Tukey's multiple comparison. ns= not significant. N=3

4.1.2.3.2 3-day old S. aureus biofilm

S. aureus SH1000 biofilms were grown for 3-days and treated with 1-hour LIPUS and 2 mg/ml vancomycin (**Figure 29a**). When the biofilms were treated with vancomycin only, the viable bacteria recovered was 9.57 x 10^7 CFU/ml, when the

biofilm was treated with vancomycin pre LIPUS treatment the CFU/ml recovered was 2.29 x 10^7, this change in CFU/ml was not significant (p=0.6, one-way ANOVA). When the vancomycin was added post LIPUS treatment the CFU/ml was 4.49 x 10^7, again this was not significantly different to the vancomycin only treated biofilms (p >0.999) or the biofilms treated with vancomycin pre LIPUS treatment (p=0.89).

When the 3-day *S. aureus* SH1000 biofilms treated with 2 mg/ml vancomycin prior to LIPUS treatment for 2-hours (**Figure 29b**) the CFU/ml was 2.62 x 10^8 which is higher than the 9.57 x 10^7 seen in vancomycin only treated biofilms but not significantly higher with a p-value of 0.22. When the biofilm was exposed to vancomycin post LIPUS treatment the CFU/ml was 2.12 x 10^8 which is not significantly different to both the vancomycin only treated biofilms (p=0.76, one-way ANOVA) and the biofilm treated with vancomycin pre LIPUS treatment (p>0.999, one-way ANOVA).

The 3-day *S. aureus* SH1000 biofilms were treated with vancomycin only, with a CFU/ml of 9.57 x 10^7 this was not significantly different from the CFU/ml (2.72 x 10^8) of the biofilms exposed to vancomycin prior to 3-hour LIPUS (p=0.25, one-way ANOVA) (**Figure 29c**). The CFU/ml recovered from the biofilms treated with vancomycin post LIPUS treatment was 2.81 x 10^8 which was not significantly higher than either the vancomycin only treated biofilm (p=0.25, one-way ANOVA) or the vancomycin pre LIPUS treated biofilm (p<0.999, one-way ANOVA). This would indicate that 30 mW/cm^2 LIPUS treatment of 1-, 2-, and 3-hours does not change the vancomycin sensitivity of *S. aureus* SH1000 3-day biofilms.

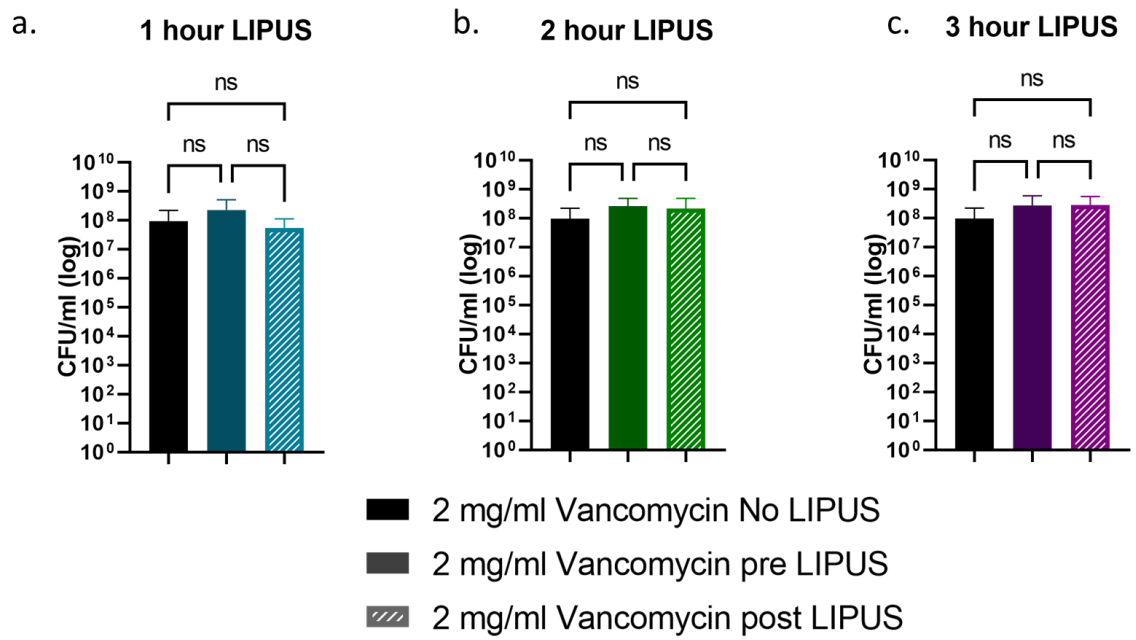

Figure 29: 3-day S. aureus SH1000 biofilm treated with 30 mW/cm² LIPUS for 1-, 2-, and 3-hours and treated with 2 mg/ml vancomycin pre and post LIPUS treatment. Error bars = +/-SEM. Analysed using one-way ANOVA with Tukey's multiple comparison. ns= not significant. N=3

4.1.2.3.3 5-day old S. aureus biofilm

S. aureus SH1000 biofilms grown for 5-days were treated with 1-hour LIPUS and 2 mg/ml vancomycin (**Figure 30a**). When the biofilms were treated with vancomycin only the number of bacteria recovered was 3.62 x 10^7 CFU/ml, this was not significantly reduced with vancomycin pre LIPUS treatment biofilms, the CFU/ml was 2.88 x 10^7 (p=0.65, one-way ANOVA). When the vancomycin was added post LIPUS treatment the CFU/ml was 1.85 x 10^7, again this was not significantly different to the vancomycin only treated biofilms (p=0.1007, one-way ANOVA) or the biofilms treated with vancomycin pre LIPUS treatment (p=0.44, one-way ANOVA).

When the 5-day *S. aureus* SH1000 biofilms were treated with 2-hour LIPUS (**Figure 30b**). The CFU/ml for biofilms treated with 2mg/ml vancomycin only was 3.62 x 10^7 CFU/ml, which was not significant different to the CFU/ml of the 2mg/ml vancomycin pre LIPUS treatment, CFU/ml (2.23 x 10^7, p=0.41, one-way ANOVA). When the

biofilms were exposed to vancomycin post LIPUS treatment the CFU/ml was 1.23 x 10^7 which is not significantly different to both the vancomycin only treated biofilms (p=0.69, one-way ANOVA) and the biofilms treated with vancomycin pre LIPUS treatment (p=0.56, one-way ANOVA).

When the 5-day *S. aureus* SH1000 biofilms were treated with LIPUS for 3-hours (**Figure 30c**) the CFU/ml recovered from the biofilms exposed to vancomycin only was 3.62 x 10^7 CFU/ml, this was not significantly reduced in the vancomycin pre LIPUS treatment biofilms, 1.36 x 10^7 CFU/ml (p=0.25, one-way ANOVA). When the biofilm was treated with vancomycin post LIPUS treatment was 2.82 x 10^7 which was not significantly higher than either the vancomycin only treated biofilms (p=0.25, one-way ANOVA) or the vancomycin pre LIPUS treated biofilms (p>0.999, one-way ANOVA). This shows that 30 mW/cm^2 LIPUS treatment of 1-, 2-, and 3-hours does not change the vancomycin sensitivity of *S. aureus* SH1000 5-day biofilms.

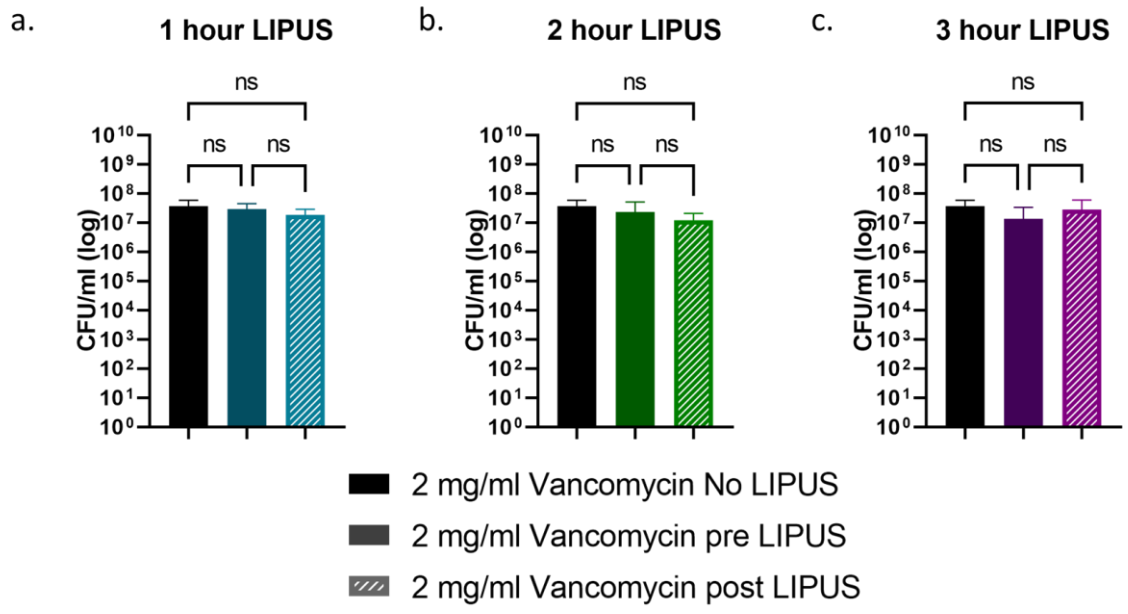

Figure 30: 5-day S. aureus SH1000 biofilm treated with 30 mW/cm^2 LIPUS for 1-, 2-, and 3-hours and treated with 2 mg/ml vancomycin pre and post LIPUS treatment. Error bars = +/-SEM. Analysed using one-way ANOVA with Tukey's multiple comparison. ns= not significant. N=3

4.1.2.3.4 7-day old S. aureus biofilm

7-day *S. aureus* SH1000 biofilms were treated with 1-hour LIPUS and 2 mg/ml vancomycin (**Figure 31a**). When the biofilms were treated with vancomycin only the CFU/ml was 3.78 x 10^7, when the biofilms were treated with vancomycin pre LIPUS treatment the CFU/ml was 3.07 x 10^7, the change in CFU/ml was not a significant reduction. When the vancomycin was added post LIPUS treatment the CFU/ml was 3.28 x 10^7. When analysed using a one-way ANOVA with multiple comparisons the p-value for all comparisons for the 1-hour LIPUS treatment was >0.999.

When 7-day *S. aureus* SH1000 biofilms were treated with 2-hour LIPUS (**Figure 31b**) there was no significant change in CFU/ml of all test conditions. The CFU/ml for biofilms treated with 2mg/ml vancomycin only was 3.78 x 10^7 when compared to 4.58 x 10^7 CFU/ml in vancomycin only treated biofilms this was not a significant reduction in viable bacteria (p=0.41, one-way ANOVA). When the biofilms were exposed to vancomycin post LIPUS treatment the CFU/ml was 1.58 x 10^7, this was again not a significant reduction in CFU with p-value >0.999 when compared to the vancomycin only treated biofilms (p>0.999, one-way ANOVA) or the vancomycin pre LIPUS biofilms (p=0.51, one-way ANOVA).

When the *S. aureus* SH1000 biofilms were treated with LIPUS for 3-hours (**Figure 31c**) the CFU/ml recovered from the biofilms exposed to vancomycin only was 3.78 x 10^7 which was not significantly different to the CFU/ml recovered from the the biofilms exposed to vancomycin pre LIPUS, 3.98 x 10^7 CFU/ml (p=0.83, one-way ANOVA). The CFU/ml recovered from the biofilms treated with vancomycin post LIPUS treatment was 2.82 x 10^7 which was not significantly higher than either the vancomycin only treated biofilm (p>0.999, one-way ANOVA) or the vancomycin pre LIPUS treated biofilm (p=0.65, one-way ANOVA). This shows that 30 mW/cm^2 LIPUS treatment of 1-, 2-, and 3-hours does not change the vancomycin sensitivity of *S. aureus* SH1000 7-day biofilms.

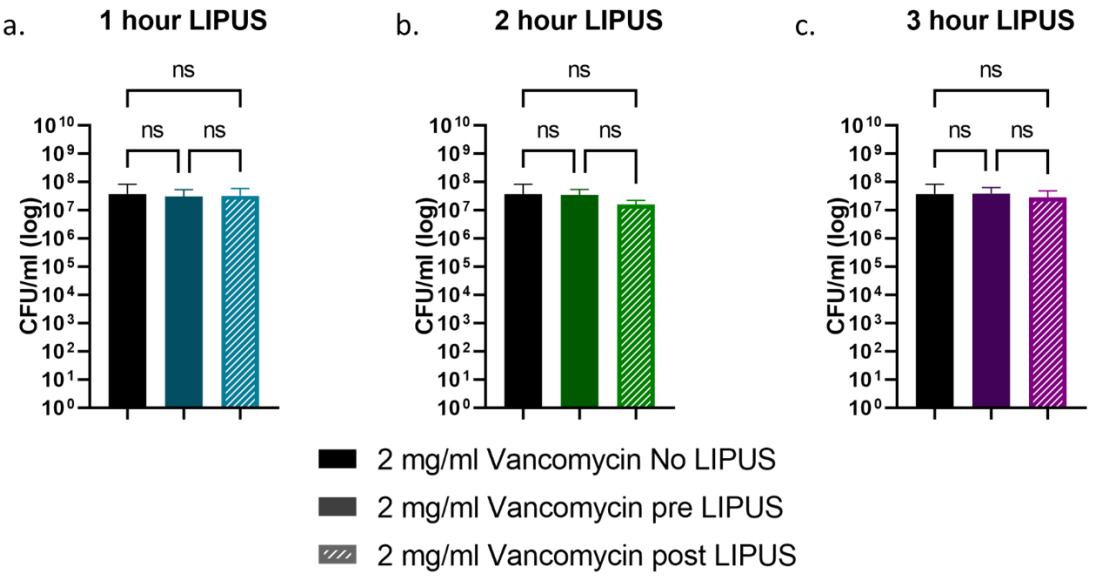

Figure 31: 7-day S. aureus SH1000 biofilm treated with 30 mW/cm^2 LIPUS for 1-, 2-, and 3-hours and treated with 2 mg/ml vancomycin pre and post LIPUS treatment. Error bars = +/-SEM. Analysed using one-way ANOVA with Tukey's multiple comparison. ns= not significant. N=3

Table 15: Summary of CFU/ml and p-value against untreated biofilms of 1-,3-, 5- and 7-day S. aureus SH1000 biofilms treated with LIPUS and gentamicin or vancomycin. Analysed using one-way ANOVA with Tukey's multiple comparison.

Age of Biofilm (days)	LIPUS Time (hours)	Antibiotic Pre/Post LIPUS	Gentamicin (mg/ml)	Vancomycin (mg/ml)	Average CFU/ml	p-value (against no LIPUS)
1	0		1		$1.45x10^7$	
1	1	Pre	1		$1x10^6$	**0.0006**
1	1	Post	1		$1.93x10^6$	0.847
1	2	Pre	1		1.58×10^6	**0.04**
1	2	Post	1		4.79×10^6	0.16
1	3	Pre	1		8.4×10^5	**0.0002**
1	3	Post	1		9.93×10^6	0.63
1	0			2	4.58×10^8	
1	1	Pre		2	8.12×10^8	>0.999
1	1	Post		2	7.86×10^8	0.54
1	2	Pre		2	5.02×10^8	>0.999
1	2	Post		2	6.91×10^8	0.37
1	3	Pre		2	2.08×10^8	>0.999
1	3	Post		2	5.12×10^8	0.37
3	0		1		2.95×10^7	
3	1	Pre	1		2.53×10^6	**0.048**
3	1	Post	1		6.67×10^5	**0.0002**
3	2	Pre	1		6.2×10^5	**0.0006**
3	2	Post	1		2.3×10^5	**0.0001**
3	3	Pre	1		1.15×10^6	**0.008**
3	3	Post	1		1.6×10^6	**0.0007**
3	0			2	9.57×10^7	
3	1	Pre		2	2.29×10^7	0.6

3	1	Post		2	4.49×10^7	>0.999
3	2	Pre		2	2.62×10^8	0.22
3	2	Post		2	2.12×10^8	0.76
3	3	Pre		2	2.72×10^8	0.25
3	3	Post		2	2.81×10^8	0.25
5	0		1		3.3×10^7	
5	1	Pre	1		4.9×10^3	**0.0008**
5	1	Post	1		1.1×10^4	0.08
5	2	Pre	1		1.06×10^5	**0.013**
5	2	Post	1		1.02×10^5	**0.007**
5	3	Pre	1		1.57×10^4	**0.004**
5	3	Post	1		1.81×10^5	**0.02**
5	0			2	3.62×10^7	
5	1	Pre		2	2.88×10^7	0.65
5	1	Post		2	1.85×10^7	0.1007
5	2	Pre		2	2.23×10^7	0.41
5	2	Post		2	1.23×10^7	0.69
5	3	Pre		2	1.36×10^7	0.25
5	3	Post		2	2.82×10^7	0.25
7	0		1		4.49×10^7	
7	1	Pre	1		2.19×10^6	**0.02**
7	1	Post	1		1.5×10^5	**0.0001**
7	2	Pre	1		3.06×10^5	**0.0047**
7	2	Post	1		4.73×10^5	**0.02**
7	3	Pre	1		4.16×10^4	**0.001**
7	3	Post	1		3.29×10^4	**0.0009**
7	0			2	3.78×10^7	

7	1	Pre		2	3.07×10^7	>0.999
7	1	Post		2	3.28×10^7	>0.999
7	2	Pre		2	4.58×10^7	0.41
7	2	Post		2	1.58×10^7	>0.999
7	3	Pre		2	3.98×10^7	0.83
7	3	Post		2	2.82×10^7	>0.999

4.1.3 Structure

Having observed increased sensitivity of biofilms to gentamicin when treated with LIPUS, the structures of biofilms at different stages of maturity were investigated with and without LIPUS treatment using confocal microscopy to ascertain if there were any structural changes in biofilm following LIPUS which may allow easier diffusion of antibiotics through the biofilm and extracellular matrix. Biofilms grown for 1- and 7-days were treated with and without LIPUS for 2-hours before being stained with polysaccharide and protein stains and visualised.

4.1.3.1.1 1-day S. aureus biofilm

When a 1-day biofilm was treated with 30 mW/cm^2 LIPUS for 2-hours there were no noticeable visual differences in the biofilms (**Figure 32a**). The bacteria within the biofilms were well dispersed with areas of higher densities of bacteria visible. These areas of higher densities of bacteria were visualised using 3D surface plots (**Figure 32b** & **c**). with raised areas on the surface indicating higher biofilm volume in those areas. When comparing the 3D surface plots of the untreated biofilms with the LIPUS treated biofilms there was no visual difference, with both containing several areas of high biofilm volume surrounded by lower biofilm volume. This would indicate that 1-day biofilms structure is not altered during 2 hours LIPUS treatment.

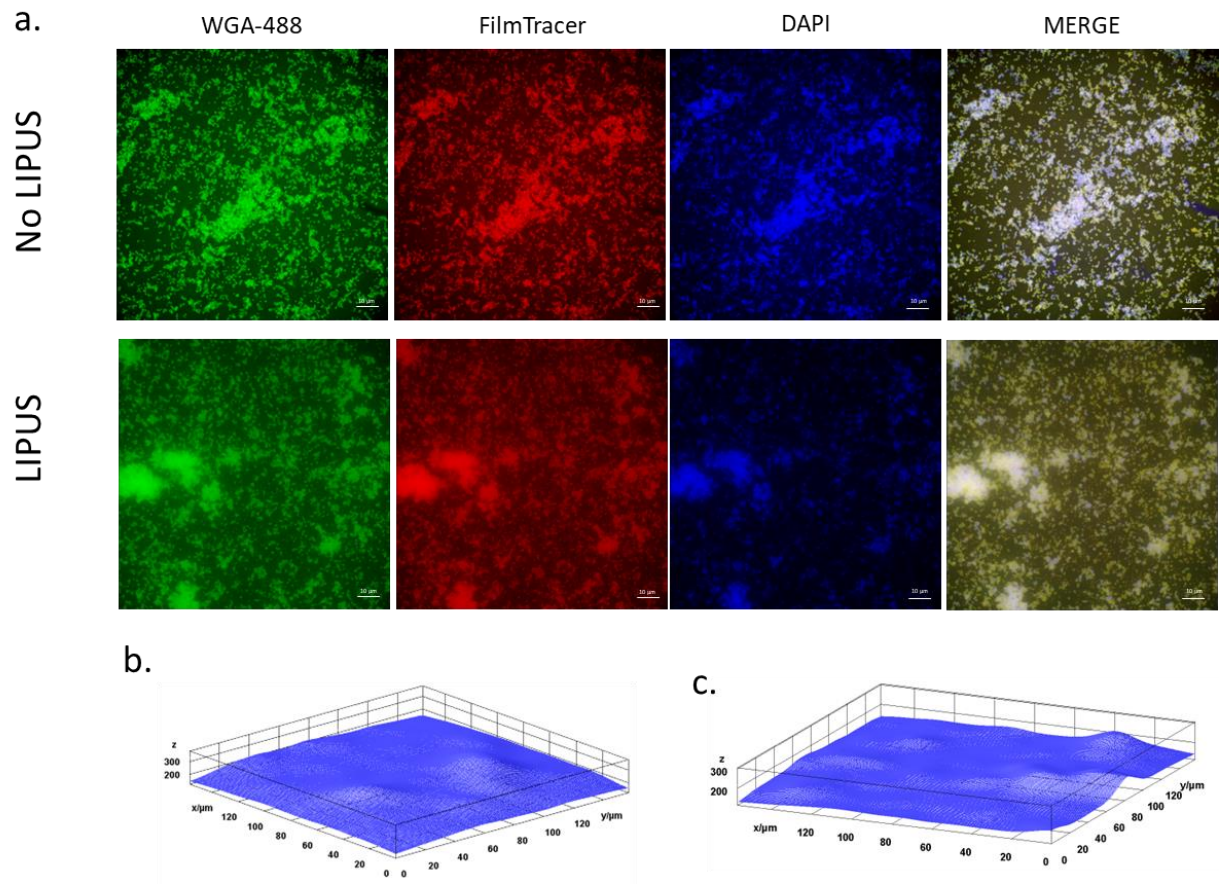

Figure 32: Confocal images of 1-day old S. aureus SH1000 biofilms with and without 30 mW/cm^2 LIPUS treatment (a). The surface plots of the biofilms were analysed using ImageJ. No LIPUS treatment biofilm (b) and LIPUS treated biofilm (c). Scale bar = 10 µm. n=2 Mag = 100x

4.1.3.1.2 7-day S. aureus biofilm

In the 7-day biofilms there was higher density of bacteria within the biofilms when comparing to the 1-day old biofilms (**Figure 32**). There is no visual difference in the biofilms when treated with 30 mW/cm^2 LIPUS for 2-hours when comparing to the untreated biofilms (**Figure 33a**). As with the 1 day old biofilms the volume of the biofilms was visualised using 3D surface plots (**Figure 33b** & **c**) When comparing the 3D surface plots of the untreated biofilms with the LIPUS treated biofilms there was no visual difference, with both containing several areas of high biofilm volume surrounded by lower biofilm volume. This would indicate that 7-day biofilms structure is also not altered during 2 hours LIPUS treatment.

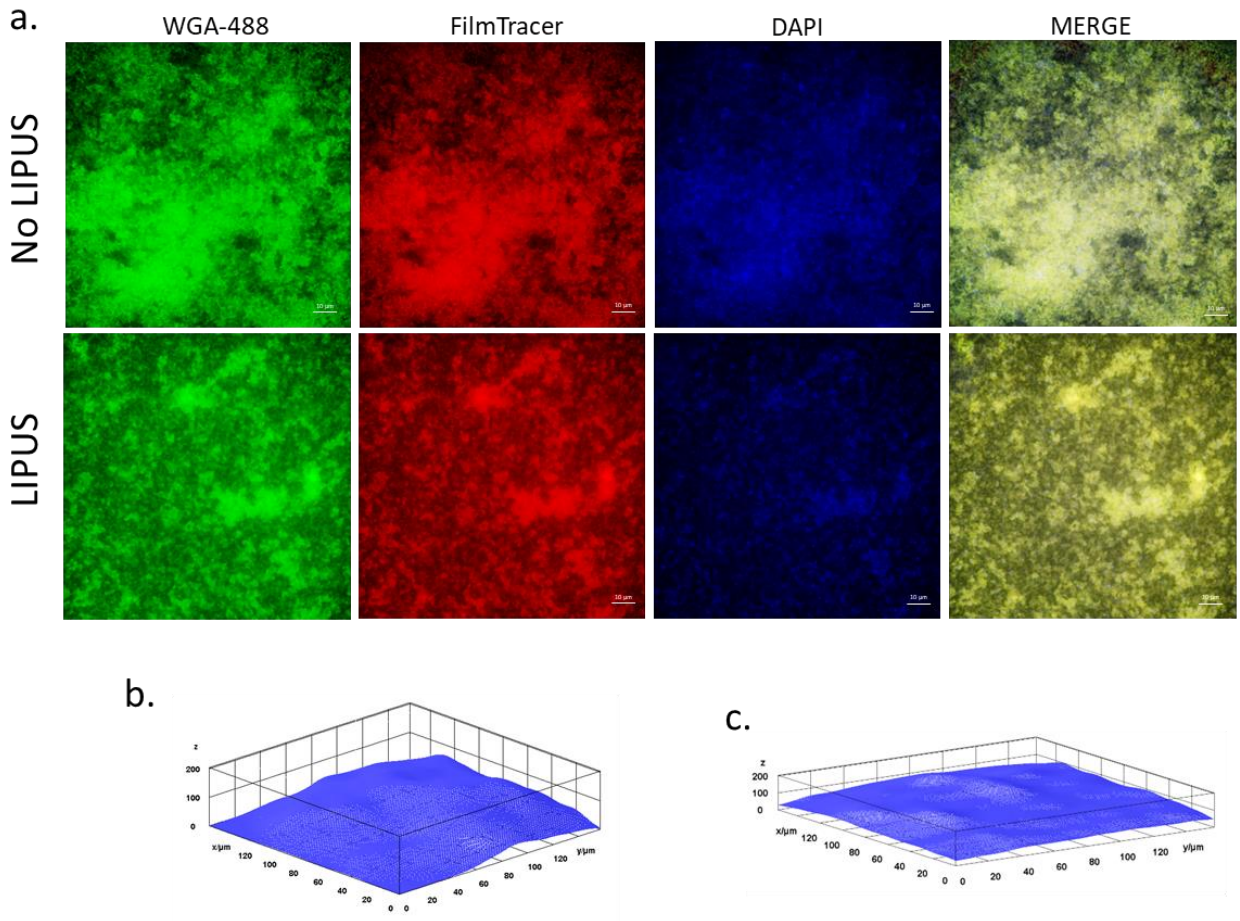

Figure 33: Confocal images of 7-day old S. aureus SH1000 biofilms with and without 30 mW/cm² LIPUS treatment (a). The surface plots of the biofilms were analysed using ImageJ. No LIPUS treatment biofilm (b) and LIPUS treated biofilm (c). Scale bar = 10 µm. Mag = 100x

4.1.4 Permeability

The permeability of biofilms and bacterial cells when treated with LIPUS were examined. In the biofilms the ability of FITC-dextran to pass through a biofilm grown in 6-well plate inserts for 1-, 3-, 5-, and 7-days was assessed by measuring fluorescence of the media surrounding the 6-well plate insert and comparing LIPUS treated biofilms with untreated biofilms. The permeability of bacterial membranes was assessed using both the ability of PI to enter the cell and β-galactosidase leakage into the growth media.

4.1.4.1 Biofilm permeability post-LIPUS

4.1.4.1.1 1-day old S. aureus biofilm

In this and following sections, RFU values (relative fluorescence units) refer to a mean RFU value from ≥3 wells.

S. aureus SH1000 biofilms were grown in well-inserts, media containing 4 kDa FITC-dextran (**Figure 34a**) was added to the insert and the fluorescence from the well surrounding the insert was measured at 1-, 2-, and 3-hour timepoints, changes in fluorescence would indicate the permeation of the biofilm by the FITC-dextran. After an hour of LIPUS treatment, the fluorescence of the media in the treated wells was a mean of 2857 RFU, while the untreated wells had a mean of 1757 RFU (not significant, p=0.088). After 2 hours of LIPUS the fluorescence in the LIPUS treated wells was significantly higher level than the untreated wells (4986 RFU vs 2051 RFU, p=0.0008). At the 3-hour timepoint the fluorescence in the untreated wells was 4011 RFU while the fluorescence in the LIPUS treated wells was 7046 RFU, while this was higher than the untreated wells, it was not significantly higher (p= 0.064).

When the higher molecular weight FITC-dextran was used (70 kDa, **Figure 34b**) the levels of fluorescence were lower than that of the lower weight FITC-dextran, indicating the molecules were not permeating the biofilm as well. At the 1-hour timepoint the fluorescence level in the untreated biofilm was not significantly different to the LIPUS treated wells (1076 RFU vs 820 RFU, p=0.72). After 2-hours LIPUS treatment the fluorescence of the untreated sample was not significantly lower than the fluorescence levels of the LIPUS treated wells (1052 vs 1753, p=0.22). At the end of the 3-hour treatment the fluorescence level had increased to 2873 RFU in the untreated wells, compared to the 3991 RFU in the LIPUS treated sample, this was a significant change (p=0.033).

The highest molecular weight FITC-dextran used was 250 kDa (**Figure 34c**), as with the 70 kDa, the fluorescence was lower indicating the molecules could not permeate the biofilm as well as the 4 kDa FITC-dextran. At the 1-hour timepoint the fluorescence level was still low with 54 RFU, in the LIPUS treated wells the fluorescence was also low with almost undetectable levels, the difference was not significant (p=0.39). After 2-hours the fluorescence of the untreated sample was not significantly different to the fluorescence in the LIPUS treated wells (763 RFU vs 534 RFU, p=0.77). At the end of the 3-hour treatment the fluorescence level had increased to 2163 RFU in the untreated wells, compared to the 1812 RFU in the LIPUS treated sample, this was not a significant change in fluorescence between the LIPUS treated wells and the untreated wells (p=0.25). In 1-day *S. aureus* SH1000 30 mW/cm^2 LIPUS treatment for 2-hours increased the ability of small weight molecules to pass through the biofilm, this was not observed with 1- and 3-hour LIPUS. LIPUS treatment does not increase the permeability of larger molecules through the *S. aureus* SH1000 biofilm.

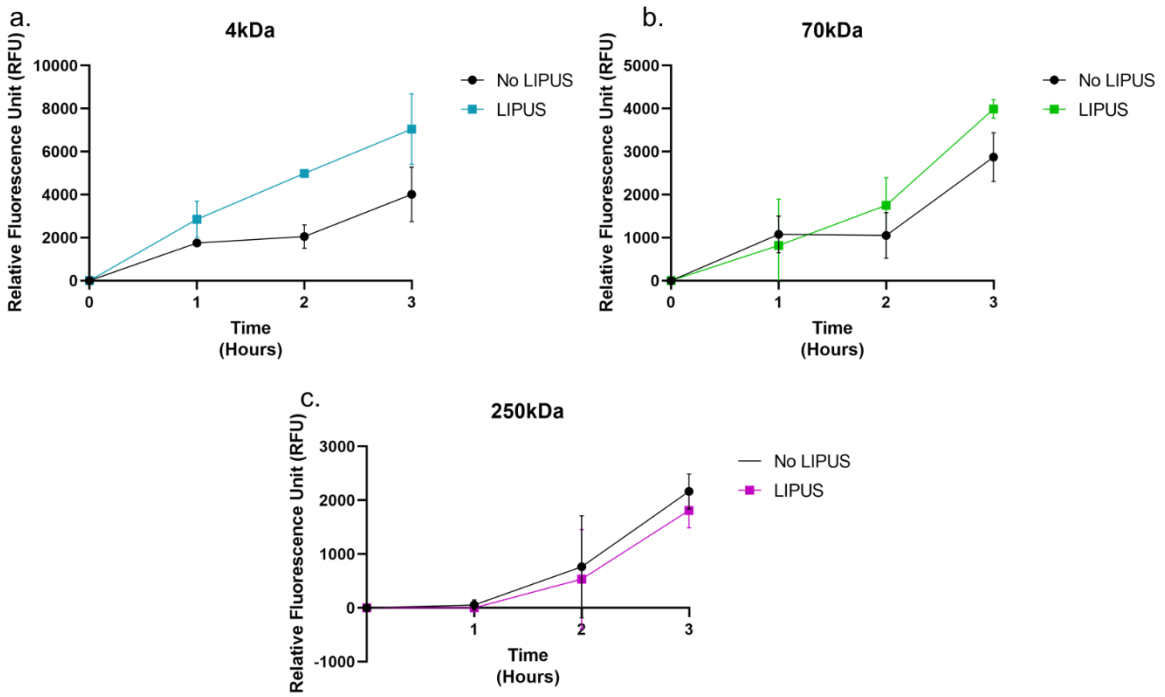

Figure 34: 1-day S. aureus SH1000 biofilm in 6-well inserts treated with 30 mW/cm2 LIPUS for 1-, 2-, and 3-hours with BHI supplemented with 4kDa (a), 70kDa (b) and 250kDa (c) FITC-Dextran, changes in

fluorescence in well surrounding the well-inserts were measured Ex:495nm Em:517nm. Error bars = +/- SEM. Analysed using multiple t-test. N=3

4.1.4.1.2 3-day old S. aureus biofilm

In 3-day *S. aureus* SH1000 biofilms treated with 30 mW/cm^2 LIPUS in the presence of low molecular weight FITC-dextran (4 kDa, **Figure 35a**), the increases in fluorescence of the media within the wells increased over the 3-hour treatment period, with the treated and untreated wells having similar levels of fluorescence throughout the treatment. At 1-hour the fluorescence in the untreated wells was not significantly different to the fluorescence in the LIPUS treated wells (4131 RFU vs 4181 RFU, p=0.93). By the 2-hour timepoint the fluorescence had increased in both the untreated and LIPUS treated wells, 7499 RFU and 7581 RFU respectively (p=0.85). At the end of the LIPUS treatment period the fluorescence had increased to 8561 RFU in the untreated well and 9407 RFU in the wells treated with LIPUS (p=0.2). The changes in the fluorescence levels were not statistically significant at any point in the 3-hour LIPUS treatment.

As with the 1-day biofilms, a decrease in fluorescence was observed in larger molecular weight FITC-dextran when compared to the lower weight FITC-dextran in the 3-day biofilms. In the wells containing 70 kDa FITC-dextran (**Figure 35b**), the levels of fluorescence increased over the 3-hour LIPUS treatment, with the levels of fluorescence remaining similar between the untreated and treated wells. At 1-hour the fluorescence in the untreated well was not significantly different to the LIPUS treated wells (770 RFU vs 759 RFU, p=0.95). After 2-hours the fluorescence had further increased to 2370 RFU in the untreated wells and 3071 in the LIPUS treated well (p=0.96). By the end of the LIPUS treatment at 3-hours the fluorescence in the untreated wells had reached 3202 RFU while the LIPUS treated wells had reached 3661 RFU (p= 0.12). Throughout the 3-hour LIPUS treatment there was no significant changes to the ability for 70 kDa FITC-dextran to permeate the 3-day *S. aureus* SH1000 biofilm.

When the 250 kDa FITC-dextran (**Figure 35c**) was used to measure the permeability of the *S. aureus* SH1000 treated with 30 mW/cm^2 LIPUS, there was again, a steady increase in fluorescence over the course of the experiment in both the LIPUS treated wells and the untreated wells with little variation in fluorescence between the treated and untreated samples. At 1-hour the fluorescence in the untreated wells was 717 RFU, while the LIPUS treated wells was 1068 RFU (p=0.41). After 2-hours the fluorescence had increased to 1987 RFU in the untreated well and 1969 RFU in the LIPUS treated wells (p=0.82). By 3-hour timepoint the fluorescence in the untreated wells had reached 2556 RFU while the LIPUS treated wells had reached 3661 RFU (p= 0.12). With no significant changes in fluorescence, LIPUS does not increase the ability of 250 kDa FITC-dextran to move through 3-day *S. aureus* SH1000 biofilms. Overall, the permeability of 3-day *S. aureus* SH1000 biofilms does not alter with the 30 mW/cm^2 LIPUS treatment.

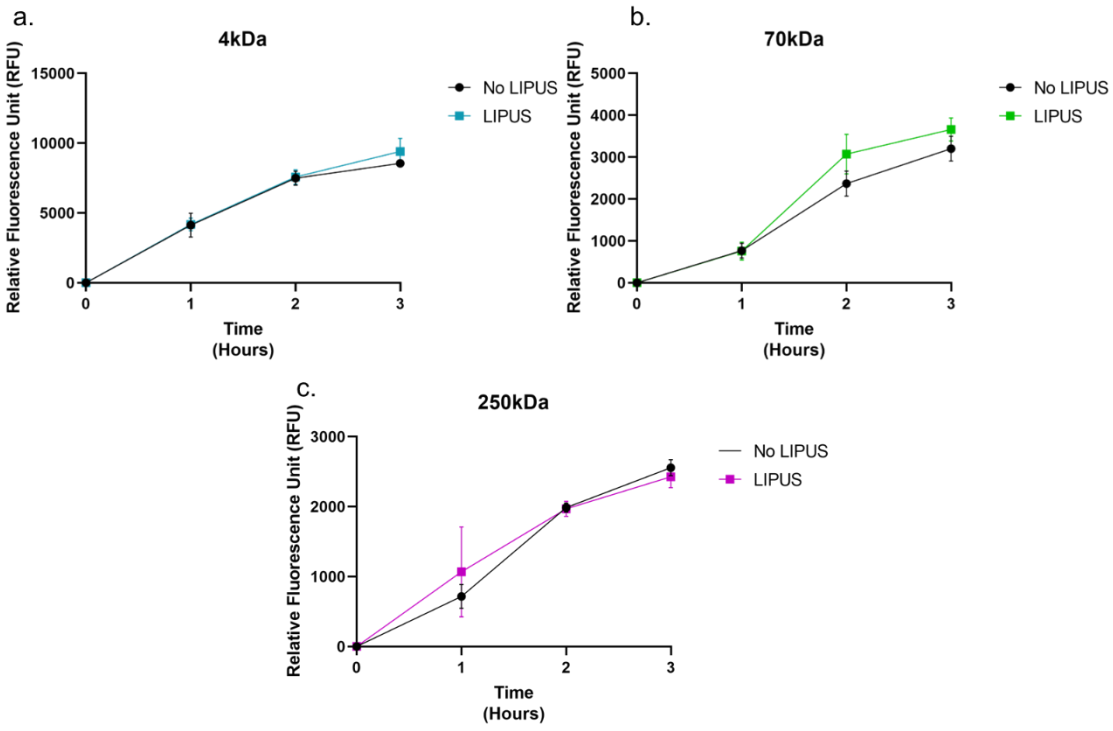

Figure 35: 3-day S. aureus SH1000 biofilm in 6-well inserts treated with 30 mW/cm^2 LIPUS for 1-, 2-, and 3-hours with BHI supplemented with 4kDa (a), 70kDa (b) and 250kDa (c) FITC-Dextran, changes in fluorescence in well surrounding the well-inserts were measured Ex:495nm Em:517nm. Error bars = +/- SEM. Analysed using multiple t-test. N=3

4.1.4.1.3 5-day old S. aureus biofilm

When 5-day *S. aureus* SH1000 biofilms were treated with LIPUS 4 kDa FITC-dextran (**Figure 36a**) moved through the biofilm into the surrounding well, by measuring the changes of fluorescence in the media in the well beneath the biofilm changes in permeability could be monitored. At the 1-hour timepoint the fluorescence in the LIPUS treated wells had increased to 1348 RFU and the untreated wells had increased to 1522 RFU. T-tests were performed and there was no significant difference in the fluorescence between the LIPUS treated wells and the untreated wells ($p=0.83$). At the 2-hour timepoint the fluorescence of the wells receiving LIPUS treatment and the wells that were untreated had further increased, fluorescence increased in the LIPUS treated wells to 5006 RFU which the untreated fluorescence was 4395 RFU this change again was not significant ($p=0.51$).Over the 3 hour total LIPUS treatment the fluorescence increased to 6216 RFU while the fluorescence in the wells not receiving LIPUS increased to 6867 RFU, by the end of the 3-hour treatment the changes in fluorescence was not significant ($p=0.61$). This shows that 30 mW/cm^2 LIPUS does not increase the ability for low weight molecules to travel through the biofilms of *S. aureus* SH1000.

When higher molecular weight FITC-dextran was used the ability for the FITC-dextran to permeate the biofilm was decreased and lower levels of fluorescence was observed. After 1-hour LIPUS treatment with media containing 70 kDa FITC-dextran (**Figure 36b**) the fluorescence for the untreated wells was 388 RFU while the LIPUS treated wells was 308 RFU, the p-value was 0.48. At the 2-hour timepoint the fluorescence had increased within the well with the untreated wells fluorescence at 1797 RFU and the LIPUS treated wells at 2418 RFU, while the RFU for the LIPUS treated wells was higher it was not a significant change ($p=0.27$). At the end of the 3-hour LIPUS treatment the untreated wells fluorescence was 2167 RFU and the LIPUS treated wells was 2409 RFU. This was again higher in the LIPUS treated well but the change was not significant ($p = 0.53$). For the wells containing 250 kDa FITC-dextran (**Figure 36c**) the fluorescence after 1-hour was 132 RFU while the LIPUS treated wells was not fluorescent, this however was not significantly different

(p=0.37). After 2-hours the untreated wells had fluorescence of 384 RFU and the LIPUS treated wells was 625 RFU, while fluorescence was higher in the LIPUS treated wells it was not a significant increase (p=0.51). After 3-hours the fluorescence had further increased to 742 RFU, while the LIPUS treated wells had decreased to 331 RFU, however this decrease was not significant (p=0.25). This demonstrates LIPUS does not increase the permeability of higher weight molecules in 5-day old *S. aureus* SH1000 biofilms.

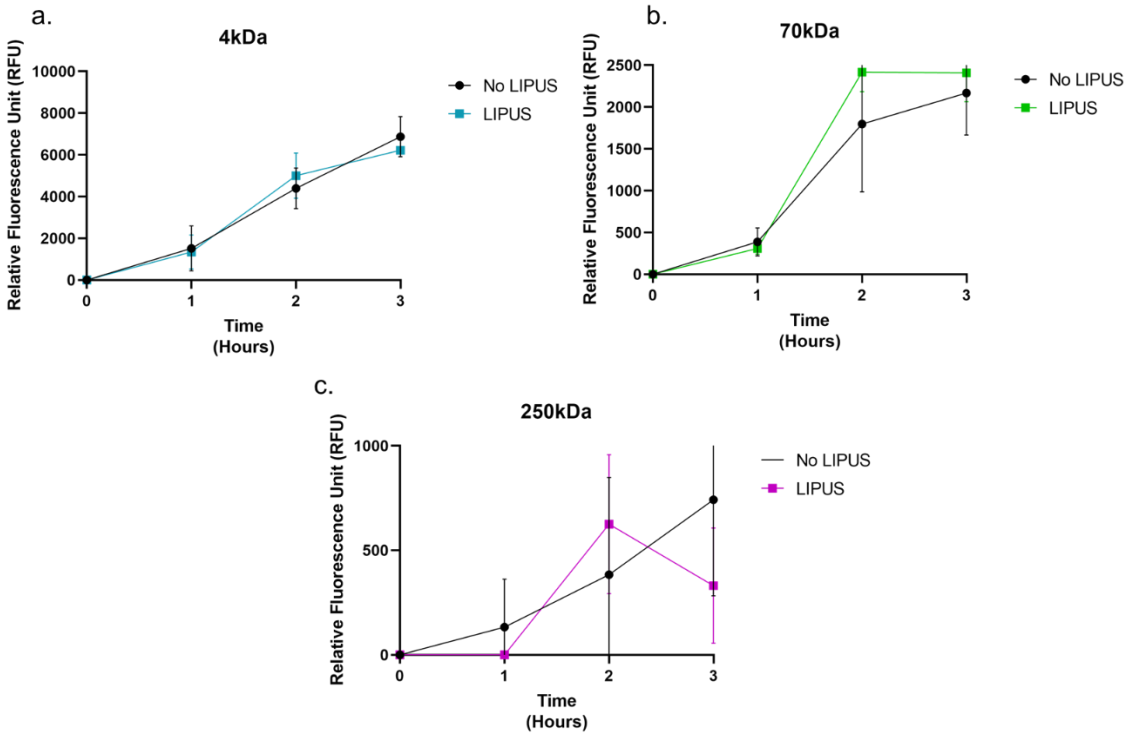

Figure 36: 5-day S. aureus SH1000 biofilm in 6-well inserts treated with 30 mW/cm^2 LIPUS for 1-, 2-, and 3-hours with BHI supplemented with 4kDa (a), 70kDa (b) and 250kDa (c) FITC-Dextran, changes in fluorescence in well surrounding the well-inserts were measured Ex:495nm Em:517nm. Error bars = +/- SEM. Analysed using multiple t-test. N=3

4.1.4.1.4 7-day old S. aureus biofilm

When *S. aureus* SH1000 biofilms were grown for 7-days and treated with 30 mW/cm^2 LIPUS in the presence of 4 kDa FITC-dextran (**Figure 37a**), the fluorescence of the media within the wells increased over the 3-hour treatment period. At 1-hour the fluorescence in the untreated wells was 1790 RFU compared to the 864 RFU in the wells treated with LIPUS (p=0.13). By the 2-hour timepoint the fluorescence had increased in both the untreated and LIPUS treated wells, 2216 RFU and 3220 RFU respectively (p=0.003). At the end of the LIPUS treatment period the fluorescence had increased to 4444 RFU in the untreated wells and 4609 RFU in the wells treated with LIPUS (p=0.79). The fluorescence levels were not statistically significant at 1- and 3-hour timepoints but at 2-hours the LIPUS treated wells had significantly increased fluorescence when compared to the untreated wells. This indicates that 2-hour LIPUS potentially increases the permeability of 4 kDa FITC-dextran through 7-day *S. aureus* SH1000.

As with the younger biofilms, lower levels of fluorescence were observed in larger molecular weight FITC-dextran experiments when compared to the lower weight FITC-dextran in the 7-day biofilms. In the wells containing 70 kDa FITC-dextran (**Figure 37b**), a steady increase in fluorescence over the course of the experiment in both the LIPUS treated wells and the untreated wells with little variation in fluorescence between the treated and untreated samples at 1- and 3-hours, and increased fluorescence at 2-hours, similar to the 4 kDa FITC-dextran samples. At 1-hour the fluorescence in the untreated wells was 491 RFU, while the LIPUS treated wells was 310 RFU (p=0.58). After 2-hours the fluorescence had further increased to 541 RFU in the untreated wells and 763 in the LIPUS treated wells (p=0.04). At the 3-hours timepoint the fluorescence in the untreated wells had reached 1549 RFU while the LIPUS treated wells had reached 1193 RFU (p= 0.58). The fluorescence levels were not statistically significant at 1- and 3-hour timepoints but at 2-hours the LIPUS treated wells had significantly increased fluorescence when compared to the untreated wells. This indicates that 2-hour LIPUS potentially increases the permeability of 70 kDa FITC-dextran through 7-day *S. aureus* SH1000.

When the 250 kDa FITC-dextran (**Figure 37c**) was used to measure the permeability of the *S. aureus* SH1000 treated with 30 mW/cm^2 LIPUS there were low levels of fluorescence at 1-hour and 3-hour LIPUS treatment as well as the untreated samples, the levels of fluorescence peaked at the 2-hour timepoint for both the treated and untreated wells. At 1-hour the fluorescence levels were undetectable in both the LIPUS treated and untreated wells. After 2-hours the fluorescence had increased to 384 RFU in the untreated wells and 625 RFU in the LIPUS treated wells (p=0.41). By 3-hour timepoint the fluorescence in the untreated wells had decreased to low levels with 13 RFU measured, the LIPUS treated wells had also fallen to 191 RFU (p= 0.31). With no significant changes in fluorescence, LIPUS does not increase the ability of 250 kDa FITC-dextran to move through 7-day *S. aureus* SH1000 biofilms.

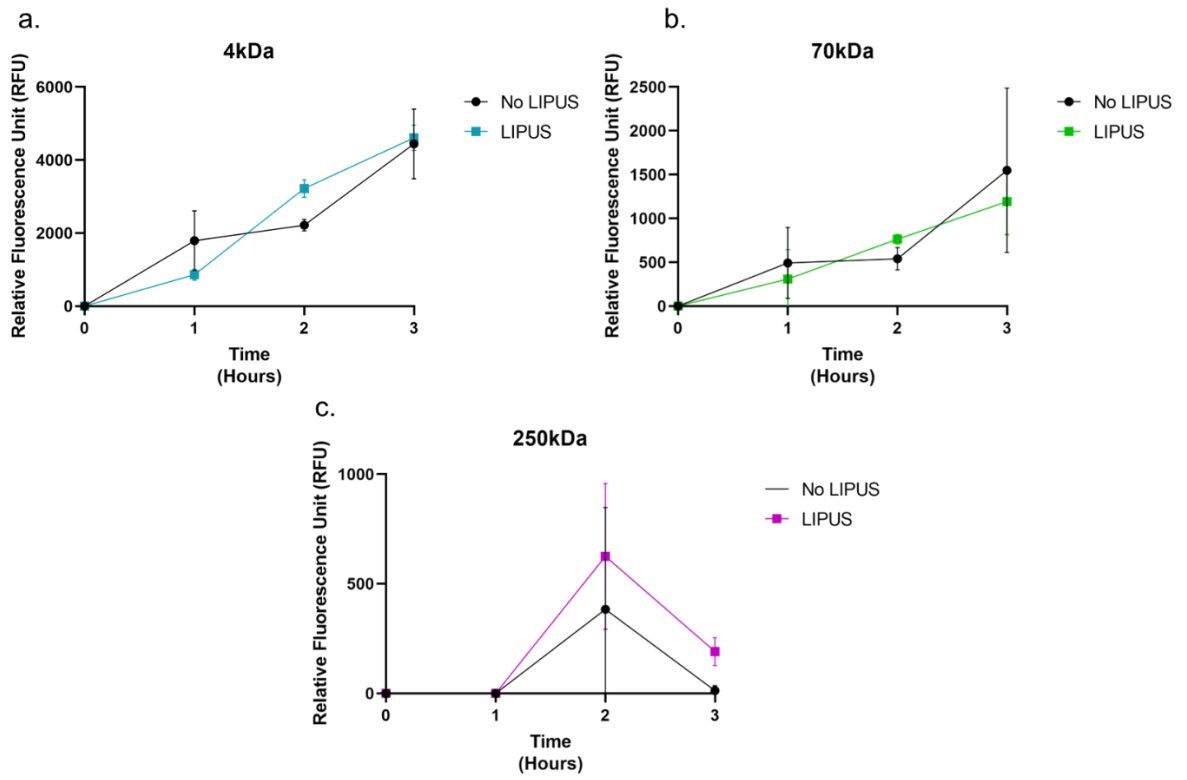

Figure 37: 7-day S. aureus SH1000 biofilm in 6-well inserts treated with 30 mW/cm^2 LIPUS for 1-, 2-, and 3-hours with BHI supplemented with 4kDa (a), 70kDa (b) and 250kDa (c) FITC-Dextran, changes in fluorescence in well surrounding the well-inserts were measured Ex:495nm Em:517nm. Error bars = +/- SEM. Analysed using multiple t-test. N=3

Small molecular weight FITC-dextran can penetrate the biofilms, with increased penetration with LIPUS in the youngest and oldest biofilms (1-day and 7-day). Larger molecular weight FITC-dextran less efficiently penetrates through biofilms and LIPUS treatment does not impact permeation of large molecules.

4.1.4.2 Planktonic cell permeability with LIPUS treatment

LIPUS treatment increased sensitivity of biofilms to gentamicin, but not vancomycin (see section 4.1.2) Gentamicin acts intracellularly, binding to the 30S subunit of the bacterial ribosome, while vancomycin binds to bacterial cell wall precursors. LIPUS treatment may create changes in permeability of bacterial cell membranes, allowing easier access for antibiotics into the cell. Changes in the membrane integrity of *S. aureus* when treated with 30 mW/cm^2 LIPUS for 2-hours were investigated using a β-galactosidase activity assay (**Figure 38**). A strain of *S. aureus* containing the *LacZ* gene, which codes for the enzyme β-galactosidase was treated with LIPUS, then 4-MUG, a substrate of β-galactosidase, was used to assess the presence of this internal enzyme in the growth media of *S. aureus*. Presence of β-galactosidase in the media may indicate the disruption of the cell wall to allow leakage of the enzyme. To measure the changes in β-galactosidase the fluorescence of the media were measured, higher fluorescence would indicate higher β-galactosidase activity. When the cells were left untreated the fluorescence was 27208 RFU, while the media taken from cells treated with LIPUS had fluorescence of 31093 RFU, this was not a statistically significant increase in fluorescence, with a p-value of 0.25 calculated with a t-test. This demonstrates no increase in β-galactosidase activity when LIPUS treatment is administered.

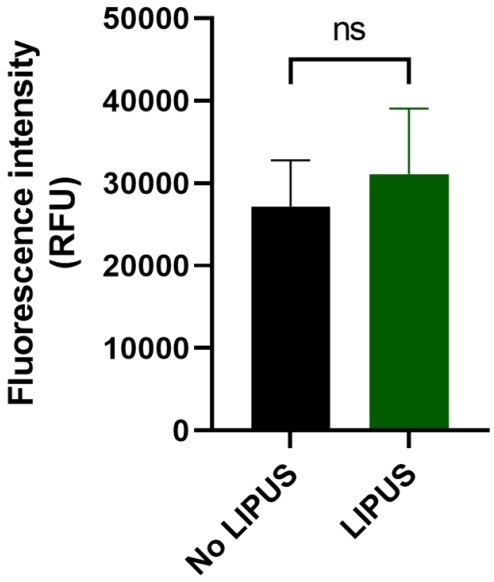

Figure 38: Planktonic S. aureus strain containing LacZ treated with 30 mW/cm² LIPUS for 2-hours, membrane leakage assessed using 4-MUG substrate for the leakage of β-galactosidase. Fluorescence measured Ex: 362 nm Em: 445 nm. ns= not significant. Error bars = +/-SEM. Analysed using t-test. N=3.

The integrity of *S. aureus* cell wall when treated with LIPUS was also investigated using propidium iodide (PI) (**Figure 39**). Planktonic *S. aureus* SH1000 were treated with 30 mW/cm^2 LIPUS for 2 hours in BHI containing SYTO 60 and PI, 10 µl of the cell suspension was then placed on microscopy slides and imaged on a fluorescent microscope. The total cells were counted and the percentage of cells containing PI stain were calculated. When the cells were untreated the number of cells containing PI was 8.5 %, while the cells treated with LIPUS was 8.9 % (p=>0.999, t-test). Therefore, this does not show an increase in cell wall permeability when *S. aureus* SH1000 is treated with 30 mW/cm^2 LIPUS for 2-hours.

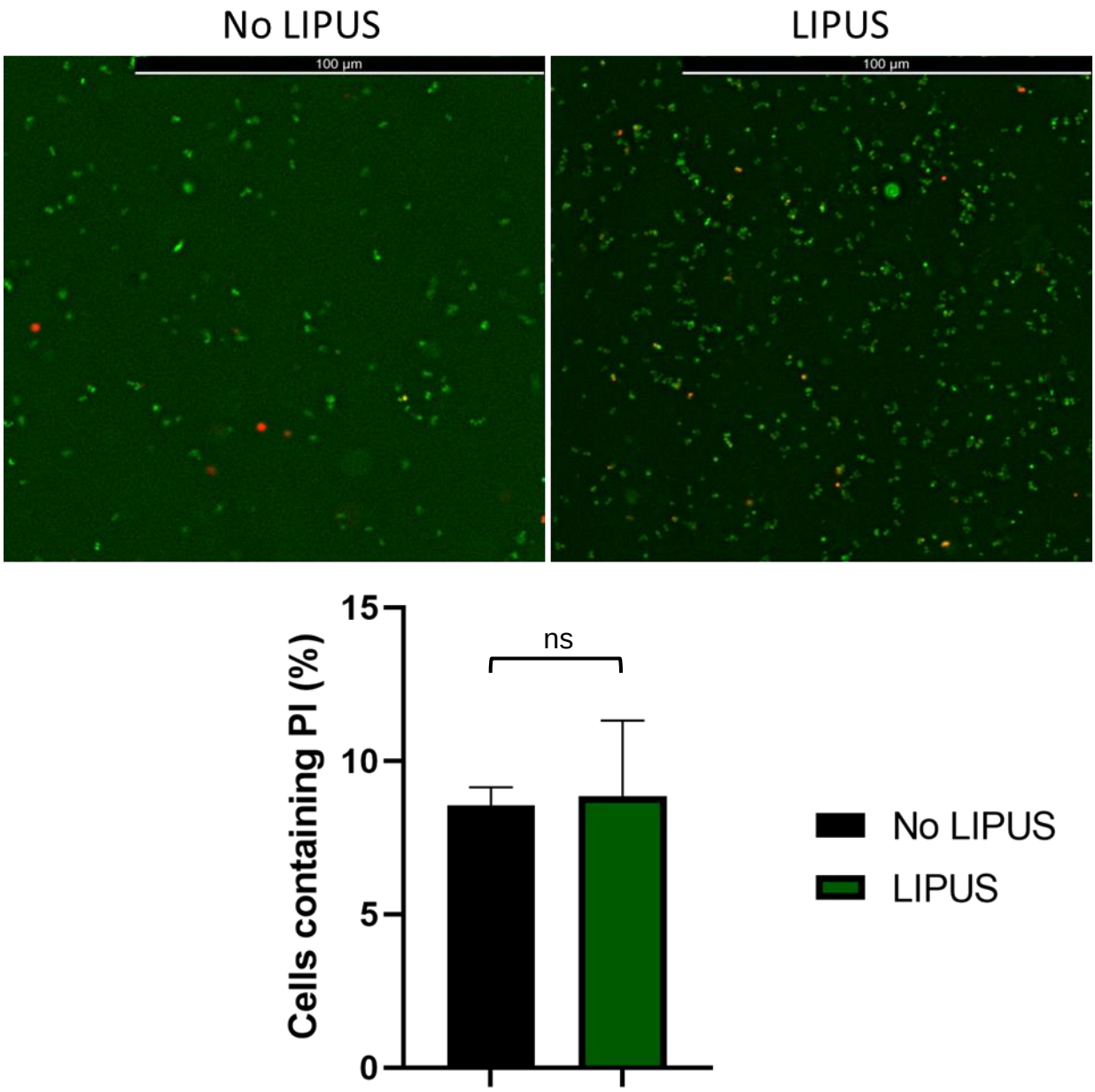

Figure 39: S. aureus SH1000 with SYTO 60 (green) and proprium iodide (red) untreated and treated with 2-hour 30 mW/cm^2 LIPUS. Percentage of cells containing PI were calculated. Error bars = +/-SEM. Ns = not significant. Analysed using t-test. N=3

These data indicate that cell membrane permeability is not affected by LIPUS in *S. aureus* SH1000 cells.

4.1.5 Metabolism

Due to the observed changes in numbers of bacteria treated with LIPUS and gentamicin (see section 4.1.2.2), changes in ATP levels within biofilms treated with LIPUS at different stages of maturity were investigated to assess changes in metabolism. BacTiter-Glo is a luciferase assay which measures luminescence relative to ATP levels. Changes in luminescence measured would correlate to the levels of ATP in a sample.

4.1.5.1.1 1-day old S. aureus biofilm

When 1-day old *S. aureus* SH1000 biofilms were untreated the luminescence in the media (**Figure 40a**) was not significantly different to the 2-hour LIPUS treated biofilms, (334000 RLU vs 271000 RLU, p=0.058, t-test), indicating LIPUS did not impact the levels of ATP in the media. Luminescence in cells taken from the untreated biofilms (**Figure 40b**) was not significantly different to the 2-hour LIPUS treated biofilms (260333 RLU vs 306000 RLU, p=0.061, t-test). This would indicate that 2-hour 30 mW/cm^2 LIPUS treatment does not impact the ATP levels within the biofilm or released into the media.

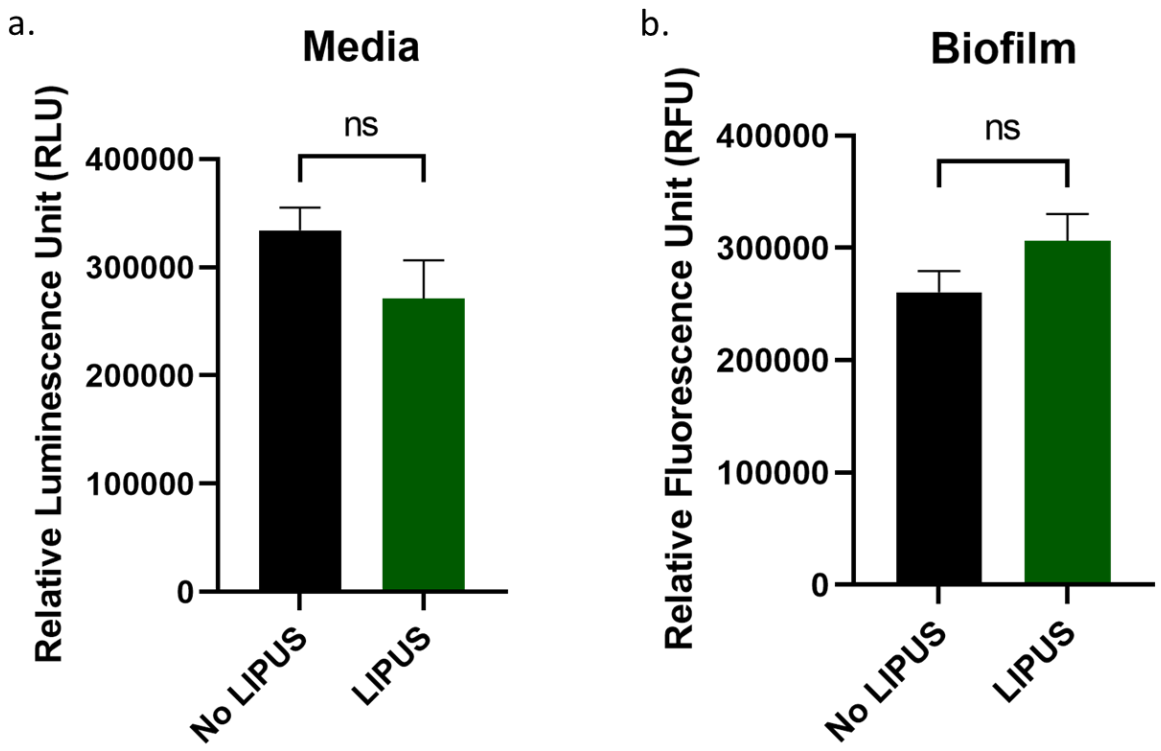

Figure 40: Relative ATP levels from 1-day S. aureus SH1000 biofilm untreated and treated with 30 mW/cm2 LIPUS in the media (a) and the whole biofilm (b). ns= not significant. Error bars = +/-SEM. Analysed using t-test. N=3

4.1.5.1.2 3-day old S. aureus biofilm

Luminescence in the media from 3-day old untreated biofilms was not significantly increased in comparison to the 2-hour LIPUS treated biofilms, (931000 RLU vs 881333 RLU, p=0.39, t-test (**Figure 41a**), indicating LIPUS did not impact the levels of ATP released into the media by a 3-day *S. aureus* SH1000 biofilm. The luminescence in cells taken the biofilm (**Figure 41b**) was not significantly different in untreated biofilms when compared to LIPUS treated biofilms (164667 RLU vs 144333 RLU, p=0.057, t-test). This would indicate that 30 mW/cm^2 does not impact the ATP levels within the biofilm of a 3-day *S. aureus* SH1000 biofilm or released into the media.

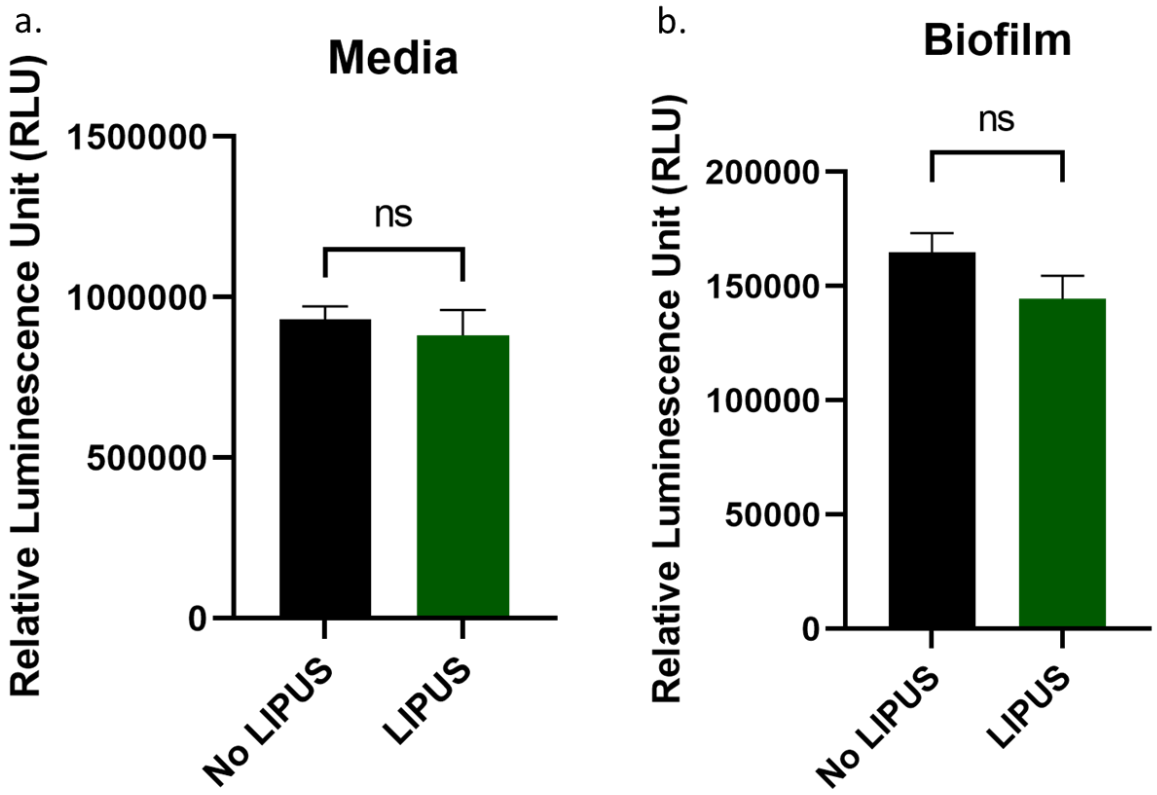

Figure 41:Relative ATP levels from 3-day S. aureus SH1000 biofilm untreated and treated with 30 mW/cm2 LIPUS in the media (a) and the whole biofilm (b). Error bars = +/-SEM. Analysed using t-test. ns= not significant. N=3

4.1.5.1.3 5-day old S. aureus biofilm

S. aureus SH1000 biofilms were grown for 5-days. The luminescence in the media taken from untreated biofilms was significantly higher than the luminescence in the 2-hour LIPUS treated biofilms (1390000 RLU vs 848333 RLU, p= 0.0003, t-test) (**Figure 42a**), indicating LIPUS significantly reduces the ATP released into the media by a 5-day *S. aureus* SH1000 biofilm. Luminescence was significantly lower in the untreated biofilms in comparison the in the LIPUS treated biofilms (182000 RLU vs 394333 RLU, p=0.009, t-test) (**Figure 42b**). This would indicate that 30 mW/cm^2 may increase the ATP within a 5-day *S. aureus* SH1000 biofilm.

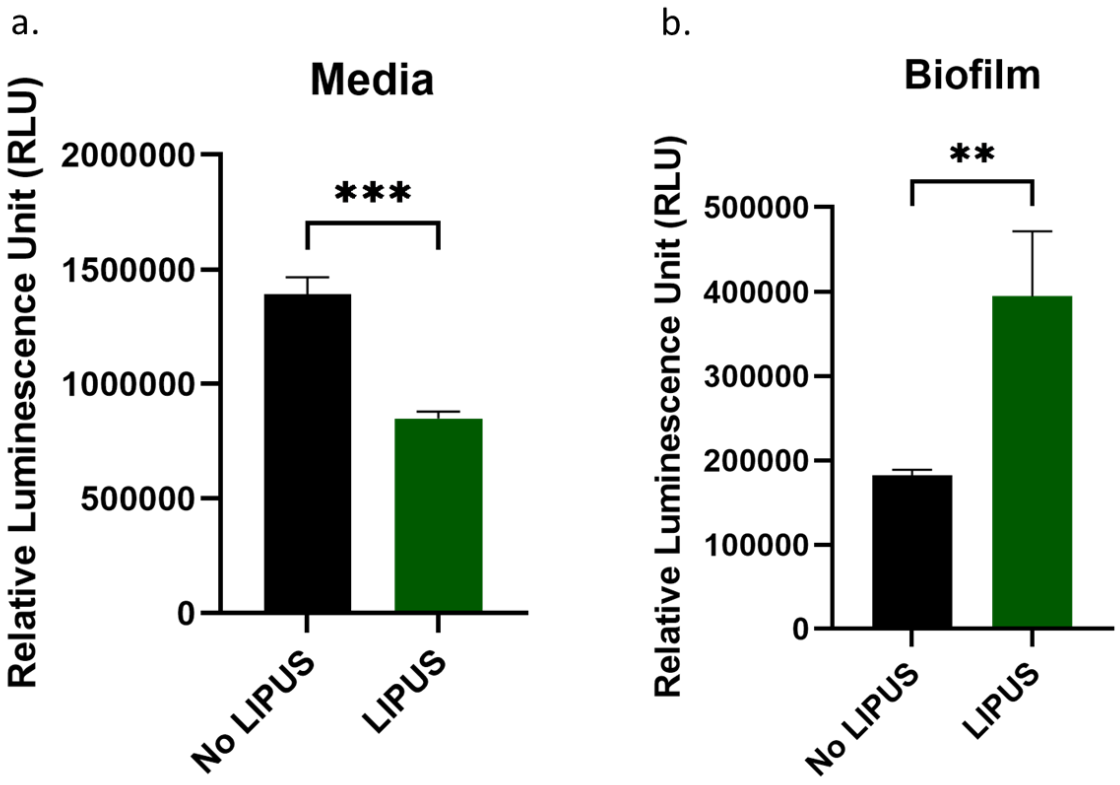

Figure 42: Relative ATP levels from 5-day S. aureus SH1000 biofilm untreated and treated with 30 mW/cm2 LIPUS in the media (a) and the whole biofilm (b). Error bars = +/-SEM. Analysed using t-test. ** = p-value < 0.01 ***= p-value <0.001. N=3

4.1.5.1.4 7-day old S. aureus biofilm

S. aureus SH1000 biofilms grown for 7-days showed a similar trend to the biofilms grown for 5-days. The luminescence was significantly higher in the media taken from the untreated biofilm compared with the 2-hour LIPUS treated biofilm (881333 RLU vs 637333 RLU, p=0.007) (**Figure 43a**), indicating LIPUS significantly reduces the ATP released into the media by a 7-day *S. aureus* SH1000 biofilm. The luminescence from the biofilm cells was significantly lower than the cells from the LIPUS treated biofilms (350000 RLU vs 540333 RLU, p=0.0001, t-test) (**Figure 43b**). This would indicate that 30 mW/cm^2 may increase the ATP within a 7-day *S. aureus* SH1000 biofilm.

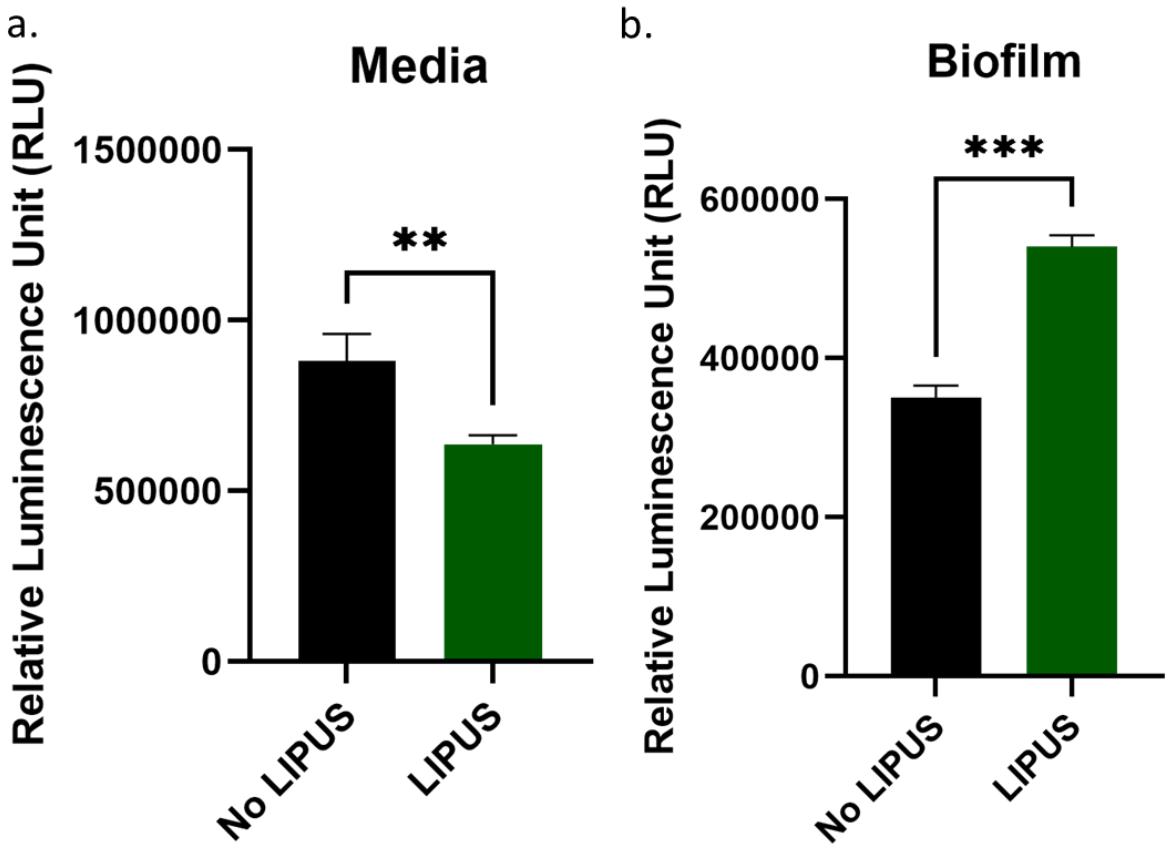

Figure 43: Relative ATP levels from 7-day S. aureus SH1000 biofilm untreated and treated with 30 mW/cm2 LIPUS in the media (a) and the whole biofilm (b). Error bars = +/-SEM. Analysed using t-test. ** = p-value < 0.01 ***= p-value <0.001 N=3

In younger biofilms (1-, 3-days) 2-hours 30 mW/cm^2 LIPUS does not influence the levels of ATP within the biofilms or the media, while in older biofilms LIPUS treatment reduces ATP release into the media, while increasing the ATP levels within the biofilms.

4.1.6 Oxygen

The levels of oxygen in media were also measured to assess whether metabolic activity changes in biofilms treated with LIPUS. An extracellular oxygen consumption assay was used. The presence of oxygen causes the emission of fluorescence; higher levels of fluorescence are correlated with higher levels of oxygen, so a

reduction in oxygen would indicate increased aerobic activity. The 1-day *S. aureus* untreated biofilm had relative fluorescence of 36989 RFU, which was significantly lower than the biofilm treated with 30 mW/cm^2 LIPUS, where the fluorescence intensity was 40021 RFU (**Figure 44**). The p-value calculated using a t-test was 0.0071. This indicates that LIPUS treatment may reduce the aerobic activity of *S. aureus* SH1000 biofilms.

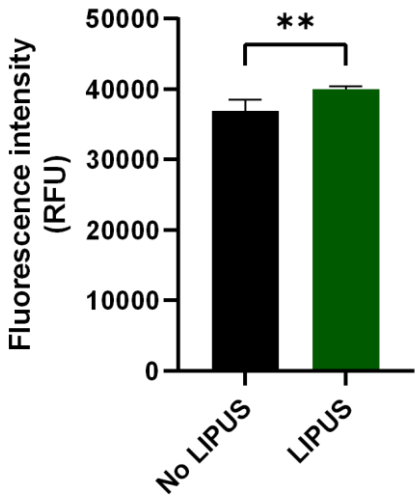

Figure 44: Relative oxygen levels in 1-day biofilm treated with 30 mW/cm^2 for 2 hours. Oxygen monitored 30-minutes post LIPUS treatment with Extracellular Oxygen Consumption assay. Error bars = +/-SEM. Analysed using t-test. **= p-value <0.01. N=3.

4.1.7 RNA Sequencing

Total RNA extracted from 1-day biofilms with or without LIPUS treatment was sequenced and analysed using gene ontology (GO) in an attempt to identify potential biological functions which may be impacted when biofilms were treated with LIPUS. GO annotations for differentially expressed genes were used for enrichment analysis to identify overrepresented annotation terms within the differentially expressed genes. Of the 146 differentially expressed genes, 63 were genes for hypothetical protein or poorly characterised proteins. For protein encoding RNA, the most over-

represented GO annotations in the differentially expressed genes can be seen in **Figure 45**. Genes associated with ATP and nucleotide binding, and transferase activity were the most over-represented molecular function. Genes involved in both the plasma membrane and the cell membrane were the most commonly affected cell component genes when biofilms were treated with LIPUS. The two biological processes most affected by LIPUS treatment of the biofilms were transmembrane transport and cytocidal processes.

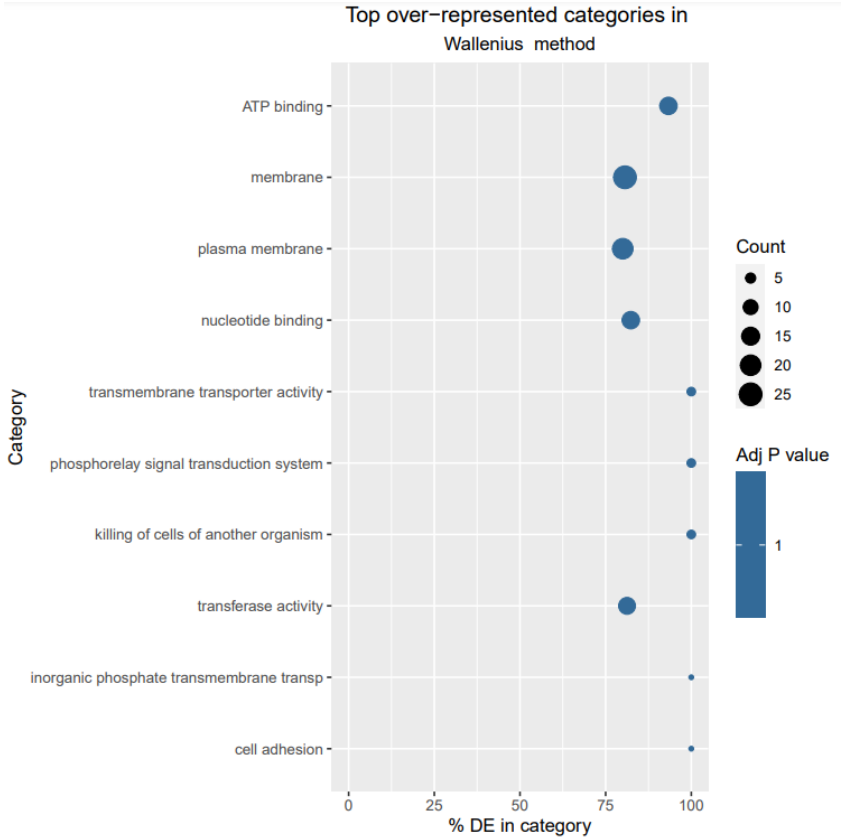

Figure 45: Gene ontology analysis of significant differentially expressed genes. N=3

Several differentially expressed genes of interest were identified, listed in **Table 16**, including upregulation of genes associated with virulence: *SAOUHSC_00715, SAOUHSC_00714, SAOUHSC_02710, SAOUHSC_02710, SAOUHSC_02709* (SaeS/R, fibronectin-binding protein, and leukocidins), and downregulation of genes associated with biosynthesis of cell wall polysaccharides: *SAOUHSC_00128,*

SAOUHSC_00115, SAOUHSC_00127, SAOUHSC_02999 (Capsule polysaccharide type 5).

Table 16: Differentially expressed genes of interest when biofilms were treated with LIPUS.

Gene ID	Gene Name	Fold change (log2)	p-value (adj)	Product/ System
SAOUHSC_00715	Response regulator	0.65482145	0.0061	SaeS/R
SAOUHSC_00714	sensor histidine kinase SaeS	0.61703659	0.0024	SaeS/R
SAOUHSC_02803	fibronectin-binding protein	0.95242244	0.039	Fibronectin-binding protein A
SAOUHSC_02710	leukocidin f subunit precursor	1.55655216	2.98×10^{-10}	leukcidins
SAOUHSC_02709	leukocidin s subunit precursor	1.59952846	8.18×10^{-9}	leukcidins
SAOUHSC_00128	cap5O protein/UDP-N-acetyl-D-mannosaminuronic acid dehydrogenase	-0.82480868	0.011	Capsule polysaccharide 5 synthesis
SAOUHSC_00115	capsular polysaccharide biosynthesis protein Cap5B	-0.91314173	0.022	Capsule polysaccharide 5 synthesis
SAOUHSC_00127	cap5N protein/UDP-glucose 4-epimerase	-0.71143717	0.043	Capsule polysaccharide 5 synthesis
SAOUHSC_02999	capsular polysaccharide biosynthesis protein Cap5B	-0.9519968	0.029	Capsule polysaccharide 5 synthesis

A sample-to sample distance heatmap is used to visualise the similarities in gene expression between individual samples within a dataset, similarly a principal component analysis (PCA) identifies clustering based on variance in gene expression between each sample. Using both the distance heat map and a PCA plot to analyse the differences and similarities in gene expression between the three repeats for each treatment condition, there is a high degree of variance in the gene expression in LIPUS treated biofilms (**Figure 46**). This variance means that solid conclusions on how LIPUS affects gene expression cannot be made based on the data presented and further repeats of RNA sequencing of LIPUS treated biofilms would be required to identify clustering and anomalies within the data.

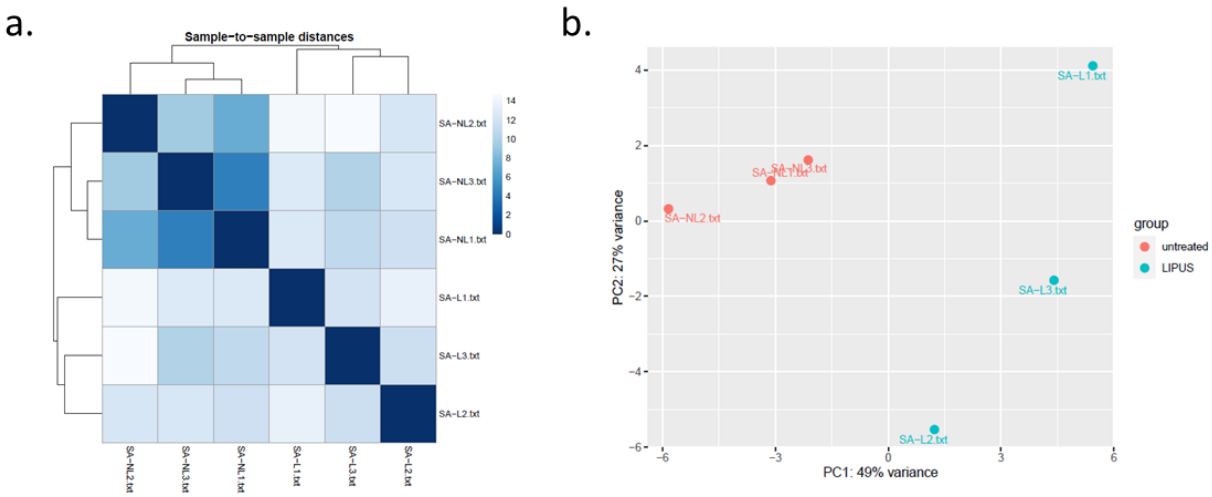

Figure 46: Heatmap of sample-to-sample distance (a). PCA plot of treatment condition, untreated (red) and LIPUS treated (blue) (b). N=3

Over-representation analysis for each of the 3 repeats was analysed individually to identify any differences in biological processes affected by LIPUS across the 3 repeats. Several differences in over-represented terms were identified. In both repeat 1 and 2 (**Figure 47** & **Figure 48**) genes associated with cell membrane and plasma membrane were affected by LIPUS, this was not seen in repeat 3 (**Figure 49**). Transferase activity was overrepresented in repeat 1, while not in repeat 2 or 3.

Toxin activity and killing of cells from another organism was only overrepresenting in repeat 3. Oxidoreductase activity was overrepresented in all three repeats. This further demonstrates the variance in the gene expression of the LIPUS treated biofilms and further repeats would be required to identify trends and biological processes affected by LIPUS.

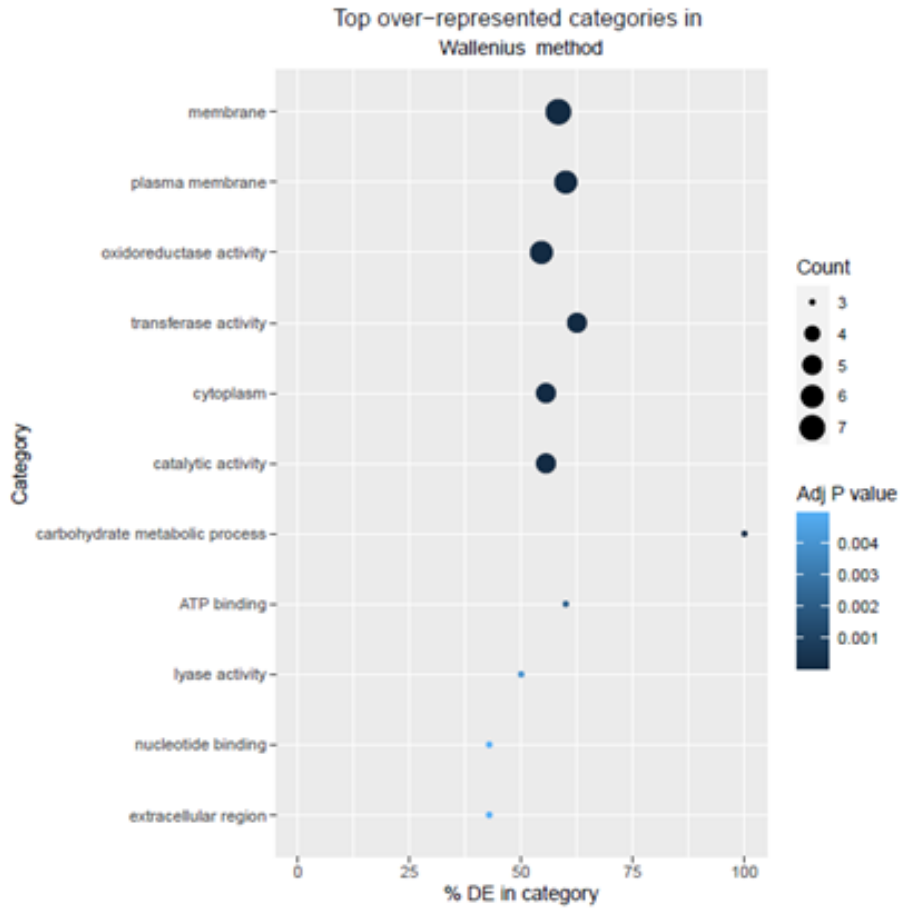

Figure 47: Over-representation analysis of gene ontology terms of statistically differentially expressed genes from Repeat 1 of RNA sequencing.

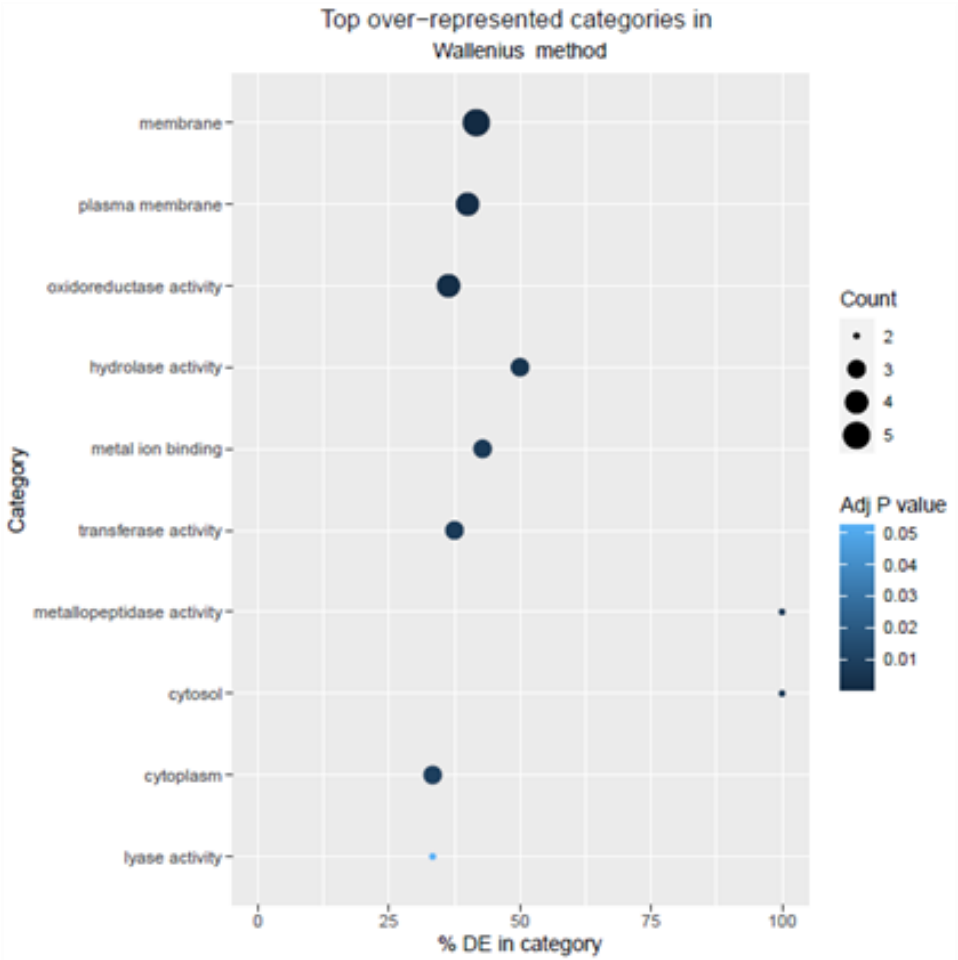

Figure 48:Over-representation analysis of gene ontology terms of statistically differentially expressed genes from Repeat 2 of RNA sequencing.

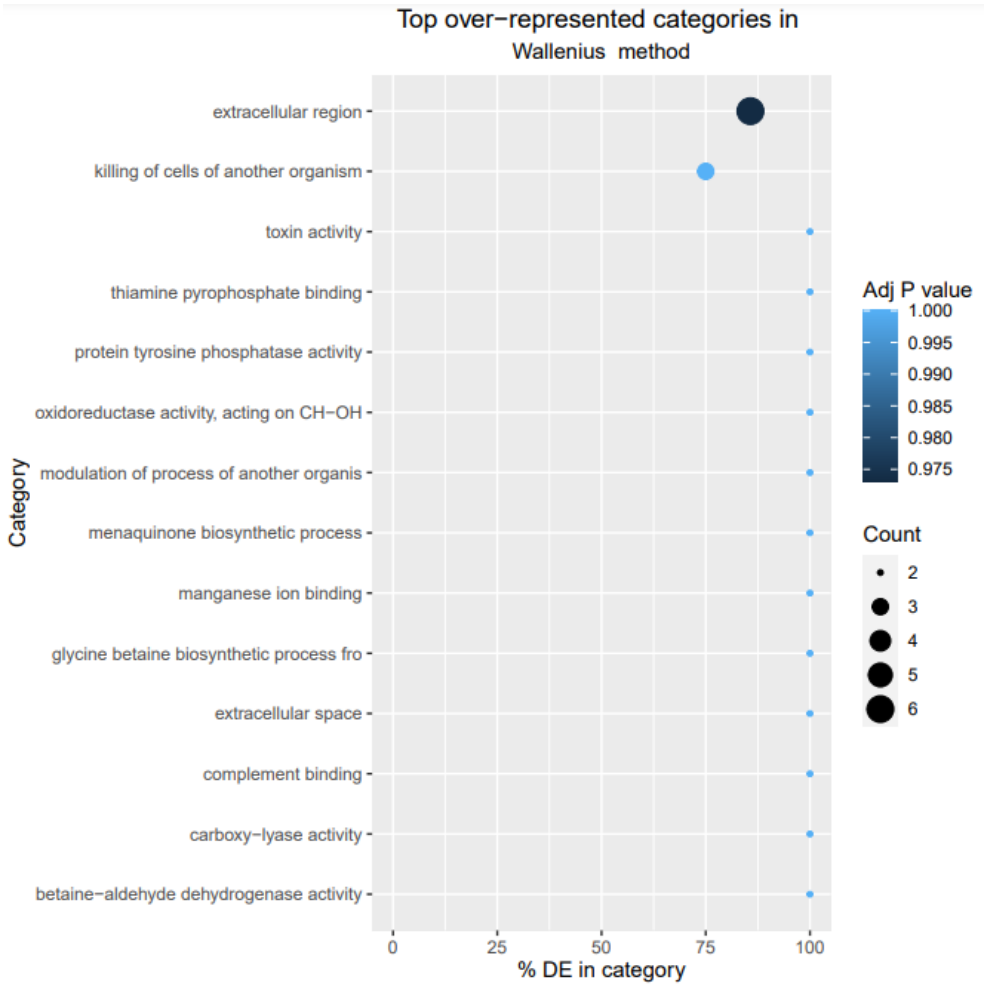

Figure 49:Over-representation analysis of gene ontology terms of statistically differentially expressed genes from Repeat 3 of RNA sequencing.

4.2 Antibiotic tolerant populations

Antibiotic tolerant (AT) populations of bacteria within biofilms are hypothesised to be associated with recurrent infections. The effects of LIPUS treatment on antibiotic sensitivity of isolated AT populations were investigated. Antibiotic tolerant cells were isolated from whole biofilms using high concentrations of ciprofloxacin and treated with LIPUS to evaluate the effects LIPUS had on the antibiotic sensitivity of this subpopulation of *S. aureus* SH1000.

4.2.1 Antibiotic tolerant population isolation

To isolate AT populations, whole biofilms were treated with high levels of antibiotics. The MICs calculated for *S. aureus* SH1000 (4.1.2.1) were used as a starting point for establish the correct concentration of ciprofloxacin. The isolation method was developed by assessing CFU extracted from samples treated with different concentrations of antibiotics, the lowest concentration yielding the greatest reduction in CFU was used as the antibiotic stress isolation concentration. When the 1-day *S. aureus* SH1000 biofilms were disrupted in BHI only the CFU/ml was 2.47 x 10^9, which reduced with increased MICs to 2.13 x 10^4 CFU/ml at 5000x MIC (see **Figure 50**, summary of CFU/ml in **Table 17**). All concentrations of ciprofloxacin yielded a significant reduction in viable bacteria with $p<0.01$. However, the greatest reduction in CFU was in the 5000x MIC, this concentration was selected to induce antibiotic stress persistence in *S. aureus* SH1000.

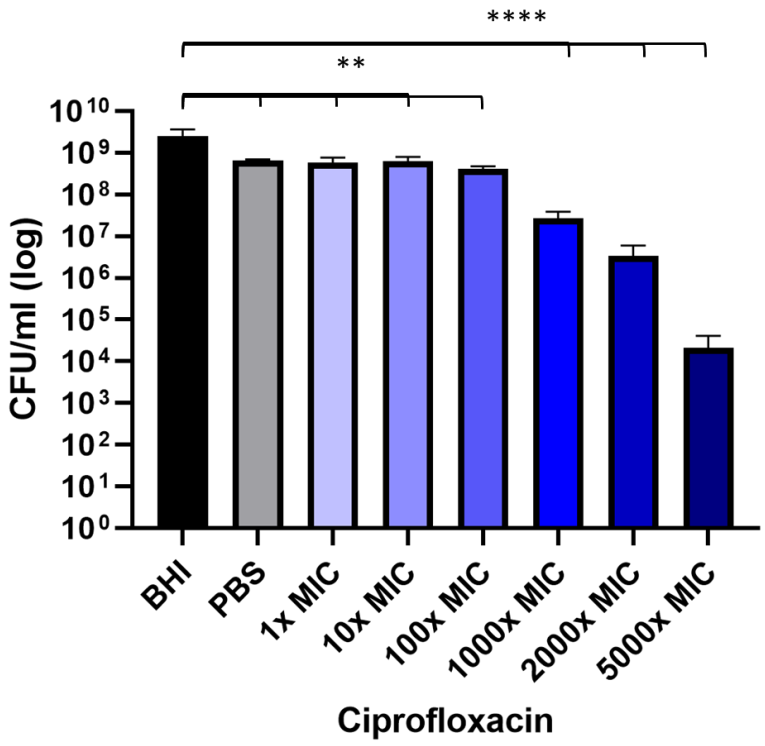

Figure 50: S. aureus SH1000 biofilms were grown for 1-day and then disrupted and incubated with 1x - 5000x MIC (0.5 µg/ml – 2500 µg/ml ciprofloxacin in PBS for 24-hours at 37 °C. Biofilms were plated using Miles-Misra to calculate CFU/ml. Error bars = +/-SEM. Analysed using one-way ANOVA with Dunnett's multiple comparison. ** = p-value < 0.01 **** = p-value <0.0001. N=3

Table 17: Summary of CFU/ml when disrupted biofilms treated with x MIC ciprofloxacin. Analysed using one-way ANOVA with Dunnett's multiple comparison.

MIC (Ciprofloxacin)	CFU/ml	P-value (against BHI only)
BHI only	2.47×10^9	
PBS only	6.47×10^8	0.0016
1x	5.73×10^8	0.0011
10x	6.40×10^8	0.0015
100x	4.13×10^8	0.0004
1000x	2.67×10^7	<0.0001
2000x	3.40×10^6	<0.0001
5000x	2.13×10^4	<0.0001

The length of antibiotic exposure was also investigated to allow the shortest possible challenge time with the greatest reduction in bacterial numbers. Disrupted *S. aureus* SH1000 biofilms were treated with 5000x MIC (2.5 µg/ml) ciprofloxacin for up to 30-hours (**Figure 51**). At the beginning of the experiment the CFU/ml was 6.33×10^8 which remained at the 2-hour timepoint. Significant reduction in bacteria was seen at the 4-hour timepoint with 2.87×10^7 CFU/ml which was further reduced by the 6-hour timepoint to 1.07×10^6. This further decreased at the 20- and 24-hour timepoint to 8×10^4 and 6×10^4 respectively. After 30-hours the level of viable bacteria began to increase again, potentially indicating the development of resistance to the ciprofloxacin. The CFU/ml for 30-hours treatment was 2.6×10^6. The difference in CFU/ml between the 20-hour and 24-hour treatment time were not significant with a p-value >0.999 when analysed with a one-way ANOVA with multiple comparisons, therefore 20-hours was selected as the length of ciprofloxacin treatment to induce persistence.

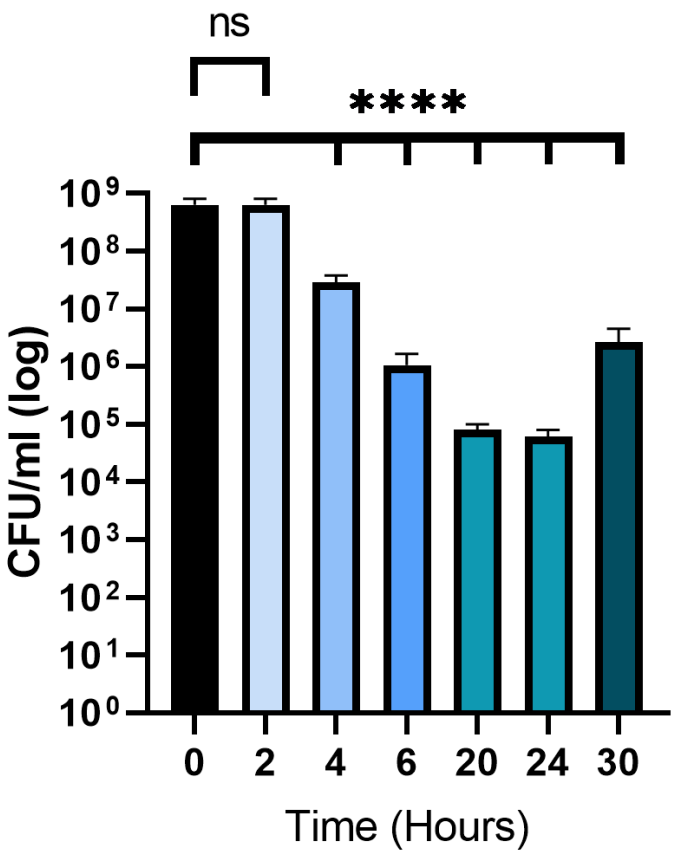

Figure 51: S. aureus SH1000 biofilms were grown for 1-day and then disrupted and incubated with 5000x MIC (2.5mg/ml) ciprofloxacin in PBS for 2 – 30-hours at 37 ºC. Biofilms were plated using Miles-Misra to calculate CFU/ml. Error bars = +/-SEM. Analysed using one-way ANOVA with Dunnett's multiple comparison. **** = p-value <0.0001. N=3

The ATP levels of whole biofilm populations and AT isolated populations were assessed using the BacTiter-Glo assay, a luciferase assay which measures luminescence relative to ATP levels. Changes in luminescence measured would correlate to the levels of ATP in a sample. Isolated AT samples and whole biofilm samples were diluted to equal OD_{600} of 0.1 to ensure equal number of cells in each sample. In the whole biofilm the relative fluorescence intensity was 1.81 x 10^6 RFU, while the AT population mean RFU was 3.44 x 10^5 (**Figure 52**). This was a significant reduction was analysed using a t-test ($p<0.0001$). This would suggest that the level of ATP in the AT population was lower than the ATP in the whole

population, validating the persistence of the AT population as lower ATP is expected in AT populations.

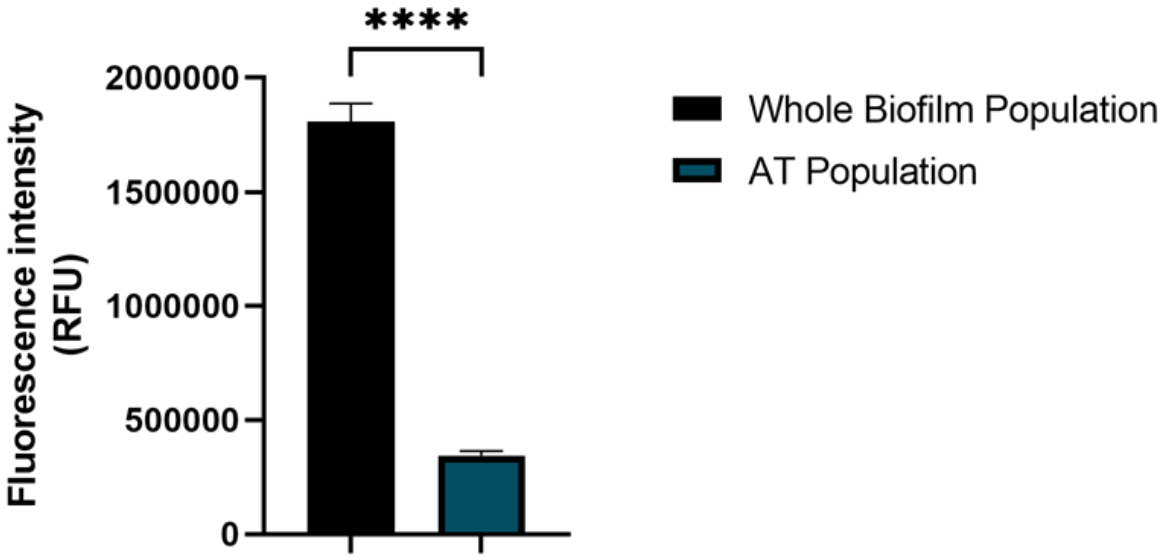

Figure 52: Relative ATP levels of whole biofilm populations and isolated AT populations from S. aureus SH1000 biofilms. Error bars = +/-SEM. Analysed using t-test. **** = p<0.0001. N = 3.

The MICs of regrown AT populations were assessed against gentamicin and ciprofloxacin to identify changes in sensitivity of the AT populations, post-isolation to assess for changes in antibiotic sensitivity driven by exposure to high concentration antibiotics. AT isolated populations from *S. aureus* SH1000 were grown in BHI supplemented with gentamicin 0.125 µg/ml – 256 µg/ml for 24-hours at 37 ^{o}C, and the optical density was read at 600nm. The MIC for gentamicin decreased from 1.34 µg/ml to 0.51 µg/ml using Gompertz fit for MIC after isolation and regrowth (**Figure 53a**). This was unexpectedly lower than the MIC calculated for *S. aureus* SH1000 (4.1.2.1) indicating increased sensitivity to gentamicin in AT populations. The MIC for ciprofloxacin increased from 0.5 µg/ml to 3.38 µg/ml (**Figure 53b**), indicating the development of resistance to ciprofloxacin in AT populations isolated from *S. aureus* SH1000.

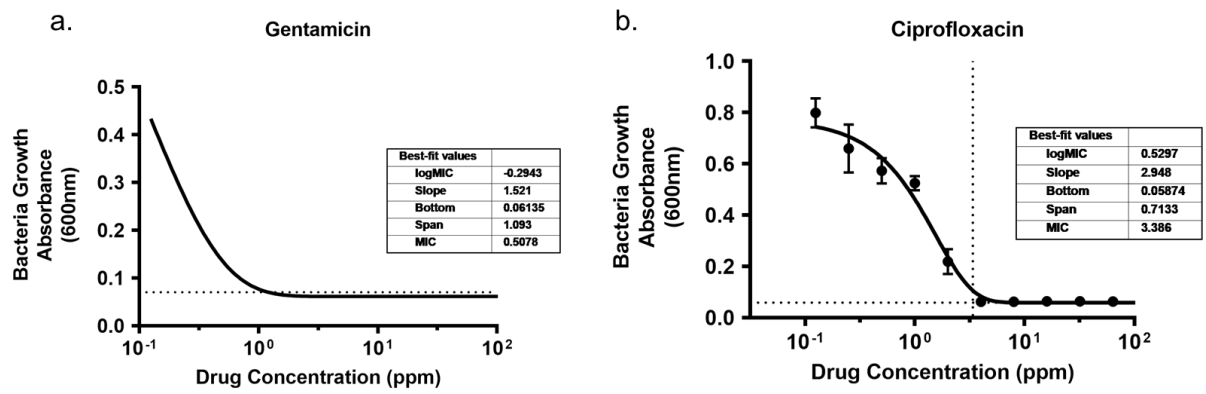

Figure 53: AT tolerant populations, isolated from S. aureus SH1000, regrown overnight in BHI at 37 °C and exposed to gentamicin (a) and ciprofloxacin (b). Error bars = +/-SEM. MIC calculated using Gompertz fit for MIC.

Growth curves for whole biofilm and AT populations were measured as AT populations are slower growing than whole biofilm, so a decreased growth rate would support confirmation of AT population isolation. Both the whole biofilm and the AT populations had a similar lag phase of 3-hours with whole biofilms having a quicker exponential growth, before reaching stationary phase by 7-hours incubation time. The AT population had a more gradual exponential phase reaching stationary phase at 11-hours incubation time **Figure 54**). When multiple t-tests were performed the growth was significantly different between 3.5-hours and 5.5-hours incubation.

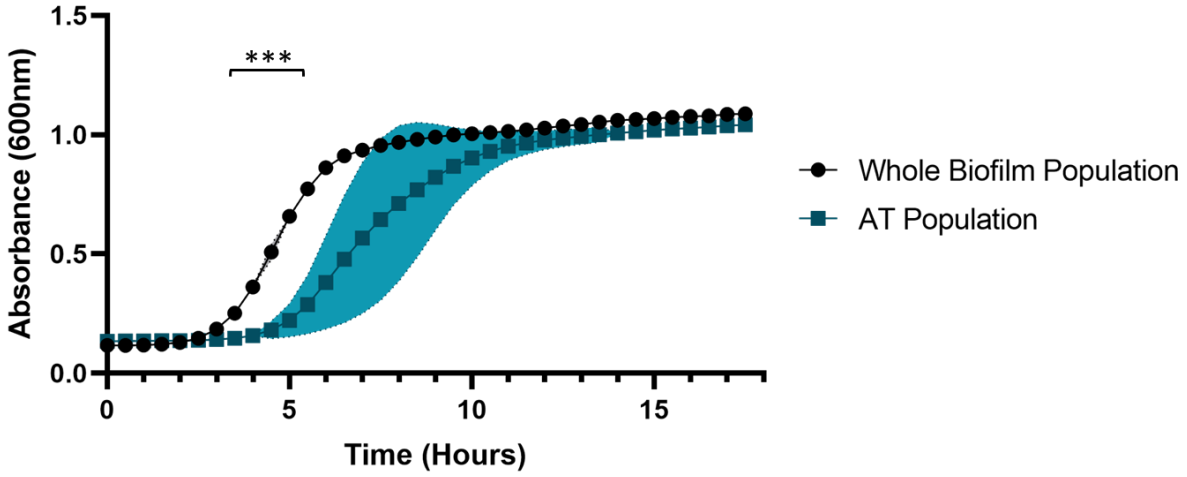

Figure 54: Isolated antibiotic tolerant populations and whole biofilm populations grown at 37 °C for 18-hours. Absorbance at 600nm was read at 30-minute intervals. Shaded area = +/-SEM. Analysed using multiple t-test *** = p-value <0.001 at time 3.5-hours – 5.5-hours. n=3

4.2.2 Changes to growth of antibiotic tolerant populations

AT populations are slow growing populations with low metabolism rates, lacking antibiotic targets hence tolerance. To assess whether LIPUS has an impact on AT growth and therefore potentially increasing antibiotic targets, AT isolated from 1-day old biofilms were treated with LIPUS for two hours and changes to the growth were assessed through CFU counts (**Figure 55**). There was no significant difference in CFU/ml in treated vs untreated AT populations (p=0.234).

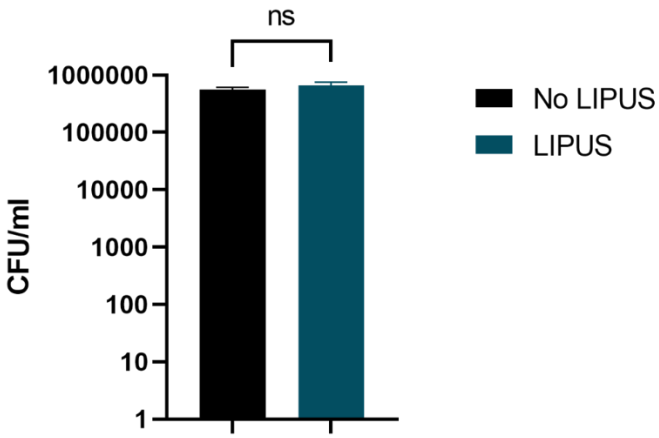

Figure 55: AT population isolated from 1-day S. aureus SH1000 biofilms treated with 30 mW/cm² LIPUS for 2-hours. CFU/ml calculated using Miles-Misra. Error bars = +/-SEM. Analysed using t-test. Ns= Not significant. N=3.

The AT population isolated from 1 day S. aureus SH1000 biofilm display a slower growth in the exponential phase (See **Figure 54**). To assess if LIPUS impacted the growth of these AT populations during the exponential phase, growth curves were measured to compare the growth rate of AT populations in comparison to whole biofilm populations following 2-hour LIPUS treatment (**Figure 56**). Whole biofilm populations entered into exponential phase after 2.5-hours of incubation and grew rapidly until entering stationary phase after incubation for 6-hours. AT populations had a longer lag phase of 4-hours and a slower growth rate in the exponential phase, reaching stationary phase after 10.5-hours. The rates of growth were statistically

significant between 2.5-hours and 6.5-hours incubation with p-values <0.05 calculated through multiple t-tests. This indicates that LIPUS does not increase AT population growth rate in comparison to whole biofilm populations from *S. aureus* SH1000 1-day biofilms.

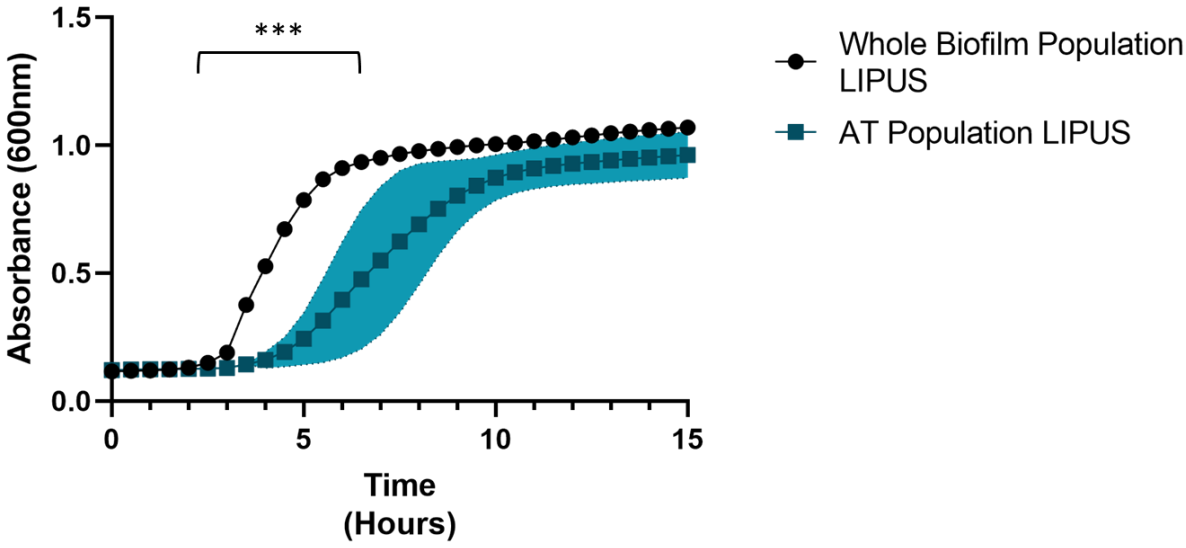

Figure 56: Growth curve of whole biofilm and isolated AT populations from S. aureus SH1000 incubated at 37 °C post 2-hour 30 mW/cm² LIPUS treatment for 15-hours. Absorbance measured at 600nm at 30-minute intervals. Shaded area = +/-SEM. *** = P-value <0.05 at 2.5-hour - 6.5-hour incubation time. Analysed using multiple t-tests. N=3

4.2.3 Changes to antibiotic sensitivity in tolerant populations

Due to the lack of antibiotic targets, AT cells are able to tolerate environments with antibiotic present. LIPUS may change AT sensitivity to antibiotics. Isolated AT along with whole biofilm populations were treated with 2-hour LIPUS and antibiotics, CFU were then calculated and compared against untreated AT and whole biofilm (**Figure 57**). When AT populations were treated with 10 µg/ml gentamicin the number of viable cells recovered from the sample was 2.1 x 10^5, however the number of viable cells significantly reduced when the AT populations were treated with 10 µg/ml gentamicin in addition to LIPUS with 5.1 x 10^4 CFU/ml. This was statistically significant when analysed using a t-test with the p-value calculated as 0.011. This

shows LIPUS treatment increases gentamicin sensitivity in AT populations isolated from *S. aureus* SH1000 biofilms.

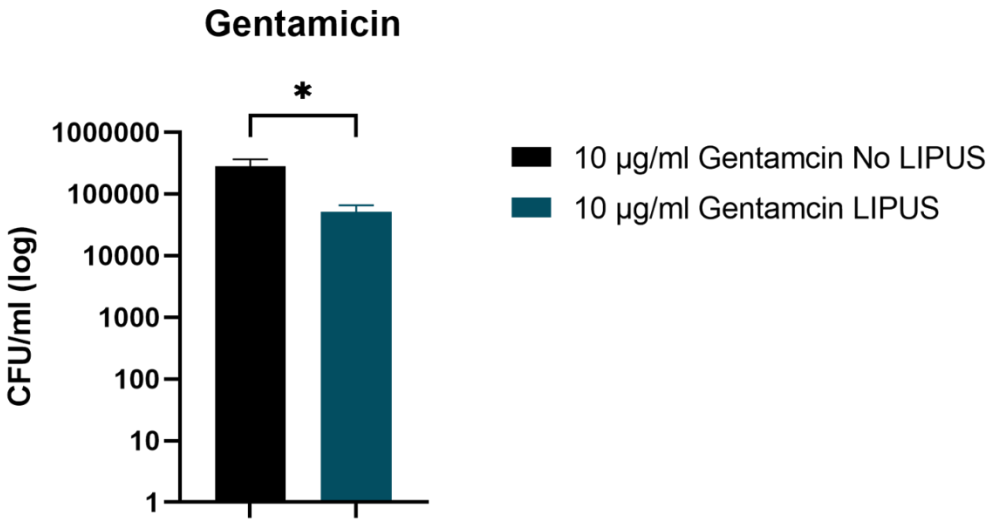

Figure 57: Antibiotic tolerant populations isolated from S. aureus SH1000 biofilms treated with 2-hour 30 mW/cm^2 LIPUS and 10 µg/ml gentamicin. Error bars = +/-SEM. Analysed using t-test. * = p<0.05. N=3

AT populations were isolated from 1 day *S. aureus* SH1000 biofilms, the growth of AT populations was not affected when treated with 30 mW/cm^2 LIPUS for 2-hours, however, antibiotic sensitivity was increased.

4.3 Tissue-engineered human skin infection model

When investigating a potential treatment option, use of 3D models can be more effective in validation of the treatment by providing a more 'realistic' environment. For this study a tissue-engineered skin infection model (TESM) was used. The TESM was grown by culturing human skin cells (HaCaT and HDF) on decellularized dermis at air liquid interface (ALI) for 14 days, infecting the TESM with *S. aureus,* and treating with LIPUS with and without gentamicin. The effects of LIPUS were assessed initially on the component cells individually in 2D monolayer, then on the 3D skin model both infected and uninfected with *S. aureus*. During this section, a synthetic wound fluid rather than tissue culture media was also used in an attempt

improve the TESM to better replicate the wound environment found in a clinical infection.

4.3.1 Cell proliferation

LIPUS is known to increase cell proliferation (Della Rocca, 2009; Katiyar *et al*., 2014), therefore it was essential to understand how LIPUS affects the cells used in the TESM. Cells were treated with 30 mW/cm^2 LIPUS for 2-hours before being quantified over a 3-day period, and changes in LIPUS treated cell numbers were compared against untreated cells. In HaCaTs, the mean number of cells counted immediately following the LIPUS treatment was 1.72 x 10^5, this was not significantly different to the mean number of cells within the LIPUS treated wells with 1.64 x 10^5 (**Figure 58a**), comparing these number with a t-test calculated a p-value of 0.9. The cells were then incubated for 1-day before cells were counted, in the untreated wells the mean number of cells had increased to 4.21 x 10^5 and the LIPUS treated wells contained a mean of 4.39 x 10^5 HaCaT cells, again this was not a significant difference with a p-value of 0.6. After 2-days of incubation post LIPUS treatment the mean number of cells in the untreated wells was 5.96 x 10^5 and in the LIPUS treated wells the mean number of cells had increased to 5.7 x 10^5, this difference was not significant (p=0.57). At the end of the 3-day incubation post LIPUS treatment the mean number of cells in the untreated wells had increased to 9.22 x 10^5 and the LIPUS treated wells contained a mean of 9.85 x 10^5 HaCaT cells. When statistically analysed using a t-test this was not significant.

HDF cells were cultured in 6-well plates and treated with 30 mW/cm^2 LIPUS for 2-hours (**Figure 58b**). The mean number of cells counted immediately following the LIPUS treatment was 6.06 x 10^4, this was the same as the number of cells in the LIPUS treated wells (p>0.9999). After 1-day incubation post LIPUS treatment the mean number of cells in the untreated wells was 1.03 x 10^5 and the LIPUS treated wells contained a mean of 9.69 x 10^4 cells, this was not a significant difference with a

p-value of 0.55. After 2-days of incubation post LIPUS treatment the mean number of cells in the untreated wells was 1.98 x 10^5 and in the LIPUS treated wells the mean number of cells had increased to 2.02 x 10^5, this difference was not significant (p=0.75). At the end of the 3-day incubation post LIPUS treatment the mean number of cells in the untreated wells had increased to 3.26 x 10^5 and the mean number of cells in the LIPUS treated wells was 3.45 x 10^5 cells. When statistically analysed using a t-test this was not significant. This demonstrates that a single treatment of 30 mW/cm^2 LIPUS for 2-hours does not increase the proliferation of either HaCaT cells or HDF cells.

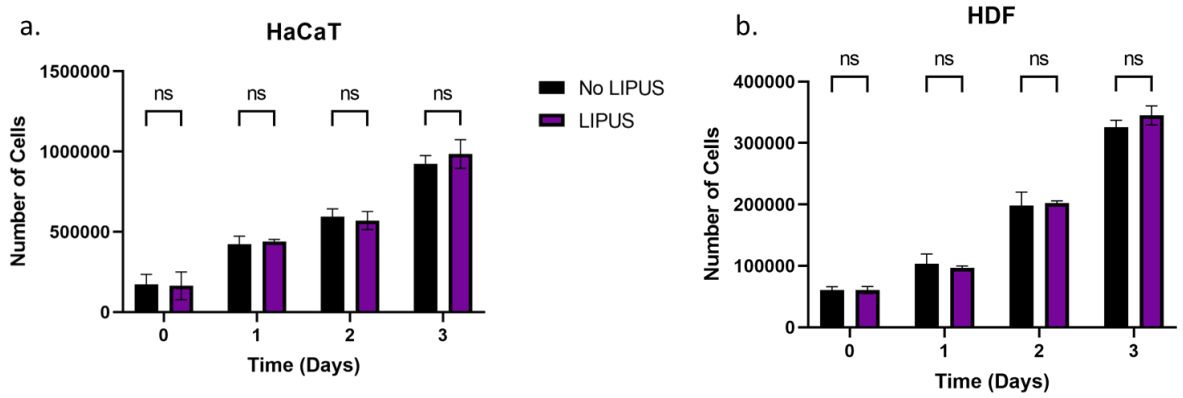

Figure 58: Cell numbers from HaCaT cells (a) and HDF cells (b) treated with 30 mW/cm^2 LIPUS for 2-hours and grown over a 3-day period at 37 ^oC 5 % CO_2. Error bars = +/-SEM. Analysed using t-test. Ns = not significant. N = 3

2-hours of LIPUS treatment does not affect cell proliferation in HaCaT or HDF cells.

A PrestoBlue assay was performed to assess viability of cells treated with LIPUS by measuring metabolism through colour change absorbance measurements. Resazurin is a blue compound in the product PrestoBlue, which is reduced to resorufin, a red compound, by cell metabolism resulting in measurable colour change proportional to metabolic activity of cells in a sample. In HaCaT cells the metabolism remained at similar levels throughout the 72-hour incubation (**Figure 59a**). Immediately following 2-hour 30 mW/cm^2 LIPUS treatment the absorbance at 570nm was 0.53, this was similar to the LIPUS treated wells with 0.58, after 1-day

the absorbance was 0.51 in the untreated wells and 0.56 in the LIPUS treated wells. After 2 days incubation the absorbance was 0.74 in the untreated wells and 0.69 in the LIPUS treated wells. Finally, the absorbance at the end of the 72-hour incubation post LIPUS treatment was 0.79 in the untreated wells and 0.73 in the LIPUS treatment wells. When analysed for a correlation the p-value was 0.82 when comparing untreated and LIPUS treated cells, indicating 2-hour 30 mW/cm^2 LIPUS treatment does not impact the metabolism of HaCaT cells.

In HDF cells, immediately post 2-hour 30 mW/cm^2 LIPUS treatment the cells had lower metabolism compared to the untreated cells, which then increased over the 3-day incubation period at similar levels to the untreated cells (**Figure 59b**). The absorbance was 0.76 in untreated wells and 0.26 in LIPUS treated wells. After 1 day incubation post LIPUS the absorbance in untreated wells had decreased to 0.57, while the LIPUS treated well had increased to 0.54. After 2-day incubation the absorbance was 0.71 in the untreated wells and 0.74 in the LIPUS treated wells. After 3-day incubation post LIPUS treatment was 0.71 in the untreated wells and 0.84 in the LIPUS treatment wells. When analysed for a correlation the p-value was 0.84 when comparing untreated and LIPUS treated cells, indicating 2-hour 30 mW/cm^2 LIPUS treatment does not impact the metabolism of HDF cells over 3-days post LIPUS treatment.

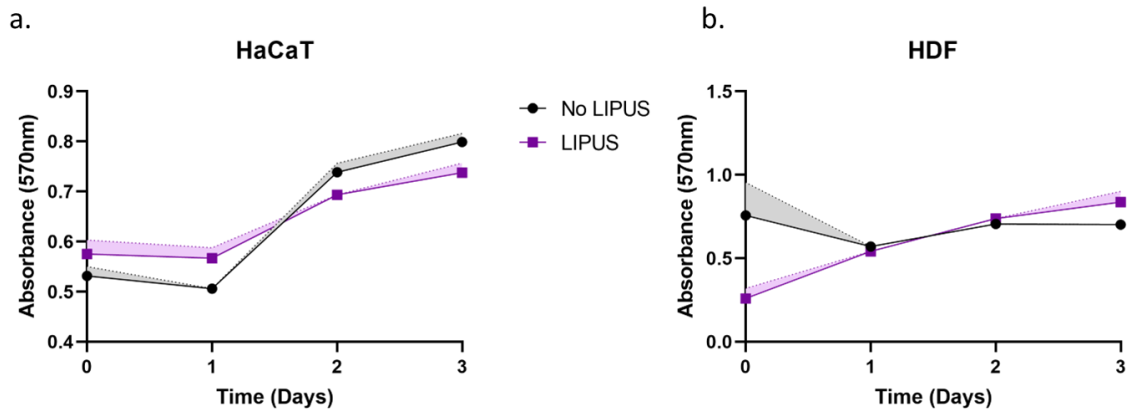

Figure 59: PrestoBlue assay was performed on monolayers of HaCaT (a) and HDF (b) treated with 30 mW/cm^2 LIPUS for 2 hours. Absorbance measured at 570nm. Shaded area = +/-SEM. Analysed using t-test. N=3

2 hours of LIPUS treatment does not affect cell viability of HaCaT or HDF cells and should therefore be a non-cytocidal treatment.

4.3.2 Permeability of monolayer

The impact of LIPUS on the permeability of skin cell monolayers was investigated to ascertain whether antibiotic penetration through skin could be affected by LIPUS, using monolayers of HaCaT and HDF cells and FITC-Dextran fluorescent molecules. HaCaT and HDF cells were grown to confluence in 6-well inserts, DMEM supplemented with 1 mg/ml 70 kDa FITC-dextran was placed within the well insert and DMEM was added to the well surrounding the insert. The wells were then treated with 30 mW/cm^2 LIPUS for 2-hours; increased fluorescence in the media surrounding the well insert would indicate an increase in permeability through the cells. In the HaCaT cells, the fluorescence intensity immediately post LIPUS treatment was mean 7075 RFU. The fluorescence intensity was slightly lower in the LIPUS treated wells at mean 6966 but this was not significantly lower (**Figure 60a**). The p-value of 0.87 was calculated when analysed using a t-test. In HDF cells, the mean fluorescence intensity immediately post LIPUS treatment was 16191, this was higher than the mean fluorescence intensity in the untreated wells at 12524, but not significantly higher (**Figure 60b**). When a t-test was performed to statistically analyse the data, the p-value was calculated at 0.074, failing to demonstrate any significant change in permeability of the HDF cells when treating with 30 mW/cm^2 LIPUS treatment.

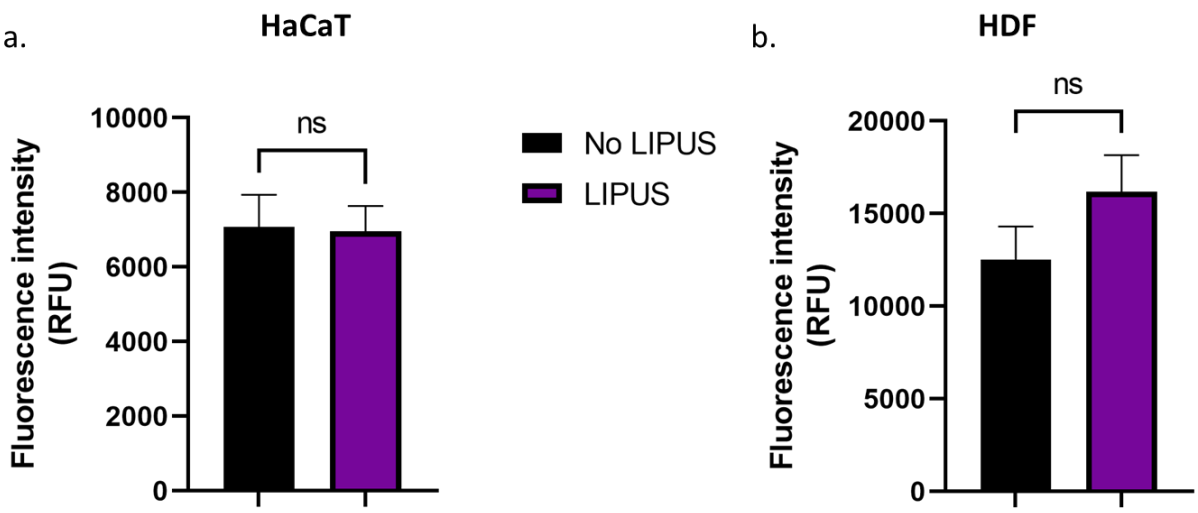

Figure 60: Confluent monolayers of HaCaT (a) and HDF (b), were grown in 6-well inserts containing DMEM supplemented with 1 mg/ml 70kDa FITC-Dextran and treated with 30 mW/cm^2 LIPUS for 2-hours. Fluorescence was read immediately post LIPUS treatment. Error bars = +/-SEM. Analysed using t-test. Ns = not significant. N=3

In the HaCaT cells, the fluorescence intensity untreated wells were mean 7265 RFU 2-hours post LIPUS treatment. The mean fluorescence intensity was slightly lower in the LIPUS treated wells at 7056 RFU but this was not significantly lower (**Figure 61a**). The p-value of 0.49 was calculated when analysed using a t-test. In HDF cells, the mean fluorescence intensity 2-hours post LIPUS treatment was 12920 RFU, this was lower than the mean fluorescence intensity in the untreated wells at 17371 RFU, but not significant (**Figure 61b**). When a t-test was performed to statistically analyse the data, the p-value was calculated at 0.072, failing to demonstrate any significant change in permeability of the HDF cells when treating with 30 mW/cm^2 LIPUS treatment.

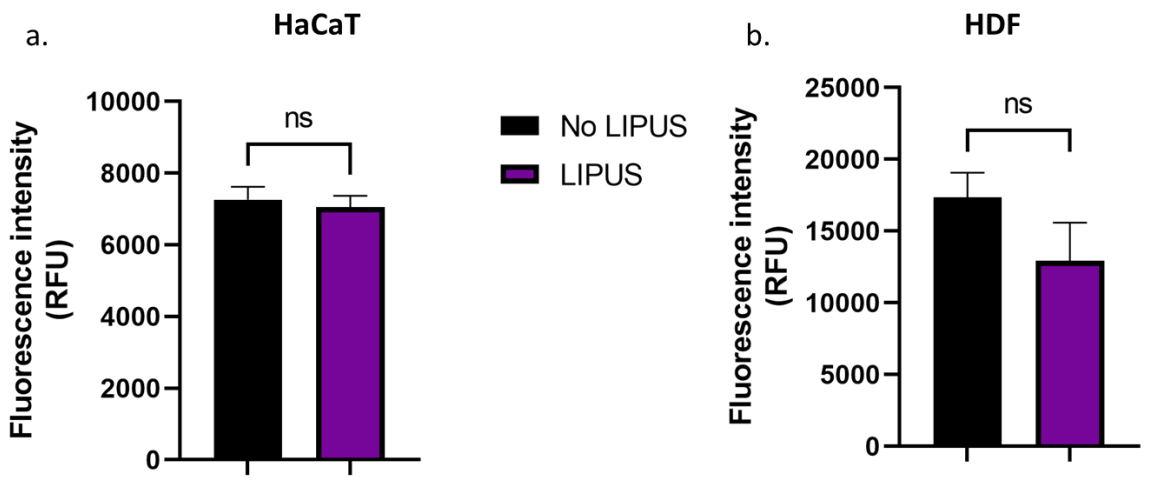

Figure 61: Confluent monolayers of HaCaT (a) and HDF (b), were grown in 6-well inserts containing DMEM supplemented with 1 mg/ml 70kDa FITC-Dextran and treated with 30 mW/cm² LIPUS for 2-hours. Fluorescence was measured 2-hours post LIPUS treatment. Error bars = +/-SEM. Analysed using t-test. Ns= not significant. N=3

2 hours of LIPUS treatment does not affect permeability of cell monolayers of HaCaT or HDF cells.

4.3.3 Wound healing

The migration of cells across a scratch wound in 2D monolayers was investigated with and without LIPUS treatment to assess potential changes in wound healing following LIPUS treatment. Monolayers of HaCaT and HDF cells were treated with Mitomycin C for 2-hours and scratched to form a wound. The monolayers were then treated with 30mW/cm^2 LIPUS for 2-hours, the closure of the wounds was monitored over 48-hours and differences in rate of closure between untreated and LIPUS treated were compared. Images taken from the HaCaT migration assay can be seen in **Figure 62**. The wound can be seen clearly at 0-hour post treatment with complete closure by 48-hours post treatment, at 18- and 24-hour post treatment partial closure of the wound can be seen.

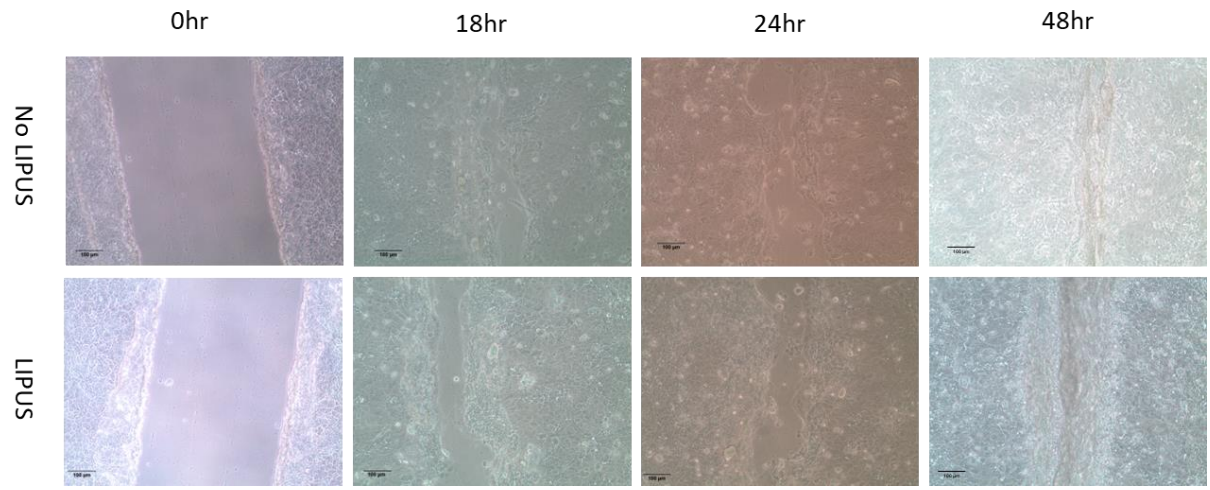

Figure 62: HaCaT cells monolayer wounded and treated with 30 mW/cm2 LIPUS and incubated for 48-hours at 37 oC 5 % CO2 imaged at 20x magnification Scale bar = 100 µm. N = 3

The total area of the wounds in HaCaT monolayers were calculated over the 48-hour period, with decreasing area indicating the closure of the wound (**Figure 63a**). The percentage of closure was also calculated (**Figure 63b**). Immediately post LIPUS treatment the area of the wounds in the untreated monolayers was 381 mm^2 while the LIPUS treated wound was 373 mm^2, this was 0% closure. After 18-hours, migration of the cells had resulted in a 75 % closure of the wounds in the untreated wells and a 69 % closure of the wounds in the LIPUS treated wells, the area of the wounds was 90 mm^2 in the untreated wells and 114 mm^2 in the LIPUS treated wells. The difference in wound closure after 18-hours was not significant (p=0.29). After 24-hours the migration of HaCaT cells had resulted in a 92 % wound closure in the untreated monolayers and an 84 % wound closure in the LIPUS treated monolayers, the wound area had decreased to 30 mm^2 in the untreated wells and 30 mm^2 in the LIPUS treatment wells, again the differences in wound closure was not significant (p=0.15). After 48-hours in both the untreated and LIPUS treated wells, the wounds had fully closed. This demonstrates that LIPUS is neither advantageous nor detrimental to HaCaT cell migration.

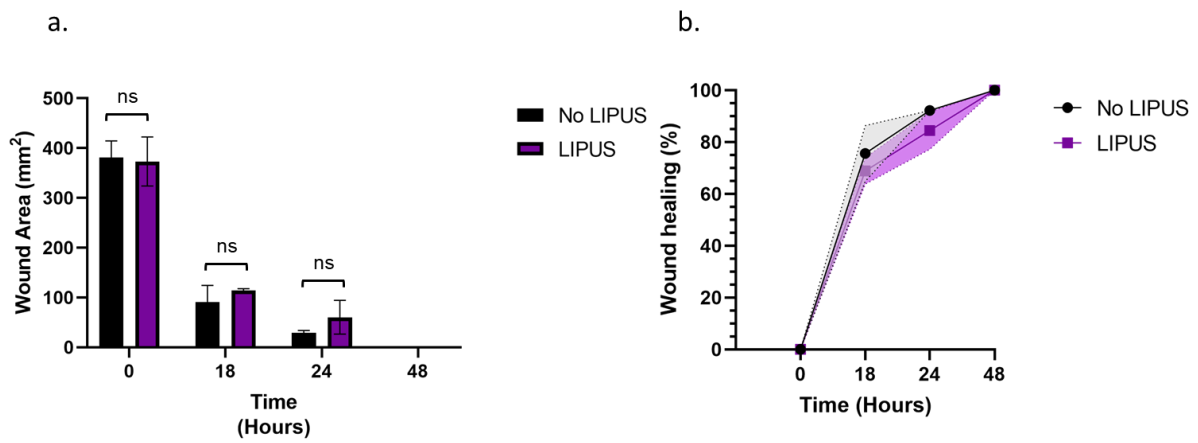

Figure 63: Wound healing over 48-hours in HaCaT cells treated with 2-hour 30 mW/cm² LIPUS. Wound area in mm² (a) and percentage of wound healing (b) was measured using ImageJ. Error bars = +/-SEM. Shaded area = +/- SEM. Analysed using t-test. Ns= not significant. N=3

Images taken from the HDF migration assay can be seen in **Figure 64**. The wounds can be seen clearly at 0-hour post treatment with complete closure by 48-hours post treatment, at 18- and 24-hour post treatment partial closure of the wounds can be seen.

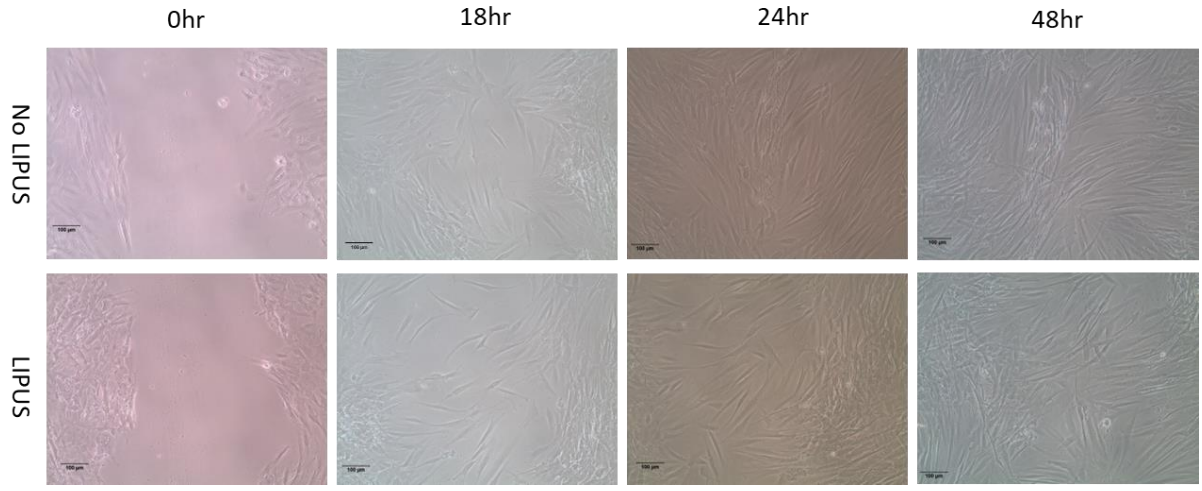

Figure 64: HDF cells monolayer wounded and treated with 30 mW/cm² LIPUS and incubated for 48-hours at 37 ºC 5 % CO_2 imaged at 20x magnification. Scale bar = 100 µm. N = 3

The total area of the wounds in HDF monolayer was calculated over the 48-hour period, with decreasing area indicating the closure of the wounds (**Figure 65a**). The percentage of closure was also calculated (**Figure 65b**). Immediately post LIPUS

treatment the area of the wounds in the untreated monolayers was 386 mm^2 while the LIPUS treated wound was 411 mm^2, this was 0% closure. After 18-hours, migration of the cells had resulted in a 69 % closure of the wounds in the untreated wells and a 59 % closure of the wound in the LIPUS treated wells, the area of the wounds was 125 mm^2 in the untreated wells and 168 mm^2 in the LIPUS treated wells, this was not a significant difference in closure with a p-value of 0.38. After 24-hours the wounds had closed 92 % in the untreated monolayers and an 76 % wound closure in the LIPUS treated monolayers, the wound area had decreased to 92 mm^2 in the untreated wells and 76 mm^2 in the LIPUS treatment wells. This was a significant difference in wound closure with the LIPUS treated wells demonstrating slower closure of the wounds (p=0.01). After 48-hours in both the untreated and LIPUS treated wells, the wounds had fully closed. This demonstrates that 2-hour 30 mW/cm^2 LIPUS may cause slowing in migration of fibroblast cells.

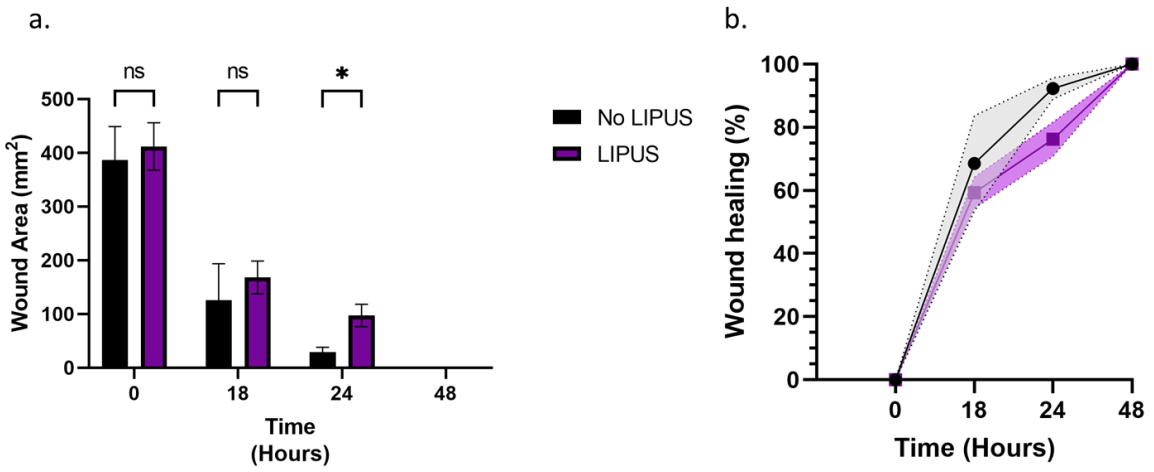

Figure 65: Wound healing over 48-hours in HDF cells treated with 2-hour 30 mW/cm^2 LIPUS. Wound area (a) and percentage of wound healing (b) was measured using ImageJ. Error bars = +/-SEM. Shaded area = +/-SEM. Analysed using t-test. Ns= not significant. * = p-value <0.05. N=3

2 hours LIPUS treatment does not affect the migration of HaCaT cells, while migration of HDF cells appears reduced, significantly at 24-hours. In both cell types complete wound closure occurred by 48-hours post LIPUS treatment.

4.3.4 Tissue-engineered skin structure

It was important to establish if LIPUS affected the structure of the model used in the study as part of evaluating its safety as a potential therapy. TESM were grown for 14-days before being treated with 30 mW/cm^2 LIPUS for 2-hours. The TESM were sectioned and then H&E stained before imaging and compared against TESM without LIPUS treatment (**Figure 66**). The epidermal layer is highlighted with the blue arrows while the border between the epidermal layer and dermal layer is highlighted by green arrows. There is no visual difference between the untreated models and the treated with 2-hour 30 mW/cm^2 LIPUS, with no separation between the epidermal and dermal layers.

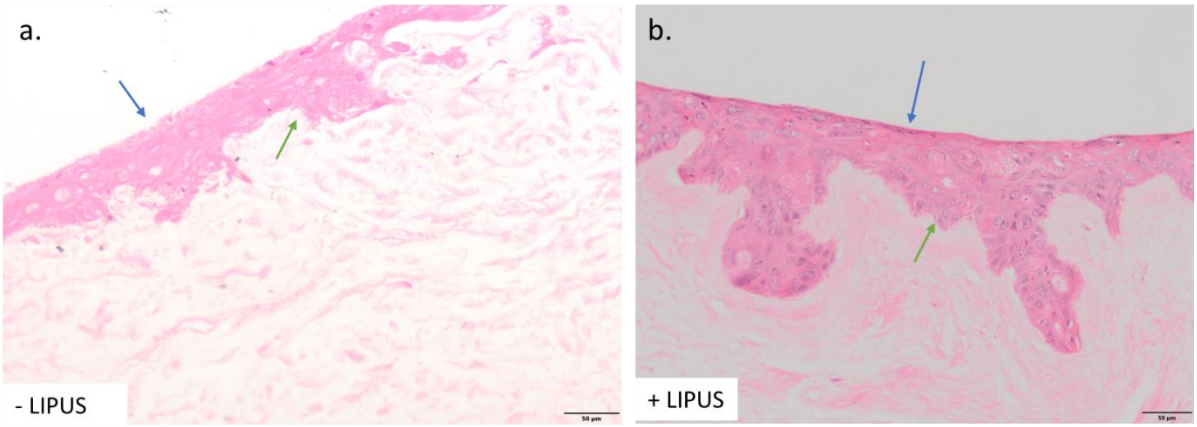

Figure 66: Histology of an untreated tissue-engineered skin model (a) and a model treated with 30 mW/cm^2 (b). Stained with haematoxylin and eosin, imaged at 20x magnification. Top of the models indicated with blue arrows, boundary between epidermis (composed mainly of HaCaT keratinocytes) and fibroblast-populated dermis in model indicated by green arrows. Scale bar = 50 µm

When infecting the TESM with *S. aureus* strains the skin model must be injured to allow an entry point for the bacteria by breaking the epidermal barrier. To injure the skin a metal loop was heated and used to burn the TESM. This injury caused the epidermal layer containing the HaCaT cells to detach from the dermal layer containing the HDF cells as shown in **Figure 67**. The uninjured TESM can be seen in **Figure 67a** with the intact epidermal layer highlighted by the orange arrow. However, the burnt TESM is shown in **Figure 67b** where the detachment of the

epidermal layer clearly seen and indicated by the blue arrow. There was not total loss of the epidermal layer within the injured model with surrounding burn site retaining the epidermal layer, indicated by the green arrow.

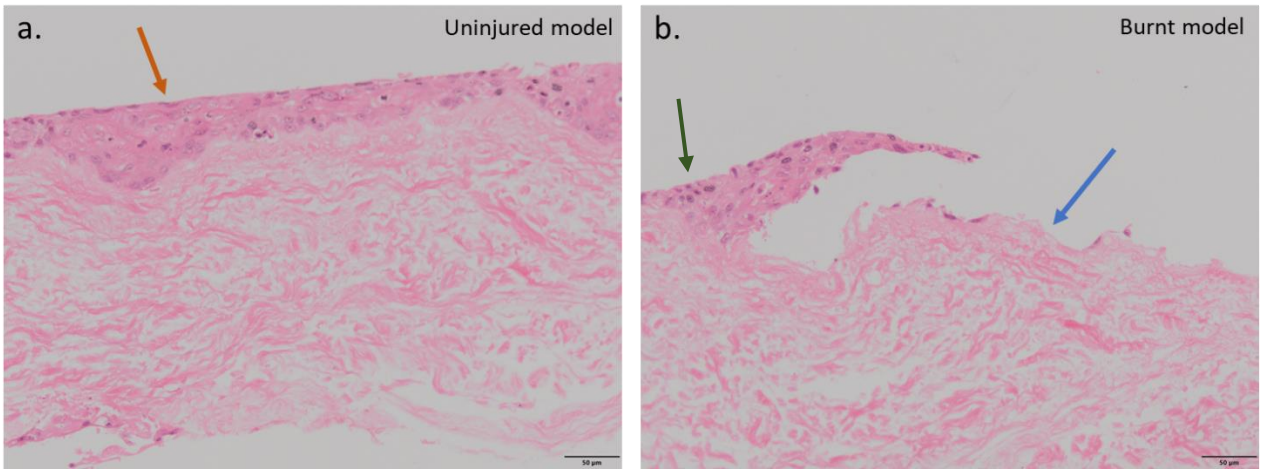

Figure 67: Histology of an uninjured tissue-engineered skin model (a) and a model treated burnt with heated metal loop(b). Stained with haematoxylin and eosin, imaged at 20x magnification. Epidermal layer indicated with orange arrow, burn site with loss of epidermal layer indicated with blue arrow, retained epidermal layer adjacent to the burn site highlighted by the green arrow. Scale bar = 50 µm

4.3.5 Infection of Tissue-Engineered Skin Model

S. aureus SH1000 was initially used to infect the TESM, however the bacteria failed to survive in the model. No CFU were recovered from the skin at 24-hour infection time with the SH1000 strain, a laboratory strain of *S. aureus* (**Figure 68**). This was in contrast to the *S. aureus* S235, a clinical isolate strain of *S. aureus*, where an average of 1.71 x 10^6 CFU/mg were recovered from the TESM. This highlights the inability for the laboratory strain to successfully colonise and infect the TESM.

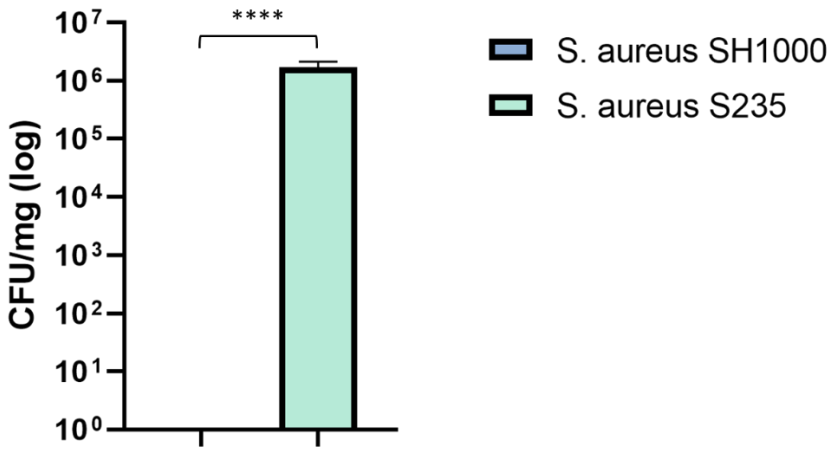

Figure 68: S. aureus SH1000 and S235 recovered from tissue-engineered models after 24-hours infection at 37°C 5 % CO_2. Error bars = +/-SEM. Analysed using t-test. **** p-value <0.0001 N=3

Due to the lack of bacteria recovered from the TESM when infected with *S. aureus* SH1000, the ability of the *S. aureus* SH1000 laboratory strain to grow in the presence of HaCaT and HDF cells and media taken from HaCaT and HDF was investigated and compared with *S. aureus* S235 (**Figure 69**). When the bacteria were grown in BHI the CFU/ml was 5.82 $x10^9$ for the SH1000 strain and 5.78 x 10^9 for the S235 strain. When grown in the presence of HaCaT cells the CFU/ml for SH1000 was 1.04 $x10^5$, while the CFU/ml for S235 was 1.96 x 10^8, the reduction in CFU for the SH1000 was significant in comparison to the S235 strain (p=0.007). When grown in the presence of HDF the CFU/ml was 3.27 x 10^4 while the CFU for S235 was 2.4 x 10^8, again this reduction in CFU in the SH1000 was significantly different to the S235 strain, the p-value was 0.002 when calculated using t-tests. In the co-culture of HaCaT and HDF cells the CFU/ml for the SH1000 was significantly lower than the CFU/ml for the S235 strain, 2.73 x 10^4 in SH1000 and 2.29 x 10^7 in S235 (p=0.0007). This demonstrates the ability of keratinocytes and fibroblasts to reduce the viability of a laboratory strain of *S. aureus* while not inhibiting the growth of a clinical strain of *S. aureus.*

Similar trends when *S. aureus* SH1000 and S235 were grown in conditioned media removed from the monolayers. When the bacteria were grown in the media removed from HaCaT cells, 2.3 x 10^4 CFU/ml of SH1000 and 1.93 x 10^8 S235 were

recovered. This was a significant reduction in viable bacteria in the SH1000 compared to S235 (p=0.014). When grown in media removed from HDF cells the CFU for SH1000 was again significantly reduced in comparison to S235 with 1.97 x 10^4 SH1000 and 3.31 x 10^8 S235 (p=0.00007). When media from the co-culture of HaCaT and HDF was used to grow the *S. aureus* strains the CFU/ml for the SH1000 was 3.22 x 10^4 and 1.69 x 10^8 for the S235, the reduction in CFU in SH1000 was significant in comparison to S235 with a p-value of 0.0043 calculated with multiple t-test.

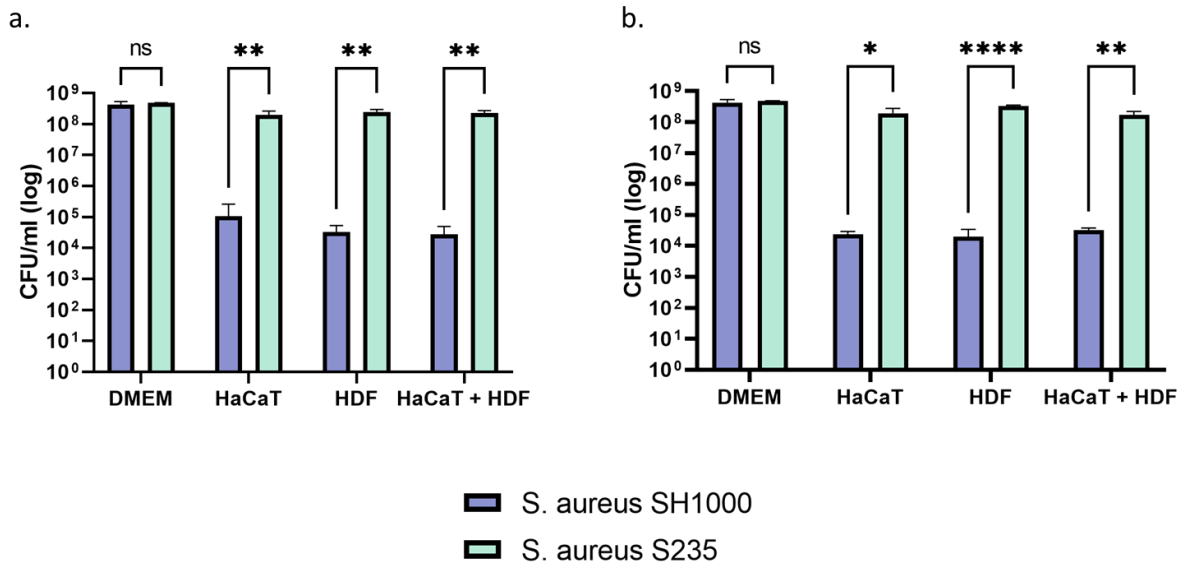

Figure 69: Colony forming units of S. aureus SH1000 and S. aureus S235 grown for 24-hours at 37 ºC 5 % CO_2 in DMEM supplemented with 10% FBS in the presence of HaCaT, HDF and co-culture of HaCaT and HDF monolayer (a), and grown for 24-hours at 37 ºC 5 % CO_2 in DMEM supplemented with 10 % FBS removed from monolayer of HaCaT, HDF and co-culture of HaCaT and HDF (b). Error bars = +/-SEM. Analysed using t-test. ns = not significant, * = p-value < 0.05, ** = p-value < 0.01, **** = p-value < 0.0001. N=3

S. aureus SH1000, unlike S. aureus S235, is unable to thrive in the presence of either HaCaT or HDF cells, or conditioned media from both cell types, suggesting release of a substance from both cell types that combats infection with this strain.

4.3.6 Antibiotic sensitivity

To test whether LIPUS is an effective adjunct to antibiotics in treatment of bacterial skin infection, an infection model was used. TESM were infected with $1x10^6$ *S. aureus* S235 for 24-hours before treatment with 20 µg/ml gentamicin with and without 2-hour 30 mW/cm^2 LIPUS treatment. Gentamicin was applied prior to LIPUS treatment and incubated for 24-hours post treatment, infected TESM without gentamicin treatment were also used as untreated controls. TESM were bisected; half of each sample was formalin fixed, processed to paraffin and wax embedded for histology, while the other half was used to calculate CFU/mg tissue in each sample. Gram staining of histology sections allowed visualisation of S. *aureus* S235 within the layers of the TESM. Images of Gram stained TESM infected (**Figure 70**) *S. aureus* S235 cells are highlighted with a blue arrow in the images.

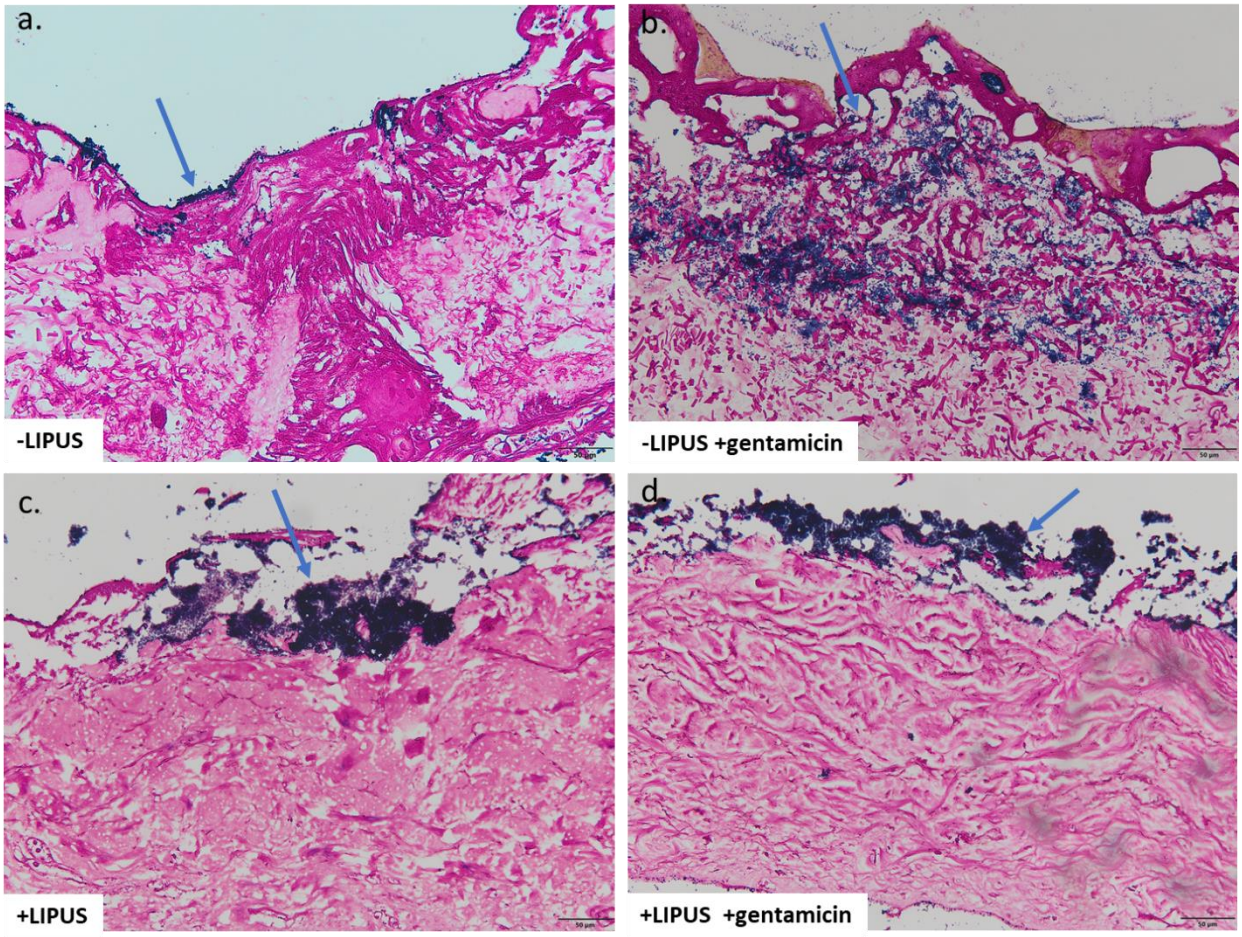

Figure 70: Gram stains of tissue-engineered skin model infected with S. aureus S235. An untreated infection model (a), an infection model treated with 10 µg/ml gentamicin only (b), an infection model treated with 30 mW/cm^2 LIPUS only (c) and an infection model treated with both 30 mW/cm^2 LIPUS and 20 µg/ml gentamicin (d). Scale bar = 50 µm

The halves of TESM for viable counts were minced using scalpels, then the *S. aureus* S235 recovered through vortexing the small pieces in PBS, which was then plated using the Miles-Misra method to calculate the number of viable bacteria in the TESM (**Figure 71**). The untreated TESM contained a mean of 1.87 x 10^7 CFU/mg, and number of viable bacteria in the LIPUS only treated TESM 2.62 x 10^7 CFU, there was no significant difference in the number of bacteria between the samples that were not treated with gentamicin (p=0.11). The infected TESM exposed to 10 µg/ml gentamicin had 7.06 x 10^4 CFU/ml *S. aureus* S235 recovered. This was a significant decrease than both the untreated TESM (p <0.0001) and the LIPUS only treated TESM (p <0.0001). When the TESM was treated with both 2-hour LIPUS treatment and 20 µg/ml gentamicin the CFU/ml recovered was 2.29 x 10^4. This was a slight reduction when compared to the gentamicin only treated TESM, but the decrease was not significant (p >0.9999). The reduction in viable bacteria in the TESM treated with LIPUS and gentamicin was significantly lower than both the untreated and LIPUS only treated TESM (p <0.0001). LIPUS does not increase gentamicin sensitivity in *S. aureus* S235 infected TESM.

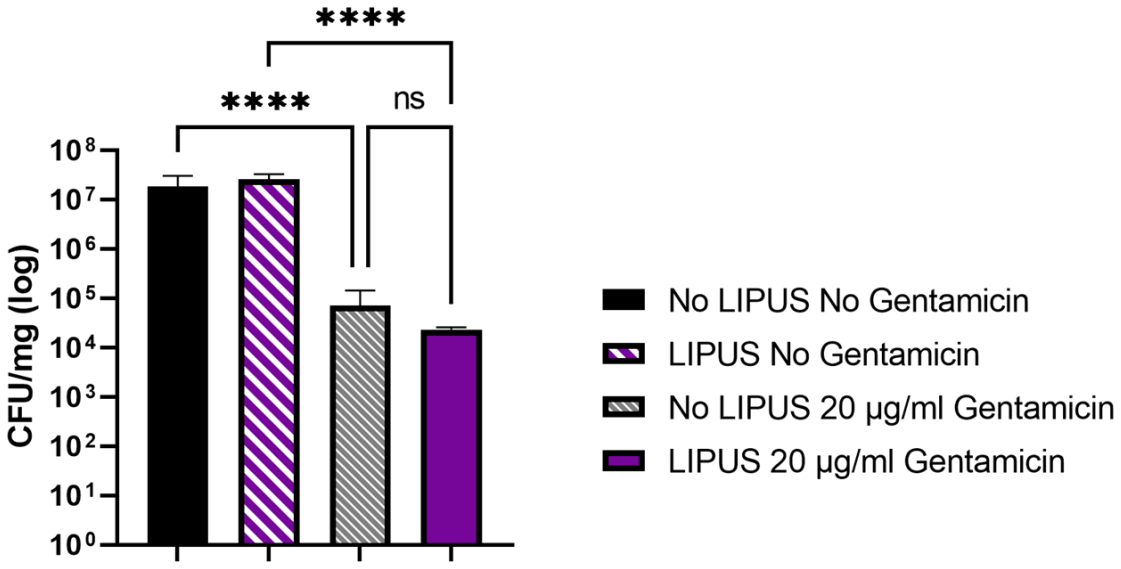

Figure 71: CFU/mg recovered from tissue-engineered skin model infected for 24-hours with S. aureus S235 before treatment with and without 30 mW/cm² LIPUS and with and without 20 µg/ml gentamicin. Statistical analysis performed using one-way ANOVA with multiple comparisons. Error bars = +/-SEM.

Analysed using one-way ANOVA with Tukey's multiple comparison. Ns= not significant, **** = p-value <0.0001. N=3

These data show LIPUS does not increase antibiotic sensitivity to gentamicin in

4.3.7 Interleukin-6 (IL-6) levels

IL-6 is a pro-inflammatory marker released during infection as part of the initial stages of immune response to infection. The use of LIPUS has been previously indicated to alter IL-6 levels released after treatment (Giantulli *et al.*, 2021). In this study changes in IL-6 levels released between TESM treated with and without LIPUS were assessed using ELISA to investigate whether the LIPUS used in this study would show similar results.

When the TESM were treated with 30 mW/cm^2 LIPUS for 2 hours it was found that IL-6 levels were elevated in the models at 0-hour and 2-hour post LIPUS treatment but by 24-hour post LIPUS treatment levels were similar across both treated and untreated TESM. At 0-hour post LIPUS treatment, the IL-6 concentration in the untreated model was mean 136 pg/ml. In contrast the LIPUS treated TESM had significantly higher IL-6 levels with 430 pg/ml (**Figure 72a**) (p = 0.027, t test).

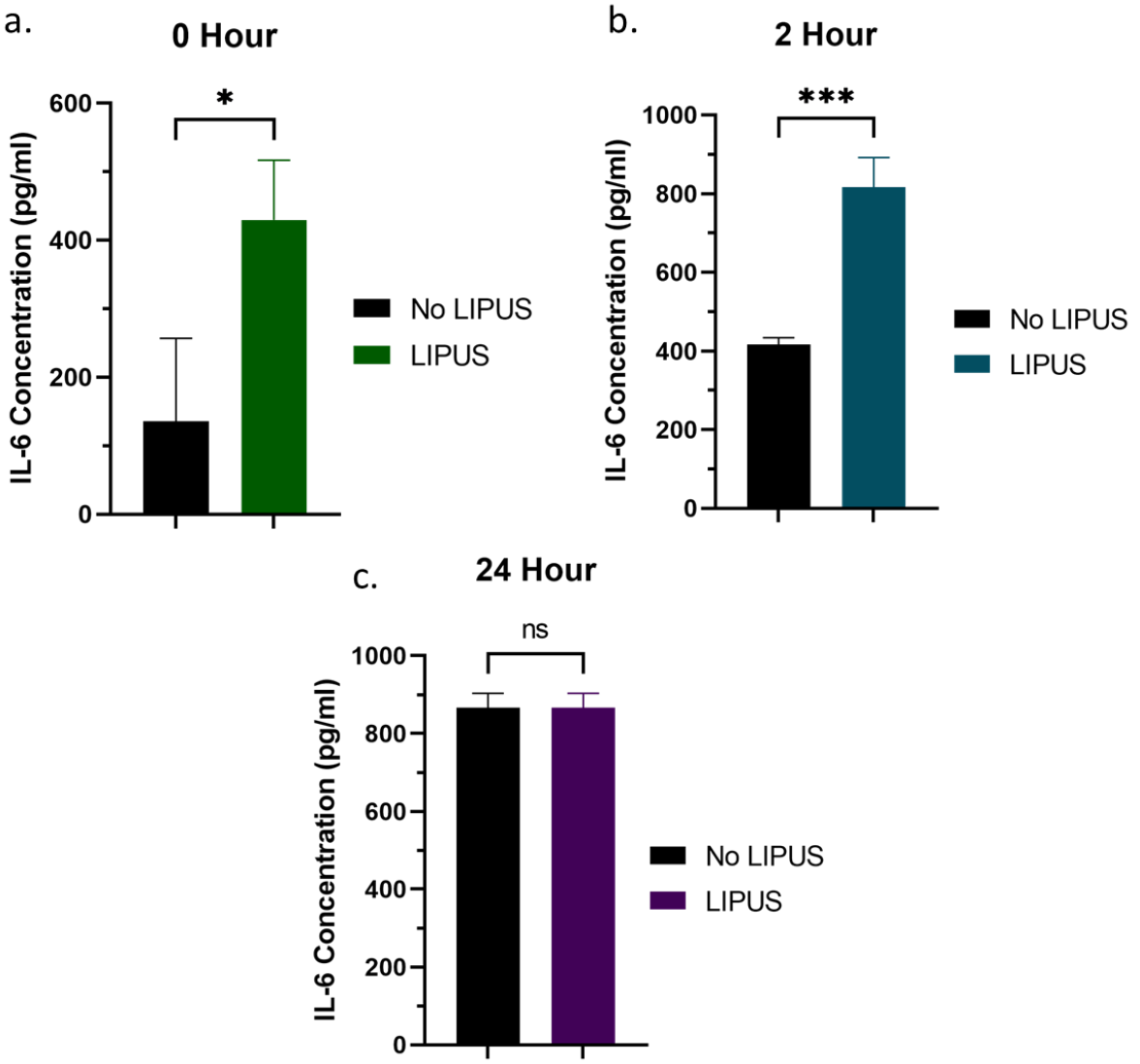

Figure 72: Tissue-engineered skin models treated with LIPUS for 2-hours, IL-6 concentrations were measured in media taken from the tissue-engineered models 0-hour post LIPUS (a), 2-hour post LIPUS (b) and 24-hour post LIPUS (c) ELISA. Error bars = +/-SEM. Analysed using t-test. ns = not significant * = p-value <0.05 *** = p-value <0.001 N=3

The IL-6 concentrations continued to increase at 2-hour post LIPUS treatment with the LIPUS treated TESM having higher concentrations of IL-6 than the untreated TESM (**Figure 72b**). The media surrounding the untreated TESM contained 416 pg/ml IL-6 while the media surrounding the LIPUS treated TESM contained significantly higher IL-6 with 816 pg/ml. A t-test was used to statistically analyse the difference in concentrations by comparing the mean of the IL-6 concentrations in the

untreated TESM with the mean of the treated TESM, the p-value was 0.008 which indicates a highly significant increase in concentrations.

After 24-hours incubation post treatment, the IL-6 concentrations in the media surrounded both LIPUS treated and LIPUS untreated TESM continued to rise, however, the difference between the two TESM had decreased (**Figure 72c**). The media surrounding the untreated TESM contained 866 pg/ml IL-6, while the media surrounded the TESM which received 2-hours LIPUS treatment had an IL-6 concentration of 805 pg/ml. These values were much closer than seen in the 0-hour and 2-hour post treatment TESM and when statistically analysed using a t-test the p-value was >0.99, meaning the difference in IL-6 levels between the two treatment conditions were no longer significant.

These data indicate that LIPUS stimulates IL-6 production in TESM immediately post LIPUS treatment and 2-hours post LIPUS treatment, by 24-hours post LIPUS IL-6 production is similar to the untreated TESM.

4.3.8 Improvement of infection model to be more clinically relevant

To improve the infection model to create a better replication of *in vivo* infections the TESM used in this study was combined with an in vitro wound milieu (IVWM) model developed by collaborators in the Kaushik lab (Dhekane *et al*., 2022). IVWM fluid was used in place of BHI to infect the TESM. To assess the differences in the infections between the IVWM and BHI, CFU/mg were calculated for viable numbers of *S. aureus* S235 recovered from the tissue, as well as imaging of Gram stains and H&E stains performed on sections taken from the TESM.

Uninfected TESM were incubated in the presence of BHI (**Figure 73a**) and IVWM (**Figure 73b**) for 24-hours. The models were fixed and sectioned before H&E

staining to visualise any changes in structure or integrity in the TESM. When comparing the TESM incubated in IVWM against the BHI incubated TESM there was no visual difference, with both models looking healthy. The epidermal layer, containing HaCaT cells, remained intact with no changes in growth or integrity, this is highlighted with the blue arrows. The same is shown of the dermal layer, containing HDF cells, with no changes in integrity or growth, highlighted with green arrows.

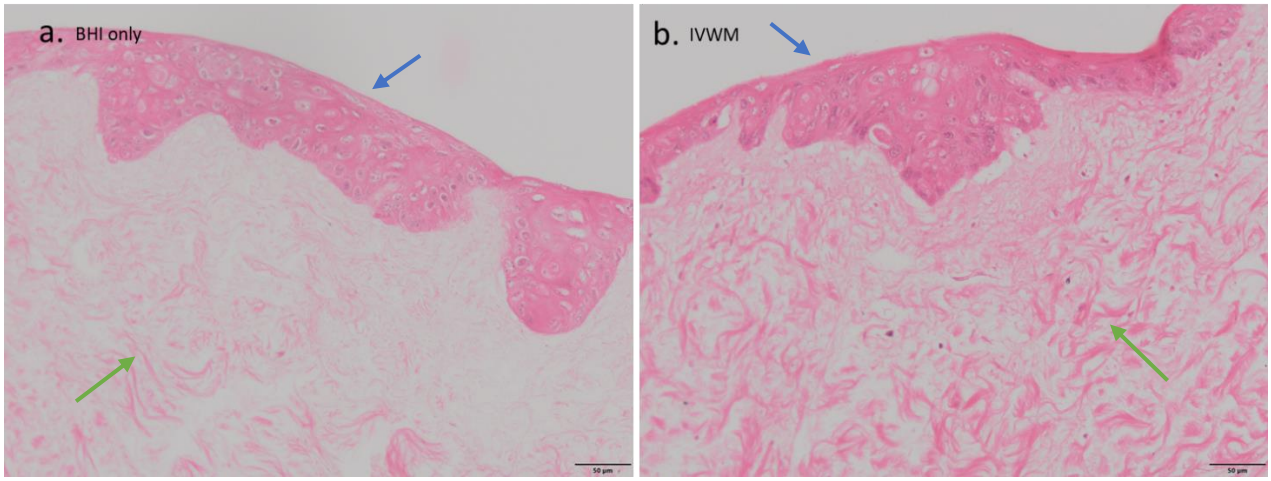

Figure 73: H&E stain of uninfected skin incubated with BHI (a) and IVWM (b). The models remained visually similar with no disruptions to either the dermal layer (green arrows) or the epidermal layer (blue arrows). Scale bar = 50 µm.

On Gram staining of infected TESM sections, there were visible differences between the two model types, with more obvious clustering of bacteria in the TESM incubated with IVWM. When the TESM were infected with *S. aureus* S235 with BHI used as the carrier of the bacteria (**Figure 74a**), the *S. aureus* S235 grow in small clusters spread along the epidermal layer of the TESM indicated by the blue arrows. However, when IVWM was used as the carrier for *S. aureus* S235 the clusters were much larger and more pronounced. This can clearly be seen in **Figure 74b** highlighted by the green arrows. This more closely replicates clustering of *S. aureus* seen *in vivo* in skin infections (Li *et al*., 2020).

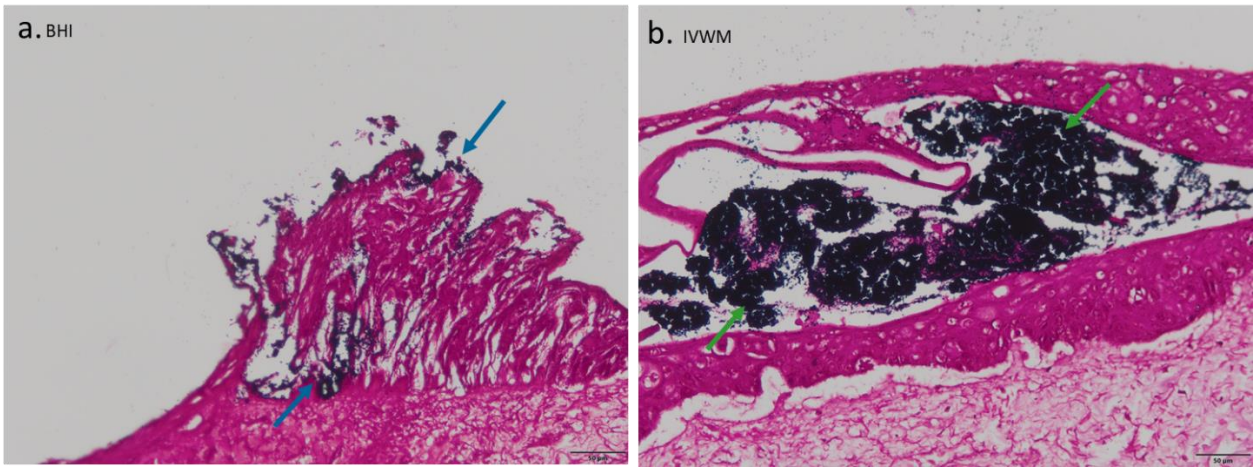

Figure 74: Gram Stain of TESM infected with S. aureus S235. S. aureus grown in BHI highlighted by blue arrows (a); larger clusters of S. aureus can be seen in models incubated with IVWM highlighted by green arrows(b). Scale bar = 50 µm.

To investigate whether IVWM impacted the ability of *S. aureus* S235 to propagate within 3D models, TESM were infected with *S. aureus* S235 using IVWM as a carrier, along with BHI which was used as the control. When BHI was used as the carrier for the bacteria the CFU/mg recovered from the TESM was 1.76 x 10^7. This was higher than the CFU/mg for the TESM infected using IVWM as the carrier for the bacteria which was 1.22 x 10^7. When analysing the difference statistically using a t-test the p-value was 0.012. While this is statistically significant difference in the number of bacteria recovered, both TESM have high levels of infection and would be classified as successful infection regardless of the carrier used for the bacteria.

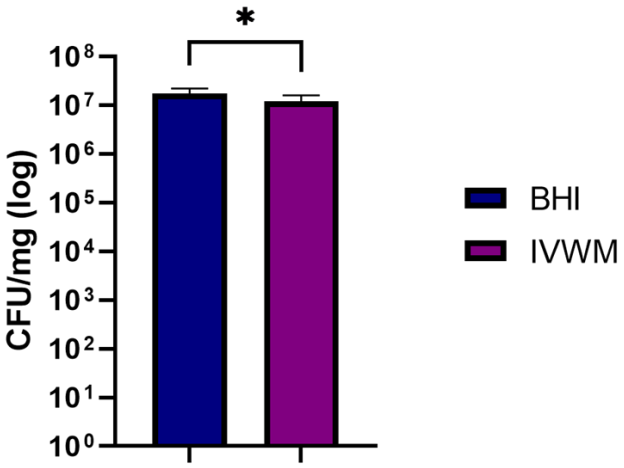

Figure 75: CFU/mg recovered from tissue-engineered skin model infected for 24-hours with S235 in BHI and IVWM. Error bars = +/-SEM. Analysed using t-test. * = p-value <0.05. N=3

4.3.9 Bacteria in IVWM

The IVWM may impact growth of bacteria as it is not a standard, optimised bacterial culture media, therefore it was important to investigate differences in behaviour of *S. aureus* S235 and SH1000 when growing in IVWM compared to BHI growth media. To assess these changes growth curves and Gram staining of both strains of *S. aureus* were performed.

BHI and IVWM were used as growth media to assess changes in growth rate for *S. aureus* S235 and *S. aureus* SH1000. When cultured in BHI *S. aureus* S235 (**Figure 76a**) reaches an OD_{600} of 1.157 at the end of 18-hours growth, reaching log phase within 3.5-hours. When grown in IVWM however, the maximum OD_{600} is 0.751, identified at 2.5hours of growth. The OD_{600} then declines to 0.607 by the end of 18-hours growth. The difference in growth is significant between 5.5-hours and 18-hours of growth in *S. aureus* S235.

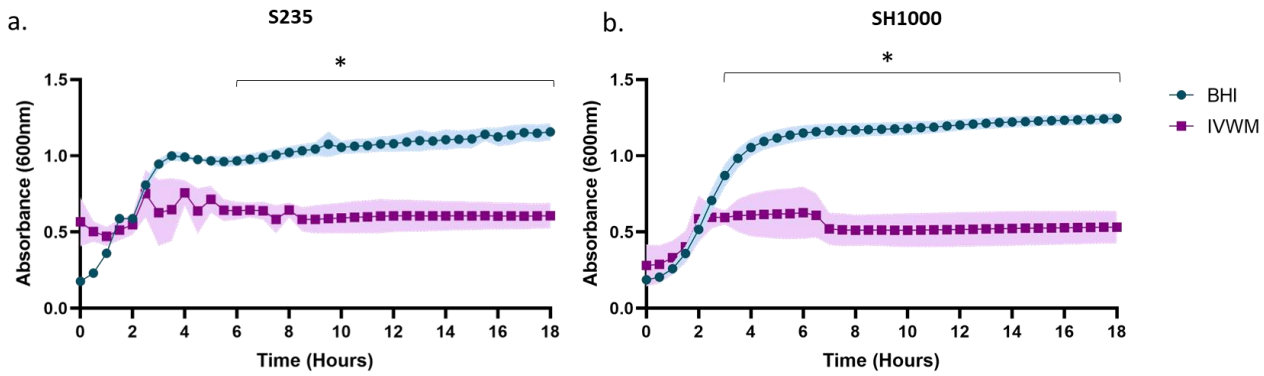

Figure 76: S. aureus S235 (a) and SH1000 (b) were grown in BHI and IVWM for 18-hours, absorbance at 600nm at 30-minute intervals. Shaded areas around growth curves indicate +/-SEM. Analysed using multiple t-test. * = p-value <0.05 N=3

When *S. aureus* SH1000 was grown in BHI and IVWM (**Figure 76b**) the initial rate of growth followed similar trends until 2-hours incubation. The *S. aureus* SH1000 grown in BHI reached OD_{600} 1.244 after 18-hours growth, also reaching log phase by 5.5-hours growth. However, when IVWM was used as the growth media, the maximum OD_{600} was reached at 2.5-hours growth with a OD_{600} of 0.596 this again declined slightly during longer incubation and the final OD_{600} at 18-hours incubation was 0.53. There was a significant difference between the growth of *S. aureus* SH1000 in BHI and IVWM between 3-hours and 18-hours with p-values calculated using multiple t-tests of <0.05.

These data indicate that IVWM is not as optimal for growth of *S. aureus* as BHI.

The CFU/ml of *S. aureus* S235 and SH1000 were calculated when grown in BHI and IVWM (**Figure 77**, summary in **Table 18** &**Table 19**). *S. aureus* S235 and SH1000 grow as well in IVWM as in BHI growth media.

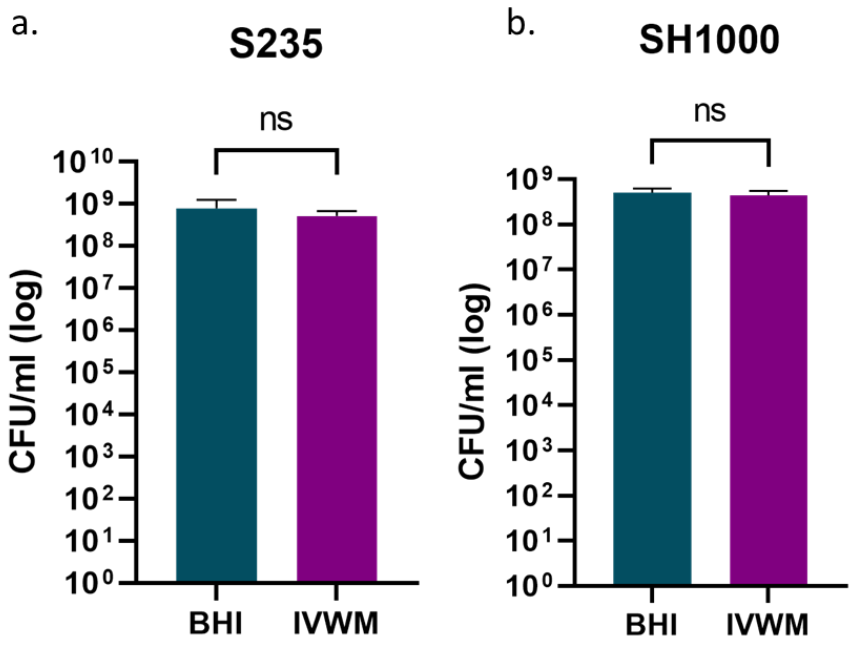

Figure 77: CFU/ml calculated from S. aureus S235 and SH1000 grown in BHI and IVWM for 24-hours. Error bars = +/-SEM. Analysed using t-test. Ns=not significant N=3

Table 18: CFU/ml of S. aureus S235 in BHI and IVWM

Treatment	CFU/ml	P-value
BHI	7.8×10^8	0.13
IVWM	5.2×10^8	

Table 19: CFU/ml of S. aureus SH1000 in BHI and IVWM

Treatment	CFU/ml	P-value
BHI	5.04×10^8	0.32
IVWM	4.38×10^8	

Due to reduced absorbance in the growth curves but similar numbers of viable *S. aureus* in the BHI and IVWM, images were captured of *S. aureus* S235 and SH1000 Gram stained after overnight growth in BHI and IVWM, to assess aggregation of the bacteria. These can be seen in **Figure 78**. When grown in BHI *S. aureus* S235 forms

small clusters (**Figure 78a**), when grown in IVWM, these clusters become aggregated forming much larger clusters of bacteria, indicated by the green arrow (**Figure 78b**). When *S. aureus* SH1000 is grown in BHI, small clusters of bacteria are also seen (**Figure 78c**), however when grown in IVWM an increase in extracellular matrix was visualised as stained pink during the Gram staining, indicated by the blue arrow. The *S. aureus* SH1000 appeared to cluster less in the IVWM, instead held together by the matrix surrounding.

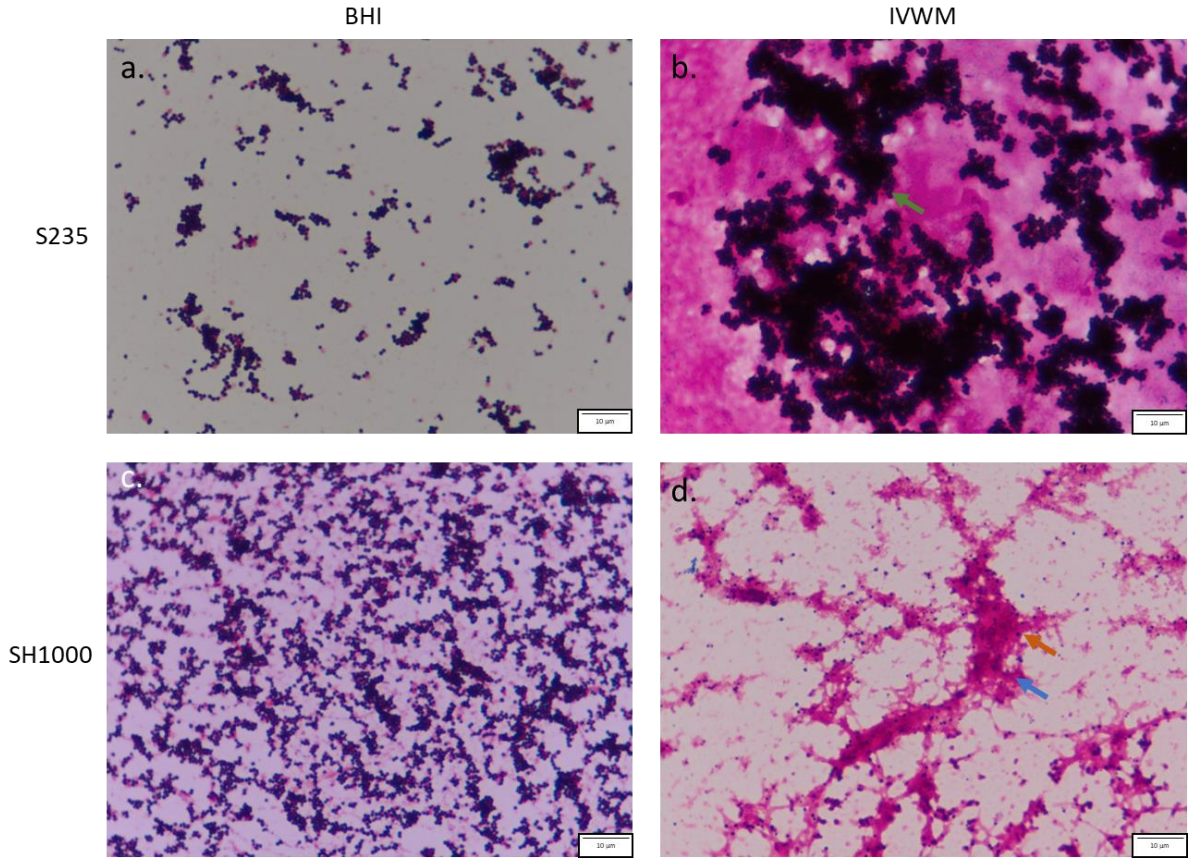

Figure 78: Gram stains of S. aureus S235 and SH1000 grown in BHI and IVWM for 24-hours at 37 ºC, large clusters of aggregated S235 indicated by the green arrow. Individual SH1000 indicated by orange arrow and fibrous extracellular matrix indicated by blue arrow. Scale bar = 10 µm Mag = 100x.

The use of IVWM produced infections representative of clinically relevant infections, with equivalent levels of infection in the TESM. The growth rates appeared reduced in IVWM compared to BHI, but similar numbers of bacteria were grown in both, the apparent reduction through reduced absorbance could be explained by aggregation of the bacteria in IVWM as visualised with Gram staining.

5 Discussion

5.1 Biofilms

Biofilms play an important role in chronic infection, and often result in prolonged and repeated antibiotic treatment. Therefore, the effective treatment of biofilms is crucial to improving antibiotic stewardship. Using LIPUS in conjunction with antibiotics has been shown to be effective at increasing antibiotic sensitivity in several pathogens and could well decrease the amount of antibiotics needed to effectively treat a chronic infection. *S. aureus* is a common pathogen found in both chronic and acute skin infections. In this study LIPUS treated *S. aureus* SH1000 biofilms were investigated to elucidate whether increased antibiotic sensitivity would occur in *S. aureus* biofilms, and the potential mechanisms behind any changes to antibiotic sensitivity explored.

5.1.1 LIPUS treatment, Growth and Dispersal

In this study the effects of 30 mW/cm^2 LIPUS treatment on *S. aureus* SH1000 biofilms were investigated. The first enquiry was to assess how growth and dispersal of the biofilm is impacted by LIPUS treatment, if at all. In this study, it was found that the growth of biofilms did not increase with 1-, 2-, or 3-hour 30 mW/cm^2 LIPUS treatment in all maturities of biofilm investigated. Previous work by (Pitt & Ross, 2003) shows an increase in bacterial numbers when treated with US for up to 3-hours. The study conducted by Pitt and Ross used Gram-positive *Staphylococcus epidermidis,* and Gram-negative *Escherichia coli* and *Pseudomonas aeruginosa;* with all three species having increased bacterial numbers indicating the effects of ultrasound on growth were independent of the structure of the cell wall and may translate to other species. The intensity of the US used in the Pitt and Ross study was much higher than the US used in this study while the frequency was lower and while it is unclear whether the US delivered in the Pitt and Ross experiments was pulsed or continuous, the use of an ultrasonic bath designed for cleaning may indicate the US was continuous. It has been established that continuous US

increases growth through raised metabolic activity in *Bacillus licheniformis* (Dai *et al., 2023)*, however, that work used higher intensity US than both Pitt and Ross, and this current study. Ensing *et al.* (Ensing *et al*., 2006) also investigated continuous US and the effects on viable cells and found similar findings to this study with no changes in viable cell numbers after US treatment. Ensing *et al.* also used low intensity US therefore the difference in intensity may contribute to the differences observed in this study rather than the frequency and intervals of wave generation, when comparing to previous work. Ayan *et al.* (Ayan et al., 2008) found that 20-minute LIPUS treatment with the Exogen machine used in this study decreased the number of viable cells in planktonic *S. aureus,* potentially demonstrating the ability of LIPUS to cause cell death in *S. aureus.* The current data presented here do not support the findings of Ayan *et al*.

When whole biofilms were stained with crystal violet, there was no change in the area of the biofilms and no visual difference in the density of the biofilm. Pitt and Ross (Pitt & Ross, 2003) measured an increase in biofilm density when treated with US, which was not observed in this study, however there were differences in frequency and intensity between the two studies which may be the reason for the differences in observations. Koibuchi *et al.* (Koibuchi *et al*., 2021) also investigated 30 mW/cm^2 LIPUS on biofilms, measuring the inhibition of *S. epidermidis* biofilm growth with LIPUS treatment. It was found that single applications of 20-minute LIPUS treatment of bacteria before biofilm establishment reduced the formation of the biofilm after 6-hours incubation, however when LIPUS was applied continuously for 12-hours there was not a reduction in biofilm. With a short incubation of 6-hours for the single short application of LIPUS the reduction in biofilm may be attributed to variations in the initial stages of biofilm formation, which is resolved as the biofilm matures. This suggests there may be an application for LIPUS in prevention of infection but as demonstrated in this study, LIPUS alone would be inappropriate as a treatment for biofilm associated infections.

The total area of *S. aureus* SH1000 biofilms reduced as the biofilms matured. Since detachment is an essential stage in a biofilm lifecycle this reduction in area may be

due to increased detachment as the biofilm increases in maturity, although it is worth considering the biofilms used in this study were grown in 6-well plates without flow, resulting in a lack of shear force on the biofilm. This lack of external stress may result in more loosely organised biofilm structure, which could increase disaggregation of areas of the biofilm as it matures due to instability. Zhang *et al.* (Zhang *et al*., 2022) found that static *P. aeruginosa* biofilms had reduced thickness when compared to biofilms exposed to dynamic flow. Berlutti *et al.* (Berlutti *et a*l., 2014) also noted increased numbers of viable cells in *S. aureus* biofilms under shear force compared with static biofilms indicating that the presence of shear force allows for improved biofilm formation.

The dispersal of the *S. aureus* biofilms when treated with LIPUS was also investigated as significant disruption to the biofilm could cause the infection to spread within the body with risk of systemic infection. In this study, dispersal of 1-, 5-, and 7- day *S. aureus* SH1000 biofilms were not altered when treated with 1-, 2-, and 3-hour 30 mW/cm^2 LIPUS treatment, however the S. *aureus* SH1000 3-day biofilm did show increased dispersal at 3-hour LIPUS treatment when analysed statistically. This may have been due to an anomaly in the datasets but due to the risk of dispersal 2-hour LIPUS treatment was selected for all future treatment time. Cavitation and shear force is needed to remove the biofilm from a surface (Wille & Coenye, 2020); while both happen in high-intensity and low-intensity US the energy in high intensity US result in inertial cavitation causing bubbles formed within a fluid to implode releasing high amplitude shockwaves. The low-intensity of the US used in this study causes stable cavitation that does not result in high energy shear force. Studies in animal models have not identified bacteraemia as a risk of low-intensity US treatment (Ensing *et al*., 2005).

5.1.2 LIPUS treatment and Antibiotic Sensitivity

The 30 mW/cm^2 LIPUS treatment increased gentamicin sensitivity in all *S. aureus* SH1000 biofilms investigated when treated with gentamicin prior to LIPUS treatment.

In older biofilms the increase in gentamicin sensitivity was not dependent on the time of LIPUS treatment in relation to the exposure to gentamicin. Maturation is a factor in antimicrobial sensitivity, therefore more mature biofilms are expected to have reduced sensitivity to antibiotics. However, the definition of a mature *S. aureus* biofilm is not clear with biofilms from 24-hours to 7-days being classed as mature (Chen *et al*., 2020; Kim *et al.*, 2018; Post *et al.*, 2017; Wu *et al.*, 2014), therefore even the youngest biofilm in this study may be classed as mature. To understand how LIPUS affects 'young' biofilms a 6-hour biofilm would be appropriate (Wu *et al*., 2014). On the other hand, LIPUS treatment in conjunction with vancomycin did not increase sensitivity to the antibiotic. This may be due to the different bacterial targets of each antibiotic. Vancomycin inhibits the synthesis of the cell wall, while gentamicin inhibits protein synthesis. This may be an indicator of the mechanism causing increased gentamicin sensitivity with LIPUS, as increased cell permeability would explain the greater gentamicin sensitivity but no change in vancomycin sensitivity.

Increased antibiotic sensitivity with US treatment has been previously observed in *S. aureus* and other microbes. Qian *et al.* (1997) and Huang *et al.* (1996) both reported increased gentamicin sensitivity in *P. aeruginosa* when used in combination with US treatment. Qian used US at intensity of 10 mW/cm^2 and varied frequencies between 70 kHz and 20 mHz, all frequencies used displayed enhanced antibacterial sensitivity when combined US and gentamicin treatment was used. Huang used a range of low US intensities between 0.2 and 15 mW/cm^2 while frequency remained 70 kHz, all intensities of US treatment tested caused a reduction in viable cells from established biofilms treated with gentamicin when compared to gentamicin only treated biofilms. Pitt *et al.* (1994) also observed increased antibiotic sensitivity in Gram-negative bacteria when treated with 0.3 W/cm^2, 67 kHz US but failed to observe changes in sensitivity in Gram-positive bacteria. Mortazavi *et al.* (2015) reported increased antibiotic susceptibility in *E. coli, S. epidermidis, S. aureus* and *Klebsiella pneumonia* when treated with diagnostic US dopplers with frequency capabilities of 7.5-13 MHz, the US power was not reported. Kvich *et al.* (2022) has reported increased antibiotic sensitivity in Gram-positive bacteria, finding 2-hour 50 kHz US treatment enhanced the bactericidal effects of both fusidic acid and clindamycin in *S. aureus* biofilms, as well as increased sensitivity in *P. aeruginosa*

biofilms to colistin and ciprofloxacin. Fusidic acid and clindamycin both have similar targets to gentamicin, inhibiting protein synthesis and ciprofloxacin also has internal targets preventing DNA synthesis, while colistin causes cell wall disruption (Fernandes, 2016; Kohanski *et al*., 2010; Sabnis *et al.*, 2021). Shi *et al.* (2013) reported decreases in number of viable intracellular *S. aureus* treated with rifampin and low-frequency US (20 kHz). Rifampin also targets internal cellular processes, preventing RNA synthesis.

Other studies have reported increased sensitivity to vancomycin when used in conjunction with US, which was not observed in this study. Hu (2018) used US targeted microbubble destruction in combination with vancomycin to enhance the effects of vancomycin in *S. epidermidis* biofilms. LIPUS mediated microbubble use in drug delivery is a different treatment option, so the observations are not comparable to LIPUS without the introduction of microbubbles, the use of microbubbles generates additional cavitation (Xiu *et al*.), this allows for more efficient penetration of antibiotics through the biofilm. Wang *et al*. (2018) found that multiple treatments of low-intensity US were more effective in increasing vancomycin sensitivity than single treatments. In bone healing patients LIPUS is administered daily with 60 doses of LIPUS as minimum (Haller *et al*., 2023). In the present study, only single treatments were used, but multiple LIPUS treatment is not unrealistic and further investigation would be useful. The intensity of the US used by Wang was higher than the intensity used in this study (92.36 mW/cm^2), which may also contribute to differences in sensitivity.

A wide range of frequencies and intensities of US appear to increase antibiotic sensitivity in many species of bacteria, however, the mechanisms behind this are poorly understood. Changes in biofilm and cell permeability, and biofilm structure have been suggested as reasons for changes in sensitivity. This study investigated this in an attempt to have a clearer picture of how antibiotic sensitivity increases with LIPUS treatment.

5.1.3 LIPUS Treatment and Structure

Due to changes in gentamicin sensitivity with LIPUS treatment the structures of whole biofilms treated with and without LIPUS were investigated to understand whether structural differences would allow for increased dispersal of antibiotics through the biofilms. In both 1-day and 7-day biofilms there was no visual difference in biofilms treated with LIPUS when compared to untreated biofilms. While few studies have investigated the effects of US only treatment, Qian *et al.* (1996) also observed no changes in biofilm structure using continuous US. Structural changes in biofilms have been observed in biofilms when LIPUS was used in conjunction with microbubbles (Xiu *et al*., 2023) due to increased cavitation caused by the presence of the microbubbles within fluid. High-intensity focused US is known to disrupt the structure of *S. aureus, P. aeruginosa* and *E. faecalis* biofilms (Bharatula *et al*., 2020; Iqbal *et al*., 2013; Yu *et al*., 2021) through thermal effects and inertial cavitation. Low-intensity US does not produce thermal effects and cavitation produced by low-intensity US is stable, reducing risks of high energy forces disrupting the structure of the biofilm. Due to the lack of changes in the structure of the biofilms treated with LIPUS, it is unlikely that structural changes to the biofilm results in the increased antimicrobial sensitivity observed.

5.1.4 LIPUS Treatment and Permeability

Biofilm permeability was investigated as a potential mechanism for increased antibiotic sensitivity in biofilms treated with LIPUS. 2 hours LIPUS treatment increased permeability of biofilms grown for 1-day to small molecules but were not more permeable to larger molecules. This was also seen in the 7-day biofilm but not the 3-, and 5-day biofilms. Previous work has reported increased permeability of *E. coli* and *P. aeruginosa* biofilms to gentamicin when treated with US (Carmen, Nelson Jl Fau - Beckstead, *et al*., 2004). The US used by Carmen was higher intensity (1.5 W/cm^2) than the US used in this study and may be a contributing factor to differences in permeability, however the difference in molecular size of the molecules used to measure permeability are most likely the cause of the difference in findings.

All weights of FITC-dextran were larger than the antibiotics used, the smallest available FITC-dextran is still significantly larger than antibiotics, therefore the use of a smaller fluorescent molecule such as fluorescently tagged antibiotics may have been more appropriate. However, permeability through the biofilm cannot be the only mechanism due to a lack of increased vancomycin sensitivity, therefore permeability of bacterial cells was also investigated.

To investigate the permeability of the *S. aureus* cell membrane, PI uptake and β-galactosidase leakage were used to assess changes in permeability. In this study neither method indicated changes in *S. aureus* membrane permeability. Other studies, on the other hand, have reported changes in permeability when treating bacterial cells with US of different intensities. (He *et al*., 2021) found the outer and inner membranes of *E. coli* were disrupted allowing for increased permeation of β-galactosidase and N-Phenyl-1-naphthylamine, however this was using high-intensity US which is known to disrupt cell membranes to lethal levels (64 W/cm^2 – 573 W/cm^2) and therefore significant increases in permeability would be expected. US has been found to increase permeability of *E. coli* cell membrane to Ca^{2+} (Li *et al*., 2018), however ions are significantly smaller than antibiotic molecules therefore it would be inappropriate to suggest antibiotics would have better permeation of cell membranes based on the increased uptake of ions. The cell wall structure of *E. coli* is different to *S. aureus*, so findings in *E. coli* may not translate into *S. aureus.* There was no increase in β-galactosidase leakage indicating a lack of substantial damage to the cell wall, however this does not give any indication of transient pore formation reported in mammalian cells treated with low-intensity US (Przystupski & Ussowicz, 2022). LIPUS is unlikely to cause significant damage in cell walls. PI uptake also did not increase in LIPUS treated cells. PI has a higher molecular weight than gentamicin and cannot passively transverse an intact membrane, while gentamicin is taken up by endocytosis therefore it may not be appropriate to conclude that LIPUS does not increase the permeability of cell membranes to molecules able to pass through an intact membrane.

5.1.5 LIPUS Treatment and Metabolism

Biofilm metabolism was investigated as another potential mechanism of increased antibiotic sensitivity. The working theory was that increased metabolism would increase the number of targets for antibiotics, for example cell wall synthesis in actively dividing cells. In young *S. aureus* biofilms the release of ATP into the media did not change with LIPUS treatment, nor did the level of ATP increase in the biofilm. However, in the 5-day and 7-day biofilms the levels of ATP decreased in the media and increased within the biofilm. Effects of US on ATP levels have been investigated in mammalian cells, finding that low-intensity US increases ATP release from bone osteoblasts (Manaka *et al*., 2015). Increased ATP release may not indicate increased metabolism, previous work in mammalian cells reported increased ATP can be associated with transient increases in membrane permeability (Arcuino *et al*., 2002), therefore it would not be appropriate to declare increased metabolism based solely on increased ATP. The reduced ATP within the media of older biofilms treated with LIPUS, suggesting that ATP is not being released from the biofilm, and an increase in ATP in cells removed from the biofilm; together suggest that 2 hours LIPUS treatment may result in increased metabolism in older biofilms.

Oxygen levels in the media taken from biofilms treated with 2-hour LIPUS were investigated to give additional indications of any changes in metabolism when the biofilms were treated with LIPUS. Oxygen levels are slightly higher in the media of biofilms treated with LIPUS; this could be interpreted as a decrease in *S. aureus* metabolism, which is not supported by the levels of ATP within the biofilm. *S. aureus* is a facultative anaerobe and is able to grow and remain active by switching metabolic processes, so the higher levels of oxygen may be attributed to reduction of specifically aerobic metabolism. As mineral oil is used to block oxygen from entering the media once the experiment has begun, it is unlikely that this higher oxygen is due to increased diffusion of oxygen into the media during the experiment. Therefore, the data collected for oxygen levels do not give useful indications as to how LIPUS impacts metabolism.

Also of note, the method for detecting the presence of oxygen does not give any indication of how oxygen is distributed within the biofilm. The biofilms are regularly a hypoxic environment, which has the potential to increase the presence of persistent cells due to stress on the bacteria (Fraiha *et al*., 2019). A theory of how US may improve the growth and antibiotic sensitivity of bacteria is through the increase of nutrients and oxygen permeating through a biofilm and increased activity of microbes deeper within the biofilm (Pitt & Ross, 2003). The use of a microelectrode needle is able to give a more detailed understanding of the levels of oxygen at various positions and depth within the biofilm and would have been beneficial to this project to give a clearer picture as to whether oxygen levels changed deeper in the biofilm rather than the extracellular oxygen consumption assay which could only give an overall view of oxygen levels within the media. The use of a microelectrode was not available during this study, therefore was not an option.

5.1.6 Gene Expression and LIPUS Treatment

Total RNA sequencing was performed to investigate whether changes in gene expression could suggest how LIPUS impacts *S. aureus* within a biofilm. Gene ontology annotations were used to identify the biological processes differentially expressed genes were involved in, changes in gene expression in bacteria with US treatment is a poorly studied area. Gene ontology enrichment analysis, using GO annotations for proteins encoded by differentially expressed genes found genes coding for proteins associated with the plasma and cell membrane were most commonly over-represented cellular components, while ATP and nucleotide binding and transferase activity were molecular functions identified as over-represented in differentially expressed genes. In terms of biological processes, transmembrane transport and cytocidal processes against other organisms, this refers to any process which induces cell death in an organism, an example would be the production of toxins which disrupt the cell membrane of host cells resulting in death of the cell, such as leukocidins, were over-represented. GO annotations give indicator to the potential functions of proteins coded by genes, therefore do not give clear indication

as to exact pathways in which changes to gene expression would impact the bacteria.

Several potential genes of interest were identified as differentially expressed in LIPUS treated samples. Four gene were identified associated with virulence. The first two genes code for serine histidine kinase, SaeS, and its associated response regulator, both were significantly upregulated in LIPUS treated *S. aureus* SH1000 biofilms. The SaeS/R system is a two-component system (TCS) which regulates the expression of exotoxins, including TSST-1, a super antigen expressed by *S. aureus* (Baroja Miren *et al*., 2016). Fibronectin-binding protein A is also regulated by SaeS/R (Steinhuber *et al*., 2003). The RNA analysis in this study also identified the upregulation of genes coding for fibronectin-binding protein A, an MSCRAMM which facilitates adhesion to host cells (Foster, 2019). The mechanical stimuli of LIPUS may impact adhesion through MSCRAMMs of *S. aureus,* as mechanical forces have been found to enhance the adhesion of clumping-factors, another type of MSCRAMM (Geoghegan & Dufrêne, 2018). Genes coding for LukS and LukF subunits were also upregulated in LIPUS treated biofilms, SaeS/R has been reported as a positive regulator of LukS and LukF (Yamazaki *et al*., 2006). Genes associated with capsule polysaccharide type 5 (CP5) were downregulated in LIPUS treated biofilms, *sae* is known to suppress expression of CP5 (Steinhuber *et al*., 2003). Harper *et al*. (2023) observed changes in TCS controlled genes when *Vibro cholerae* was exposed to mechanical stimuli. The ability of SaeS/R to recognise and respond to mechanical stimuli has not been reported. Therefore, further investigation into the changes in gene expression related to SaeS/R would need to be performed to confirm and further probe this observation.

There was a high degree of variation between the LIPUS treated replicates, meaning more repeats would be required to fully identify differentially expressed genes with LIPUS treatment. Due to time restrictions the potential of the changes in gene expression were not fully examined and further replicates and analysis would be required to fully understand the influence of US treatment on gene expression in *S. aureus* and how this would impact *S. aureus* during infection.

Several genes have been implicated in the formation of AT populations, including *Agr* and its regulators (*CodY, SigB, SarU, RsaE,*) (Bui & Kidd, 2015; Gaio *et al*., 2021; Kinkel Traci *et al*., 2013; Xu *et al*., 2017). In this work, there were no changes in the expression of these genes in *S. aureus* when treated with LIPUS. However, AT cells are a small percentage of whole biofilms, and fluctuations in these genes may not be noticeable in whole biofilm population RNA sequencing. RNA sequencing should be performed on isolated AT populations to understand if LIPUS could impact these populations.

5.2 Antibiotic Tolerant Population

Antibiotic tolerant (AT) cells are found in almost all bacterial populations, including biofilms, and these AT cells are associated with recurring infections after treatment. Due to the AT cells very low metabolic activity, the cells lack targets for antibiotics which often target growth processes, such as cell wall synthesis, protein synthesis and DNA synthesis. When antibiotic treatment is applied these AT cells are able to survive, and when treatment is ceased these cells can become once again metabolically active and re-establish an infection. In this study AT tolerant cells were isolated and validated and the use of LIPUS as a treatment option was investigated through the growth and antibiotic sensitivity of AT cells when treated with LIPUS.

5.2.1 Isolation of Antibiotic Tolerant Population

The first step in investigating AT tolerant cells was to successfully isolate this subpopulation from the whole biofilm. The concentration of ciprofloxacin and the time of antibiotic challenge was optimised by calculating number of viable cells. AT populations are around 1 % of the whole population. 5000x MIC ciprofloxacin for 20-hours was selected as the isolation conditions. Validation of AT populations was done to confirm successful isolation. The ATP levels in AT populations was

investigated as decreased ATP is known to indicate persistence (Conlon *et al*., 2016). There were significantly lower levels of ATP in populations isolated using ciprofloxacin relative to the whole population. The growth rate of AT cells isolated from *S. aureus* biofilms was also investigated. Slow growth with prolonged lag phase is indicative of AT populations (Vulin *et al*., 2018) and this was observed in this study, with a lag phase around 2-hours longer in the population treated with ciprofloxacin. These indicate successful AT population isolation.

The MICs of resurrected AT cells was investigated against ciprofloxacin and gentamicin to assess for the development of resistance. Concerningly the AT populations, resurrected in BHI overnight, demonstrated an increased resistance to ciprofloxacin, compared to previous MICs performed on whole *S. aureus* populations, indicating the development of resistance to ciprofloxacin. In future experiments the use of a dual antibiotic AT cell isolation method could reduce the concentration of antibiotics required and reducing the risk of the development of antibiotic resistance. The resurrected AT populations also demonstrated an increased sensitivity to gentamicin, the expected MIC would be similar to previous MICs (Li *et al*., 2023). The cause for this increased sensitivity is unclear and would require further investigation.

5.2.2 Growth of Antibiotic Tolerant Populations with LIPUS Treatment

The growth of AT cells was investigated following LIPUS treatment, as increased growth would imply an increase in antibiotic targets. Both the number of viable cells and the rate of growth were investigated. When treated with 30 mW/cm^2 LIPUS for 2 hours there was no change in the number of viable cells recovered from the samples compared to untreated samples, therefore there was no increase in growth. The same was true for the growth rate in with a prolonged lag phase still observed in AT populations treated with LIPUS compared to whole biofilm populations. With both the number of viable cells and the rate of growth there is no indication that LIPUS would increase growth of AT cells. The presence of AT populations is often associated with

environmental stresses such as nutrient and oxygen starvation (Cabral *et al*., 2018), and the mechanism in which other authors have suggested observations made in previous studies using US has been the increased availability of oxygen and nutrients (Pitt & Ross, 2003). If this were the case an increase in growth in AT population when treated with LIPUS would be expected but is not observed here. However, no increase in growth was observed in the whole biofilms treated with LIPUS, therefore the behaviour of LIPUS treated AT populations is matched to the behaviour of the whole biofilm.

5.2.3 Changes to Antibiotic Sensitivity in Tolerant Populations with LIPUS Treatment

The number of viable cells in AT cells isolated from *S. aureus* biofilms treated with 30 mW/cm^2 LIPUS and gentamicin was investigated to assess whether increased gentamicin sensitivity in whole biofilms was the result of changes in sensitivity in AT cells. There was a significant reduction in the number of viable cells in the LIPUS treated samples when compared to the untreated samples. The increased sensitivity was similar to the levels of increased sensitivity seen in whole biofilms. Therefore, the mechanism is unlikely to be the increased sensitivity in AT cells, rather the same mechanism is working on both AT cells and whole biofilm cells.

5.3 Tissue-Engineered Skin

The use of models is necessary when investigating viable treatment options for clinical application. In the first instance an *in vitro* model is appropriate to assess the capability of the treatment, and using a 3D model is ideal as cells and host/pathogen interactions behave differently in a 3D environment when compared to a 2D environment. In this study, effects of LIPUS on the cells used in the TE skin model were investigated as well as effects of LIPUS on both the model and the antibiotic sensitivity of an infection established in the model. A synthetic wound fluid was also

used, in an attempt to improve the infection model by recreating a more physiologically relevant infection.

5.3.1 LIPUS Treatment and Cell Proliferation

The effects of 2-hour 30 mW/cm^2 LIPUS treatment on the proliferation and viability of keratinocytes and fibroblasts (HaCaT and HDF) used in the TESM were investigated to confirm LIPUS did not negatively affect the mammalian cells and support the idea that treatment times suggested by the biofilm antibiotic sensitivity data could be used in the TESM. Both proliferation and viability remained unchanged, indicating there was no beneficial or adverse effects of LIPUS treatment in the keratinocytes and fibroblasts used in this study.

The effects of US on proliferation and viability of human cells have previously been examined with varying results. Osteoblast proliferation is known to increase when treated with LIPUS (Katiyar *et al*., 2014) and LIPUS is currently used in clinic to enhance bone fracture healing time (Rutten *et al*., 2008). The mechanisms for increased proliferation in osteoblasts are thought to through the mechanical stimuli caused during US treatment and the increased uptake of Ca^{2+} *(Costa Alvarenga et al.*, 2010; Katiyar *et al.*, 2014). It was reported that proliferation of breast epithelial cells (MCF-12A) was not altered when treated with 30 mW/cm^2 low-intensity US. Enhancement of proliferation was observed in higher intensity US (50 & 100 mW/cm^2), although proliferation of a carcinoma cell line (T47D) was inhibited with US treatment (Katiyar *et al*., 2020). These data suggest influences on proliferation depend on the intensity of the US. Fibroblasts from mice also exhibited increased proliferation when treated with low-intensity US, however the intensity (0.2 & 0.6 W/cm^2) was still higher than the intensity used in this study (Franco de Oliveira *et al*., 2011). This suggests that intensities greater than 50 mW/cm^2 may induce increased proliferation in epithelial and fibroblast cells, while the intensity used in this study does not induce that same increase. Gingival fibroblasts receiving repeated LIPUS (30 mW/cm^2) treatment over a 28-day period did not demonstrate an increase in

viability (Mostafa *et al*., 2009), indicating similarly to this current study that viability of fibroblasts is not influenced by LIPUS.

5.3.2 LIPUS Treatment and Monolayer Permeability

The permeability of dermal keratinocyte and fibroblast monolayers with and without LIPUS treatment was investigated using fluorescence (FITC labelled dextran). Increased permeability could indicate the antibiotics would have better penetration within the skin but may also indicate disruption of tight junctions and therefore bacteria may penetrate deeper within the skin. No significant increase in permeability of HaCaT or HDF monolayers treated with 30 mW/cm^2 to 70 kDa FITC-dextran was observed, with the same permeation of the cells treated with LIPUS and untreated cells both immediately post treatment and 2 hours post treatment. Allison *et al.* (2023) investigated the changes in permeability to macromolecules (40 kDa, 70 kDa & 150 kDa) in cornea and similarly found no increase in permeability in 70 kDa molecules when treated with pulsed US (0.5 & 1 W/cm^2). The smaller molecule (40 kDa) did exhibit increased permeability with US treatment. Antibiotic molecular weight is significantly smaller than the dextran used, (gentamicin, 478 Da; vancomycin, 1,449 Da) so to investigate whether antibiotic permeability would increase following LIPUS in future a smaller fluorescent molecule would be more informative.

5.3.3 Wound healing

The impact of LIPUS on wound healing was investigated using a migration assay in both dermal keratinocytes and fibroblasts (HaCaT and HDF), to understand if the length of LIPUS treatment suggested by the biofilm antibiotic sensitivity data would impact the rate of healing. Chronic wounds are characterised by the failure to heal and treatment for chronic wounds would ideally improve healing or not exacerbate poor healing.

The scratch wounds in HaCaT cell monolayers healed within 48 hours, with no difference in rate of migration between the LIPUS treated and untreated cells. The wounds in the HDF cells also fully healed within 48 hours, with similar rates of closure with the exception of the 24-hour time point. By hour 24 the wounds in the untreated HDF cells had closed to a significantly higher degree than the LIPUS treated wounds, indicating long LIPUS treatment may inhibit the migration of fibroblast cells. Gonzalez *et al.* (2023) also observed a reduction in migration of pancreatic cancer cells when treated with low-intensity US (<100 mW/cm^2), although the US used by Gonzalez was continuous rather than pulsed. However, as low-intensity US has been demonstrated to negatively impact proliferation of cancerous cells while enhancing healthy cells at intensities above 50 mW/cm^2, comparisons of cancerous pancreatic cells to healthy fibroblasts and keratinocytes may not be appropriate (Katiyar *et al*., 2020). Hill *et al.* (2005) used healthy epithelial cells from urinary tracts to assess wound healing in monolayers and found LIPUS (30 mW/cm^2) did not change the rate of reepithelialisation, this reflects the data collected in this study, with keratinocyte rate of wound closure remaining the same in LIPUS treated wounds as untreated wounds. Intensity of US may, as seen in proliferation, play a key role in changes to migration as Iwanabe *et al.* (2016) reported enhanced wound closer when treated with low-intensity US higher than used in this study (160 & 240 mW/cm^2). Live cell imaging would have been beneficial in this study, to allow for deeper understanding in the rate of closure, as imaging was performed at widely spaced intervals, unfortunately at the time of experimentation live imaging was unavailable.

5.3.4 Tissue-engineered Skin Structure with LIPUS Treatment

2 hours of LIPUS treatment does not affect the structure of the skin in our TESM experiments. This is expected as 30 mW/cm^2 LIPUS is used in clinic for 20-minute treatments with no deleterious effects; however, as the treatment used in this study was much longer than current clinical treatment time, it was essential that there was confirmation the longer treatment did not affect the skin. As the dermal scaffold used

in this study was taken from donors, there was variation in the thickness of the DED, therefore the models were not uniform across the repeats. The use of a collagen hydrogel would eliminate the variations in thickness, however this would compromise the presence of diverse proteins found in the dermal ECM of the DED.

5.3.5 Infection of model with S. aureus Clinical and Laboratory Strains

S. aureus SH1000 was not only unable to infect the 3D model but was unable to survive in the 3D model environment. This is in contrast to the clinical S235 strain of *S. aureus*. This was further investigated, and it was found that *S. aureus* SH1000 also failed to grow to similar levels in the media taken from HaCaT and HDF cells, and also in the presence of HaCaT and HDF monolayers. This was an unexpected finding as *S. aureus* SH1000 has been used in previous *in vivo* and *in vitro* infection models (Cho *et al*., 2011; Lamret *et al*., 2023). Differences in virulence factors expressed by the laboratory strain are hypothesised to be the cause of this reduction in survival and growth. The phenomenon of reduced pathogenicity in laboratory strains has been observed in other bacterial species. Hayashi *et al.* (2001) reported a reduction in virulence associated genes in laboratory strains of *E. coli* compared with clinical strains. Bundy *et al.* (2005) noted that laboratory strains of *Bacillus cereus* were genetically indistinguishable from clinical isolates but the metabolite profile of clinical strains was distinctly different to laboratory strain, suggesting phenotypical differences in the laboratory strains which may contribute to changes in virulence. Strobel *et al.* (2016) demonstrated a reduction in several proteins expressed by SH1000 when compared with four other strains of *S. aureus* (Cowan1, USA300, LS1 and 6850). FnBPA, Eap and α-toxin were all expressed at very low levels, as well as low expression of enzymes: SplA, SplB, lipase and aureolysin. FnBPA and Eap are both virulence factors associated with adhesion to host extracellular matrix (Hansen *et al*., 2006; Speziale & Pietrocola, 2020). A-toxin is a barrel-forming cytotoxin produced by *S. aureus* (Berube & Bubeck Wardenburg, 2013) SplA, SplB, lipase, and aureolysin associated with disruption of epithelial barrier as well as modulation of host immune response (Singh & Phukan, 2019; Tanaka *et al*., 2018). These are all important virulence factors for *S. aureus* infection

therefore reduction in these proteins may contribute to the lack of pathogenesis observed in this study. To confirm this a direct comparison of *S. aureus* SH1000 and S235 genome and protein expression would be beneficial, which was beyond the scope of the current work.

5.3.6 LIPUS Treatment and Antibiotic Sensitivity in Tissue-Engineered Skin

Gentamicin was the only antibiotic used on the tissue-engineered skin models as *S. aureus* SH1000 biofilms did not display any enhanced sensitivity to vancomycin when used in combination with LIPUS. Gentamicin was introduced prior to the LIPUS treatment as the difference between antibiotic challenging the biofilms prior and post LIPUS was not significant. There was no increase in gentamicin sensitivity when treating infected TESM with LIPUS, this would indicate that LIPUS is not an appropriate adjunctive to antibiotics in a clinical setting. Carmen *et al.* (2004) used rabbit *in vivo* models infected with *S. epidermidis* and found that combined US treatment and vancomycin significantly reduced the number of viable cells recovered 48-hours post treatment, when *in vitro* biofilms were treated this reduction with combined treatment was not observed. Ensing *et al.* (2005) reported similar findings with *E. coli* infected rabbits having enhanced responses to gentamicin treatment with a reduction in viable cells on implanted biofilm disks when the rabbits received US treatment compared to rabbits without US treatment.

This increased sensitivity to antibiotics observed in *in vivo* models was not seen in the *in vitro* 3D models in this study, this could be due to the difference in pathogens investigated. However, it must be considered that the setup of the *in vitro* experiment does not truly represent the physiological environment of skin infections seen in clinic. One possible reason for this lack of increased gentamicin sensitivity is that the US wavelengths may not be optimal for reaching the upper layer of the well. The frequency used in this study was 1.5 MHz, the range of penetration for 1 MHz ultrasound is 3-5 cm while higher frequency of 3 MHz has a lower range of penetration of 1-2 cm (Takebe *et al*., 2014), therefore the depth of penetration for 1.5

MHz will be close to the 3-5 cm penetration of 1 MHz, which is significantly more than the distance between the transducer and the TESM in a well insert, therefore it is unlikely that the distance the LIPUS needs to travel is the reason. Another possible factor in this lack of increased sensitivity could be attenuation of the wave as it travels though materials. In *in vitro* experimentation the plastic of the wells used may alter the propagation of the US, however, Leskinen and Hynynen (Leskinen & Hynynen, 2012) found polystyrene, the material of 6-well plates, allows low-frequency soundwaves to pass relatively effectively and may not contribute completely to reduced propagation of soundwaves. The attenuation may also be slightly enhanced by the change of medium the US must travel through in the experiment with the coupling medium, the material of the well, and the cell culture media all possessing different densities and impacting the speed of the US wave (Snehota *et al*., 2020). There is also the factor of the TESM absorbing the soundwaves from the LIPUS, there is suggestion that keratin levels in the epidermis, and the variance in the orientation of collagen in the dermis may increase the scattering and decrease the propagation of soundwaves through skin (Moran *et al*., 1995). This coupled with attenuation from the other materials in the experimental set up may contribute to preventing US waves from reaching the bacteria found on the top layers of the skin, protecting the bacterial cells from the effects seen in the biofilm only experiments.

In clinic it is suggested the LIPUS would be applied directly on top of the wound, therefore experimental design would need to reflect that, potentially removing the infected TESM from the well insert and placing in the well, inverted to place the infection directly above the transducer. This, however, risks disturbing the TESM infection mechanically and media would need to be placed on top of the TESM to ensure survival of the cells during experimentation, leading to the risk of washing the bacteria from the wound.

It is also important to note that in a skin infection in humans antibiotics do not work alone, there are also immune cells working to clear the infection, with antibiotics supporting this by reducing replication and survival of bacteria to levels the immune

system can control. The model from this study is lacking immune cells and including them in this study was unrealistic, however it may be an appropriate suggestion to improve the model by including immune cells. The effects of ultrasound on immune cells activated during infection has been poorly researched, with focus on high-intensity US treatment of tumours being prominent in current research, therefore the effects of LIPUS on immune cells would be a potentially interesting area to investigate when considering LIPUS as an infection treatment option.

5.3.7 LIPUS Treatment and IL-6

Il-6 is a proinflammatory cytokine released form several cells within the skin in the initial stages of the innate immune response to infection, including keratinocytes which are immune competent cells within the skin, both present in the TESM during infection. Levels of IL-6 were investigated to give an indication as to whether LIPUS treatment could enhance the immune response initiated during infection. When treating TESM with LIPUS the level of IL-6 was higher in LIPUS treated models when compared to the untreated model at 0-hour and 2-hour post LIPUS treatment, by 24-hour post LIPUS treatment the levels of IL-6 were the same in both treated and untreated samples. Increased IL-6 release from LIPUS treated keratinocytes has previously been reported. (Giantulli *et al*., 2021) reported increased IL-6 secretion post LIPUS treatment at 15-minutes post treatment. Similarly to the data presented in the current study, Giantulli *et al.* also found IL-6 secretion 24-hours post LIPUS treatment was unchanged compared with untreated samples. The current study recorded higher IL-6 secretion at 2-hour post LIPUS treatment, while Giantulli reported IL-6 secretion of similar levels between the 2 test conditions at 3-hour post LIPUS treatment. The difference in IL-6 secretion at 2 and 3-hour post LIPUS treatment may be attributed to Giantulli using a monolayer of HaCaT cells, while this study used a 3D TESM containing both HaCaT and HDF cells. It is well reported that cells in 3D models behave differently to cells in monolayer (Jensen & Teng, 2020).

IL-6 (100 ng/ml) stimulates antimicrobial peptide (AMP) production in keratinocytes the absence of bacteria (Ching *et al*., 2018; Erdag & Morgan, 2002). AMPs play a crucial role in modulating the innate immune response to pathogens, acting as chemoattractants for T-cells, neutrophils and macrophages (Chertov *et al.*, 1996; Chertov *et al*., 1997; Soruri *et al*., 2007) and therefore LIPUS could potentially enhance the innate immune response to infection. To further investigate effects on the immune response to LIPUS, other cytokines responsible for modulation of the innate immune response and the production of AMP, such as IL-1 and IL-8, as well as the production of AMPs, such as LL-37 and β-defensins, at lower cytokine concentrations should be investigated.

5.3.8 Improvement of physiological relevance of skin infection model

The skin model used in this study can be further improved to represent a more physiological infection of *S. aureus*. To do this a synthetic wound fluid (IVWM) was developed by collaborators in Pune, India (Dhekane *et al*., 2022), and combined with the skin model used in this study. The infected model remained grossly visually the same when incubated with BHI and IVWM. However, on histological examination of the *S. aureus* infected TESM the infections were morphologically different; large clusters of *S. aureus* were seen in the samples with IVWM as the carrier and only small clusters in the BHI samples. This clustering is similar to that seen in *in vivo* modelling (Li *et al.*, 2020) and therefore better representative of clinically relevant infection.

The number of bacteria removed from the 3D models where IVWM was used as the carrier was significantly lower than the 3D models where BHI was used as the carrier but well within the range of CFU/mg of infected tissue, so while the number of bacteria present may be lower, the models were still successfully infected. When *S. aureus* SH1000 and S235 were grown in IVWM and BHI there was a small but insignificant reduction in the number of both S235 and SH1000 cells recovered from the IVWM. When growth curves were performed IVWM produced a significantly

lower absorbance than the BHI, indicating reduced growth. However, the number of viable bacteria recovered from both the BHI and IVWM was similar, showing *S. aureus* SH1000 and S235 were able to grow in both. Therefore, it is hypothesized the reduction in absorbance is caused by the clumping of the bacteria in the IVWM. This was confirmed in the S235 strain, as when Gram stains were performed on bacteria grown in IVWM there was a significant amount of clustering of the bacteria when compared to the S235 in the BHI. In the SH1000 there was the presence of a fibrous extracellular matrix surrounding the bacteria which stained with the counterstain in Gram staining that is not visible in the BHI staining. The composition of this matrix was not investigated but it would be interesting to analyse this further in future research to identify the origins of the matrix. Again, differences in the protein expression of SH1000 and S235 would need to be further examined to determine the cause of visual differences observed, with particular interest in adherence related proteins.

6 Conclusion

This study aimed to investigate if 30 mW/cm^{2,} 1.5 MHz LIPUS, currently used in clinical practice for bone healing could be used to improve treatment of skin infections and improve antibiotic stewardship through reduction of antibiotic usage. To do this, *S. aureus,* a common skin pathogen, was used as a model microbe. How LIPUS affects the *S. aureus* biofilm was investigated, along with subpopulations of antibiotic tolerant *S. aureus*, and finally a tissue-engineered skin model was used to assess the efficacy of treating a skin infection in a 3D model.

This study showed that 30 mW/cm^2 LIPUS was effective in increasing antibiotic sensitivity to gentamicin in all maturities of biofilms investigated, with older biofilms having increased sensitivity to gentamicin independent of the time of gentamicin challenge in relation to LIPUS treatment. This was not the case for vancomycin treatment; no increased sensitivity in any biofilms tested was observed.

After a systematic process to elucidate the mechanisms of the increased gentamicin sensitivity, the project was unable to definitively identify how this increased sensitivity occurs. However, the increased permeability of the youngest and oldest biofilms to the smallest fluorescent molecules may indicate that LIPUS could increase the permeability of biofilms to smaller molecules such as antibiotics, however no structural changes in the biofilm were identified. It was established that increased growth was unlikely to occur with 30 mW/cm^2 LIPUS as well as low risk for dispersal of the biofilm, meaning the use of LIPUS would not increase the infection or risk infection becoming systemic through bacteria dispersing into other areas of the body including the bloodstream. This study indicates older biofilms have higher levels of ATP which may indicate an increase in metabolism. However, no significant changes in gene expression relating to metabolism were identified. The leading theory is that LIPUS may increase the ability of the antibiotic to cross the cell membrane, however, further work would be required to confirm this is the case.

AT populations were isolated from biofilms and treated with LIPUS. There was no increase in number of viable cells when the AT cells were treated with LIPUS, nor did the rate of growth increase, however AT populations had increased sensitivity to gentamicin when treated with LIPUS. This was similar to the increase in gentamicin sensitivity seen in whole biofilms when treated with LIPUS.

Proliferation and metabolism in human keratinocytes and fibroblasts were not changed by 2 hours of 30 mW/cm^2 LIPUS treatment. Also the permeability of monolayers of HaCaT and HDF cells was not changed after LIPUS treatment. The migration of HaCaT cells was not affected by LIPUS treatment, however in HDF cells there was a reduction in migration at 24-hours post LIPUS treatment, therefore long LIPUS treatment may result in inhibition of wound healing and would require further investigation if LIPUS was found to be a viable adjunctive treatment option for SSTI. No structural changes in TESM were observed after LIPUS treatment, showing skin damage was unlikely, even in long LIPUS treatment. There was no increased gentamicin sensitivity in *S. aureus* S235 infected TESM treated with LIPUS, when compared to infected TESM treated with gentamicin only, indicating the antibiotic

adjunct LIPUS treatment tested in this study does not confer any advantage for clinical use. Changes to treatment protocol could be investigated further to identify if other treatment conditions altered effectiveness of combined LIPUS and antibiotic. LIPUS treated TESM produced higher levels of IL-6 when compared to untreated TESM immediately following LIPUS treatment and also 2-hours post LIPUS treatment, a phenomenon which also warrants further investigation.

The laboratory strain *S. aureus* SH1000 was unable to survive and infect the TESM, while the clinical strain *S. aureus* S235 was able to successfully infect the TESM. There was a reduction in the number of viable *S. aureus* SH1000 cells in monolayers of HaCaT, HDF and co-cultures of HaCaT and HDF cells in comparison to *S. aureus* S235. The same reduction in *S. aureus* SH1000 numbers was seen in media removed from HaCaT, HDF and co-cultures of HaCaT and HDF cells, while *S. aureus* S235 were able to survive. Differences in virulence factors in laboratory strains and clinical strains are likely to cause this change in behaviour and is an interesting avenue to pursue further research.

Finally, the use of a synthetic wound fluid produced infections closer resembling physiological infections. This is beneficial in infection research as behaviours of *S. aureus* in *in vitro* infections would closer align with the behaviours of the pathogen observed in *in vivo* experimentation.

7 Future work

Due to funding and time limitations, there are still outstanding questions from this project as well as new questions raised which give rise to further research projects. While this project fails to fully understand the mechanisms surrounding the increased gentamicin sensitivity in *S. aureus* SH1000 biofilms, it makes good progress in elucidating the mechanisms. To further understand the effects LIPUS has on *S. aureus* it would be beneficial to use live imaging to identify transient pore formation

in the cell membrane of *S. aureus*. Unfortunately, this technology is currently unavailable, therefore it is not possible to gather this data at this time.

There was a lack of increased sensitivity to gentamicin plus LIPUS treatment in *S. aureus* S235 when infecting a skin model. It is possible this could be due to the distance LIPUS waves are able to travel being unable to reach the skin model placed within a well, although it could also be due to repeated LIPUS treatments being required. Given more time and funding it would have been valuable to this project to conduct experiments over several days with repeated LIPUS treatment. In a clinical setting, one off LIPUS treatment would be unlikely, as in bone healing patients use repeated short periods of LIPUS over several weeks to improve the healing time in a fracture. It would be helpful to apply this to the biofilms and infected tissue-engineered models to observe if the antibiotic sensitivity increase seen in the biofilms in this study could be further improved as well as assess if repeated treatments over a longer period of time could induce increased antibiotic sensitivity in the infected skin models. Using repeated treatments could lead to potentially decreasing the length of the LIPUS treatment required to induce the increased sensitivity which would be advantageous if combined LIPUS and antibiotic treatment were to be used in a clinical setting. 20-minute LIPUS treatment is currently used in fracture clinics whereas 2-hour LIPUS treatment for infection may not be well tolerated by patients.

Potential projects in the future:

<u>Project: Effects of LIPUS on Polymicrobial Biofilms</u>

Aims: To investigate how LIPUS affects multispecies biofilms

Objectives:

1. Establish a multispecies biofilm in model skin infections.

2. Investigate how multispecies biofilms are affected by LIPUS – metabolism, structure, antibiotic sensitivity.
3. Produce a multispecies infection in tissue-engineered models and whether LIPUS can affect antibiotic sensitivity.

Project: How mammalian cells prevent growth and survival of *S. aureus* laboratory strains

Aims: To investigate how HaCaT and HDF cells prevent the growth and survival of the laboratory strain *S. aureus* SH1000

Objectives:

1. To identify the proteomic profile of laboratory and clinical strains of *S. aureus.*
2. Investigate if other laboratory strains of *S. aureus* demonstrate similar failure to survive in 3D skin models.
3. To identify AMPs secreted by keratinocytes and fibroblasts and the response of clinical and laboratory strains of *S. aureus*.

8 References

Abraham, J., & Mathew, S. (2019). Merkel Cells: A Collective Review of Current Concepts. *Int J Appl Basic Med Res*, *9*(1), 9-13. https://doi.org/10.4103/ijabmr.IJABMR_34_18

Abu-Zidan, F. M., Hefny, A. F., & Corr, P. (2011). Clinical ultrasound physics. *Journal of emergencies, trauma, and shock*, *4*(4), 501-503. https://doi.org/10.4103/0974-2700.86646

Abushaheen, M. A., Muzaheed, Fatani, A. J., Alosaimi, M., Mansy, W., George, M.,…Jhugroo, P. (2020). Antimicrobial resistance, mechanisms and its clinical significance. *Disease-a-Month*, *66*(6), 100971. https://doi.org/https://doi.org/10.1016/j.disamonth.2020.100971

Agerer, F., Lux, S., Michel, A., Rohde, M., Ohlsen, K., & Hauck, C. R. (2005). Cellular invasion by Staphylococcus aureus reveals a functional link between focal adhesion kinase and cortactin in integrin-mediated internalisation. *Journal of Cell Science*, *118*(10), 2189. https://doi.org/10.1242/jcs.02328

Ahmad, N. I., Yean Yean, C., Foo, P. C., Mohamad Safiee, A. W., & Hassan, S. A. (2020). Prevalence and association of Panton-Valentine Leukocidin gene with the risk of sepsis in patients infected with Methicillin Resistant Staphylococcus aureus. *Journal of Infection and Public Health*. https://doi.org/https://doi.org/10.1016/j.jiph.2020.06.018

Baroja Miren, L., Herfst Christine, A., Kasper Katherine, J., Xu Stacey, X., Gillett Daniel, A., Li, J.,…McCormick John, K. (2016). The SaeRS Two-Component System Is a Direct and Dominant Transcriptional Activator of Toxic Shock Syndrome Toxin 1 in Staphylococcus aureus. *Journal of Bacteriology*, *198*(19), 2732-2742. https://doi.org/10.1128/jb.00425-16

Bharatula, L. D., Marsili, E., Rice, S. A., & Kwan, J. J. (2020). Influence of High Intensity Focused Ultrasound on the Microstructure and c-di-GMP Signaling of Pseudomonas aeruginosa Biofilms [Original Research]. *Frontiers in Microbiology*, *11*.

Bhattacharya, S., & Mishra, R. K. (2015). Pressure ulcers: Current understanding and newer modalities of treatment. *Indian journal of plastic surgery : official publication of the Association of Plastic Surgeons of India*, *48*(1), 4-16. https://doi.org/10.4103/0970-0358.155260

Bien, J., Sokolova, O., & Bozko, P. (2011). Characterization of Virulence Factors of Staphylococcus aureus: Novel Function of Known Virulence Factors That Are Implicated in Activation of Airway Epithelial Proinflammatory Response. *J Pathog*, *2011*, 601905. https://doi.org/10.4061/2011/601905

Bochu, W., Lanchun, S., Jing, Z., Yuanyuan, Y., & Yanhong, Y. (2003). The influence of Ca2+ on the proliferation of S. cerevisiae and low ultrasonic on the concentration of Ca2+ in the S. cerevisiae cells. *Colloids and Surfaces B: Biointerfaces*, *32*(1), 35-42. https://doi.org/https://doi.org/10.1016/S0927-7765(03)00129-2

Boguniewicz, M., & Leung, D. Y. M. (2011). Atopic dermatitis: a disease of altered skin barrier and immune dysregulation. *Immunological reviews*, *242*(1), 233-246. https://doi.org/10.1111/j.1600-065X.2011.01027.x

Boutte, C. C., & Crosson, S. (2013). Bacterial lifestyle shapes stringent response activation. *Trends Microbiol*, *21*(4), 174-180. https://doi.org/10.1016/j.tim.2013.01.002

Bowler, P. G., Duerden, B. I., & Armstrong, D. G. (2001). Wound microbiology and associated approaches to wound management. *Clinical microbiology reviews*, *14*(2), 244-269. https://doi.org/10.1128/CMR.14.2.244-269.2001

Boyko, T. V., Longaker, M. T., & Yang, G. P. (2018). Review of the Current Management of Pressure Ulcers. *Advances in wound care*, *7*(2), 57-67. https://doi.org/10.1089/wound.2016.0697

Bukvić Mokos, Z., Markota Čagalj, A., & Marinović, B. (2023). Epidemiology of hidradenitis suppurativa. *Clinics in Dermatology*, *41*(5), 564-575. https://doi.org/https://doi.org/10.1016/j.clindermatol.2023.08.020

Casqueiro, J., Casqueiro, J., & Alves, C. (2012). Infections in patients with diabetes mellitus: A review of pathogenesis. *Indian J Endocrinol Metab*, *16 Suppl 1*, S27-36. https://doi.org/10.4103/2230-8210.94253

Cazander, G., Pritchard, D. I., Nigam, Y., Jung, W., & Nibbering, P. H. (2013). Multiple actions of Lucilia sericata larvae in hard-to-heal wounds. *BioEssays*, *35*(12), 1083-1092. https://doi.org/https://doi.org/10.1002/bies.201300071

Centre for Disease Control and Prevention. (2007). *National Vital Statistic System: Life Expectancy*. Centre for Disease Control and Prevention,. Retrieved April 2020 from https://www.cdc.gov/nchs/nvss/life-expectancy.htm#data

Cheng, A. G., DeDent, A. C., Schneewind, O., & Missiakas, D. (2011). A play in four acts: Staphylococcus aureus abscess formation. *Trends in microbiology*, *19*(5), 225-232. https://doi.org/10.1016/j.tim.2011.01.007

Cheng, A. G., McAdow, M., Kim, H. K., Bae, T., Missiakas, D. M., & Schneewind, O. (2010). Contribution of Coagulases towards Staphylococcus aureus Disease and Protective Immunity. *PLOS Pathogens*, *6*(8), e1001036. https://doi.org/10.1371/journal.ppat.1001036

Chertov, O., Michiel, D. F., Xu, L., Wang, J. M., Tani, K., Murphy, W. J.,…Oppenheim, J. J. (1996). Identification of Defensin-1, Defensin-2, and CAP37/Azurocidin as T-cell Chemoattractant Proteins Released from Interleukin-8-stimulated Neutrophils (∗). *Journal of Biological Chemistry*, *271*(6), 2935-2940. https://doi.org/10.1074/jbc.271.6.2935

Chertov, O., Ueda, H., Xu, L. L., Tani, K., Murphy, W. J., Wang, J. M.,…Oppenheim, J. J. (1997). Identification of Human Neutrophil-derived Cathepsin G and Azurocidin/CAP37 as Chemoattractants for Mononuclear Cells and Neutrophils. *Journal of Experimental Medicine*, *186*(5), 739-747. https://doi.org/10.1084/jem.186.5.739

Cheung, G. Y., Joo, H. S., Chatterjee, S. S., & Otto, M. (2014). Phenol-soluble modulins--critical determinants of staphylococcal virulence. *FEMS Microbiol Rev*, *38*(4), 698-719. https://doi.org/10.1111/1574-6976.12057

Ching, C. B., Gupta, S., Li, B., Cortado, H., Mayne, N., Jackson, A. R.,…Becknell, B. (2018). Interleukin-6/Stat3 signaling has an essential role in the host antimicrobial response to urinary tract infection. *Kidney International*, *93*(6), 1320-1329. https://doi.org/https://doi.org/10.1016/j.kint.2017.12.006

Chomarat, P., Banchereau, J., Davoust, J., & Karolina Palucka, A. (2000). IL-6 switches the differentiation of monocytes from dendritic cells to macrophages. *Nature Immunology*, *1*(6), 510-514. https://doi.org/10.1038/82763

Church, D., Elsayed, S., Reid, O., Winston, B., & Lindsay, R. (2006). Burn Wound Infections. *Clinical microbiology reviews*, *19*(2), 403. https://doi.org/10.1128/CMR.19.2.403-434.2006

Cichorek, M., Wachulska, M., Stasiewicz, A., & Tymińska, A. (2013). Skin melanocytes: biology and development. *Postepy Dermatol Alergol*, *30*(1), 30-41. https://doi.org/10.5114/pdia.2013.33376

Cieri, B., Conway, E. L., Sellick, J. A., & Mergenhagen, K. A. (2019). Identification of risk factors for failure in patients with skin and soft tissue infections. *The American Journal of Emergency Medicine*, *37*(1), 48-52. https://doi.org/https://doi.org/10.1016/j.ajem.2018.04.046

Conlon, B. P., Rowe, S. E., Gandt, A. B., Nuxoll, A. S., Donegan, N. P., Zalis, E. A.,…Lewis, K. (2016). Persister formation in Staphylococcus aureus is associated with ATP depletion. *Nature Microbiology*, *1*(5). https://doi.org/10.1038/nmicrobiol.2016.51

Costa Alvarenga, É., Rodrigues, R., Caricati-Neto, A., Silva-Filho, F. C., Paredes-Gamero, E. J., & Ferreira, A. T. (2010). Low-intensity pulsed ultrasound-dependent osteoblast proliferation occurs by via activation of the P2Y receptor: Role of the P2Y1 receptor. *Bone*, *46*(2), 355-362. https://doi.org/https://doi.org/10.1016/j.bone.2009.09.017

Cunningham, R., Cockayne, A., & Humphreys, H. (1996). Clinical and molecular aspects of the pathogenesis of Staphylococcus aureus bone and joint infections. *Journal of Medical Microbiology*, *44*(3), 157-164. https://doi.org/https://doi.org/10.1099/00222615-44-3-157

Della Rocca, G. J. (2009). The science of ultrasound therapy for fracture healing. *Indian J Orthop*, *43*(2), 121-126. https://doi.org/10.4103/0019-5413.50845

DeLongchamp, J., Saleh, M., & Ferroni, G. (2011). Structure and Function of Bacterial and Fungal Cell Walls. In (pp. 7-16).

Dengler, V., Foulston, L., DeFrancesco, A. S., & Losick, R. (2015). An Electrostatic Net Model for the Role of Extracellular DNA in Biofilm Formation by Staphylococcus aureus. *Journal of Bacteriology*, *197*(24), 3779. https://doi.org/10.1128/JB.00726-15

Dhekane, R., Mhade, S., & Kaushik, K. S. (2022). Adding a new dimension: Multi-level structure and organization of mixed-species Pseudomonas aeruginosa and Staphylococcus aureus biofilms in a 4-D wound microenvironment. *Biofilm*, *4*, 100087. https://doi.org/https://doi.org/10.1016/j.bioflm.2022.100087

DiNubile, M. J., & Lipsky, B. A. (2004). Complicated infections of skin and skin structures: when the infection is more than skin deep. (0305-7453 (Print)).

Diwan, A. D., Wang, M. X., Jang, D., Zhu, W., & Murrell, G. A. (2000). Nitric oxide modulates fracture healing. *J Bone Miner Res*, *15*(2), 342-351. https://doi.org/10.1359/jbmr.2000.15.2.342

Dong, Y., Li, J., Li, P., & Yu, J. (2018). Ultrasound Microbubbles Enhance the Activity of Vancomycin Against Staphylococcus epidermidis Biofilms In Vivo. *Journal of Ultrasound in Medicine*, *37*(6), 1379-1387. https://doi.org/10.1002/jum.14475

Doroshenko, N., Rimmer, S., Hoskins, R., Garg, P., Swift, T., Spencer, H. L. M.,…Shepherd, J. (2018). Antibiotic functionalised polymers reduce bacterial biofilm and bioburden in a simulated infection of the cornea [10.1039/C8BM00201K]. *Biomaterials Science*, *6*(8), 2101-2109. https://doi.org/10.1039/C8BM00201K

Doroshenko, N., Tseng, B. S., Howlin, R. P., Deacon, J., Wharton, J. A., Thurner, P. J.,…Stoodley, P. (2014). Extracellular DNA impedes the transport of vancomycin in Staphylococcus epidermidis biofilms preexposed to subinhibitory concentrations of vancomycin. *Antimicrobial Agents and Chemotherapy*, *58*(12), 7273-7282. https://doi.org/10.1128/AAC.03132-14

Dowd, S. E., Wolcott, R. D., Sun, Y., McKeehan, T., Smith, E., & Rhoads, D. (2008). Polymicrobial nature of chronic diabetic foot ulcer biofilm infections determined using bacterial tag encoded FLX amplicon pyrosequencing (bTEFAP). *PLoS One*, *3*(10), e3326-e3326. https://doi.org/10.1371/journal.pone.0003326

Dryden, M., Baguneid, M., Eckmann, C., Corman, S., Stephens, J., Solem, C.,…Haider, S. (2015). Pathophysiology and burden of infection in patients with diabetes mellitus and peripheral vascular disease: focus on skin and soft-tissue infections. *Clinical Microbiology and Infection*, *21*, S27-S32. https://doi.org/https://doi.org/10.1016/j.cmi.2015.03.024

Dryden, M. S. (2010). Complicated skin and soft tissue infection. *Journal of Antimicrobial Chemotherapy*, *65*(suppl_3), iii35-iii44. https://doi.org/10.1093/jac/dkq302

Dumville, J. C., Worthy, G., Soares, M. O., Bland, J. M., Cullum, N., Dowson, C.,…Torgerson, D. J. (2009). VenUS II: a randomised controlled trial of larval therapy in the management of leg ulcers. *13*, 55. https://doi.org/10.3310/hta13550

Ekanayake-Mudiyanselage, S., Aschauer, H., Schmook, F. P., Jensen, J. M., Meingassner, J. G., & Proksch, E. (1998). Expression of epidermal keratins and the cornified envelope protein involucrin is influenced by permeability barrier disruption. *J Invest Dermatol*, *111*(3), 517-523. https://doi.org/10.1046/j.1523-1747.1998.00318.x

Ennis, W. J., Valdes, W., Gainer, M., & Meneses, P. (2006). Evaluation of Clinical Effectiveness of MIST Ultrasound Therapy for the Healing of Chronic Wounds. *Advances in Skin & Wound Care*, *19*(8).

Erdag, G., & Morgan, J. R. (2002). Interleukin-1alpha and interleukin-6 enhance the antibacterial properties of cultured composite keratinocyte grafts. (0003-4932 (Print)).

Erdogan, O., & Esen, E. (2009). Biological aspects and clinical importance of ultrasound therapy in bone healing. *J Ultrasound Med*, *28*(6), 765-776. https://doi.org/10.7863/jum.2009.28.6.765

Fabiilli, M. L., Haworth, K. J., Fakhri, N. H., Kripfgans, O. D., Carson, P. L., & Fowlkes, J. B. (2009). The role of inertial cavitation in acoustic droplet vaporization. *IEEE transactions on ultrasonics, ferroelectrics, and frequency control*, *56*(5), 1006-1017. https://doi.org/10.1109/TUFFC.2009.1132

Falugi, F., Kim, H. K., Missiakas, D. M., & Schneewind, O. (2013). Role of Protein A in the Evasion of Host Adaptive Immune Responses by Staphylococcus aureus. *mBio*, *4*(5), e00575-00513. https://doi.org/10.1128/mBio.00575-13

Feng, J., Kessler, D. A., Ben-Jacob, E., & Levine, H. (2014). Growth feedback as a basis for persister bistability. *Proceedings of the National Academy of Sciences of the United States of America*, *111*(1), 544-549. https://doi.org/10.1073/pnas.1320396110

Fisher, B., Hiller, C., & Rennie, S. (2003). A comparison of continuous ultrasound and pulsed ultrasound on soft tissue injury markers in the rat. *Journal of Physical Therapy Science*, *15*, 65-70.
Fisher, R. A., Gollan, B., & Helaine, S. (2017). Persistent bacterial infections and persister cells. *Nat Rev Microbiol*, *15*(8), 453-464. https://doi.org/10.1038/nrmicro.2017.42
Foster, T. J. Antibiotic resistance in Staphylococcus aureus. Current status and future prospects. (1574-6976 (Electronic)).
Foster, T. J. (2017). Antibiotic resistance in Staphylococcus aureus. Current status and future prospects. *FEMS Microbiology Reviews*, *41*(1574-6976 (Electronic)).
Foster, T. J. (2019). The MSCRAMM Family of Cell-Wall-Anchored Surface Proteins of Gram-Positive Cocci. *Trends Microbiol*, *27*(11), 927-941. https://doi.org/10.1016/j.tim.2019.06.007
Frykberg, R. G., & Banks, J. (2015). Challenges in the Treatment of Chronic Wounds. (2162-1918 (Print)).
Gade, N. D., & Qazi, M. S. (2013). Fluoroquinolone Therapy in Staphylococcus aureus Infections: Where Do We Stand? *J Lab Physicians*, *5*(2), 109-112. https://doi.org/10.4103/0974-2727.119862
Gallo, M., Ferrara, L., & Naviglio, D. (2018). Application of Ultrasound in Food Science and Technology: A Perspective. *Foods*, *7*(10). https://doi.org/10.3390/foods7100164
Gardner, S. E., Hillis, S. L., Heilmann, K., Segre, J. A., & Grice, E. A. (2013). The neuropathic diabetic foot ulcer microbiome is associated with clinical factors. *Diabetes*, *62*(3), 923-930. https://doi.org/10.2337/db12-0771
Gebhard, F., Pfetsch, H., Steinbach, G., Strecker, W., Kinzl, L., & Brückner, U. B. (2000). Is Interleukin 6 an Early Marker of Injury Severity Following Major Trauma in Humans? *Archives of Surgery*, *135*(3), 291-295. https://doi.org/10.1001/archsurg.135.3.291
Gelens, L., Hill, L., Vandervelde, A., Danckaert, J., & Loris, R. (2013). A general model for toxin-antitoxin module dynamics can explain persister cell formation in E. coli. *PLoS Comput Biol*, *9*(8), e1003190. https://doi.org/10.1371/journal.pcbi.1003190
Geoghegan, J. A., & Dufrêne, Y. F. (2018). Mechanomicrobiology: How Mechanical Forces Activate Staphylococcus aureus Adhesion. *Trends in Microbiology*, *26*(8), 645-648. https://doi.org/https://doi.org/10.1016/j.tim.2018.05.004
Giantulli, S., Tortorella, E., Brasili, F., Scarpa, S., Cerroni, B., Paradossi, G.,…Domenici, F. (2021). Effect of 1-MHz ultrasound on the proinflammatory interleukin-6 secretion in human keratinocytes. *Scientific Reports*, *11*(1), 19033. https://doi.org/10.1038/s41598-021-98141-2
Gloag, E. S., Fabbri, S., Wozniak, D. J., & Stoodley, P. (2020). Biofilm mechanics: Implications in infection and survival. *Biofilm*, *2*, 100017. https://doi.org/https://doi.org/10.1016/j.bioflm.2019.100017
Greenhalgh, D. G. (2017). Sepsis in the burn patient: a different problem than sepsis in the general population. *Burns & Trauma*, *5*(1), 23. https://doi.org/10.1186/s41038-017-0089-5
Guest, J. F., Fuller, G. W., & Vowden, P. (2018). Diabetic foot ulcer management in clinical practice in the UK: costs and outcomes. *International Wound Journal*, *15*(1), 43-52. https://doi.org/10.1111/iwj.12816

Gunderson, C. G. (2011). Cellulitis: Definition, Etiology, and Clinical Features. *The American Journal of Medicine*, *124*(12), 1113-1122. https://doi.org/10.1016/j.amjmed.2011.06.028

Guo, Y., Song, G., Sun, M., Wang, J., & Wang, Y. (2020). Prevalence and Therapies of Antibiotic-Resistance in Staphylococcus aureus [10.3389/fcimb.2020.00107]. *Frontiers in cellular and infection microbiology*, *10*, 107.

Gupta, P., Sarkar, S., Das, B., Bhattacharjee, S., & Tribedi, P. (2016). Biofilm, pathogenesis and prevention—a journey to break the wall: a review. *Archives of Microbiology*, *198*(1), 1-15. https://doi.org/10.1007/s00203-015-1148-6

Hall, C. W., & Mah, T.-F. (2017). Molecular mechanisms of biofilm-based antibiotic resistance and tolerance in pathogenic bacteria. *FEMS Microbiology Reviews*, *41*(3), 276-301. https://doi.org/10.1093/femsre/fux010

Hanzelmann, D., Joo, H.-S., Franz-Wachtel, M., Hertlein, T., Stevanovic, S., Macek, B.,…Peschel, A. (2016). Toll-like receptor 2 activation depends on lipopeptide shedding by bacterial surfactants. *Nature Communications*, *7*(1), 12304. https://doi.org/10.1038/ncomms12304

Harms, A., Fino, C., Sorensen, M. A., Semsey, S., & Gerdes, K. (2017). Prophages and Growth Dynamics Confound Experimental Results with Antibiotic-Tolerant Persister Cells. *mBio*, *8*(6). https://doi.org/10.1128/mBio.01964-17

Harper, C. E., Zhang, W., Lee, J., Shin, J.-H., Keller, M. R., van Wijngaarden, E.,…Hernandez, C. J. (2023). Mechanical stimuli activate gene expression via a cell envelope stress sensing pathway. *Scientific Reports*, *13*(1), 13979. https://doi.org/10.1038/s41598-023-40897-w

Hazan, Z., Zumeris, J., Jacob, H., Raskin, H., Kratysh, G., Vishnia, M.,…Lavie, G. (2006). Effective Prevention of Microbial Biofilm Formation on Medical Devices by Low-Energy Surface Acoustic Waves. *Antimicrobial Agents and Chemotherapy*, *50*(12), 4144-4152. https://doi.org/10.1128/aac.00418-06

Hemmige, V., McNulty, M., Silverman, E., & David, M. Z. (2015). Recurrent skin and soft tissue infections in HIV-infected patients during a 5-year period: incidence and risk factors in a retrospective cohort study. *BMC Infectious Diseases*, *15*(1), 455. https://doi.org/10.1186/s12879-015-1216-1

Hohl, D., Mehrel, T., Lichti, U., Turner, M. L., Roop, D. R., & Steinert, P. M. (1991). Characterization of human loricrin. Structure and function of a new class of epidermal cell envelope proteins. *Journal of Biological Chemistry*, *266*(10), 6626-6636.

Hoiby, N., Bjarnsholt, T., Givskov, M., Molin, S., & Ciofu, O. (2010). Antibiotic resistance of bacterial biofilms. *Int J Antimicrob Agents*, *35*(4), 322-332. https://doi.org/10.1016/j.ijantimicag.2009.12.011

Horsburgh, M., J., Aish, J., L., White, I., J., Shaw, L., Lithgow, J., K., & Foster, S., J. (2002). σB Modulates Virulence Determinant Expression and Stress Resistance: Characterization of a Functional rsbU Strain Derived from Staphylococcus aureus 8325-4. *Journal of Bacteriology*, *184*(19), 5457-5467. https://doi.org/10.1128/jb.184.19.5457-5467.2002

Hu, C., Xiong, N., Zhang, Y., Rayner, S., & Chen, S. (2012). Functional characterization of lipase in the pathogenesis of Staphylococcus aureus. *Biochemical and Biophysical Research Communications*, *419*(4), 617-620. https://doi.org/https://doi.org/10.1016/j.bbrc.2012.02.057

Huang, Y.-Y., Lin, C.-W., Yang, H.-M., Hung, S.-Y., & Chen, I. W. (2018). Survival and associated risk factors in patients with diabetes and amputations caused

by infectious foot gangrene. *Journal of Foot and Ankle Research*, *11*(1), 1. https://doi.org/10.1186/s13047-017-0243-0
Hynes, W. L., & Walton, S. L. (2000). Hyaluronidases of Gram-positive bacteria. *FEMS Microbiology Letters*, *183*(2), 201-207. https://doi.org/10.1111/j.1574-6968.2000.tb08958.x
Ibberson, C. B., Jones, C. L., Singh, S., Wise, M. C., Hart, M. E., Zurawski, D. V., & Horswill, A. R. (2014). Staphylococcus aureus hyaluronidase is a CodY-regulated virulence factor. *Infect Immun*, *82*(10), 4253-4264. https://doi.org/10.1128/IAI.01710-14
Iqbal, K., Ohl, S.-W., Khoo, B.-C., Neo, J., & Fawzy, A. S. (2013). Effect of High-Intensity Focused Ultrasound on Enterococcus Faecalis Planktonic Suspensions and Biofilms. *Ultrasound in Medicine & Biology*, *39*(5), 825-833. https://doi.org/https://doi.org/10.1016/j.ultrasmedbio.2012.12.006
Irving, S. E., & Corrigan, R. M. (2018). Triggering the stringent response: signals responsible for activating (p)ppGpp synthesis in bacteria. *Microbiology (Reading)*, *164*(3), 268-276. https://doi.org/10.1099/mic.0.000621
Izadifar, Z., Babyn, P., & Chapman, D. (2017). Mechanical and Biological Effects of Ultrasound: A Review of Present Knowledge. *Ultrasound Med Biol*, *43*(6), 1085-1104. https://doi.org/10.1016/j.ultrasmedbio.2017.01.023
Izadifar, Z., Chapman, D., & Babyn, P. (2020). An Introduction to High Intensity Focused Ultrasound: Systematic Review on Principles, Devices, and Clinical Applications. *J Clin Med*, *9*(2). https://doi.org/10.3390/jcm9020460
Izumi, Y., Satterfield, K., Lee, S., Harkless, L. B., & Lavery, L. A. (2009). Mortality of first-time amputees in diabetics: A 10-year observation. *Diabetes Research and Clinical Practice*, *83*(1), 126-131. https://doi.org/https://doi.org/10.1016/j.diabres.2008.09.005
Jacoby, G. A. (2005). Mechanisms of Resistance to Quinolones. *Clinical Infectious Diseases*, *41*(Supplement_2), S120-S126. https://doi.org/10.1086/428052
James, G. A., Swogger, E., Wolcott, R., Pulcini, E., Secor, P., Sestrich, J.,…Stewart, P. S. (2008). Biofilms in chronic wounds. *Wound Repair Regen*, *16*(1), 37-44. https://doi.org/10.1111/j.1524-475X.2007.00321.x
Jeschke, M. G., van Baar, M. E., Choudhry, M. A., Chung, K. K., Gibran, N. S., & Logsetty, S. (2020). Burn injury. *Nature reviews. Disease primers*, *6*(1), 11-11. https://doi.org/10.1038/s41572-020-0145-5
Ji, H., & Li, X.-K. (2016). Oxidative Stress in Atopic Dermatitis. *Oxidative Medicine and Cellular Longevity*, *2016*(1), 2721469. https://doi.org/https://doi.org/10.1155/2016/2721469
Jneid, J., Lavigne, J. P., La Scola, B., & Cassir, N. (2017). The diabetic foot microbiota: A review. *Human Microbiome Journal*, *5-6*, 1-6. https://doi.org/https://doi.org/10.1016/j.humic.2017.09.002
Kang, J., Dietz, M. J., & Li, B. (2019). Antimicrobial peptide LL-37 is bactericidal against Staphylococcus aureus biofilms. *PLoS One*, *14*(6), e0216676. https://doi.org/10.1371/journal.pone.0216676
Kapałczyńska, M., Kolenda, T., Przybyła, W., Zajączkowska, M., Teresiak, A., Filas, V.,…Lamperska, K. (2018). 2D and 3D cell cultures - a comparison of different types of cancer cell cultures. *Arch Med Sci*, *14*(4), 910-919. https://doi.org/10.5114/aoms.2016.63743
Katayama, Y., Ito, T., & Hiramatsu, K. (2000). A new class of genetic element, staphylococcus cassette chromosome mec, encodes methicillin resistance in

Staphylococcus aureus. *Antimicrob Agents Chemother*, *44*(6), 1549-1555. https://doi.org/10.1128/aac.44.6.1549-1555.2000

Kateel, R., Augustine, A. J., Prabhu, S., Ullal, S., Pai, M., & Adhikari, P. (2018). Clinical and microbiological profile of diabetic foot ulcer patients in a tertiary care hospital. *Diabetes & Metabolic Syndrome: Clinical Research & Reviews*, *12*(1), 27-30. https://doi.org/https://doi.org/10.1016/j.dsx.2017.08.008

Katiyar, A., Duncan, R. L., & Sarkar, K. (2014). Ultrasound stimulation increases proliferation of MC3T3-E1 preosteoblast-like cells. *Journal of Therapeutic Ultrasound*, *2*(1), 1. https://doi.org/10.1186/2050-5736-2-1

Kee, K. K., Nair, H. K. R., & Yuen, N. P. (2019). Risk factor analysis on the healing time and infection rate of diabetic foot ulcers in a referral wound care clinic. *Journal of Wound Care*, *28*(Sup1), S4-S13. https://doi.org/10.12968/jowc.2019.28.Sup1.S4

Keren, I., Kaldalu, N., Spoering, A., Wang, Y., & Lewis, K. (2004). Persister cells and tolerance to antimicrobials. *FEMS Microbiology Letters*, *230*(1), 13-18. https://doi.org/10.1016/s0378-1097(03)00856-5

Kerr, M., Barron, E., Chadwick, P., Evans, T., Kong, W. M., Rayman, G.,…Jeffcoate, W. J. (2019). The cost of diabetic foot ulcers and amputations to the National Health Service in England. *Diabetic Medicine*, *36*(8), 995-1002. https://doi.org/10.1111/dme.13973

Ki, V., & Rotstein, C. (2008). Bacterial skin and soft tissue infections in adults: A review of their epidemiology, pathogenesis, diagnosis, treatment and site of care. *Can J Infect Dis Med Microbiol*, *19*(2), 173-184. https://doi.org/10.1155/2008/846453

Koibuchi, H., Fujii, Y., Sato'o, Y., Mochizuki, T., Yamada, T., Cui, L., & Taniguchi, N. (2021). Inhibitory effects of ultrasound irradiation on Staphylococcus epidermidis biofilm. *Journal of Medical Ultrasonics*, *48*(4), 439-448. https://doi.org/10.1007/s10396-021-01120-3

Kong, K. F., Schneper, L., & Mathee, K. (2010). Beta-lactam antibiotics: from antibiosis to resistance and bacteriology. *APMIS*, *118*(1), 1-36. https://doi.org/10.1111/j.1600-0463.2009.02563.x

Korch, S. B., Henderson, T. A., & Hill, T. M. (2003). Characterization of the hipA7 allele of Escherichia coli and evidence that high persistence is governed by (p)ppGpp synthesis. *Mol Microbiol*, *50*(4), 1199-1213. https://doi.org/10.1046/j.1365-2958.2003.03779.x

Kuipers, A., Stapels, D. A. C., Weerwind, L. T., Ko, Y. P., Ruyken, M., Lee, J. C.,…Rooijakkers, S. H. M. (2016). The Staphylococcus aureus polysaccharide capsule and Efb-dependent fibrinogen shield act in concert to protect against phagocytosis. *Microbiology (Reading)*, *162*(7), 1185-1194. https://doi.org/10.1099/mic.0.000293

Kumar, A., & Schweizer, H. P. (2005). Bacterial resistance to antibiotics: active efflux and reduced uptake. *Adv Drug Deliv Rev*, *57*(10), 1486-1513. https://doi.org/10.1016/j.addr.2005.04.004

Kussell, E., Kishony, R., Balaban, N. Q., & Leibler, S. (2005). Bacterial persistence: a model of survival in changing environments. *Genetics*, *169*(4), 1807-1814. https://doi.org/10.1534/genetics.104.035352

Lacey, K. A., Mulcahy, M. E., Towell, A. M., Geoghegan, J. A., & McLoughlin, R. M. (2019). Clumping factor B is an important virulence factor during Staphylococcus aureus skin infection and a promising vaccine target. *PLoS Pathog*, *15*(4), e1007713. https://doi.org/10.1371/journal.ppat.1007713

Lambert, P. A. (2002). Cellular impermeability and uptake of biocides and antibiotics in Gram-positive bacteria and mycobacteria. *Journal of Applied Microbiology*, *92*(s1), 46S-54S. https://doi.org/10.1046/j.1365-2672.92.5s1.7.x

Laurens, N., Koolwijk, P., & de Maat, M. P. (2006). Fibrin structure and wound healing. *J Thromb Haemost*, *4*(5), 932-939. https://doi.org/10.1111/j.1538-7836.2006.01861.x

Le, K. Y., & Otto, M. (2015). Quorum-sensing regulation in staphylococci—an overview [Mini Review]. *Frontiers in Microbiology*, *6*.

Lebre, M. C., van der Aar, A. M. G., van Baarsen, L., van Capel, T. M. M., Schuitemaker, J. H. N., Kapsenberg, M. L., & de Jong, E. C. (2007). Human Keratinocytes Express Functional Toll-Like Receptor 3, 4, 5, and 9. *Journal of Investigative Dermatology*, *127*(2), 331-341. https://doi.org/https://doi.org/10.1038/sj.jid.5700530

Leclercq, R. (2002). Mechanisms of Resistance to Macrolides and Lincosamides: Nature of the Resistance Elements and Their Clinical Implications. *Clinical Infectious Diseases*, *34*(4), 482-492. https://doi.org/10.1086/324626

Lewis, K. (2001). Riddle of biofilm resistance. *Antimicrob Agents Chemother*, *45*(4), 999-1007. https://doi.org/10.1128/AAC.45.4.999-1007.2001

Lewis, K. (2007). Persister cells, dormancy and infectious disease. *Nat Rev Microbiol*, *5*(1), 48-56. https://doi.org/10.1038/nrmicro1557

Li, J., Ma, L., Liao, X., Liu, D., Lu, X., Chen, S.,…Ding, T. (2018). Ultrasound-Induced. *Front Microbiol*, *9*, 2486. https://doi.org/10.3389/fmicb.2018.02486

Li, J., Ma, L., Liao, X., Liu, D., Lu, X., Chen, S.,…Ding, T. (2018). Ultrasound-Induced Escherichia coli O157:H7 Cell Death Exhibits Physical Disruption and Biochemical Apoptosis [Original Research]. *Frontiers in Microbiology*, *9*.

Li, T., Wang, G., Yin, P., Li, Z., Zhang, L., & Tang, P. (2020). Adaptive expression of biofilm regulators and adhesion factors of Staphylococcus aureus during acute wound infection under the treatment of negative pressure wound therapy in vivo. *Exp Ther Med*, *20*(1), 512-520. https://doi.org/10.3892/etm.2020.8679

Liu, X., Deng, S., Huang, J., Huang, Y., Zhang, Y., Yan, Q.,…Jia, X. (2017). Dissemination of macrolides, fusidic acid and mupirocin resistance among. *Oncotarget*, *8*(35), 58086-58097. https://doi.org/10.18632/oncotarget.19491

Llor, C., & Bjerrum, L. (2014). Antimicrobial resistance: risk associated with antibiotic overuse and initiatives to reduce the problem. *Ther Adv Drug Saf*, *5*(6), 229-241. https://doi.org/10.1177/2042098614554919

Lowy, F. D. (2003). Antimicrobial resistance: the example of Staphylococcus aureus. *J Clin Invest*, *111*(9), 1265-1273. https://doi.org/10.1172/JCI18535

Lu, S. H., & McLaren, A. M. (2017). Wound healing outcomes in a diabetic foot ulcer outpatient clinic at an acute care hospital: a retrospective study. *Journal of Wound Care*, *26*(Sup10), S4-S11. https://doi.org/10.12968/jowc.2017.26.Sup10.S4

Maciag, M., Kochanowska, M., Lyzeń, R., Wegrzyn, G., & Szalewska-Pałasz, A. (2010). ppGpp inhibits the activity of Escherichia coli DnaG primase. *Plasmid*, *63*(1), 61-67. https://doi.org/10.1016/j.plasmid.2009.11.002

Macià, M. D., Rojo-Molinero, E., & Oliver, A. (2014). Antimicrobial susceptibility testing in biofilm-growing bacteria. *Clinical Microbiology and Infection*, *20*(10), 981-990. https://doi.org/10.1111/1469-0691.12651

Mackenzie, P. (2017). *North West Coast Strategic Clinical Network Diabetes Footcare Pathway Blueprint*.

Makrantonaki, E., Ganceviciene, R., & Zouboulis, C. (2011). An update on the role of the sebaceous gland in the pathogenesis of acne. *Dermatoendocrinol*, *3*(1), 41-49. https://doi.org/10.4161/derm.3.1.13900

Malik, A., Mohammad, Z., & Ahmad, J. (2013). The diabetic foot infections: Biofilms and antimicrobial resistance. *Diabetes & Metabolic Syndrome: Clinical Research & Reviews*, *7*(2), 101-107. https://doi.org/https://doi.org/10.1016/j.dsx.2013.02.006

Mann, E. E., Rice, K. C., Boles, B. R., Endres, J. L., Ranjit, D., Chandramohan, L.,…Bayles, K. W. (2009). Modulation of eDNA Release and Degradation Affects Staphylococcus aureus Biofilm Maturation. *PLoS One*, *4*(6), e5822. https://doi.org/10.1371/journal.pone.0005822

Mason, T. J. (2011). Therapeutic ultrasound an overview. *Ultrason Sonochem*, *18*(4), 847-852. https://doi.org/10.1016/j.ultsonch.2011.01.004

Mavrogenis, A. F., Megaloikonomos, P. D., Antoniadou, T., Igoumenou, V. G., Panagopoulos, G. N., Dimopoulos, L.,…Lazaris, A. (2018). Current concepts for the evaluation and management of diabetic foot ulcers. *EFORT Open Rev*, *3*(9), 513-525. https://doi.org/10.1302/2058-5241.3.180010

McAdow, M., DeDent, A. C., Emolo, C., Cheng, A. G., Kreiswirth, B. N., Missiakas, D. M., & Schneewind, O. (2012). Coagulases as determinants of protective immune responses against Staphylococcus aureus. *Infect Immun*, *80*(10), 3389-3398. https://doi.org/10.1128/IAI.00562-12

McAdow, M., Missiakas, D. M., & Schneewind, O. (2012). Staphylococcus aureus secretes coagulase and von Willebrand factor binding protein to modify the coagulation cascade and establish host infections. *J Innate Immun*, *4*(2), 141-148. https://doi.org/10.1159/000333447

Midorikawa, K., Ouhara, K., Komatsuzawa, H., Kawai, T., Yamada, S., Fujiwara, T.,…Sugai, M. (2003). Staphylococcus aureus Susceptibility to Innate Antimicrobial Peptides, β-Defensins and CAP18, Expressed by Human Keratinocytes. *Infection and Immunity*, *71*(7), 3730-3739. https://doi.org/10.1128/iai.71.7.3730-3739.2003

Moormeier, D. E., & Bayles, K. W. (2017). Staphylococcus aureus biofilm: a complex developmental organism. *Molecular Microbiology*, *104*(3), 365-376. https://doi.org/10.1111/mmi.13634

Mudge, E., Price, P., Neal, W., & Harding, K. G. (2014). A randomized controlled trial of larval therapy for the debridement of leg ulcers: Results of a multicenter, randomized, controlled, open, observer blind, parallel group study. *Wound Repair and Regeneration*, *22*(1), 43-51. https://doi.org/https://doi.org/10.1111/wrr.12127

Muhammad, M. H., Idris, A. L., Fan, X., Guo, Y., Yu, Y., Jin, X.,…Huang, T. (2020). Beyond Risk: Bacterial Biofilms and Their Regulating Approaches. *Front. Microbiol.*, *11*.

Mulani, M. S., Kamble, E. E., Kumkar, S. N., Tawre, M. S., & Pardesi, K. R. (2019). Emerging Strategies to Combat ESKAPE Pathogens in the Era of Antimicrobial Resistance: A Review. *Frontiers in Microbiology*, *10*, 539-539. https://doi.org/10.3389/fmicb.2019.00539

Mulcahy, M. E., Geoghegan, J. A., Monk, I. R., O'Keeffe, K. M., Walsh, E. J., Foster, T. J., & McLoughlin, R. M. (2012). Nasal Colonisation by Staphylococcus aureus Depends upon Clumping Factor B Binding to the Squamous Epithelial Cell Envelope Protein Loricrin. *PLOS Pathogens*, *8*(12), e1003092. https://doi.org/10.1371/journal.ppat.1003092

Navratna, V., Nadig, S., Sood, V., Prasad, K., Arakere, G., & Gopal, B. (2010). Molecular Basis for the Role of Staphylococcus aureus Penicillin Binding Protein 4 in Antimicrobial Resistance. *Journal of Bacteriology*, *192*(1), 134. https://doi.org/10.1128/JB.00822-09

Ndosi, M., Wright-Hughes, A., Brown, S., Backhouse, M., Lipsky, B. A., Bhogal, M.,…Nelson, E. A. (2018). Prognosis of the infected diabetic foot ulcer: a 12-month prospective observational study. *Diabetic medicine : a journal of the British Diabetic Association*, *35*(1), 78-88. https://doi.org/10.1111/dme.13537

Newman, C. M. H., & Bettinger, T. (2007). Gene therapy progress and prospects: Ultrasound for gene transfer. *Gene Therapy*, *14*(6), 465-475. https://doi.org/10.1038/sj.gt.3302925

Ngo, Q. V., Faass, L., Sähr, A., Hildebrand, D., Eigenbrod, T., Heeg, K., & Nurjadi, D. (2022). Inflammatory Response Against Staphylococcus aureus via Intracellular Sensing of Nucleic Acids in Keratinocytes [Original Research]. *Frontiers in Immunology*, *13*.

NHS. (2023). *Hospital Admitted Patient Care Activity 2022-23*. NHS. Retrieved 10-11-2023 from https://digital.nhs.uk/data-and-information/publications/statistical/hospital-admitted-patient-care-activity/2022-23

NICE. (2019a). *Cellulitis and erysipelas: antimicrobial prescribing*. https://www.nice.org.uk/guidance/ng141

NICE. (2019b). *Diabetic foot problems: prevention and management*. https://www.nice.org.uk/guidance/ng19

NICE. (2020a). *Impetigo: antimicrobial prescribing*. https://www.nice.org.uk/guidance/ng153

NICE. (2020b). Leg ulcer infection: antimicrobial prescribing. In.

O'Neill, A. J., Miller, K., Oliva, B., & Chopra, I. (2004). Comparison of assays for detection of agents causing membrane damage in Staphylococcus aureus. *Journal of Antimicrobial Chemotherapy*, *54*(6), 1127-1129. https://doi.org/10.1093/jac/dkh476

Oksala, O., Salo, T., Tammi, R., Häkkinen, L., Jalkanen, M., Inki, P., & Larjava, H. (1995). Expression of proteoglycans and hyaluronan during wound healing. *Journal of Histochemistry & Cytochemistry*, *43*(2), 125-135. https://doi.org/10.1177/43.2.7529785

Oliveira, D., Borges, A., & Simões, M. (2018). Toxins and Their Molecular Activity in Infectious Diseases. *Toxins (Basel)*, *10*(6). https://doi.org/10.3390/toxins10060252

Onesti, M. G., Fioramonti, P., Fino, P., Sorvillo, V., Carella, S., & Scuderi, N. (2016). Effect of enzymatic debridement with two different collagenases versus mechanical debridement on chronic hard-to-heal wounds. *International Wound Journal*, *13*(6), 1111-1115. https://doi.org/https://doi.org/10.1111/iwj.12421

Open University. (2023). *Infection and Immunity*. Open University. https://www.open.edu/openlearn/mod/oucontent/view.php?id=28153&section=4.1

Otto, M. (2008). Staphylococcal biofilms. *Curr Top Microbiol Immunol*, *322*, 207-228. https://doi.org/10.1007/978-3-540-75418-3_10

Pace, E., Gjomarkaj, M., Melis, M., Profita, M., Spatafora, M., Vignola, A. M.,…Mody, C. H. (1999). Interleukin-8 Induces Lymphocyte Chemotaxis into the Pleural

Space. *American Journal of Respiratory and Critical Care Medicine*, *159*(5), 1592-1599. https://doi.org/10.1164/ajrccm.159.5.9806001

Peetermans, M., Vanassche, T., Liesenborghs, L., Claes, J., Vande Velde, G., Kwiecinksi, J.,…Verhamme, P. (2014). Plasminogen activation by staphylokinase enhances local spreading of S. aureus in skin infections. *BMC Microbiology*, *14*(1), 310. https://doi.org/10.1186/s12866-014-0310-7

Percival, S. L., Malone, M., Mayer, D., Salisbury, A.-M., & Schultz, G. (2018). Role of anaerobes in polymicrobial communities and biofilms complicating diabetic foot ulcers. *International Wound Journal*, *15*(5), 776-782. https://doi.org/10.1111/iwj.12926

Periasamy, S., Joo, H.-S., Duong, A. C., Bach, T.-H. L., Tan, V. Y., Chatterjee, S. S.,…Otto, M. (2012). How Staphylococcus aureus biofilms develop their characteristic structure. *Proceedings of the National Academy of Sciences*, *109*(4), 1281. https://doi.org/10.1073/pnas.1115006109

Pfisterer, K., Shaw, L. E., Symmank, D., & Weninger, W. (2021). The Extracellular Matrix in Skin Inflammation and Infection [Review]. *Frontiers in Cell and Developmental Biology*, *9*.

Pitt, W. G., McBride, M. O., Lunceford, J. K., Roper, R. J., & Sagers, R. D. (1994). Ultrasonic enhancement of antibiotic action on gram-negative bacteria. *Antimicrob Agents Chemother*, *38*(11), 2577-2582. https://doi.org/10.1128/aac.38.11.2577

Pitt, W. G., & Ross, S. A. (2003). Ultrasound increases the rate of bacterial cell growth. *Biotechnology Progress*, *19*(3), 1038-1044. https://doi.org/10.1021/bp0340685

Pivarcsi, A., Bodai, L., Réthi, B., Kenderessy-Szabó, A., Koreck, A., Széll, M.,…Kemény, L. (2003). Expression and function of Toll-like receptors 2 and 4 in human keratinocytes. *International Immunology*, *15*(6), 721-730. https://doi.org/10.1093/intimm/dxg068

Pontes, D., Innocentin, S., Del Carmen, S., Almeida, J. F., Leblanc, J.-G., de Moreno de Leblanc, A.,…Chatel, J.-M. (2012). Production of Fibronectin Binding Protein A at the surface of Lactococcus lactis increases plasmid transfer in vitro and in vivo. *PLoS One*, *7*(9), e44892-e44892. https://doi.org/10.1371/journal.pone.0044892

Postma, B., Poppelier, M. J., van Galen, J. C., Prossnitz, E. R., van Strijp, J. A. G., de Haas, C. J. C., & van Kessel, K. P. M. (2004). Chemotaxis Inhibitory Protein of Staphylococcus aureus Binds Specifically to the C5a and Formylated Peptide Receptor. *The Journal of Immunology*, *172*(11), 6994. https://doi.org/10.4049/jimmunol.172.11.6994

Powles, A., Martin, D., Wells, I., & Goodwin, C. (2018). Physics of Ultrasound. *Phsics*, *19*(4), 202-205.

Prieto-Pérez, L., Pérez-Tanoira, R., Petkova-Saiz, E., Pérez-Jorge, C., Lopez-Rodriguez, C., Alvarez-Alvarez, B.,…Esteban, J. (2014). Osteomyelitis: a descriptive study. (2005-4408 (Electronic)).

Pulido-Cejudo, A., Guzmán-Gutierrez, M., Jalife-Montaño, A., Ortiz-Covarrubias, A., Martínez-Ordaz, J. L., Noyola-Villalobos, H. F., & Hurtado-López, L. M. (2017). Management of acute bacterial skin and skin structure infections with a focus on patients at high risk of treatment failure. *Ther Adv Infect Dis*, *4*(5), 143-161. https://doi.org/10.1177/2049936117723228

Quaresma, J. A. S. (2019). Organization of the Skin Immune System and Compartmentalized Immune Responses in Infectious Diseases. *Clin Microbiol Rev*, *32*(4). https://doi.org/10.1128/cmr.00034-18

Rademacher, F., Simanski, M., Gläser, R., & Harder, J. (2018). Skin microbiota and human 3D skin models. *Experimental Dermatology*, *27*(5), 489-494. https://doi.org/https://doi.org/10.1111/exd.13517

Ramisetty, B. C. M., Ghosh, D., Roy Chowdhury, M., & Santhosh, R. S. (2016). What Is the Link between Stringent Response, Endoribonuclease Encoding Type II Toxin-Antitoxin Systems and Persistence? *Frontiers in Microbiology*, *7*, 1882-1882. https://doi.org/10.3389/fmicb.2016.01882

Ramundo, J., & Gray, M. (2008). Is ultrasonic mist therapy effective for debriding chronic wounds? *J Wound Ostomy Continence Nurs*, *35*(6), 579-583. https://doi.org/10.1097/01.WON.0000341470.41191.51

Rastogi, A., Sukumar, S., Hajela, A., Mukherjee, S., Dutta, P., Bhadada, S. K., & Bhansali, A. (2017). The microbiology of diabetic foot infections in patients recently treated with antibiotic therapy: A prospective study from India. *J Diabetes Complications*, *31*(2), 407-412. https://doi.org/10.1016/j.jdiacomp.2016.11.001

Reiber, G. E., Vileikyte, L., Boyko, E. J., del Aguila, M., Smith, D. G., Lavery, L. A., & Boulton, A. J. (1999). Causal pathways for incident lower-extremity ulcers in patients with diabetes from two settings. *Diabetes Care*, *22*(1), 157-162. https://doi.org/10.2337/diacare.22.1.157

Reygaert, W. C. (2018). An overview of the antimicrobial resistance mechanisms of bacteria. *AIMS Microbiol*, *4*(3), 482-501. https://doi.org/10.3934/microbiol.2018.3.482

Riordan, K., & Lee, J. C. (2004). Staphylococcus aureus Capsular Polysaccharides. *Clinical Microbiology Reviews*, *17*(1), 218. https://doi.org/10.1128/CMR.17.1.218-234.2004

Roilides, E., Simitsopoulou, M., Katragkou, A., & Walsh, T. J. (2015). How Biofilms Evade Host Defenses. *Microbiol Spectr*, *3*(3). https://doi.org/10.1128/microbiolspec.MB-0012-2014

Rollof, J., Hedström, S. A., & Nilsson-Ehle, P. (1987). Lipolytic activity of Staphylococcus aureus strains from disseminated and localized infections. *Acta Pathol Microbiol Immunol Scand B*, *95*(2), 109-113. https://doi.org/10.1111/j.1699-0463.1987.tb03096.x

Roper, J. A., Williamson, R. C., Bally, B., Cowell, C. A. M., Brooks, R., Stephens, P.,…Bass, M. D. (2015). Ultrasonic Stimulation of Mouse Skin Reverses the Healing Delays in Diabetes and Aging by Activation of Rac1. *J Invest Dermatol*, *135*(11), 2842-2851. https://doi.org/10.1038/jid.2015.224

Rutten, S., Nolte, P. A., Korstjens, C. M., van Duin, M. A., & Klein-Nulend, J. (2008). Low-intensity pulsed ultrasound increases bone volume, osteoid thickness and mineral apposition rate in the area of fracture healing in patients with a delayed union of the osteotomized fibula. *Bone*, *43*(2), 348-354. https://doi.org/10.1016/j.bone.2008.04.010

Ryu, S., Song, P. I., Seo, C. H., Cheong, H., & Park, Y. (2014). Colonization and infection of the skin by S. aureus: immune system evasion and the response to cationic antimicrobial peptides. *International journal of molecular sciences*, *15*(5), 8753-8772. https://doi.org/10.3390/ijms15058753

Sadykov, M. R., & Bayles, K. W. (2012). The control of death and lysis in staphylococcal biofilms: a coordination of physiological signals. *Curr Opin Microbiol*, *15*(2), 211-215. https://doi.org/10.1016/j.mib.2011.12.010

Salgado, G., Ng, Y. Z., Koh, L. F., Goh, C. S. M., & Common, J. E. (2017). Human reconstructed skin xenografts on mice to model skin physiology. *Differentiation*, *98*, 14-24. https://doi.org/10.1016/j.diff.2017.09.004

Schröder, A., Schröder, B., Roppenser, B., Linder, S., Sinha, B., Fässler, R., & Aepfelbacher, M. (2006). Staphylococcus aureus fibronectin binding protein-A induces motile attachment sites and complex actin remodeling in living endothelial cells. *Molecular biology of the cell*, *17*(12), 5198-5210. https://doi.org/10.1091/mbc.e06-05-0463

Selan, L., Papa, R., Barbato, G., Scoarughi, G. L., Vrenna, G., & Artini, M. (2019). Ultrasound affects minimal inhibitory concentration of ampicillin against methicillin resistant Staphylococcus aureus USA300. *New Microbiologica*, *42*(1), 52-54.

Service, N. H. (2023). *Hospital Admitted Patient Care Activity 2022-23*. NHS. Retrieved 10-11-2023 from https://digital.nhs.uk/data-and-information/publications/statistical/hospital-admitted-patient-care-activity/2022-23

Seth, A., Attri, A. K., Kataria, H., Kochhar, S., Seth, S. A., & Gautam, N. (2019). Clinical Profile and Outcome in Patients of Diabetic Foot Infection. *International journal of applied & basic medical research*, *9*(1), 14-19. https://doi.org/10.4103/ijabmr.IJABMR_278_18

Seth, D., Cheldize, K., Brown, D., & Freeman, E. F. (2017). Global Burden of Skin Disease: Inequities and Innovations. *Curr Dermatol Rep*, *6*(3), 204-210. https://doi.org/10.1007/s13671-017-0192-7

Shahi, S. K., & Kumar, A. (2015). Isolation and Genetic Analysis of Multidrug Resistant Bacteria from Diabetic Foot Ulcers. *Front Microbiol*, *6*, 1464. https://doi.org/10.3389/fmicb.2015.01464

Shaikh, S., Fatima, J., Shakil, S., Rizvi, S. M., & Kamal, M. A. Antibiotic resistance and extended spectrum beta-lactamases: Types, epidemiology and treatment. (1319-562X (Print)).

Shaikh, S., Fatima, J., Shakil, S., Rizvi, S. M., & Kamal, M. A. (2015). Antibiotic resistance and extended spectrum beta-lactamases: Types, epidemiology and treatment. (1319-562X (Print)).

Shanei, A., & Sazgarnia, A. (2019). An overview of therapeutic applications of ultrasound based on synergetic effects with gold nanoparticles and laser excitation. *Iranian journal of basic medical sciences*, *22*(8), 848-855. https://doi.org/10.22038/ijbms.2019.29584.7142

Shepherd, J., Douglas, I., Rimmer, S., Swanson, L., & MacNeil, S. (2009). Development of three-dimensional tissue-engineered models of bacterial infected human skin wounds. *Tissue Eng Part C Methods*, *15*(3), 475-484. https://doi.org/10.1089/ten.tec.2008.0614

Singer, A. J., & McClain, S. A. (2002). Persistent wound infection delays epidermal maturation and increases scarring in thermal burns. *Wound Repair and Regeneration*, *10*(6), 372-377. https://doi.org/10.1046/j.1524-475X.2002.10606.x

Soares, G. M., Figueiredo, L. C., Faveri, M., Cortelli, S. C., Duarte, P. M., & Feres, M. (2012). Mechanisms of action of systemic antibiotics used in periodontal

treatment and mechanisms of bacterial resistance to these drugs. *J Appl Oral Sci*, *20*(3), 295-309. https://doi.org/10.1590/s1678-77572012000300002

Soruri, A., Grigat, J., Forssmann, U., Riggert, J., & Zwirner, J. (2007). β-Defensins chemoattract macrophages and mast cells but not lymphocytes and dendritic cells: CCR6 is not involved. *European Journal of Immunology*, *37*(9), 2474-2486. https://doi.org/https://doi.org/10.1002/eji.200737292

Speziale, P., Pietrocola, G., Foster, T. J., & Geoghegan, J. A. (2014). Protein-based biofilm matrices in Staphylococci. *Front Cell Infect Microbiol*, *4*, 171. https://doi.org/10.3389/fcimb.2014.00171

Spilsbury, K., Cullum, N., Dumville, J. C., O'Meara, S., Petherick, E. S., & Thompson, C. (2008). Exploring patient perceptions of larval therapy as a potential treatment for venous leg ulceration. *11*, 148-159.

Steinhuber, A., Goerke, C., Bayer, M. G., Döring, G., & Wolz, C. (2003). Molecular architecture of the regulatory Locus sae of Staphylococcus aureus and its impact on expression of virulence factors. *J Bacteriol*, *185*(21), 6278-6286. https://doi.org/10.1128/jb.185.21.6278-6286.2003

Stern, R., Asari, A. A., & Sugahara, K. N. (2006). Hyaluronan fragments: An information-rich system. *European Journal of Cell Biology*, *85*(8), 699-715. https://doi.org/https://doi.org/10.1016/j.ejcb.2006.05.009

Sugimoto, S., Sato, F., Miyakawa, R., Chiba, A., Onodera, S., Hori, S., & Mizunoe, Y. (2018). Broad impact of extracellular DNA on biofilm formation by clinically isolated Methicillin-resistant and -sensitive strains of Staphylococcus aureus. *Sci Rep*, *8*(1), 2254. https://doi.org/10.1038/s41598-018-20485-z

Sugita, Y., Mizuno, S., Nakayama, N., Iwaki, T., Murakami, E., Wang, Z.,…Furuhata, H. (2008). Nitric oxide generation directly responds to ultrasound exposure. *Ultrasound Med Biol*, *34*(3), 487-493. https://doi.org/10.1016/j.ultrasmedbio.2007.08.008

Sullivan, T., & de Barra, E. (2018). Diagnosis and management of cellulitis. *Clinical medicine (London, England)*, *18*(2), 160-163. https://doi.org/10.7861/clinmedicine.18-2-160

T.M., B., & K., K. (2022). *Histology, Dermis.* StatPearls Publishing.

Tabur, S., Eren, M. A., Çelik, Y., Dağ, O. F., Sabuncu, T., Sayiner, Z. A., & Savas, E. (2015). The major predictors of amputation and length of stay in diabetic patients with acute foot ulceration. *Wien Klin Wochenschr*, *127*(1-2), 45-50. https://doi.org/10.1007/s00508-014-0630-5

Takeuchi, O., Hoshino, K., & Akira, S. (2000). Cutting Edge: TLR2-Deficient and MyD88-Deficient Mice Are Highly Susceptible to Staphylococcus aureus Infection1. *The Journal of Immunology*, *165*(10), 5392-5396. https://doi.org/10.4049/jimmunol.165.10.5392

Takeuchi, O., Hoshino, K., Kawai, T., Sanjo, H., Takada, H., Ogawa, T.,…Akira, S. (1999). Differential roles of TLR2 and TLR4 in recognition of gram-negative and gram-positive bacterial cell wall components. *Immunity*, *11*(4), 443-451. https://doi.org/10.1016/s1074-7613(00)80119-3

Thomas, D. C., Tsu, C. L., Nain, R. A., Arsat, N., Fun, S. S., & Sahid Nik Lah, N. A. (2021). The role of debridement in wound bed preparation in chronic wound: A narrative review. (2049-0801 (Print)).

Tombulturk, F. K., & Kanigur-Sultuybek, G. (2021). A molecular approach to maggot debridement therapy with Lucilia sericata and its excretions/secretions in wound healing. *Wound Repair and Regeneration*, *29*(6), 1051-1061. https://doi.org/https://doi.org/10.1111/wrr.12961

Tong, S. Y. C., Davis, J. S., Eichenberger, E., Holland, T. L., & Fowler, V. G., Jr. (2015). Staphylococcus aureus infections: epidemiology, pathophysiology, clinical manifestations, and management. *Clinical microbiology reviews*, *28*(3), 603-661. https://doi.org/10.1128/CMR.00134-14

Ugwu, E., Adeleye, O., Gezawa, I., Okpe, I., Enamino, M., & Ezeani, I. (2019). Predictors of lower extremity amputation in patients with diabetic foot ulcer: findings from MEDFUN, a multi-center observational study. *J Foot Ankle Res*, *12*, 34. https://doi.org/10.1186/s13047-019-0345-y

Uhm, C., Jeong, H., Lee, S. H., Hwang, J. S., Lim, K.-M., & Nam, K. T. (2023). Comparison of structural characteristics and molecular markers of rabbit skin, pig skin, and reconstructed human epidermis for an ex vivo human skin model. *Toxicological Research*, *39*(3), 477-484. https://doi.org/10.1007/s43188-023-00185-1

Vandenesch, F., Lina, G., & Henry, T. (2012). Staphylococcus aureus hemolysins, bi-component leukocidins, and cytolytic peptides: a redundant arsenal of membrane-damaging virulence factors? *Frontiers in cellular and infection microbiology*, *2*, 12. https://doi.org/10.3389/fcimb.2012.00012

Veening, J.-W., Smits, W. K., & Kuipers, O. P. (2008). Bistability, Epigenetics, and Bet-Hedging in Bacteria. *Annual Review of Microbiology*, *62*(1), 193-210. https://doi.org/10.1146/annurev.micro.62.081307.163002

Vowden, K. R., & Vowden, P. (1999). Wound debridement, Part 2: Sharp techniques. (0969-0700 (Print)).

Walsh, E. J., O'Brien, L. M., Liang, X., Hook, M., & Foster, T. J. (2004). Clumping Factor B, a Fibrinogen-binding MSCRAMM (Microbial Surface Components Recognizing Adhesive Matrix Molecules) Adhesin of Staphylococcus aureus, Also Binds to the Tail Region of Type I Cytokeratin 10. *Journal of Biological Chemistry*, *279*(49), 50691-50699.

Wang, D. D., Jamjoom, R. A., Alzahrani, A. H., Hu, F. B., & Alzahrani, H. A. (2016). Prevalence and Correlates of Lower-Extremity Amputation in Patients With Diabetic Foot Ulcer in Jeddah, Saudi Arabia. *Int J Low Extrem Wounds*, *15*(1), 26-33. https://doi.org/10.1177/1534734615601542

Wang, E., Qiang, X., Li, J., Zhu, S., & Wang, P. (2016). The in Vitro Immune-Modulating Properties of a Sweat Gland-Derived Antimicrobial Peptide Dermcidin. *Shock*, *45*(1), 28-32. https://doi.org/10.1097/shk.0000000000000488

Wang, H., Teng, F., Yang, X., Guo, X., Tu, J., Zhang, C., & Zhang, D. (2017). Preventing microbial biofilms on catheter tubes using ultrasonic guided waves. (2045-2322 (Electronic)).

Wang, J., Wen, K., Liu, X., Weng, C.-x., Wang, R., & Cai, Y. (2018). Multiple Low Frequency Ultrasound Enhances Bactericidal Activity of Vancomycin against Methicillin-Resistant Staphylococcus aureus Biofilms. *BioMed Research International*, *2018*, 6023101. https://doi.org/10.1155/2018/6023101

Wang, X., & Wood, T. K. (2011). Toxin-antitoxin systems influence biofilm and persister cell formation and the general stress response. *Appl Environ Microbiol*, *77*(16), 5577-5583. https://doi.org/10.1128/AEM.05068-11

Wood, T. K., & Song, S. (2020). Forming and waking dormant cells: The ppGpp ribosome dimerization persister model. *Biofilm*, *2*, 100018. https://doi.org/https://doi.org/10.1016/j.bioflm.2019.100018

World Health Organisation. (2018). *Antimicrobial Resistance*. https://www.who.int/en/news-room/fact-sheets/detail/antimicrobial-resistance

World Health Organisation. (2020). *Antibiotic Resistance*. Retrieved 17/08/2020 from https://www.who.int/news-room/fact-sheets/detail/antibiotic-resistance

Xie, X., Bao, Y., Ni, L., Liu, D., Niu, S., Lin, H.,…Luo, Z. (2017). Bacterial Profile and Antibiotic Resistance in Patients with Diabetic Foot Ulcer in Guangzhou, Southern China: Focus on the Differences among Different Wagner's Grades, IDSA/IWGDF Grades, and Ulcer Types. *International journal of endocrinology*, *2017*, 8694903-8694903. https://doi.org/10.1155/2017/8694903

Xu, S. X., & McCormick, J. K. (2012). Staphylococcal superantigens in colonization and disease. *Frontiers in cellular and infection microbiology*, *2*, 52-52. https://doi.org/10.3389/fcimb.2012.00052

Yamazaki, K., Kato, F., Kamio, Y., & Kaneko, J. (2006). Expression of γ-hemolysin regulated by sae in Staphylococcus aureus strain Smith 5R. *FEMS Microbiology Letters*, *259*(2), 174-180. https://doi.org/10.1111/j.1574-6968.2006.00236.x

Yao, L., Berman, J. W., Factor, S. M., & Lowy, F. D. (1997). Correlation of histopathologic and bacteriologic changes with cytokine expression in an experimental murine model of bacteremic Staphylococcus aureus infection. *Infect Immun*, *65*(9), 3889-3895. https://doi.org/10.1128/iai.65.9.3889-3895.1997

Yarbrough, P., Kukhareva, P., Spivak, E., Hopkins, C., & Kawamoto, K. (2015). Evidence-Based Care for Cellulitis. *Journal of Hospital Medicine*, *10*(12), 780-786. https://doi.org/10.1002/jhm.2433

Yoong, P. (2013). Immunomodulation by the Panton-Valentine leukocidin can benefit the host during Staphylococcus aureus infections. *Virulence*, *4*(1), 92-96. https://doi.org/10.4161/viru.23165

Young, T. (2012). Skin failure and wound debridement. *Nursing and Residential Care*, *14*(2), 74-79. https://doi.org/10.12968/nrec.2012.14.2.74

Zalis, E. A., Nuxoll, A. S., Manuse, S., Clair, G., Radlinski, L. C., Conlon, B. P.,…Lewis, K. (2019). Stochastic Variation in Expression of the Tricarboxylic Acid Cycle Produces Persister Cells. *mBio*, *10*(5). https://doi.org/10.1128/mBio.01930-19

Zhong, C., Wu, Y., Lin, H., & Liu, R. (2023). Advances in the antimicrobial treatment of osteomyelitis. *Composites Part B: Engineering*, *249*, 110428. https://doi.org/https://doi.org/10.1016/j.compositesb.2022.110428

Zhou, S., Schmelz, A., Seufferlein, T., Li, Y., Zhao, J., & Bachem, M. G. (2004). Molecular mechanisms of low intensity pulsed ultrasound in human skin fibroblasts. *J Biol Chem*, *279*(52), 54463-54469. https://doi.org/10.1074/jbc.M404786200

Zhu, H.-X., Cai, X.-Z., Shi, Z.-L., Hu, B., & Yan, S.-G. (2014). Microbubble-mediated ultrasound enhances the lethal effect of gentamicin on planktonic Escherichia coli. *BioMed research international*, *2014*, 142168-142168. https://doi.org/10.1155/2014/142168